

Advances

in Clinical and Experimental Medicine

MONTHLY ISSN 1899-5276 (PRINT) ISSN 2451-2680 (ONLINE)

advances.umw.edu.pl

2022, Vol. 31, No. 10 (October)

Impact Factor (IF) – 1.736
Ministry of Science and Higher Education – 70 pts
Index Copernicus (ICV) – 168.52 pts



WROCLAW
MEDICAL UNIVERSITY

Advances
in Clinical and Experimental
Medicine



Advances in Clinical and Experimental Medicine

ISSN 1899-5276 (PRINT)

ISSN 2451-2680 (ONLINE)

advances.umw.edu.pl

MONTHLY 2022
Vol. 31, No. 10
(October)

Advances in Clinical and Experimental Medicine (*Adv Clin Exp Med*) publishes high-quality original articles, research-in-progress, research letters and systematic reviews and meta-analyses of recognized scientists that deal with all clinical and experimental medicine.

Editorial Office

ul. Marcinkowskiego 2–6
50-368 Wrocław, Poland
Tel.: +48 71 784 12 05
E-mail: redakcja@umw.edu.pl

Publisher

Wrocław Medical University
Wybrzeże L. Pasteura 1
50-367 Wrocław, Poland

Online edition is the original version
of the journal

Editor-in-Chief

Prof. Donata Kurpas

Deputy Editor

Prof. Wojciech Kosmala

Managing Editor

Marek Misiak, MA

Scientific Committee

Prof. Sabine Bährer-Kohler
Prof. Antonio Cano
Prof. Breno Diniz
Prof. Erwan Donal
Prof. Chris Fox
Prof. Naomi Hachiya
Prof. Carol Holland
Prof. Markku Kurkinen
Prof. Christos Lionis

Section Editors

Anesthesiology

Prof. Marzena Zielińska

Basic Sciences

Prof. Iwona Bil-Lula
Prof. Bartosz Kempisty
Dr. Wiesława Kranc
Dr. Anna Lebedeva
Dr. Mateusz Olbromski
Dr. Maciej Sobczyński

Clinical Anatomy, Legal Medicine, Innovative Technologies

Prof. Rafael Boscolo-Berto

Statistical Editors

Wojciech Bombała, MSc
Katarzyna Giniewicz, MSc Eng.
Anna Kopszak, MSc
Dr. Krzysztof Kujawa

Manuscript editing

Marek Misiak, MA, Jolanta Krzyżak, MA

Prof. Raimundo Mateos

Prof. Zbigniew W. Ras
Prof. Jerzy W. Rozenblit
Prof. Silvana Santana
Prof. James Sharman
Prof. Jamil Shibli
Prof. Michal Toborek
Prof. László Vécsei
Prof. Cristiana Vitale

Dentistry

Prof. Marzena Dominiak
Prof. Tomasz Gedrange
Prof. Jamil Shibli

Dermatology

Prof. Jacek Szepietowski

Emergency Medicine, Innovative Technologies

Prof. Jacek Smereka

Gynecology and Obstetrics

Prof. Olimpia Sipak-Szmigiel

Histology and Embryology

Prof. Marzena Podhorska-Okołów

Internal Medicine

Angiology

Dr. Angelika Chachaj

Cardiology

Prof. Wojciech Kosmala

Dr. Daniel Morris

Endocrinology

Prof. Marek Bolanowski

Gastroenterology

Assoc. Prof. Katarzyna Neubauer

Hematology

Prof. Andrzej Deptała

Prof. Dariusz Wołowicz

Nephrology and Transplantology

Assoc. Prof. Dorota Kamińska

Assoc. Prof. Krzysztof Letachowicz

Pulmonology

Prof. Anna Brzecka

Microbiology

Prof. Marzenna Bartoszewicz

Assoc. Prof. Adam Junka

Molecular Biology

Dr. Monika Bielecka

Prof. Jolanta Saczko

Neurology

Assoc. Prof. Magdalena Koszewicz

Assoc. Prof. Anna Pokryszko-Dragan

Dr. Masaru Tanaka

Neuroscience

Dr. Simone Battaglia

Oncology

Prof. Andrzej Deptała

Dr. Marcin Jędryka

Gynecological Oncology

Dr. Marcin Jędryka

Ophthalmology

Dr. Agnieszka Rafalska

Orthopedics

Prof. Paweł Reichert

Otolaryngology

Assoc. Prof. Tomasz Zatoński

Pediatrics

Pediatrics, Metabolic Pediatrics, Clinical Genetics, Neonatology, Rare Disorders

Prof. Robert Śmigiel

Pediatric Nephrology

Prof. Katarzyna Kiliś-Pstrusińska

Pediatric Oncology and Hematology

Assoc. Prof. Marek Ussowicz

Pharmaceutical Sciences

Assoc. Prof. Marta Kepinska

Prof. Adam Matkowski

Pharmacoeconomics, Rheumatology

Dr. Sylwia Szafraniec-Buryło

Psychiatry

Prof. Jerzy Leszek

Public Health

Prof. Monika Sawhney

Prof. Izabella Uchmanowicz

Qualitative Studies, Quality of Care

Prof. Ludmiła Marcinowicz

Radiology

Prof. Marek Sęsiadek

Rehabilitation

Prof. Jakub Taradaj

Surgery

Assoc. Prof. Mariusz Chabowski

Prof. Renata Taboła

Telemedicine, Geriatrics, Multimorbidity

Assoc. Prof. Maria Magdalena

Bujnowska-Fedak

Editorial Policy

Advances in Clinical and Experimental Medicine (Adv Clin Exp Med) is an independent multidisciplinary forum for exchange of scientific and clinical information, publishing original research and news encompassing all aspects of medicine, including molecular biology, biochemistry, genetics, biotechnology and other areas. During the review process, the Editorial Board conforms to the "Uniform Requirements for Manuscripts Submitted to Biomedical Journals: Writing and Editing for Biomedical Publication" approved by the International Committee of Medical Journal Editors (www.ICMJE.org). The journal publishes (in English only) original papers and reviews. Short works considered original, novel and significant are given priority. Experimental studies must include a statement that the experimental protocol and informed consent procedure were in compliance with the Helsinki Convention and were approved by an ethics committee.

For all subscription-related queries please contact our Editorial Office:

redakcja@umw.edu.pl

For more information visit the journal's website:

advances.umw.edu.pl

Pursuant to the ordinance No. 134/XV R/2017 of the Rector of Wrocław Medical University (as of December 28, 2017) from January 1, 2018 authors are required to pay a fee amounting to 700 euros for each manuscript accepted for publication in the journal Advances in Clinical and Experimental Medicine.

Indexed in: MEDLINE, Science Citation Index Expanded, Journal Citation Reports/Science Edition, Scopus, EMBASE/Excerpta Medica, Ulrich's™ International Periodicals Directory, Index Copernicus

Typographic design: Piotr Gil, Monika Kołęda

DTP: Wydawnictwo UMW

Cover: Monika Kołęda

Printing and binding: Drukarnia I-BiS Bierońscy Sp.k.

Contents

Editorials

- 1061 Marta Wleklík, Michał Czapla, Quin Denfeld, Roman Przybylski, Krzysztof Reczuch, Izabella Uchmanowicz
The how and why of assessing frailty syndrome in cardiac surgery
- 1065 Marek Misiak, Donata Kurpas
**Checklists for reporting research in *Advances in Clinical and Experimental Medicine*:
How to choose a proper one for your manuscript?**

Original papers

- 1073 Lijuan Sun, Hongyun Li, Qun Fu, Shuangmin Hu, Wenfei Zhao
**Significance of detecting the levels of miR-29a, survivin and interferon gamma release assay
in patients with lung cancer and tuberculosis**
- 1081 Mengtian Xu, Li Zhu, Jingjuan Yang
**Nurse-led cancer palliative care compared to oncologist-led cancer palliative care:
A retrospective analysis of Chinese patients suffering from cancer and receiving chemotherapy**
- 1087 Cui Xu, Xiangxiu Qi
Development and validation of a 4-lncRNA combined prediction model for patients with hepatocellular carcinoma
- 1099 Xixi Lin, Sijie Yang
**A prognostic signature based on the expression profile of the ferroptosis-related long non-coding RNAs
in hepatocellular carcinoma**
- 1111 Gulşah Yildirim, Hakki Muammer Karakas
Artery-first microwave ablation in the treatment of benign thyroid nodules
- 1121 Radosław Andrzej Konieczny, Ewa Żurawska-Płaksej, Konrad Kaaz,
Hanna Czapór-Irzabek, Wojciech Bombała, Andrzej Mysiak, Wiktor Kuliczkowski
Citrulline and long-term mortality in patients with cardiovascular disease
- 1129 Dawid Żyrek, Anastasija Krzemińska, Nina Żyrek, Andrzej Wajda, Wojciech Pabian, Michał Pacholski, Mateusz Sokolski, Robert Zymlński
**Effects of exposure to air pollution on acute cardiovascular and respiratory admissions to the hospital
and early mortality at emergency department**
- 1139 Anna Gładka, Tomasz Zatoński, Joanna Rymaszewska
Association between the long-term exposure to air pollution and depression

Reviews

- 1153 Vasilios Tanos, Jennifer Laidlaw, Panayiotis Tanos, Anna Papadopoulou
New insights into the neural network of the nongravid uterus
- 1163 Magdalena Maria Zawadzka, Marcin Grabowski, Agnieszka Kapłon-Cieślicka
Phenotyping in heart failure with preserved ejection fraction: A key to find effective treatment

The how and why of assessing frailty syndrome in cardiac surgery

Marta Wleklík^{1,2,A–F}, Michał Czapla^{2,3,D–F}, Quin Denfeld^{4,D–F},
Roman Przybylski^{2,5,E,F}, Krzysztof Reczuch^{2,6,E,F}, Izabella Uchmanowicz^{1,6,A,D–F}

¹ Department of Nursing and Obstetrics, Faculty of Health Sciences, Wrocław Medical University, Poland

² Institute of Heart Diseases, University Hospital, Wrocław, Poland

³ Department of Emergency Medical Service, Wrocław Medical University, Poland

⁴ School of Nursing, Oregon Health & Science University, Portland, USA

⁵ Department of Cardiac Surgery and Heart Transplantation, Institute of Heart Diseases, Wrocław Medical University, Poland

⁶ Institute of Heart Diseases, Wrocław Medical University, Poland

A – research concept and design; B – collection and/or assembly of data; C – data analysis and interpretation;

D – writing the article; E – critical revision of the article; F – final approval of the article

Advances in Clinical and Experimental Medicine, ISSN 1899–5276 (print), ISSN 2451–2680 (online)

Adv Clin Exp Med. 2022;31(10):1061–1064

Address for correspondence

Michał Czapla

E-mail: michal.czapla@umw.edu.pl

Funding sources

None declared

Conflict of interest

None declared

Received on July 30, 2022

Reviewed on September 22, 2022

Accepted on October 11, 2022

Published online on October 24, 2022

Abstract

Frailty syndrome (FS) is one of the most important variables that have a proven impact on the increased risk of morbidity and mortality in cardiac surgery. However, FS assessment is not routinely incorporated into daily clinical practice or included in commonly used risk assessment models. The inclusion of FS in perioperative risk prediction models in cardiac surgery would not only allow for a more accurate assessment but could also assist in the selection of an appropriate treatment strategy while favoring the appropriate use of clinical resources. The identification of FS in the qualification process must not be seen as an absolute contraindication to cardiac surgery but as an opportunity to adequately prepare the patient for the procedure. However, the literature is heterogeneous in terms of the selection of an appropriate tool for identifying FS. Selected tools commonly used in the assessment of FS in patients with cardiovascular disease, including those of greatest relevance in cardiac surgery, are presented in this editorial.

Key words: cardiac surgery, frailty syndrome, older adult, perioperative risk

Cite as

Wleklík M, Czapla M, Denfeld Q, Przybylski R, Reczuch K, Uchmanowicz I. The how and why of assessing frailty syndrome in cardiac surgery. *Adv Clin Exp Med.* 2022;31(10):1061–1064. doi: 10.17219/acem/155306

DOI

10.17219/acem/155306

Copyright

Copyright by Author(s)

This is an article distributed under the terms of the Creative Commons Attribution 3.0 Unported (CC BY 3.0) (<https://creativecommons.org/licenses/by/3.0/>)

Introduction

Cardiac surgery is currently facing a preponderance of older adult patients with coexisting frailty syndrome (FS), which poses significant clinical, social and economic challenges.¹ Worldwide, there has been a deterioration in the clinical profile of patients qualified for cardiac surgery. Indeed, patients are characterized by higher than before perioperative risk and more comorbidities, with the average duration of surgery and stay in the postoperative ward increasing.² The qualification and perioperative risk stratification should consider all variables that will determine treatment outcomes in the short and long term. Frailty syndrome is one of the most important variables that have a proven impact on the increased risk of morbidity and mortality in cardiac surgery.^{3,4} However, FS assessment is not routinely incorporated into everyday clinical practice or included in commonly used risk assessment models, such as The European System for Cardiac Operative Risk Evaluation II (EuroSCORE II) or The Society of Thoracic Surgeons (STS) risk score. In clinical decision-making, frailty is still assessed using unstandardized methods, either at the bedside (e.g., foot-of-the-bed assessment) or by using the so-called “eyeball test”.⁵ However, these rapid and subjective assessment methods are not reliable for assessing frailty.⁶ There is still no consensus on a specific multidimensional tool for assessing FS in cardiac surgery that has a high-risk predictive value. Incorporating FS into perioperative risk prediction models in cardiac surgery would allow for a more accurate assessment and help select an appropriate treatment strategy while promoting the appropriate use of clinical resources. Importantly, these risk scales can aid during Heart Team discussions to ensure balanced multidisciplinary decision-making in cardiac surgery, especially in line with the patient’s goals and values. The overarching goals of cardiac surgery management should always be patient-centered. Cardiac surgery is designed to alleviate symptoms of disease and improve patient survival. The identification of FS in the qualification process must not be seen as an absolute contraindication for cardiac surgery, but rather an opportunity to adequately prepare the patient for this procedure. Given the high importance of FS in cardiac surgery, it is important to continue research efforts aimed at improving models that predict perioperative risk, as well as to implement routine assessment of FS during the qualification process. The literature, however, is heterogeneous in terms of choosing an appropriate tool for identifying FS. This is due to the development and availability of multiple research tools, as well as the existence of different approaches to operationalizing frailty. Broadly speaking, there are unidimensional tools for assessing frailty, most often physical frailty, and multidimensional tools that assess frailty in both physical and psychosocial aspects.

Commonly used assessment tools

A selection of commonly used tools for assessing FS in patients with cardiovascular disease, including those of greatest relevance in cardiac surgery, are described below.

The 5-meter gait speed is often used in research studies of cardiac surgery as a tool that reliably predicts the risk of perioperative complications. Walking a distance of 5 m in ≥ 6 s is considered a slow gait speed.¹⁰ Many researchers recognize the superiority of this test over others in predicting perioperative complications in cardiac surgery.⁷

The frailty phenotype consists of 5 criteria to identify frailty, including weight loss, feelings of exhaustion, decreased physical activity, slowed gait speed, and weakened handgrip strength. Frailty is diagnosed when a minimum of 3 criteria are met, whilst meeting from 1 to 2 criteria indicates pre-frailty, a condition predisposing to frailty.⁸

The frailty index was developed from the Canadian Study of Health and Aging. It assesses the accumulation of deficits such as decreased mobility, cognitive impairment, reduced energy and functional capacity, worse mood, lack of social support, unintentional weight loss, and loss of appetite, among others.^{9,10}

The Clinical Frailty Scale involves clinically assessing patients and classifying them into one of 9 states, where No. 1 means that the patient is very fit, and No. 9 means that the patient is terminally ill and has a life expectancy of less than 6 months. Each score on the scale corresponds to a written description of frailty that is supplemented by a corresponding graphic to support the frailty classification. A score ≥ 5 indicates frailty.¹⁰

The Tilburg Frailty Indicator is a multidimensional assessment tool for FS. It consists of 25 questions and provides data on general frailty, as well as frailty in terms of physical, mental and societal domains. Frailty is recognized with a score ≥ 5 points.^{11–13}

The Groningen Frailty Indicator is a multidimensional tool composed of 15 items that include physical, cognitive, social, and psychological factors. Scores range from a minimum score (0 points) to a score ≥ 4 points, which indicates frailty.¹⁴

The simple frailty questionnaire (FRAIL) scale consists of 5 items that address subjective feelings of fatigue, difficulty walking 10 steps without resting, difficulty walking several hundred meters, chronic disease, comorbidities, and unintentional weight loss. Frailty is identified when from 3 to 5 elements are reported, whilst pre-frailty is diagnosed when 1 to 2 elements are reported.¹⁵

The Edmonton Frail Scale takes into account the assessment of cognitive function, general health, functional independence, social support, medication intake, nutritional status, mood, incontinence, and functional capacity. The scores range from 0 (no frailty) to 17 (severe frailty).¹⁶

The Essential Frailty Toolset predicts the annual risk of death in patients scheduled for either transcatheter

or surgical aortic valve surgery. The tool assesses preoperative anemia, hypoalbuminemia, 5 repetitions of standing up from a chair to a standing position without the use of arms, and cognitive impairment. A score of 5 indicates a high risk of 1-year mortality (65% for transcatheter and 50% for surgical), whilst a score of 0–1 indicates a risk of 1-year mortality of 6% for transcatheter and 3% for surgical intervention.¹⁷

Comprehensive assessment of frailty was introduced as a more precise preoperative assessment of frailty in elderly cardiac surgery patients. This assessment includes elements specific to the frailty phenotype and clinical frailty assessment. In addition, it assesses performance in basic and complex activities of daily living, balance and physical fitness. It also includes the results of laboratory tests (albumin, creatinine, natriuretic peptide) and takes into account the functional status of the respiratory system.¹⁸

Frailty Predicts Death One Year after Elective Cardiac Surgery Test (FORECAST) is a simplified version of the comprehensive assessment of frailty, consisting of 5 items with the highest predictive value. Tests involve sitting down and getting up from a chair, patient-declared feelings of weakness within 2 weeks, climbing stairs,

assessment using the Clinical Frailty Scale, and serum creatinine level. This assessment has shown promising results in predicting annual mortality in the cardiac surgery patient population.¹⁹

Conclusions

Identification of FS in cardiac surgery may have different practical purposes. Screening tools are appropriate for perioperative risk stratification, while formal, in-depth FS assessment may be necessary to define specific and individualized preoperative management to optimize the patient's condition and reduce complications.²⁰ In an ideal clinical setting, FS assessment tools should have the ability to differentiate between potentially reversible frailty and irreversible frailty. This aims to enhance the identification of patients who may not only be candidates for cardiac surgery but are also highly likely to survive it while maintaining or improving their quality of life.^{21,22}

Table 1 shows issues related to the assessment of frailty in cardiac surgery. Table 2 presents selected methods used to assess frailty in cardiac surgery.

Table 1. Issues related to the assessment of frailty in cardiac surgery

<p>Analysis of frailty in valvular heart disease</p>	<p>ESC/EACTS Guidelines* → decision-making should take into account frailty, which is associated with an increased risk of morbidity and mortality after both SAVR and TAVI. The basis for assessing frailty should not be subjective but a combination of various objective indicators. In patients at increased surgical risk (STS risk score or EuroSCORE II ≥ 4% or logistic EuroSCORE I ≥ 10% or other risk factors not included in the above scales, such as frailty syndrome), the choice between SAVR and TAVI should be made at the Heart Team meeting and should be preceded by careful individual evaluation of each patient. Increased frailty (presence of >2 Katz scale factors) is a factor in favor of choosing TAVI.²³</p> <p>ACC/AHA guidelines** → decision-making should be individualized on the basis of patient-specific factors that affect longevity or quality of life, such as comorbid cardiac and noncardiac conditions, frailty, dementia, and other factors. Frailty score provides the assessment of risk of procedure and chance of recovery of quality of life. Validated frailty scores include the Katz Score (independence in feeding, bathing, dressing, transferring, toileting, and urinary continence) plus independence in ambulation (no walking aid or assistance required, or completion of a 5-m eter walk in <6 s). Other scoring systems can be applied to calculate no, mild or moderate to severe frailty.²⁴</p>
<p>Frailty as a contraindication to cardiac surgery</p>	<p>The clinical decision to select appropriate interventions or to decline cannot be made solely on the basis of calculated perioperative risk, taking into account frailty assessment. Achieving optimal clinical outcomes always requires the use of expert judgement (Heart Team assessment), taking into account patient preferences. Risk prediction models such as STS risk score or EuroSCORE II extended with FS assessment are therefore intended to support, but not guide, clinical decisions.</p>

* 2021 European Society of Cardiology/European Association for Cardio-Thoracic Surgery (ESC/EACTS) Guidelines for the management of valvular heart disease; ** 2020 American College of Cardiology/American Heart Association (ACA/AHA) Guideline for the Management of Patients with Valvular Heart Disease; TAVI – transcatheter aortic valve implantation; SAVR – surgical aortic valve replacement; EuroSCORE – The European System for Cardiac Operative Risk Evaluation; STS – The Society of Thoracic Surgeons.

Table 2. The selected methods to assess frailty in cardiac surgery

Method	Scoring
<p>The 5-meter gait speed – simple measure of frailty that identifies slowed gait speed. It is very often used in cardiac surgery research as a tool that predicts the risk of perioperative complications in elderly patients.¹⁰</p>	<p>frailty – distance of 5 m in ≥6 s (gait speed ≥0.83 m/s)</p>
<p>The Clinical Frailty Scale – simple clinical assessment that classifies a patient into one of 9 clinical states, where state No. 1 means that the patient is fit, and state No. 9 means that the patient is terminally ill and has a life expectancy of less than 6 months. Each point on the scale corresponds to a written description of frailty, supplemented by a corresponding graphic to support the frailty classification.¹⁰</p>	<p>frailty – score ≥5</p>
<p>The Essential Frailty Toolset – 4-item based frailty assessment scale that predicts the annual risk of death in patients scheduled for either transcatheter or conventional aortic valve surgery. The tool takes into account preoperative anemia, hypoalbuminemia, 5 repetitions of standing up from a chair to a standing position without the use of arms, and cognitive impairment.¹⁷</p>	<p>frailty status: robust = 0, prefrail = 1–2, frail = 3–5</p>

ORCID iDs

Marta Wleklík  <https://orcid.org/0000-0001-9574-4448>
 Michał Czapla  <https://orcid.org/0000-0002-4245-5420>
 Quin Denfeld  <https://orcid.org/0000-0001-7568-9568>
 Roman Przybylski  <https://orcid.org/0000-0003-2399-5111>
 Krzysztof Reczuch  <https://orcid.org/0000-0002-1699-739X>
 Izabella Uchmanowicz  <https://orcid.org/0000-0001-5452-0210>

References

- Singh M, Stewart R, White H. Importance of frailty in patients with cardiovascular disease. *Eur Heart J*. 2014;35(26):1726–1731. doi:10.1093/eurheartj/ehu197
- Szychta W, Majstrak F, Opolski G, Filipiak KJ. Change in the clinical profile of patients referred for coronary artery bypass grafting from 2004 to 2008: Trends in a single-centre study. *Kardiol Pol*. 2015; 73(7):493–501. doi:10.5603/KP.a2015.0055
- Bagnall NM, Faiz O, Darzi A, Athanasiou T. What is the utility of pre-operative frailty assessment for risk stratification in cardiac surgery? *Interact Cardiovasc Thorac Surg*. 2013;17(2):398–402. doi:10.1093/icvts/ivt197
- Wilson CM, Kostsucu SR, Boura JA. Utilization of a 5-meter walk test in evaluating self-selected gait speed during preoperative screening of patients scheduled for cardiac surgery. *Cardiopulm Phys Ther J*. 2013;24(3):36–43. PMID:23997690. PMID:PMC3751713.
- Bridgman PG, Lainchbury JG, Hii TBK. Does frailty lie in the eyes of the beholder? *Heart Lung Circ*. 2015;24(12):1238. doi:10.1016/j.hlc.2015.08.001
- Hii TBK, Lainchbury JG, Bridgman PG. Frailty in acute cardiology: Comparison of a quick clinical assessment against a validated frailty assessment tool. *Heart Lung Circ*. 2015;24(6):551–556. doi:10.1016/j.hlc.2014.11.024
- Chen MA. Frailty and cardiovascular disease: Potential role of gait speed in surgical risk stratification in older adults. *J Geriatr Cardiol*. 2015;12(1):44–56. doi:10.11909/j.jissn.1671-5411.2015.01.006
- Fried LP, Tangen CM, Walston J, et al. Frailty in older adults: Evidence for a phenotype. *J Gerontol A Biol Sci Med Sci*. 2001;56(3):M146–M157. doi:10.1093/gerona/56.3.M146
- Robinson TN, Walston JD, Brummel NE, et al. Frailty for surgeons: Review of a National Institute on Aging Conference on Frailty for Specialists. *J Am Coll Surg*. 2015;221(6):1083–1092. doi:10.1016/j.jamcollsurg.2015.08.428
- Rockwood K. A global clinical measure of fitness and frailty in elderly people. *Can Med Assoc J*. 2005;173(5):489–495. doi:10.1503/cmaj.050051
- Gobbens RJJ, van Assen MALM, Luijckx KG, Wijnen-Sponselee MTH, Schols JMGA. The Tilburg Frailty Indicator: Psychometric properties. *J Am Med Dir Assoc*. 2010;11(5):344–355. doi:10.1016/j.jamda.2009.11.003
- Uchmanowicz I, Gobbens R, Jankowska-Polanska B, Loboz-Rudnicka M, Manulik S, Loboz-Grudzien K. Cross-cultural adaptation and reliability testing of the Tilburg Frailty Indicator for optimizing care of Polish patients with frailty syndrome. *Clin Interv Aging*. 2014;9:997. doi:10.2147/CIA.S64853
- Gobbens RJJ, Boersma P, Uchmanowicz I, Santiago LM. The Tilburg Frailty Indicator (TFI): New evidence for its validity. *Clin Interv Aging*. 2020;15:265–274. doi:10.2147/CIA.S243233
- Dent E, Kowal P, Hoogendijk EO. Frailty measurement in research and clinical practice: A review. *Eur J Intern Med*. 2016;31:3–10. doi:10.1016/j.ejim.2016.03.007
- Morley JE, Malmstrom TK, Miller DK. A simple frailty questionnaire (FRAIL) predicts outcomes in middle aged African Americans. *J Nutr Health Aging*. 2012;16(7):601–608. doi:10.1007/s12603-012-0084-2
- Graham MM, Galbraith PD, O'Neill D, Rolfson DB, Dando C, Norris CM. Frailty and outcome in elderly patients with acute coronary syndrome. *Can J Cardiol*. 2013;29(12):1610–1615. doi:10.1016/j.cjca.2013.08.016
- Afilalo J, Lauck S, Kim DH, et al. Frailty in older adults undergoing aortic valve replacement. *J Am Coll Cardiol*. 2017;70(6):689–700. doi:10.1016/j.jacc.2017.06.024
- Sündermann S, Dademasch A, Praetorius J, et al. Comprehensive assessment of frailty for elderly high-risk patients undergoing cardiac surgery. *Eur J Cardiothorac Surg*. 2011;39(1):33–37. doi:10.1016/j.ejcts.2010.04.013
- Sundermann S, Dademasch A, Rastan A, et al. One-year follow-up of patients undergoing elective cardiac surgery assessed with the Comprehensive Assessment of Frailty test and its simplified form. *Interact Cardiovasc Thorac Surg*. 2011;13(2):119–123. doi:10.1510/icvts.2010.251884
- Robinson TN, Walston JD, Brummel NE, et al. Frailty for surgeons: Review of a National Institute on Aging Conference on Frailty for Specialists. *J Am Coll Surg*. 2015;221(6):1083–1092. doi:10.1016/j.jamcollsurg.2015.08.428
- Joyce E. Frailty in advanced heart failure. *Heart Fail Clin*. 2016;12(3):363–374. doi:10.1016/j.hfc.2016.03.006
- Kluszczyńska M, Młynarska A. Influence of frailty syndrome on patient prognosis after coronary artery bypass grafting. *Adv Clin Exp Med*. 2021;30(9):923–931. doi:10.17219/acem/137558
- Vahanian A, Beyersdorf F, Praz F, et al. 2021 ESC/EACTS Guidelines for the management of valvular heart disease. *Eur Heart J*. 2022;43(7):561–632. doi:10.1093/eurheartj/ehab395
- Otto CM, Nishimura RA, Bonow RO, et al. 2020 ACC/AHA Guideline for the Management of Patients With Valvular Heart Disease: A Report of the American College of Cardiology/American Heart Association Joint Committee on Clinical Practice Guidelines. *Circulation*. 2021; 143(5):e35–e71. doi:10.1161/CIR.0000000000000923

Checklists for reporting research in *Advances in Clinical and Experimental Medicine*: How to choose a proper one for your manuscript?

Marek Misiak^{1,B–F}, Donata Kurpas^{2,A–F}

¹ Wrocław Medical University Press, Wrocław Medical University, Poland

² Department of Family Medicine, Faculty of Medicine, Wrocław Medical University, Poland

A – research concept and design; B – collection and/or assembly of data; C – data analysis and interpretation;

D – writing the article; E – critical revision of the article; F – final approval of the article

Advances in Clinical and Experimental Medicine, ISSN 1899–5276 (print), ISSN 2451–2680 (online)

Adv Clin Exp Med. 2022;31(10):1065–1072

Address for correspondence

Marek Misiak

E-mail: marek.misiak@umw.edu.pl

Funding sources

None declared

Conflict of interest

None declared

Acknowledgements

Marek Misiak, MA, would like to thank
Ia Sudoplatova, PhD, for her support.

Received on September 10, 2022

Reviewed on September 19, 2022

Accepted on September 19, 2022

Published online on October 24, 2022

Abstract

Various guidelines for authors of research papers and the checklists that often accompany these statements play an important role in the creation of carefully written scientific papers – for authors, they serve as tools to ensure the correct structure and content of the manuscript, increasing the chances that a paper will be published in a journal with a high rejection rate. The aim of this editorial is to provide a concise outline of the checklists most frequently used to guide the structuring of papers published in *Advances in Clinical and Experimental Medicine*, and to support current and prospective authors of this journal in choosing a checklist for their manuscript.

The EQUATOR website is presented as a useful tool in choosing a checklist: <https://www.equator-network.org/>. Then, 8 checklists that are most popular among authors who publish their work in *Advances in Clinical and Experimental Medicine* are outlined: STROBE – for observational studies; ARRIVE – for any area of bioscience research using laboratory animals; CASP – for qualitative studies; CONSORT – for parallel group randomized trials; PRISMA – for all reviews and meta-analyses; SQUIRE – for studies on quality improvement in healthcare; STARD – for diagnostic accuracy studies; REMARK – for tumor marker prognostic studies. Each of the 8 presented checklists is discussed in a following order: 1) the name of the checklist is explained; 2) the type of articles to which it is intended is pointed out; 3) the structure of the checklist is explained; 4) if there are any extensions of the presented checklist for specific subtypes of papers, they are listed; 5) the most important literature on the presented checklist is provided.

As a take-home message, basic tips for choosing a checklist are formulated. Finally, examples of papers adhering to each discussed checklist are provided.

Key words: quality, checklist, scientific journal, EQUATOR network, medical writing

Cite as

Misiak M, Kurpas D. Checklists for reporting research
in *Advances in Clinical and Experimental Medicine*:
How to choose a proper one for your manuscript?
Adv Clin Exp Med. 2022;31(10):1065–1072.
doi:10.17219/acem/155921

DOI

10.17219/acem/155921

Copyright

Copyright by Author(s)

This is an article distributed under the terms of the
Creative Commons Attribution 3.0 Unported (CC BY 3.0)
(<https://creativecommons.org/licenses/by/3.0/>)

Introduction

Authors of research papers often – and for various reasons – fail to report specific details about their study.¹ In response to the poor quality of reporting medical research, guidelines intended for various types of study designs have been developed. Implementation of these guidelines will lead to improvements in the quality of medical research reporting – to accurate reporting, complete transparency and easier assessment of the validity of reported research findings. That means that the proper utilization of the checklists as a tool for enhancing the quality of papers is beneficial for both authors and journal editors. For the former, it increases the possibility that the paper will be published and cited; for the latter, it ensures the quality of the submitted papers and may result in a higher citation score and prestige of the journal.

Currently, the EQUATOR network (Enhancing the QUALity and Transparency Of health Research) has registered 256 guidelines on varying topics of medical research.^{2–6} In 1988, the International Committee of Medical Journal Editors (ICMJE) stated in its guidelines that statistical methods should be presented precisely and exhaustively enough to allow a reviewer to verify the results. In 1994, the first attempt was made to develop reporting guidelines, which eventually formed the basis for the development of the Consolidated Standards of Reporting Trials (CONSORT) in 1996.⁷ Since then, many other checklists to be used for various types of medical papers have been released, and the use of several such tools has been endorsed, recommended or required by editorial offices of many high-profile medical journals.

In our journal, it is mandatory to use the EQUATOR website to select the appropriate checklist for the study: <https://www.equator-network.org/>. For qualitative studies, the CASP checklist is required: <https://casp-uk.net/casp-tools-checklists/>. Eight checklists are presented in this editorial, to which most manuscripts published in *Advances in Clinical and Experimental Medicine* conform, in the order in which they were most frequently selected by our authors. The presented checklists have been chosen for 2 reasons: they are the checklists most frequently chosen for papers published in *Advances in Clinical and Experimental Medicine*, and, because the scope of this journal encompasses a broad array of medical sciences, this set of checklists partly reflects the most popular tools of this kind among authors of scientific medical papers in general.

Notes of the editor

The mandatory use of checklists was introduced in *Advances in Clinical and Experimental Medicine* in 2020. Based on more than 2 years of experience with these tools, the following observations can be made:

1. Although various checklists have gradually become a part of the scientific landscape in the last 10–15 years, not only in medical field, still many researchers declare that they encounter them for the first time when they submit a manuscript to our journal. However, it should be emphasized that such tools are more and more often used by the editors of scientific journals to improve the quality of the submitted papers and to maintain their satisfactory methodological level. It is therefore of utmost importance for all researchers to familiarize themselves with the most common checklists in their field.

2. Before filling out a particular checklist, you should read it carefully, because the formats of the various instruments of this type are by no means uniform. Some require authors to provide page numbers where relevant sections of the manuscript are located; others stipulate that a relevant passage of text be included; still others require only a yes/no response to one or more items. Not only must the checklist be completed – it must be completed correctly.

3. Common mistakes that less experienced authors make when preparing the checklist include: resubmitting the cover letter or main body of the text instead of a completed relevant checklist, submitting an incomplete checklist, and selecting the wrong checklist (in some cases, the Preferred Reporting Items for Systematic Reviews and Meta-Analyses (PRISMA) checklist is submitted with an original paper even though it is clearly intended for reviews and meta-analyses only).

Objectives

The aim of this editorial is to provide a concise outline of the checklists most frequently used to guide the structuring of papers published in *Advances in Clinical and Experimental Medicine*, and to support current and prospective authors of this journal in choosing a checklist for their manuscript. Selecting a proper checklist and submitting its filled-in form is a prerequisite for the initial assessment of the manuscript in this journal; at the same time, we are aware that such choice poses a problem for many authors.

Each of the 8 presented checklists is discussed in a following order: 1) the name of the checklist is explained; 2) the type of articles to which it is intended is pointed out; 3) the structure of the checklist is explained; 4) if there are any extensions of the presented checklist for specific subtypes of papers, they are listed; 5) the most important literature on the presented checklist is provided. To complement this guide, examples of papers adhering to each discussed checklist are provided in Table 1.

STROBE

STrengthening the Reporting of OBservational studies in Epidemiology (STROBE) serves as a guide for reporting

all observational studies, particularly cohort, case-control and cross-sectional studies. There are separate STROBE checklists for these 3 types of studies and a combined version for all 3.

These guidelines were developed in order to ensure that observational research is reported transparently to let the readers understand what was planned, investigated and elucidated, and what conclusions were reached. The STROBE statement consists of a 22-item checklist divided into 6 sections: 1) title and abstract; 2) introduction (background/rationale and objectives); 3) methods (study design, setting, participants, variables, data sources/measurement, bias, study size, quantitative variables, and statistical methods); 4) results (participants, descriptive data, outcome data, main results, and other analyses); 5) discussion (key results, limitations, interpretation, and generalizability); and 6) other information (funding). Eighteen of the items are identical for the 3 types of studies (cohort, case-control and cross-sectional studies), while 4 items differ; therefore, make sure you have chosen the right version of this checklist or use the combined version. The STROBE checklist is available in PDF and DOC/DOCX formats, but please note these versions are not identical – the latter is fillable and is the one, not simply the statement in PDF, that should be used. For each element in each item, a page number should be provided where the respective issue is mentioned, and if it is not discussed, a dash or N/A (not applicable) should be written. The guide is not to be followed strictly – the presentation of information should depend on the style of the journal, preferences of the authors and traditions of a given research field.

Several extensions of this checklist have been released, including a version for genetic association studies (STREGA), observational studies in molecular epidemiology (STROBE-ME), studies on molecular epidemiology for infectious diseases (STROME-ID), studies in epidemiology for respondent-driven sampling studies (STROBE-RDS), epidemiological studies on antimicrobial resistance (STROBE-AMS), studies on nutritional epidemiology (STROBE-nut), studies of newborn infections (STROBE-NI), and studies in epidemiology using Mendelian randomization (STROBE-MR).

Two fundamental papers on the STROBE guidelines were published by Vandembroucke et al. and von Elm et al.^{8,9} Experiences from using this checklist were summarized by Ghaferi et al. and Cuschieri,^{10,11} while da Costa et al. provided an overview of the misuse of this tool.¹²

ARRIVE

We require that Animal Research: Reporting of In Vivo Experiments (ARRIVE) checklist be followed in the preparation of studies involving live animals, from mammals to fish and invertebrates.

The goal of this tool is to optimize the quality and reliability of published work, which ensures completeness and transparency, and allows other researchers to evaluate and replicate the research and results presented. The authors can choose between 2 versions of this checklist – basic and full. The ARRIVE Essential 10 (E10) constitutes the minimum requirements for reporting animal research and includes information allowing reviewers and readers to assess the reliability of the findings. The Recommended Set complements the E10 and adds important context to the study described. Reporting this information is considered the best practice.

The ARRIVE E10 consists of 10 items which cover different, but interconnected aspects of the study. These are: 1) study design; 2) sample size; 3) inclusion and exclusion criteria (introduced to prevent ad hoc exclusion of data); 4) randomization; 5) blinding; 6) outcome measures; 7) statistical methods; 8) experimental animals; 9) experimental procedures; and 10) results. Each item points out what details should be provided regarding this particular aspect of research. These items are the basic minimum to include in a manuscript. Without this information, readers and reviewers cannot assess the reliability of the findings. When filling in this checklist, the authors must report a section/line number where the respective issue is discussed, or a reason for not reporting.

The 2.0 version of the ARRIVE checklist was published in 2020 by Percie du Sert et al.¹³ Percie du Sert et al. have explained this tool in more detail,^{14,15} while Kilkenny et al. have provided valuable explanations of how this checklist should be used.^{16,17}

CASP

The Critical Appraisal Skills Programme (CASP) core checklists are not a single tool, but a group of checklists of similar design. Regarding papers submitted to *Advances in Clinical and Experimental Medicine*, the CASP checklist for qualitative studies is required. This is the only checklist not included in the EQUATOR website – it can be downloaded from the CASP initiative website (<https://casp-uk.net/casp-tools-checklists/>).

The CASP checklist for qualitative studies consists of 10 questions, whose main objective is to guide the authors in systematic thinking about the reported issues. The first 3 questions are screening ones and can be answered promptly: 1) Was there a clear statement of the aims of the research?; 2) Is a qualitative methodology appropriate?; 3) Was the research design appropriate to address the aims of the research? If the answer to both questions is “yes”, it is worth continuing with the remaining 7 questions: 4) Was the recruitment strategy appropriate to the aims of the research?; 5) Was the data collected in a way that addressed the research issue?; 6) Has

the relationship between researcher and participants been adequately considered?; 7) Have ethical issues been taken into consideration?; 8) Was the data analysis sufficiently rigorous?; 9) Is there a clear statement of findings?; 10) How valuable is the research? Some of the questions overlap, but should be answered nevertheless. Most questions ask you to answer “yes”, “no” or “cannot say”. A series of prompts in italics follows each question to remind why it is important. No page numbers from the manuscript need to be provided.

All CASP checklists are based on the 1994 *Journal of the American Medical Association (JAMA)* guides to the medical literature.¹⁸ The most extensive presentation of this tool was published by Long et al.¹⁹ Nadelson and Nadelson discussed it the context of teaching evidence-based practice,²⁰ while Chenail reported his experiences in using the tool during methodology courses.²¹

CONSORT

Consolidated Standards of Reporting Trials (CONSORT) is a guideline for reporting parallel group randomized controlled trials, intended to promote complete reporting and transparent research; its latest version dates from 2010.

Indirectly, this tool also influences study design, conduct and publication in order to prevent inadequately designed studies from being published. In addition, it contains a flowchart that provides an overview of the phases that patients go through in the study.

The CONSORT checklist consists of 25 points divided into 6 sections: 1) title and abstract; 2) introduction (background and objectives); 3) methods (trial design, participants, interventions, outcomes, sample size, randomization, allocation concealment mechanism, blinding, and statistical methods); 4) results (participant flow, recruitment, baseline data, numbers analyzed, outcomes and estimation, ancillary analyses, and harms); 5) discussion (limitations, generalizability and interpretation); and 6) other information (registration, protocol and funding). Some of the items contain 1 or 2 leading questions detailing the issues that need to be addressed. For each element in each item, a page number should be provided where the respective issue is discussed, and if it is not discussed, a dash or N/A should be written.

A detailed presentation of this tool was published by Moher et al.,²² while Falci and Marques offered a more concise guide to its use.²³ Pandis et al. proposed an extension for person randomized trials,²⁴ while Schulz updated the CONSORT checklist for use in parallel group randomized trials.²⁵ Blanco et al. investigated whether CONSORT checklists submitted by authors properly summarize information that is actually reported in published articles,²⁶ and Turner et al. – whether the use of this tool makes the reporting of randomized controlled trials more complete.²⁷

PRISMA

Preferred Reporting Items for Systematic Reviews and Meta-Analyses (PRISMA) are intended for all reviews and meta-analyses. They were designed to help systematic reviewers transparently report why the review was done, what the authors did and what they found.

The PRISMA checklist consists of 27 items divided into 7 categories: 1) title; 2) abstract; 3) introduction (rationale and objectives); 4) methods (eligibility criteria, information sources, search strategy, selection process, data collection process, data items, study risk of bias assessment, effect measures, synthesis methods, reporting bias assessment, and certainty assessment); 5) results (study selection, study characteristics, risk of bias in studies, results of individual studies, results of syntheses, reporting biases, and certainty of evidence); 6) discussion; and 7) other information (registration and protocol, financial support, competing interests, and availability of data, code and other materials). Some of the items are divided into subitems, and all contain leading questions detailing the issues that need to be addressed.

Several extensions of this checklist have been released, including a version for studies in health equity (PRISMA-Equity), for abstracts only (PRISMA-Abstracts), for systematic reviews and meta-analysis protocols (PRISMA-P), for systematic reviews and meta-analyses of individual participant data (PRISMA-IPD), for systematic reviews and meta-analyses of complex interventions (PRISMA-CI), for systematic reviews and meta-analyses of diagnostic test accuracy studies (PRISMA-DTA), for scoping reviews (PRISMA-ScR), and for literature searches in systematic reviews (PRISMA-S).

The PRISMA checklist was first presented in 2005 as an update of QUality Of Reporting Of Meta-analyses (QUOROM) statement to reflect conceptual and practical advances in the science of systematic reviews.²⁸ The most important publications on PRISMA are a paper by Moher et al.²⁹ and a detailed presentation of an updated version of this checklist published by Page et al.³⁰ Liberati et al. provided a meticulous explanation and elaboration of its practical application,³¹ while Sarkis-Onofre et al. offered a more concise guide for authors.³²

It is important to emphasize that when submitting a manuscript that adheres to the PRISMA guidelines, the flowchart depicting the selection process of the studies analyzed must be included as one of the figures.

SQUIRE

The Standards for Quality Improvement Reporting Excellence (SQUIRE) checklist is intended for reports that describe system-level work to improve the quality, safety and value of health-care, and use various methods to demonstrate that observed outcomes are related

to the intervention(s). The SQUIRE checklist can be adapted to many approaches in this field of study.

SQUIRE 2.0, published in 2015,³³ contains 18 items divided into 6 sections related to each part of the paper: 1) title and abstract; 2) introduction (problem description, available knowledge, rationale, and specific objectives); 3) methods (context, intervention(s), study of intervention(s), measures, analyses, and ethical considerations); 4) results; 5) discussion (summary, interpretation, limitations, and conclusions); and 6) information on funding sources.

This checklist does not require filling in – authors have to carefully confront their paper with the requirements listed in each item, and then submit the used checklist together with the manuscript. Authors should consider each item from SQUIRE, but including each item in the paper may be inappropriate or unnecessary. The items can be used in the manuscript in an order different to the sequence in which they appear in the checklist.

The most important publication on this instrument is the presentation of SQUIRE 2.0 by Ogrinc et al.³³ A team led by the same investigator also provided a valuable explanation and elaboration of the previous version of this checklist – most of their comments apply to the revised version as well.³⁴ McQuillan and Wong also provided valuable explanations of this instrument,³⁵ while Goodman et al. discussed version 2.0 in detail.³⁶

STARD

The Standards for Reporting Diagnostic Accuracy (STARD) statement is intended for diagnostic accuracy studies. A study is identified as a diagnostic accuracy study if the authors used at least 1 measure of accuracy, such as sensitivity, specificity, predictive values, or area under the curve (AUC). The STARD statement was designed to apply to all types of medical tests.

The 30-item STARD checklist is organized into 7 sections: 1) title and abstract (identification as a study of diagnostic accuracy); 2) abstract (its structure); 3) introduction (scientific and clinical background and study objectives and hypotheses); 4) methods (study design, participants, test methods, and analysis); 5) results (flow of participants using a diagram, test results); 6) discussion (study limitations, including sources of potential bias and statistical uncertainty, generalizability, implications for practice, including the intended use and clinical role of the index test); and 7) other information (registration, where the full study protocol can be accessed, and funding).

The tool was created by the STARD initiative.³⁷ The most recent version is STARD 2015, presented by Bossuyt et al.,³⁸ and each item was explained in detail and with examples by Cohen et al.³⁹ A special version of this checklist for journal and conference abstracts only was published by Cohen et al.⁴⁰ The impact of implementing this tool was reported by Stahl et al., who investigated whether

the STARD statement improved the quality of reporting of diagnostic accuracy studies published in *European Radiology*.⁴¹

REMARK

REporting recommendations for tumor MARKer prognostic studies (REMARK) is a more specific checklist developed for studies exploring only 1 (albeit extensively researched) area – tumor marker prognostic studies.

This checklist generally applies to any studies involving prognostic factors (whether these factors are biological markers, imaging assessments, clinical assessments, or measures of functional status in activities of daily living), as well as to studies on other diseases in addition to cancer. The processes of measuring and reporting the aforementioned factors may be different in different papers, but the study reporting principles remain the same.

Similarly to several other such tools, the REMARK checklist uses the IMRaD (Introduction, Methods, Results, and Discussion) structure and provides authors with detailed guidelines for each section of a given manuscript. Therefore, this checklist consists of 20 items grouped into 4 sections. The Introduction should state the markers studied, the study objectives and any prespecified hypotheses. In the Methods section, information about patients, sample characteristics, test methods, study design, and statistical analysis methods should be provided. The Results guidelines explain how the obtained data should be presented and interpreted (with separate suggestions for univariate and multivariate analyses). The Discussion section should interpret the results in the context of the hypotheses formulated and relevant studies cited, identify the limitations of the study, and discuss implications for future research and clinical utility.

A paper by McShane et al. presents this tool,⁴² while Altman et al. and Sauerbrei et al. provided elaborations and explanations of each item in this checklist.^{43,44} Mallett et al. published a review of articles related to the guidelines from REMARK.⁴⁵

Discussion

When comparing the 8 checklists presented above, it can be observed that all of them, excluding the CASP tool, follow the IMRaD structure, although the number of categories into which the items are divided ranges from 5 to 7. A situation when all or virtually all items apply to one paper seems impossible, but when the authors leave an N/A acronym or a dash in most of the items, it can imply that a wrong checklist has been chosen. Such danger stems from the fact that several items, especially those outside the Methods and Results section (which are specific to a given type of articles), address similar issues and

it is possible to apply them to manuscripts of a type different from the checklist is intended to check.

Ideally, the checklist should be chosen before writing the paper – following the selected guidelines will ensure a proper structure and content of the article and result in a quicker initial assessment of the paper after the submission since deeper changes in order to conform to the requirements of the checklist will not be necessary. The influence of adhering to a given checklist is more profound when its requirements and recommendations are implemented already when the paper is being written than when it is adjusted to the editor's comments during the initial assessment.

Limitations

In the authors' view, the most important limitation of this paper is that it presents only some of the checklists used by authors of medical articles published in English. Several frequently chosen checklists were not discussed – e.g., CARE (for case reports), AGREE (for reporting clinical practice guidelines), ENTREQ (for syntheses of qualitative research), and SPIRIT (for reporting clinical trial reports and related documents) – because the present paper focuses solely on checklists for which examples of usage

can be found in papers published in *Advances in Clinical and Experimental Medicine*.

Conclusions

Checklists play an important role in the preparation of carefully written scientific papers – for authors, they serve as a tool to ensure the correct structure and content of the manuscript, which in turn increases the chances that a paper will be published in a journal with a high rejection rate. They serve this purpose only if authors not only select and complete an appropriate checklist, but also modify the manuscript to meet the requirements of a particular checklist. Therefore, it is advisable to select a checklist not when submitting the paper, but already when deciding on the type and form of the paper – changes (e.g., restructuring the Materials and Methods section) are then not necessary during the initial assessment by the editorial office following submission. The EQUATOR network diagram facilitates the selection of a suitable checklist – it is important to analyze this tool thoroughly, because for most papers submitted to scientific medical journals a suitable checklist can be found in this diagram. Choosing the most appropriate checklist and implementing it in one's own work is a win-win strategy: both the authors

Table 1. Examples of papers adhering to respective checklists, published in *Advances in Clinical and Experimental Medicine* in 2021 and 2022^{46–65}

Checklist and URL	Authors	Reference
ARRIVE – for any area of bioscience research using laboratory animals https://arriveguidelines.org/resources/author-checklists	Yu et al.	[46]
	Tosun et al.	[47]
	Gündüz et al.	[48]
CASP – for qualitative studies https://casp-uk.net/images/checklist/documents/CASP-Qualitative-Studies-Checklist/CASP-Qualitative-Checklist-2018.pdf	Wang et al.	[49]
	İçduygu et al.	[50]
	Wang et al.	[51]
CONSORT – for parallel group randomized trials https://www.consort-statement.org/	Tong et al.	[52]
	Kara et al.	[53]
	Ada et al.	[54]
PRISMA – for all reviews and meta-analyses https://prisma-statement.org/PRISMAStatement/Checklist.aspx	Rachwalik et al.	[55]
	Liu et al.	[56]
	Rakoczy et al.	[57]
REMARK – for tumor marker prognostic studies https://www.equator-network.org/reporting-guidelines/reporting-recommendations-for-tumour-marker-prognostic-studies-remark/	Annus et al.	[58]
SQUIRE – for studies on quality improvement in healthcare http://www.squire-statement.org/index.cfm?fuseaction=Page.ViewPage&PageID=471	Charong et al.	[59]
	Kolasa et al.	[60]
STARD – for diagnostic accuracy studies https://www.equator-network.org/reporting-guidelines/stard/	Fang et al.	[61]
	Yang et al.	[62]
STROBE – for observational studies (cohort, case-control and cross-sectional studies) https://www.strobe-statement.org/checklists/	Dominiak et al.	[63]
	Floer et al.	[64]
	Rams et al.	[65]

ARRIVE – Animal Research: Reporting of In Vivo Experiments; CASP – Critical Appraisal Skills Programme; CONSORT – Consolidated Standards of Reporting Trials; PRISMA – Preferred Reporting Items for Systematic Reviews and Meta-Analyses; REMARK – REporting recommendations for tumor MARKer prognostic studies; SQUIRE – Standards for QUALity Improvement Reporting Excellence; STARD – Standards for Reporting Diagnostic Accuracy; STROBE – STrengthening the Reporting of OBServational studies in Epidemiology.

as well as the editors and reviewers benefit from popularization of such tools.

As an important complement, we would like to offer readers 20 examples of good papers published in our journal in the last 2 years that conform to 8 different checklists, along with links to the respective checklists (Table 1).

Take-home message – practical suggestions

1. The checklists should be seen not only as another requirement, but as a way to improve the quality of the manuscript by following guidelines formulated by experienced researchers.


2. To choose a checklist, enter the EQUATOR website: <https://www.equator-network.org/>. If your manuscript is a qualitative study, use the CASP checklist: <https://casp-uk.net/casp-tools-checklists/>.

3. We suggest choosing a checklist before you start writing the paper.

4. The choice of the checklist for a manuscript should be based on the type of the article – there is always only one possibility for a given type of manuscript, and the checklists available on the EQUATOR website together with the CASP checklists cover all types of manuscripts submitted to *Advances in Clinical and Experimental Medicine*. The type of papers for which the given checklist is intended appears either in its title/heading or on the subpage of a given checklist on the EQUATOR website. When in doubt, the authors are recommended to read the checklists carefully and decide which is the most appropriate, even if some of the items of the chosen checklist would not be applicable.

ORCID iDs

Marek Misiak  <https://orcid.org/0000-0003-2208-2193>

Donata Kurpas  <https://orcid.org/0000-0002-6996-8920>

References

- McEvoy NL, Tume LN, Trapani J. What are publication reporting checklists and why are they so important? *Nurs Crit Care*. 2022;27(3):291–293. doi:10.1111/nicc.12771
- Altman DG, Simera I. A history of the evolution of guidelines for reporting medical research: The long road to the EQUATOR Network. *J R Soc Med*. 2016;109(2):67–77. doi:10.1177/0141076815625599
- Simera I, Moher D, Hirst A, Hoey J, Schulz KF, Altman DG. Transparent and accurate reporting increases reliability, utility, and impact of your research: Reporting guidelines and the EQUATOR Network. *BMC Med*. 2010;8(1):24. doi:10.1186/1741-7015-8-24
- Pandis N, Fedorowicz Z. The international EQUATOR network: Enhancing the quality and transparency of health care research. *J Appl Oral Sci*. 2011;19(5):0. doi:10.1590/S1678-77522011000500001
- Simera I, Moher D, Hoey J, Schulz KF, Altman DG. A catalogue of reporting guidelines for health research. *Eur J Clin Invest*. 2010;40(1):35–53. doi:10.1111/j.1365-2362.2009.02234.x
- Gould KA. The EQUATOR Network: A resource for authors. *Dimens Crit Care Nurs*. 2016;35(6):350. doi:10.1097/DCC.0000000000000213
- Johansen M, Thomsen SF. Guidelines for reporting medical research: A critical appraisal. *Int Sch Res Notices*. 2016;2016:1346026. doi:10.1155/2016/1346026
- Vandenbroucke JP, von Elm E, Altman DG, et al. Strengthening the Reporting of Observational Studies in Epidemiology (STROBE): Explanation and elaboration. *PLoS Med*. 2007;4(10):e297. doi:10.1371/journal.pmed.0040297
- von Elm E, Altman DG, Egger M, et al. The Strengthening the Reporting of Observational Studies in Epidemiology (STROBE) Statement: Guidelines for reporting observational studies. *PLoS Med*. 2007;4(10):e296. doi:10.1371/journal.pmed.0040296
- Ghaferi AA, Schwartz TA, Pawlik TM. STROBE reporting guidelines for observational studies. *JAMA Surg*. 2021;156(6):577. doi:10.1001/jamasurg.2021.0528
- Cuschieri S. The STROBE guidelines. *Saudi J Anaesth*. 2019;13(5):31. doi:10.4103/sja.SJA_543_18
- da Costa BR, Cevallos M, Altman DG, Rutjes AWS, Egger M. Uses and misuses of the STROBE statement: Bibliographic study. *BMJ Open*. 2011;1(1):e000048. doi:10.1136/bmjopen-2010-000048
- Percie du Sert N, Hurst V, Ahluwalia A, et al. The ARRIVE guidelines 2.0: Updated guidelines for reporting animal research. *PLoS Biol*. 2020;18(7):e3000410. doi:10.1371/journal.pbio.3000410
- Percie du Sert N, Hurst V, Ahluwalia A, et al. Revision of the ARRIVE guidelines: Rationale and scope. *BMJ Open Sci*. 2018;2(1):e000002. doi:10.1136/bmjopen-2018-000002
- Percie du Sert N, Ahluwalia A, Alam S, et al. Reporting animal research: Explanation and elaboration for the ARRIVE guidelines 2.0. *PLoS Biol*. 2020;18(7):e3000411. doi:10.1371/journal.pbio.3000411
- Kilkenny C, Browne WJ, Cuthill IC, Emerson M, Altman DG. Improving bioscience research reporting: The ARRIVE guidelines for reporting animal research. *PLoS Biol*. 2010;8(6):e1000412. doi:10.1371/journal.pbio.1000412
- Kilkenny C, Browne W, Cuthill I, Emerson M, Altman D; NC3Rs Reporting Guidelines Working Group. Animal research: Reporting in vivo experiments. The ARRIVE guidelines. *J Physiol*. 2010;588(14):2519–2521. doi:10.1113/jphysiol.2010.192278
- Guyatt GH, Sackett D, Cook D. Users' guides to the medical literature. II. How to use an article about therapy or prevention. B. What were the results and will they help me in caring for my patients? Evidence-Based Medicine Working Group. *JAMA*. 1994;271(1):59–63. doi:10.1001/jama.271.1.59
- Long HA, French DP, Brooks JM. Optimising the value of the Critical Appraisal Skills Programme (CASP) tool for quality appraisal in qualitative evidence synthesis. *Res Methods Med Health Sci*. 2020;1(1):31–42. doi:10.1177/2632084320947559
- Nadelson S, Nadelson LS. Evidence-based practice article reviews using CASP tools: A method for teaching EBP. *Worldviews Evid Based Nurs*. 2014;11(5):344–346. doi:10.1111/wvn.12059
- Chenail R. Learning to appraise the quality of qualitative research articles: A contextualized learning object for constructing knowledge. *Qual Rep*. 2014;16(1):236–248. doi:10.46743/2160-3715/2011.1049
- Moher D, Hopewell S, Schulz KF, et al. CONSORT 2010 explanation and elaboration: Updated guidelines for reporting parallel group randomised trials. *BMJ*. 2010;340:c869. doi:10.1136/bmj.c869
- Falci SGM, Marques LS. CONSORT: When and how to use it. *Dental Press J Orthod*. 2015;20(3):13–15. doi:10.1590/2176-9451.20.3.013-015.ebo
- Pandis N, Chung B, Scherer RW, Elbourne D, Altman DG. CONSORT 2010 statement: Extension checklist for reporting within person randomised trials. *BMJ*. 2017;357:j2835. doi:10.1136/bmj.j2835
- Schulz KF. CONSORT 2010 statement: Updated guidelines for reporting parallel group randomized trials. *Ann Intern Med*. 2010;152(11):726. doi:10.7326/0003-4819-152-11-201006010-00232
- Blanco D, Biggane AM, Cobo E; MiRoR network. Are CONSORT checklists submitted by authors adequately reflecting what information is actually reported in published papers? *Trials*. 2018;19(1):80. doi:10.1186/s13063-018-2475-0
- Turner L, Shamsseer L, Altman DG, Schulz KF, Moher D. Does use of the CONSORT statement impact the completeness of reporting of randomised controlled trials published in medical journals? A Cochrane review. *Syst Rev*. 2012;1(1):60. doi:10.1186/2046-4053-1-60
- Ming T, Li X, Zhou Q, Moher D, Ling C, Yu W. From QUOROM to PRISMA: A survey of high-impact medical journals' instructions to authors and a review of systematic reviews in anesthesia literature. *PLoS One*. 2011;6(11):e27611. doi:10.1371/journal.pone.0027611

29. Moher D, Liberati A, Tetzlaff J, Altman DG; The PRISMA Group. Preferred Reporting Items for Systematic Reviews and Meta-Analyses: The PRISMA statement. *PLoS Med.* 2009;6(7):e1000097. doi:10.1371/journal.pmed.1000097
30. Page MJ, McKenzie JE, Bossuyt PM, et al. The PRISMA 2020 statement: An updated guideline for reporting systematic reviews. *PLoS Med.* 2021;18(3):e1003583. doi:10.1371/journal.pmed.1003583
31. Liberati A, Altman DG, Tetzlaff J, et al. The PRISMA statement for reporting systematic reviews and meta-analyses of studies that evaluate healthcare interventions: Explanation and elaboration. *BMJ.* 2009;339:b2700. doi:10.1136/bmj.b2700
32. Sarkis-Onofre R, Catalá-López F, Aromataris E, Lockwood C. How to properly use the PRISMA statement. *Syst Rev.* 2021;10(1):117. doi:10.1186/s13643-021-01671-z
33. Ogrinc G, Davies L, Goodman D, Batalden P, Davidoff F, Stevens D. SQUIRE 2.0 (Standards for QUality Improvement Reporting Excellence): Revised publication guidelines from a detailed consensus process. *BMJ Qual Saf.* 2016;25(12):986–992. doi:10.1136/bmjqs-2015-004411
34. Ogrinc G, Mooney SE, Estrada C, et al. The SQUIRE (Standards for QUality Improvement Reporting Excellence) guidelines for quality improvement reporting: Explanation and elaboration. *Qual Saf Health Care.* 2008;17(Suppl 1):i13–i32. doi:10.1136/qshc.2008.029058
35. McQuillan RF, Wong BM. The SQUIRE Guidelines: A scholarly approach to quality improvement. *J Grad Med Educ.* 2016;8(5):771–772. doi:10.4300/JGME-D-16-00558.1
36. Goodman D, Ogrinc G, Davies L, et al. Explanation and elaboration of the SQUIRE (Standards for Quality Improvement Reporting Excellence) Guidelines, V.2.0: Examples of SQUIRE elements in the healthcare improvement literature. *BMJ Qual Saf.* 2016;25(12):e7. doi:10.1136/bmjqs-2015-004480
37. Richards D. The STARD initiative. *Evid Based Dent.* 2003;4(2):21–22. doi:10.1038/sj.ebd.6400183
38. Bossuyt PM, Reitsma JB, Bruns DE, et al. STARD 2015: An updated list of essential items for reporting diagnostic accuracy studies. *BMJ.* 2015;351:h5527. doi:10.1136/bmj.h5527
39. Cohen JF, Korevaar DA, Altman DG, et al. STARD 2015 guidelines for reporting diagnostic accuracy studies: Explanation and elaboration. *BMJ Open.* 2016;6(11):e012799. doi:10.1136/bmjopen-2016-012799
40. Cohen JF, Korevaar DA, Gatsonis CA, et al. STARD for Abstracts: Essential items for reporting diagnostic accuracy studies in journal or conference abstracts. *BMJ.* 2017;358:j3751. doi:10.1136/bmj.j3751
41. Stahl AC, Tietz AS, Kendziora B, Dewey M. Has the STARD statement improved the quality of reporting of diagnostic accuracy studies published in European Radiology? [published online as ahead of print on July 30, 2022]. *Eur Radiol.* 2022. doi:10.1007/s00330-022-09008-7
42. McShane LM, Altman DG, Sauerbrei W, Taube SE, Gion M, Clark GM. Reporting Recommendations for Tumor Marker Prognostic Studies (REMARK). *J Natl Cancer Inst.* 2005;97(16):1180–1184. doi:10.1093/jnci/dji237
43. Altman DG, McShane LM, Sauerbrei W, Taube SE. Reporting Recommendations for Tumor Marker Prognostic Studies (REMARK): Explanation and elaboration. *PLoS Med.* 2012;9(5):e1001216. doi:10.1371/journal.pmed.1001216
44. Sauerbrei W, Taube SE, McShane LM, Cavenagh MM, Altman DG. Reporting Recommendations for Tumor Marker Prognostic Studies (REMARK): An abridged explanation and elaboration. *J Natl Cancer Inst.* 2018;110(8):803–811. doi:10.1093/jnci/djy088
45. Mallett S, Timmer A, Sauerbrei W, Altman DG. Reporting of prognostic studies of tumour markers: A review of published articles in relation to REMARK guidelines. *Br J Cancer.* 2010;102(1):173–180. doi:10.1038/sj.bjc.6605462
46. Yu M, Bian Y, Wang L, Chen F. Low-intensity pulsed ultrasound enhances angiogenesis in rabbit capsule tissue that acts as a novel vascular bed in vivo. *Adv Clin Exp Med.* 2021;30(6):581–589. doi:10.17219/acem/134115
47. Tosun M, Olmez H, Unver E, et al. Oxidative and pro-inflammatory lung injury induced by desflurane inhalation in rats and the protective effect of rutin. *Adv Clin Exp Med.* 2021;30(9):941–948. doi:10.17219/acem/136194
48. Gündüz Z, Aktas F, Vatansev H, Solmaz M, Erdogan E. Effects of amantadine and topiramate on neuronal damage in rats with experimental cerebral ischemia-reperfusion. *Adv Clin Exp Med.* 2021;30(10):1013–1023. doi:10.17219/acem/138327
49. Wang Y, Wang Y, Ren C, Wang H, Zhang Y, Xiu Y. Upregulation of centromere protein K is crucial for lung adenocarcinoma cell viability and invasion. *Adv Clin Exp Med.* 2021;30(7):691–699. doi:10.17219/acem/133820
50. İçduygu F, Samli H, Ozgoz A, Vatansever B, Hekimler Ozturk K, Akgun E. Possibility of paclitaxel to induce the stemness-related characteristics of prostate cancer cells. *Adv Clin Exp Med.* 2021;30(12):1283–1291. doi:10.17219/acem/140590
51. Wang W, Xiao C, Chen H, Li F, Xia D. Radiation induces submandibular gland damage by affecting Cdkn1a expression and regulating expression of miR-486a-3p in a xerostomia mouse model. *Adv Clin Exp Med.* 2021;30(9):933–939. doi:10.17219/acem/136457
52. Tong L, Cheng J, Zuo H, Li J. MicroRNA-197 promotes proliferation and inhibits apoptosis of gallbladder cancer cells by targeting insulin-like growth factor-binding protein 3. *Adv Clin Exp Med.* 2021;30(7):661–672. doi:10.17219/acem/134833
53. Kara H, Çağlar C, Asiltürk M, Karahan S, Uğurlu M. Comparison of a manual walking platform and the CatWalk gait analysis system in a rat osteoarthritis model. *Adv Clin Exp Med.* 2021;30(9):949–956. doi:10.17219/acem/137536
54. Ada F, Kasimzade F, Mendil A, Gocmez H. Effects of nano-sized titanium dioxide powder and ultraviolet light on superficial veins in a rabbit model. *Adv Clin Exp Med.* 2021;30(12):1255–1262. doi:10.17219/acem/141501
55. Rachwalik M, Hurkacz M, Sienkiewicz-Oleszkiewicz B, Jasiński M. Role of resistin in cardiovascular diseases: Implications for prevention and treatment. *Adv Clin Exp Med.* 2021;30(8):865–874. doi:10.17219/acem/135978
56. Liu J, Chen Y, Li S, Zhao Z, Wu Z. Machine learning in orthodontics: Challenges and perspectives. *Adv Clin Exp Med.* 2021;30(10):1065–1074. doi:10.17219/acem/138702
57. Rakoczy K, Szlasa W, Saczko J, Kulbacka J. Therapeutic role of vanillin receptors in cancer. *Adv Clin Exp Med.* 2021;30(12):1293–1301. doi:10.17219/acem/139398
58. Annus Á, Tömösi F, Rárosi F, et al. Kynurenic acid and kynurenine aminotransferase are potential biomarkers of early neurological improvement after thrombolytic therapy: A pilot study. *Adv Clin Exp Med.* 2021;30(12):1225–1232. doi:10.17219/acem/141646
59. Charong N, Kooltheat N, Plyduang T. High-sensitivity detection of clinically significant red blood cell antibodies by the column agglutination technique. *Adv Clin Exp Med.* 2021;30(11):1205–1214. doi:10.17219/acem/140317
60. Kolasa J, Frączek-Jucha M, Grabowski M, et al. A quasi-experimental study examining a nurse-led educational program to improve disease knowledge and self-care for patients with acute decompensated heart failure with reduced ejection fraction. *Adv Clin Exp Med.* 2021;31(3):267–275. doi:10.17219/acem/143989
61. Fang Y, Liu J, Long Y, Wen J, Huang D, Xin L. Knockdown of circular RNA hsa_circ_0003307 inhibits synovial inflammation in ankylosing spondylitis by regulating the PI3K/AKT pathway. *Adv Clin Exp Med.* 2022;31(7):781–788. doi:10.17219/acem/146830
62. Yang JW, Chu M, Qi Y, et al. Correlation between age and curative effects of selective dorsal neurectomy for primary premature ejaculation. *Adv Clin Exp Med.* 2022;31(8):837–845. doi:10.17219/acem/147426
63. Dominiak S, Karuga-Kuźniewska E, Popecki P, Kubasiewicz-Ross P. PRF versus xenograft in sinus augmentation in case of HA-coating implant placement: A 36-months retrospective study. *Adv Clin Exp Med.* 2021;30(6):633–640. doi:10.17219/acem/134202
64. Floer M, Clausen M, Meister T, Vollenberg R, Bettenworth D, Tepasse PR. Soluble syndecan-1 as marker of intestinal inflammation: A preliminary study and evaluation of a new panel of biomarkers for non-invasive prediction of active ulcerative colitis. *Adv Clin Exp Med.* 2021;30(7):655–660. doi:10.17219/acem/139040
65. Rams A, Koszałka-Węgiel J, Kuszmiersz P, et al. Characteristics of idiopathic inflammatory myopathies with novel myositis-specific autoantibodies. *Adv Clin Exp Med.* 2021;30(12):1239–1248. doi:10.17219/acem/141181

Significance of detecting the levels of miR-29a, survivin and interferon gamma release assay in patients with lung cancer and tuberculosis

Lijuan Sun^{A,B,D-F}, Hongyun Li^{A,B,D-F}, Qun Fu^{B-D,F}, Shuangmin Hu^{B-D,F}, Wenfei Zhao^{C,D,F}

Department of Respiratory and Critical Care, The Fifth Affiliated Hospital of Zhengzhou University, China

A – research concept and design; B – collection and/or assembly of data; C – data analysis and interpretation; D – writing the article; E – critical revision of the article; F – final approval of the article

Advances in Clinical and Experimental Medicine, ISSN 1899–5276 (print), ISSN 2451–2680 (online)

Adv Clin Exp Med. 2022;31(10):1073–1080

Address for correspondence

Lijuan Sun
E-mail: sunlijuan_2020@126.com

Funding sources

None declared

Conflict of interest

None declared

Received on November 2, 2021

Reviewed on December 6, 2021

Accepted on May 20, 2022

Published online on September 12, 2022

Abstract

Background. When lung cancer is combined with concurrent tuberculosis (TB), it increases the difficulty of diagnosis and treatment, leading to missed and/or misdiagnosed cases.

Objectives. To provide reference markers for the clinical diagnosis of patients with lung cancer complicated by active pulmonary TB (APT).

Materials and methods. The concentration of survivin in diseased tissue, and miR-29a and IGRAs interferon gamma (IFN- γ) in serum were evaluated in 25 patients with non-small cell lung carcinoma (NSCLC) complicated by APT, 32 patients with NSCLC and 30 patients with APT.

Results. The expression of miR-29a in serum of patients with APT was higher than in patients with NSCLC complicated by APT (least significant difference (LSD)- $t = 4.724$, $p < 0.001$), and the NSCLC group (LSD- $t = 6.619$, $p < 0.001$). Furthermore, patients with NSCLC complicated by APT had higher miR-29a concentration than the NSCLC group. The rate of positive survivin expression in NSCLC ($\chi^2 = 23.418$, $p < 0.001$) and NSCLC combined with APT group ($\chi^2 = 17.160$, $p < 0.001$) was significantly higher than in patients with APT. The concentration of IFN- γ in serum of the NSCLC complicated by APT group (LSD- $t = 2.912$, $p = 0.004$) and the APT group (LSD- $t = 4.452$, $p < 0.001$) was higher than in the NSCLC group. The level of IFN- γ in serum of the NSCLC complicated by APT group were higher than in the APT group, but there was no statistical difference.

Conclusions. The levels of MiR-29a, Survivin and IFN- γ was helpful for differential diagnosis of lung cancer and tuberculosis.

Key words: NSCLC, miR-29a, survivin, APT, IGRAs

Cite as

Sun L, Li H, Fu Q, Hu S, Zhao W. Significance of detecting the levels of miR-29a, survivin and interferon gamma release assay in patients with lung cancer and tuberculosis.

Adv Clin Exp Med. 2022;31(10):1073–1080.

doi:10.17219/acem/150306

DOI

10.17219/acem/150306

Copyright

Copyright by Author(s)

This is an article distributed under the terms of the Creative Commons Attribution 3.0 Unported (CC BY 3.0)

(<https://creativecommons.org/licenses/by/3.0/>)

Background

Lung cancer is a very common malignant tumor, posing a significant threat to human health and life. Its morbidity and mortality are increasing year by year. Tuberculosis (TB) is endemic in China, causing a great economic burden. Improving TB diagnosis and treatment has become an urgent public health issue.¹ The incidence rate of TB in China is 58/100,000, while the incidence of lung cancer in these patients is 10.9 times that of patients without TB (26.3 compared to 2.41 per 10,000 person-years).² Therefore, the incidence of both lung cancer and TB in China is relatively high. When lung cancer is combined with concurrent TB infection, it increases the difficulty of diagnosis and treatment, and leads to missed or misdiagnosed cases of both diseases. In such situations, bronchoscopy, computed tomography (CT) and transthoracic lung biopsy should be performed. If diagnosis is unclear after all diagnostic tests are performed, a biopsy is necessary. When lung imaging indicates space-occupying or exudative changes, the probability of lung cancer diagnosis complicated with TB is not high. In clinical evaluations, it is essential to be vigilant. When some biomarkers are abnormal, it is often necessary to perform lesion biopsy or lesion resection once again to confirm the diagnosis.

MicroRNAs (miRNAs/miRs) are small RNA molecules that can be stably expressed in body fluids such as serum, plasma or saliva, and can be detected with high sensitivity. MicroRNAs are also stably expressed in exosomes and can be transmitted through this mechanism. Studies have found that miRNAs can affect a variety of biological processes, such as DNA damage repair, cell cycle arrest, cell hypoxia, proliferation and apoptosis, etc. This enables miRNAs to act as a biological factor predicting non-small cell lung cancer (NSCLC) in patients.⁴ Some scholars have found that after *Mycobacterium tuberculosis* spp. invades macrophages, miRNAs participate in the anti-TB infection process of the body.⁵ In a study by Das et al.,⁶ after THP-1 macrophages were infected with H37Rv and H37Ra, the expression of miR-29a in THP-1 cells increased.

Survivin is a new member of the inhibitor of apoptosis (IAP) family and it is the strongest IAP found so far. It has complex functions and can inhibit cell apoptosis, promote cell transformation, participate in cell mitosis and angiogenesis, and cause tumor cells to develop drug resistance.^{7,8} The *survivin* gene is 15 kb in length, located at 17q25, and has 4 exons and 3 introns. Its coding product consists of 142 amino acids and has a molecular weight of 16.2 kD. Other members of the IAP family generally contain baculovirus IAP repeat (BIR) molecules composed of 2–3 tandem cysteine/histidine consensus sequences of 70 amino acids, and terminal hydroxyl RING finger structure, in which the BIR molecule exerts an anti-apoptotic effect. However, survivin contains only a single BIR functional region, while the terminal hydroxyl does not

contain a ring finger structure, but an interwoven spiral structure, in contrast to other IAP family members.

Interferon gamma (IFN- γ) release assays (IGRAs) are used as an auxiliary diagnostic test for TB infection. They evaluate the ability of T cells to release IFN- γ upon stimulation with TB-specific antigens.⁹ Latent TB infection is very common in adults. Recently, IGRAs have been utilized clinically to diagnose active adult TB.^{10–12}

Objectives

Survivin is tumor-specific, being expressed only in tumor and embryonic tissues, while miR-29a and IFN- γ are mostly used in the differential diagnosis of TB. The aim of this study was to establish the clinical diagnosis value of miR-29a, survivin and IFN- γ in patients with NSCLC combined with active pulmonary TB (APT).

Materials and methods

Research objects

Patients with NSCLC combined with APT (n = 25), those with NSCLC (n = 32) and patients with APT diagnosed from March 2017 to September 2019 (n = 30) in our center were selected to participate in this prospective study. The diagnosis of NSCLC was confirmed by lung biopsy, bronchoscopy, surgical pathological tissue, lymph node biopsy, and imaging examination. The TNM staging standards refer to the National Comprehensive Cancer Network (NCCN) NSCLC Clinical Practice Guidelines.¹³ The diagnosis of APT conforms to the 2018 version of the diagnostic criteria issued by National Health and Family Planning Commission of the People's Republic of China for TB.¹⁴ The detailed diagnostic process was shown in Fig. 1. We performed the lung biopsy only for TB patients with difficult diagnoses, and included them in the study. Immunohistochemistry was used to diagnose and classify lung disease markers including TTF-1, Napsin A, CK7, p63/p40, CK5/6, DSG3, CgA, Syn, CD56, Ki67, and Bacillus Calmette-Guerin (BCG). Patients diagnosed with NSCLC combined with APT may be diagnosed with both diseases at the same time, or one of them may be diagnosed successively. Among patients with NSCLC combined with APT, in 3 cases NSCLC and APT were diagnosed at the same time, 9 cases were diagnosed as APT before the diagnosis of NSCLC, and 13 cases were diagnosed as NSCLC before the diagnosis of APT. Exclusion criteria included retreated TB, a history of a malignant tumor, a history of anti-TB or tumor treatment before enrollment, or other obvious complications, such as infection. Every patient signed an informed consent form before participating in the study. The study was conducted

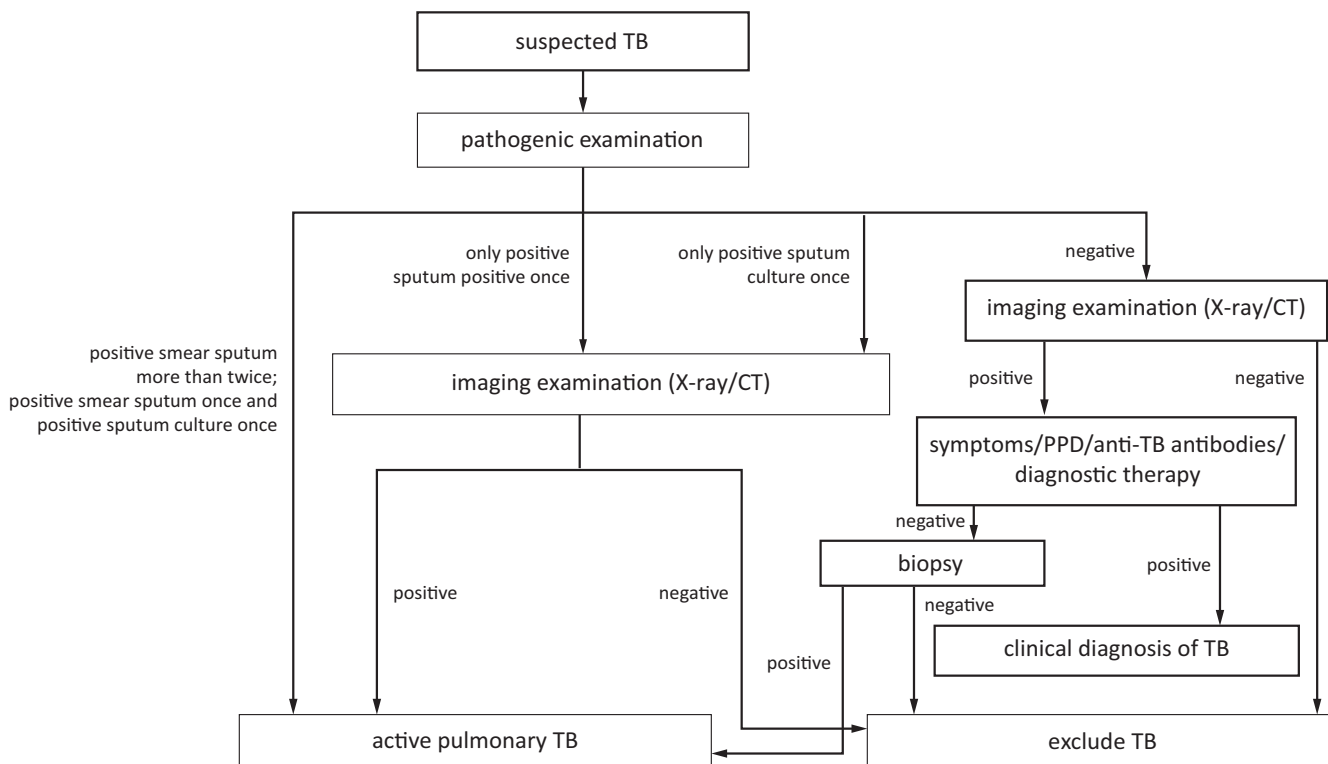


Fig. 1. Flowchart of active tuberculosis (TB) diagnosis
 CT – computed tomography; PPD – purified protein derivative.

in accordance with the Declaration of Helsinki and approved by the Ethics Committee of The Fifth Affiliated Hospital of Zhengzhou University, Zhengzhou, China (approval No. 2017003).

Detection method

Survivin detection method

We used immunohistochemistry to detect survivin protein expression. After the tissue wax section was dewaxed, debenzened and hydrated with gradient ethanol, the endogenous peroxidase activity was blocked using 3% hydrogen peroxide, with the antigen being repaired by high pressure and high temperature. After washing with phosphate-buffered saline (PBS) and blocking with normal goat serum (supplied in the kit) for 10 min, the survivin antibody (cat. No. ZN2428; 1:2000 dilution; Beijing Baiaolaibo Technology Co., Ltd., Beijing, China) was added and incubated at 4°C for 12 h. Next, the slides were washed and the biotin-labeled secondary antibody was added dropwise with labeled streptavidin and incubated overnight at 4°C. Slides were washed following incubation, and then the secondary antibody and horseradish enzyme-labeled streptavidin (Beijing Baiaolaibo Technology Co., Ltd.) were added dropwise and incubated overnight at 4°C. Samples were then washed with PBS and 3,3'-diaminobenzidine (DAB) (Beijing Baiaolaibo Technology Co., Ltd.) added dropwise, and incubated at room temperature for 5 min

to develop color. Then, the samples were washed with water, counterstained with hematoxylin (Beijing Baiaolaibo Technology Co., Ltd.), dehydrated and dried, and finally coverslipped for observation under a microscope (model CX31-LV320; Olympus Corp., Tokyo, Japan). Survivin protein expression was identified according to the following criteria: 5 high-power fields were randomly selected for each slice and scored according to the percentage of positive cells. The percentage of positive cells >75% was counted as 4 points, ≥50–75% as 3 points, ≥25–50% as 2 points, ≥5–25% as 1 point, and <5% scored 0 points. According to the intensity of color development, brown meant 3 points, brown yellow 2 points, light yellow 1 point, and no color 0 points. The score was calculated by multiplying the 2 items, and it was segregated from high to low. A score of 9 or more meant high expression, 5–8 medium expression, 2–4 low expression, and 0–1 negative expression. In this study, high, medium and low results were defined as positive expressions (representative images of immunohistochemical staining are shown in Fig. 2).

Detection method of miR-29a

Quantitative reverse transcription polymerase chain reaction (qRT-PCR) was used to detect the levels of miR-29a in peripheral blood. Fasting venous blood was collected, centrifuged at 2000 rpm/min for 20 min at 4°C, and the supernatant was collected into a centrifuge tube and stored at –80°C for testing. The TRIzol (Thermo Fisher Scientific, Waltham,

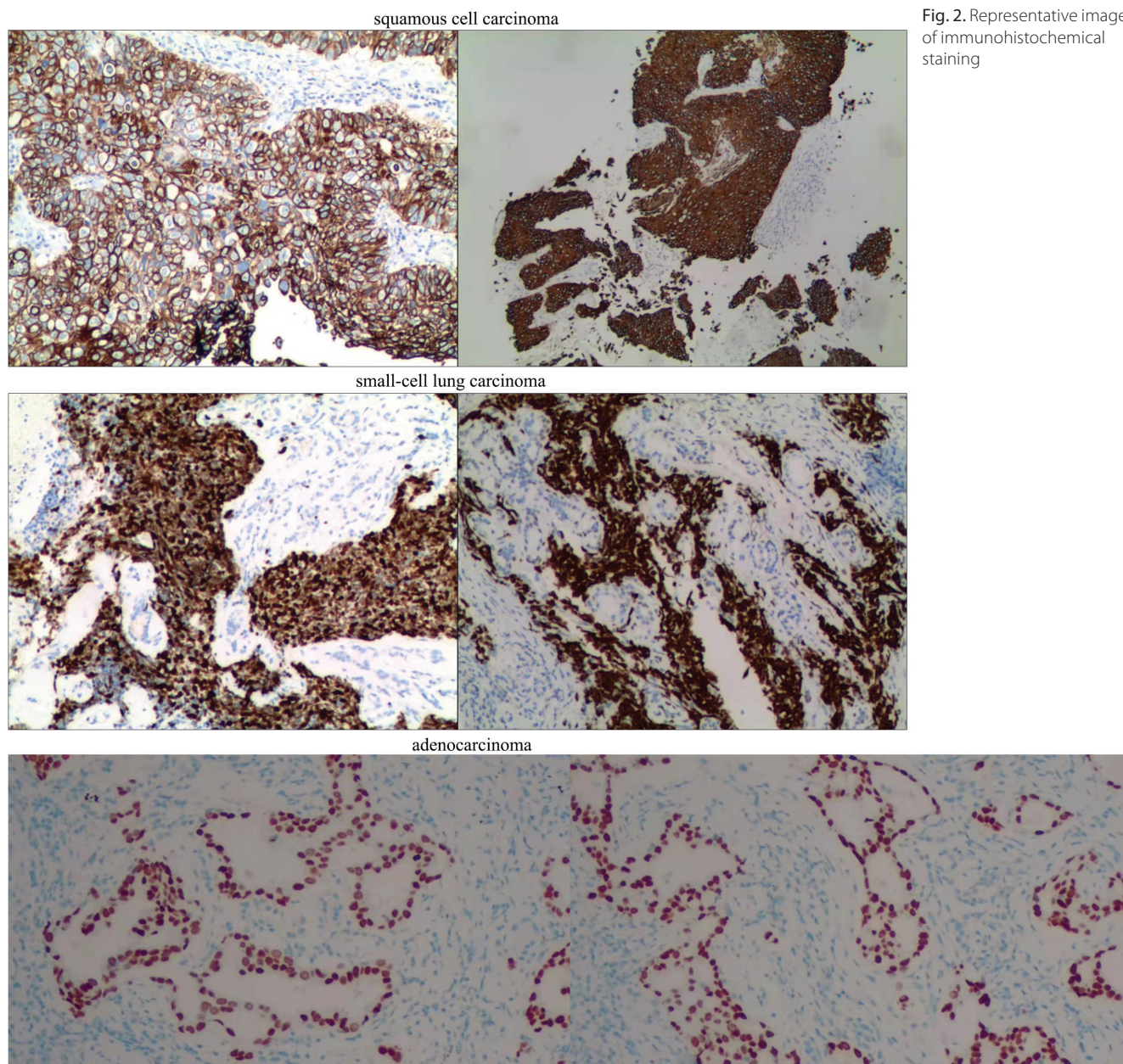


Fig. 2. Representative images of immunohistochemical staining

USA) was used to extract total RNA from the collected cellular material, and after detection of nucleic acid concentration, reverse transcription of miRNA was performed to generate cDNA. Using cDNA as a template and U6 as an internal reference gene, SYBR Premix EX Taq™ II (TaKaRa Bio Inc., Kusatsu, Japan) was used to detect the expression of miR-29a, using the following primer sequences: upstream primer: 5'-GGGTAGCACCATCTGAAA-3', downstream primer: 5'-CAGTGC GTGTCCTGGAGT-3', U6 primer: 5'-GACTTATGTTAGGAGACGA-3'. The reaction system consisted of 20 μ L, including cDNA (2 μ L), miR-29a primer (1 μ L), SYBR Premix EX Taq™ II (10 μ L), and double distilled water (ddH₂O) (7 μ L). A total of 40 cycles were performed, and the relative expression of miR-29a was calculated using the $2^{-\Delta\Delta C_t}$ method. The experiment was repeated 3 times to ensure validity.

IFN- γ detection method

Peripheral venous blood was collected, divided (1 mL per tube) into N (negative control), T (test culture) and P (positive control) tubes, and mixed gently for 2 h. Tubes were incubated at 37°C for 24 h, then centrifuged at 3000 rpm for 10 min, and the upper layer of plasma was used for testing. A human IFN- γ enzyme-linked immunosorbent assay (ELISA) kit (cat. No. 1605023) was purchased from Shanghai Jianglai Biotech Co., Ltd. (Shanghai, China) and the absorbance (A) was measured using a microplate reader at 450 nm. A standard curve was prepared according to the calibrator to calculate the IFN- γ level. When the value of IFN- γ is 0–14 pg/mL, it indicates a negative result. If it exceeds 14.0 pg/mL, it indicates a positive result, and the patient may have TB infection.¹⁵ A positive test result (IFN- γ (+)) was interpreted

as latent *M. tuberculosis* spp. infection, whereas a negative IGRA (IFN- γ (-)) result meant no infection with *M.tb*.

Statistical analyses

All data were analyzed using IBM SPSS v. 20.0 software (IBM Corp., Armonk, USA). The Shapiro–Wilk test was used to test normality and the Levene's test was used to test homogeneity of variance. The measurement data were expressed as mean \pm standard deviation (M \pm SD). The comparison between groups was performed using t-test or one-way analysis of variance (ANOVA) followed by least significant difference (LSD) test. The count data were expressed as a percentage, and the comparison between groups was performed using Fisher's exact test or χ^2 test. The value of $p < 0.05$ indicated a statistically significant difference.

Results

General information

The average age in the NSCLC group was 52.92 \pm 4.63 years. Among 15 cases of lung squamous cell carcinoma, 14 cases were p63+, 10 cases were syn+ and 15 cases were CK 5/6+. Among 17 cases of lung adenocarcinoma, 16 cases were TTF-1+, 13 cases were Napsin A and 17 cases were CK 7+. The TNM stage ranged between I and IV. In the APT group, the average age was 50.62 \pm 4.88 years. The NSCLC combined with APT group had an average age of 55.06 \pm 5.17 years. Of these patients, 13 cases were diagnosed as lung squamous cell carcinoma, and 12 cases were diagnosed as lung adenocarcinoma. The TNM stage ranged between I and IV (Table 1). There was no statistically significant difference in gender or age of the 3 groups.

Table 1. Clinical and demographic characteristics of enrolled patients

Variable	NSCLC	APT	NSCLC+APT
Gender, n (%)			
male	22 (68.75)	21 (70.00)	18 (72.00)
female	10 (21.25)	9 (30.00)	7 (28.00)
Age, range [years]	46–65	42–68	49–71
Cytological typing, n (%)			
Squamous cell carcinoma, n (%)	15 (46.88)	–	13 (52.00)
p63+	14 (93.33)	–	–
syn+	10 (66.67)	–	–
CK 5/6+	15 (100.00)	–	–
Adenocarcinoma, n (%)	17 (53.12)	–	12 (48.00)
TTF-1+	16 (94.12)	–	–
Napsin A	13 (76.47)	–	–
CK 7+	17 (100.00)	–	–
TNM stage, n (%)			
I–IIIa	13 (40.63)	–	12 (48.00)
IIIb–IV	19 (59.37)	–	13 (52.00)

NSCLC – non-small cell lung carcinoma patients; APT – patients with pulmonary tuberculosis; NSCLC+APT – patients with NSCLC combined with APT.

The expression and comparison of survivin, miR-29a and IFN- γ in the 3 groups

Results for survivin, miR-29a and IFN- γ in the 3 groups are shown in Table 2, including normality and homogeneity of variance. The positive rate of survivin in NSCLC (NSCLC compared to APT, 78.12% compared to 16.67%, $\chi^2 = 23.418$, $p < 0.001$) and NSCLC combined with APT group (NSCLC combined with APT compared to APT, 72.00% compared to 16.67%, $\chi^2 = 17.160$, $p < 0.001$) was significantly higher than in the APT group. However, there was no statistical difference between the NSCLC group and the NSCLC combined with APT group (NSCLC compared to NSCLC combined with APT, 78.12% compared to 72%, $\chi^2 = 0.284$, $p = 0.758$). The survivin expression had no significant relationship with the age, sex, pathological type, or clinical stage of NSCLC combined with APT patients (Table 3).

One-way ANOVA followed by the LSD-t-test was used to analyze the differences between 3 groups. The expression of miR-29a in the APT group was significantly higher than in the NSCLC combined with APT group (APT compared to NSCLC combined with APT, 4.43 \pm 1.91 compared to 2.27 \pm 1.98, post hoc LSD-t-test, LSD-t = 4.724, $p < 0.001$) and the NSCLC group (APT compared to NSCLC, 4.43 \pm 1.91 compared to 1.59 \pm 1.53, post hoc LSD-t-test, LSD-t = 6.619, $p < 0.001$). However, there was no statistical difference between the NSCLC combined with APT group and the NSCLC group (NSCLC combined with APT compared to NSCLC, 2.27 \pm 1.98 compared to 1.59 \pm 1.53, post hoc LSD-t-test, LSD-t = 1.509, $p = 0.151$) (Table 2 and Fig. 3A). The expression of miR-29a had no significant relationship with the age, gender and pathological type of NSCLC combined with APT patients, but was related to the clinical stage. Moreover, the difference in TNM stage between the 2 groups was also significant (2.87 \pm 1.65 compared to 1.33 \pm 0.92, t-test, $t = 2.861$, $p = 0.011$) (Table 3).

The concentration of IFN- γ in the APT group (APT compared to NSCLC, 132.43 \pm 122.28 compared to 36.72 \pm 50.66, post hoc LSD-t-test, LSD-t = 4.452, $p < 0.001$) and the NSCLC combined with APT (NSCLC combined with APT compared to NSCLC, 102.48 \pm 60.55 compared to 36.72 \pm 50.66, post hoc LSD-t-test, LSD-t = 2.912, $p = 0.004$) was higher than that in the NSCLC group. Furthermore, the IFN- γ level in the NSCLC combined with APT group was lower than that in the APT group, although there was no statistical difference between them (102.48 \pm 60.55 compared to 132.43 \pm 122.28, post hoc LSD-t-test, LSD-t = 1.307, $p = 0.195$) (Table 2 and Fig. 3B).

Discussion

Survivin is the most powerful inhibitor of apoptosis within the IAP family, and it is only expressed in embryonic and developing fetal tissues. It is not expressed

Table 2. Expression of survivin, miR-29a and IFN- γ in 3 groups of patients

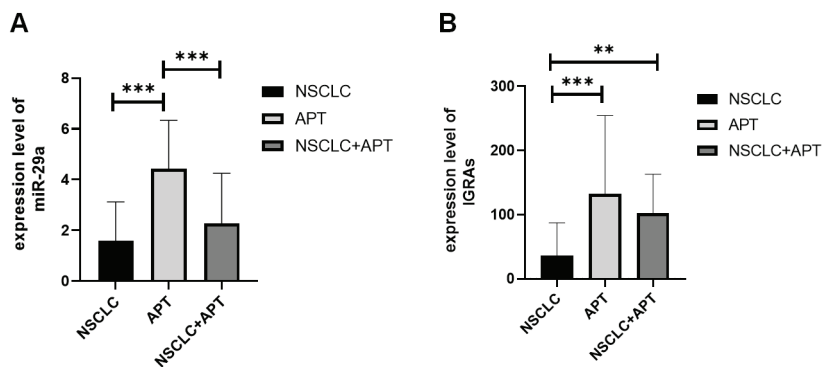
Group	Value	NSCLC (n = 32)	APT (n = 30)	NSCLC+APT (n = 25)
Survivin, n (%)	positive	25 (78.12)	5 (16.67)	18 (72.00)
	negative	7 (21.88)	25 (83.33)	7 (28.00)
	χ^2 *	23.418	17.160	0.284
	p-value	<0.001 ^a	<0.001 ^b	0.758 ^c
miR-29a (M \pm SD)	–	1.59 \pm 1.53	4.43 \pm 1.91	2.27 \pm 1.98
Shapiro–Wilk test	Sig.	0.093	0.114	0.337
Homogeneity of variances test	p-value	0.24		
	t-value**	6.619	4.724	4.724
	p-value	<0.001 ^a	<0.001 ^b	0.151 ^c
IFN- γ (M \pm SD)	–	36.72 \pm 50.66	132.43 \pm 122.28	102.48 \pm 60.55
Shapiro–Wilk test	Sig.	0.236	0.522	0.417
Homogeneity of variances test	p-value	0.09		
	t-value**	4.452	1.307	2.912
	p-value	<0.001 ^a	0.195 ^b	0.004 ^c

IFN- γ – interferon gamma; M – mean; SD – standard deviation; NSCLC – non-small cell lung cancer patients; APT – patients with pulmonary tuberculosis; NSCLC+APT – patients with NSCLC combined with APT; * significance testing performed using χ^2 test; ** significance testing was done using one-way analysis of variance (ANOVA) followed by the least significant difference (LSD) t-test; ^a NSCLC compared to APT; ^b APT compared to NSCLC+APT; ^c NSCLC compared to NSCLC+APT.

Table 3. Expression of survivin and miR-29a in patients with NSCLC+APT

Clinicopathological features	n	Survivin			miR-29a		
		positive	negative	Fisher's exact p-value*	M \pm SD	t-value	p-value**
Age							
≤55 years	10	7	3	0.601	2.29 \pm 1.73	0.570	0.577
>55 years	15	11	4		1.92 \pm 1.39		
Sex				0.607		–0.652	0.532
male	18	12	6		1.92 \pm 1.35		
female	7	5	2		2.45 \pm 1.94		
Cytological typing				0.560		–1.349	0.193
squamous cell carcinoma	13	8	5		1.68 \pm 1.19		
adenocarcinoma	12	8	4		2.50 \pm 1.76		
TNM stages				0.440		2.861	0.011
I–IIa	12	7	5		2.87 \pm 1.65		
IIa–IV	13	9	4		1.33 \pm 0.92		

NSCLC+APT – patients with non-small cell lung carcinoma (NSCLC) combined with APT; * significance testing was performed using Fisher's exact test; ** significance testing was done using t-test; M – mean; SD – standard deviation.

**Fig. 3.** The expression level of indicated genes, miR-29a (A) and interferon gamma (IFN- γ) (B)

IGRAs – interferon gamma release assays; NSCLC – non-small cell lung cancer patients; APT – patients with pulmonary tuberculosis; NSCLC+APT – patients with NSCLC combined with APT.

in most of the normal, mature adult tissues, but has abnormal expression in many tumors.^{16–18} Survivin promotes the occurrence and development of NSCLC by inhibiting the apoptosis of cancer cells, thereby allowing them

to escape from monitoring remain undetected. Tamm et al. detected the expression of survivin in 60 human tumor cell lines, of which the expression was the highest in lung and breast cancer.¹⁹ Our results demonstrated

that survivin was highly expressed in the NSCLC and the NSCLC combined with APT groups, and its expression was significantly higher than the positive rate of benign lung lesions and consistent with related reports.²⁰ In addition, the present study found that positive survivin expression is not related to clinical tumor stage ($p > 0.05$). Interestingly, this result is consistent with those of Zhao and Zheng,²¹ but Niu et al.²² found that the positive rate of survivin was related to TNM staging. The later the TNM staging was performed, the higher the positive rate of survivin. We consider this discrepancy to be due to variation in cases included in each report.

MicroRNAs are a type of non-coding RNAs with 19–22 nucleotides. Because they can directly target a variety of proteins, they have multiple functions. The miR-29a is a part of the small RNA family which, in addition to the 3'untranslated region (3'UTR), can interact with miRNA regulatory elements (MRE) in the non-3'UTR region. For example, there are a total of 14 miR-29a-binding sites in the 3'UTR region and coding region of elastin. It was confirmed using luciferase reporter gene analysis that miR-29a could simultaneously bind to the MRE in the coding region and 3'UTR region to inhibit elastin expression.²³ Studies found that miR-29a could directly inhibit the expression of a variety of collagen molecules, with target genes being mainly extracellular matrix and migration protein.^{24,25} The miR-29a target gene-related proteins participated in multiple signaling pathways, and could inhibit extracellular matrix remodeling by combining with the downstream of the transforming growth factor (TGF- β)/Smad-3 signaling pathway.²⁶ Furthermore, the expression of miR-29a in normal lung tissues gradually increases as the lung matures.²⁷ Moreover, miRNAs participate in the proliferation and apoptosis of various tumors by regulating the expression of oncogenes. The expression of miR-29a was downregulated in NSCLC tissues, which was significantly correlated to tumor staging and metastasis, and had certain value for NSCLC diagnosis and the evaluation of the disease.²⁸ Studies found that miR-29a also played an important role in the body's immune response, and had certain clinical value in the diagnosis of APT. Fu et al. used a microarray-based expression profiling to screen the serum of patients with active TB and found that the expression of miR-29a was significantly upregulated, which was consistent with the upregulation of miR-29a in the sputum of patients with APT.²⁹ Sharbati et al. also confirmed that *M.tb* could upregulate the expression of miR-29a after infecting human macrophages.³⁰

The incidence of TB is relatively high, and infection is most common in the lungs. Tumor patients are susceptible to TB due to low immunity. At this stage, the most commonly used screening method for TB infection in China is the tuberculin skin test (TST), but its specificity is reduced because the pure protein derivative of the antigen is similar to the antigen of the BCG vaccine. When the body's immune function declines, the sensitivity

of TST diagnosis also decreases,³¹ and it is prone to cross-reaction and false positive results.^{32,33} The bacteriological examination is a common method for diagnosing active TB, but it takes a long time to culture tubercle bacillus. Therefore, finding a fast and accurate detection method is particularly important for the prevention and diagnosis of TB. Interferon gamma is a specific cytokine released by T lymphocytes sensitized by TB. In recent years, IGRAs have become a new type of immunological diagnosis method, which is gradually applied in the clinical diagnosis of TB.³⁴ After an individual is infected with *M.tb*, 2 specific antigens, namely CFP-10 and ESAT-6, can be produced. These antigens stimulate T lymphocytes to produce IFN- γ . Therefore, by detecting the level of IFN- γ in the peripheral blood of patients, it is possible to determine whether there is *M.tb* infection, and to distinguish true TB infection, eliminating the interference of vaccination and nontuberculous infection.³⁵ Research by Huang and Chen found that malignant tumors and purulent infections can also cause IFN- γ to increase.³⁶ Furthermore, other results have confirmed that IGRAs show high sensitivity and specificity in diagnosis, and is more useful than TST in auxiliary diagnosis of APT.³⁷

In clinical practice, doctors need to treat patients with high suspicion of tumor or TB with caution during diagnosis and treatment; the possibility of lung cancer complicated with TB should be fully considered. A correct diagnosis in patients with the coexistence of TB and lung cancer is difficult. In such cases, bronchoscopy, CT and transthoracic lung biopsy should be performed. If diagnosis is unclear after these diagnostic tests, surgery becomes necessary. The 3 biomarkers (survivin, IFN- γ and miR-29) proposed in this study can provide other avenues for differential diagnoses. However, we should be vigilant to patients with APT complicated by lung cancer, especially those with low serum expression of miR-29a, and high expression of survivin in diseased tissues who have been pathologically diagnosed with APT. According to the clinical situation, a reasonable diagnosis and treatment plan can be developed to avoid missed or misdiagnosed cases, which is of great significance for patients with lung cancer complicated with TB.

Limitations

The present study has several limitations. First, although abovementioned biomarkers (survivin, IFN- γ and miR-29) could be seen to help diagnose lung cancer in patients with TB, we did not take cost into account. Second, this study did not include the prognostic information of each group, and the significance of those biomarkers for the prognosis of lung cancer combined with TB could not be evaluated. However, it will be evaluated in future studies. Finally, this study is limited to the conditions of local population, and the discussed issue requires larger, multi-center, multi-field future studies.

Conclusions

In the present study, our results demonstrated that detecting the levels of miR-29a, survivin and IFN- γ was helpful for differential diagnosis of lung cancer and TB.

ORCID iDs

Lijuan Sun  <https://orcid.org/0000-0002-4105-1678>
 Hongyun Li  <https://orcid.org/0000-0001-8205-1036>
 Qun Fu  <https://orcid.org/0000-0002-4819-0697>
 Shuangmin Hu  <https://orcid.org/0000-0001-5679-7934>
 Wenfei Zhao  <https://orcid.org/0000-0002-2494-4925>

References

- Yu YH, Liao CC, Hsu WH, et al. Increased lung cancer risk among patients with pulmonary tuberculosis: A population cohort study. *J Thorac Oncol*. 2011;6(1):32–37. doi:10.1097/JTO.0b013e3181fb4fcc
- Wallis RS, Kim P, Cole S, et al. Tuberculosis biomarkers discovery: Developments, needs, and challenges. *Lancet Infect Dis*. 2013;13(4):362–372. doi:10.1016/S1473-3099(13)70034-3
- Tomasetti M, Lee W, Santarelli L, Neuzil J. Exosome-derived microRNAs in cancer metabolism: Possible implications in cancer diagnostics and therapy. *Exp Mol Med*. 2017;49(1):e285–e285. doi:10.1038/emmm.2016.153
- Chen X, Xu Y, Liao X, et al. Plasma miRNAs in predicting radiosensitivity in non-small cell lung cancer. *Tumor Biol*. 2016;37(9):11927–11936. doi:10.1007/s13277-016-5052-8
- Bao M, Fu YR, Yi ZJ. Research progress of microRNA in anti-tuberculosis immunity and tuberculosis diagnosis [in Chinese]. *Zhonghua Jie He He Hu Xi Za Zhi*. 2015;38(12):918–921.
- Das K, Saikolappan S, Dhandayuthapani S. Differential expression of miRNAs by macrophages infected with virulent and avirulent *Mycobacterium tuberculosis*. *Tuberculosis*. 2013;93:S47–S50. doi:10.1016/S1472-9792(13)70010-6
- Münscher A, Prochnow S, Gulati A, et al. Survivin expression in head and neck squamous cell carcinomas is frequent and correlates with clinical parameters and treatment outcomes. *Clin Oral Invest*. 2019;23(1):361–367. doi:10.1007/s00784-018-2444-8
- Zhang S, Xiao JY, Xie CN, Liu Y, Wang CL, Tian YQ. Effect of survivin gene silencing on malignant phenotype of nasopharyngeal carcinoma cell line CNE-2 [in Chinese]. *Ji Nan Da Xue Xue Bao*. 2011;32(6):607–610.
- Pai M, Dheda K, Cunningham J, Scano F, O'Brien R. T-cell assays for the diagnosis of latent tuberculosis infection: Moving the research agenda forward. *Lancet Infect Dis*. 2007;7(6):428–438. doi:10.1016/S1473-3099(07)70086-5
- Jiang W, Shao L, Zhang Y, et al. High-sensitive and rapid detection of *Mycobacterium tuberculosis* infection by IFN- γ release assay among HIV-infected individuals in BCG-vaccinated area. *BMC Immunol*. 2009;10(1):31. doi:10.1186/1471-2172-10-31
- Goletti D, Raja A, Ahamed Kabeer BS, et al. IFN- γ , but not IP-10, MCP-2 or IL-2 response to RD1 selected peptides associates to active tuberculosis. *J Infect*. 2010;61(2):133–143. doi:10.1016/j.jinf.2010.05.002
- Abdel-Samea SA, Ismail YM, Fayed SMA, Mohammad AA. Comparative study between using QuantiFERON and tuberculin skin test in diagnosis of *Mycobacterium tuberculosis* infection. *Egypt J Chest Dis Tuberc*. 2013;62(1):137–143. doi:10.1016/j.ejcd.2013.02.003
- Ettinger DS, Wood DE, Akerley W, et al; National Comprehensive Cancer Network. Non-small cell lung cancer, version 6.2015. *J Natl Compr Canc Netw*. 2015;13(5):515–524. doi:10.6004/jnccn.2015.0071
- National Health and Family Planning Commission of the People's Republic of China. Diagnostic criteria for tuberculosis (WS 288-2017) [in Chinese]. *Electron J Emerg Infect Dis*. 2018;3(1):59–61.
- Tao YH, Yang XL, Jin FX, Lv QQ, Dong HQ. Application of T lymphocyte interferon gamma release test in the diagnosis of tuberculosis [in Chinese]. *Zhong Hua Yi Yuan Gan Ran Xue Za Zhi*. 2017;27(18):4081–4084.
- Altieri DC. Survivin, cancer networks and pathway-directed drug discovery. *Nat Rev Cancer*. 2008;8(1):61–70. doi:10.1038/nrc2293
- Ambrosini G, Adida C, Altieri DC. A novel anti-apoptosis gene, survivin, expressed in cancer and lymphoma. *Nat Med*. 1997;3(8):917–921. doi:10.1038/nm0897-917
- Roshdy N, Mostafa T. Seminal plasma survivin in fertile and infertile males. *J Urol*. 2009;181(3):1269–1272. doi:10.1016/j.juro.2008.10.158
- Tamm I, Wang Y, Sausville E, et al. IAP-family protein survivin inhibits caspase activity and apoptosis induced by Fas (CD95), Bax, caspases, and anticancer drugs. *Cancer Res*. 1998;58(23):5315–5320. PMID:9850056.
- Cao Y, Dilimulati T, Yang HG. Clinical significance of survivin and p53 protein expression in non-small cell lung cancer [in Chinese]. *Chin J Cancer Prev Treat*. 2011;18(10):773–775.
- Zhao SC, Zheng DR. Expression and significance of PPTG, survivin and bFGF mRNA in non-small cell lung cancer [in Chinese]. *J Clin Pulm Med*. 2017;22(3):542–545.
- Niu YQ, Deng LY, Wang YF. Expression and clinicopathological significance of Sox2 and Survivin in non-small cell lung cancer [in Chinese]. *J Diagn Pathol*. 2015;22(10):594–597.
- Liu SJ, Zhang F, Wei W, et al. Expression of miR-29a-3p and miR-365a-3p in peripheral blood of patients with active pulmonary tuberculosis and latent tuberculosis infection [in Chinese]. *Clin Study*. 2013;10(22):36–38.
- Gebeshuber CA, Zatloukal K, Martinez J. miR-29a suppresses tristetraprolin, which is a regulator of epithelial polarity and metastasis. *EMBO Rep*. 2009;10(4):400–405. doi:10.1038/embor.2009.9
- Fort A, Borel C, Migliavacca E, Antonarakis SE, Fish RJ, Neerman-Arbez M. Regulation of fibrinogen production by microRNAs. *Blood*. 2010;116(14):2608–2615. doi:10.1182/blood-2010-02-268011
- Wang Y, Liu J, Chen J, Feng T, Guo Q. MiR-29 mediates TGF β 1-induced extracellular matrix synthesis through activation of Wnt/ β -catenin pathway in human pulmonary fibroblasts. *Technol Health Care*. 2015;23(s1):S119–S125. doi:10.3233/thc-150943
- Cushing L, Kuang PP, Qian J, et al. miR-29 is a major regulator of genes associated with pulmonary fibrosis. *Am J Respir Cell Mol Biol*. 2011;45(2):287–294. doi:10.1165/rcmb.2010-0323OC
- Xiao J, Meng XM, Huang XR, et al. miR-29 inhibits bleomycin-induced pulmonary fibrosis in mice. *Mol Ther*. 2012;20(6):1251–1260. doi:10.1038/mt.2012.36
- Fu Y, Yi Z, Wu X, Li J, Xu F. Circulating microRNAs in patients with active pulmonary tuberculosis. *J Clin Microbiol*. 2011;49(12):4246–4251. doi:10.1128/JCM.05459-11
- Sharbati J, Lewin A, Kutz-Lohroff B, Kamal E, Einspanier R, Sharbati S. Integrated micro-RNA-mRNA-analysis of human monocyte derived macrophages upon *Mycobacterium avium* subsp. *hominissuis* infection. *PLoS ONE*. 2011;6(5):e20258. doi:10.1371/journal.pone.0020258
- Li TX, He Y, Zhou G, et al. The value of whole blood interferon gamma release test in the diagnosis of tuberculosis [in Chinese]. *Chin J Tuberculosis*. 2016;38(8):623–629.
- Huebner RE, Schein MF, Bass JB. The tuberculin skin test. *Clin Infect Dis*. 1993;17(6):968–975. doi:10.1093/clinids/17.6.968
- Black GF, Weir RE, Floyd S, et al. BCG-induced increase in interferon-gamma response to mycobacterial antigens and efficacy of BCG vaccination in Malawi and the UK: Two randomised controlled studies. *Lancet*. 2002;359(9315):1393–1401. doi:10.1016/S0140-6736(02)08353-8
- Wu Y, Li Q, Zhang ZD. The value of interferon gamma release test in the diagnosis of senile pulmonary tuberculosis [in Chinese]. *Chin J Tuberculosis*. 2016;38(2):122–128.
- Zeng Y, Li TS, Song MM, Huang L. The value of interferon gamma release test in the diagnosis of active pulmonary tuberculosis [in Chinese]. *J Clin Lung*. 2017;22(5):777–780.
- Huang X, Chen J. Laboratory diagnosis of tuberculous pleural effusion [in Chinese]. *J Mod Lab Med*. 2014;29(1):97–100.
- Zhang SM, Zhou H, Fu YQ, Shen YH, Zhou JY. The clinical value of γ -interferon release test in the diagnosis of active tuberculosis [in Chinese]. *Chin J Tuberc Resp Dis*. 2014;37:372–373.

Nurse-led cancer palliative care compared to oncologist-led cancer palliative care: A retrospective analysis of Chinese patients suffering from cancer and receiving chemotherapy

Mengtian Xu^{B,E,F}, Li Zhu^{C,E,F}, Jingjuan Yang^{A,D–F}

Department of Infectious Diseases, First Affiliated Hospital of Soochow University, Suzhou, China

A – research concept and design; B – collection and/or assembly of data; C – data analysis and interpretation; D – writing the article; E – critical revision of the article; F – final approval of the article

Advances in Clinical and Experimental Medicine, ISSN 1899–5276 (print), ISSN 2451–2680 (online)

Adv Clin Exp Med. 2022;31(10):1081–1086

Address for correspondence

Jingjuan Yang
E-mail: jingjuan.y1ang@gmail.com

Funding sources

None declared

Conflict of interest

None declared

Acknowledgements

The authors would like to thank the medical and nursing staff of the First Affiliated Hospital of Soochow University, Suzhou, China.

Received on November 22, 2021

Reviewed on February 20, 2022

Accepted on May 9, 2022

Published online on June 6, 2022

Cite as

Xu M, Zhu L, Yang J. Nurse-led cancer palliative care compared to oncologist-led cancer palliative care: A retrospective analysis of Chinese patients suffering from cancer and receiving chemotherapy. *Adv Clin Exp Med.* 2022;31(10):1081–1086. doi:10.17219/acem/149915

DOI

10.17219/acem/149915

Copyright

Copyright by Author(s)

This is an article distributed under the terms of the Creative Commons Attribution 3.0 Unported (CC BY 3.0) (<https://creativecommons.org/licenses/by/3.0/>)

Abstract

Background. Cancer palliative care is recommended by guidelines for patients with early stage of cancer. Unlike the Western countries, in mainland China, cancer patients receive specialist-led cancer palliative care. Nurse-led cancer palliative care (NUC) is not well established yet.

Objectives. To compare the clinical outcome measures, quality of life and symptom distress in patients suffering from cancer who received NUC with the same results in patient who received consulting oncologist-led cancer palliative care (ONC).

Materials and methods. The study was a chart review of a database of patients suffering from cancer. Data regarding clinical outcome measures, quality of life and symptom distress of patients suffering from cancer who were receiving chemotherapy and NUC (NUC cohort, n = 185) or ONC (ONC cohort, n = 170) were collected and analyzed. One oncologist or 1 nurse was involved in treating 1 patient during the patient's hospital visit. Each visit took 30 min. The Chinese version of the Symptom Distress Scale was used for the evaluation of the degree of symptom distress. The simplified Chinese version of the European Organization for Research and Treatment Quality of Life Questionnaire (the EORTC QLQ-C30) v. 3.0 was used for evaluation of the quality of life.

Results. Female patients preferred NUC ($p < 0.0001$). The pain intensity (4.13 ± 1.71 compared to 3.35 ± 1.01 , $p < 0.0001$), dyspnea (3.89 ± 1.48 compared to 2.82 ± 0.97 , $p < 0.0001$), constipation (3.56 ± 1.78 compared to 3.06 ± 1.89 , $p = 0.0107$), and degree of symptom distress (38.09 ± 7.26 compared to 35.05 ± 7.92 , $p = 0.0002$) were reported higher among patients from the ONC cohort than among those from the NUC cohort. Patients from the NUC cohort reported a better quality of life than those from the ONC cohort (70.41 ± 13.62 compared to 45.63 ± 7.94 , $p < 0.0001$).

Conclusions. The NUC results in better clinical outcome measures and higher quality of life than ONC for patients receiving chemotherapy.

Key words: cancer, cancer palliative care, nurse, oncologist, quality of life

Background

Cancer is a widespread disease responsible for mortality and death.¹ At the time of diagnosis, most patients are in an advanced stage of cancer (IIIb or IV) and very few are in an early stage.² Patients diagnosed at an advanced stage have a poor prognosis, lower survival rate and a higher symptom burden than those diagnosed at an early stage.^{1,3} Chemotherapy has adverse effects on the health of patients.¹ Advances in technology and radiotherapy and/or chemotherapy make the conditions of patients during the treatment period complex.^{4,5} Nurses are members of the oncology multidisciplinary team and contribute to the well-being of patients before and after the cancer treatment.⁶

Outcomes after chemotherapies are required to be predicted before further chemotherapy treatment cycles for the success of the previous intervention(s) and to avoid emergency condition(s). Guidelines recommend cancer palliative care for patients with an early stage of the disease.⁷ The clinics operated with nurse-led cancer palliative care (NUC) model have better clinical outcomes than those operated with clinician-led cancer palliative care (ONC).⁸ Unlike the Western countries, in mainland China, cancer patients receive ONC. Therefore, the NUC is not well established yet. Pilot studies performed in the 947 Hospital of PLA, Kashgar Shule, China, the Hong Kong Polytechnic University, Hong Kong, and Queen Elizabeth Hospital, Hong Kong,^{1,5} meta-analyses^{9,10} and randomized trials on adult patients with acute lymphoblastic leukemia¹¹ reported that NUC results in better clinical outcomes than non-nurse-led cancer palliative care in patients with cancer. However, ONC is the preferred supportive adjuvant care modality among cancer patients.¹² There are only a few studies available to compare the effectiveness of NUC and ONC or non-nurse-led cancer palliative care in Chinese cancer patients.

Objectives

The objectives of this non-randomized, non-treatment and retrospective study were to compare the clinical outcome measures (pain, dyspnea and constipation), quality of life, symptom distress, and survival of Chinese patients suffering from cancer and receiving chemotherapy who received NUC to those of patients who received ONC.

Materials and methods

Ethics approval and consent to participate

The study was a chart review of a database of patients suffering from cancer. Therefore, informed consent from patients, registration into the Chinese trial

registry or approval from the human ethics committee of the First Affiliated Hospital of Soochow University, Suzhou, China, were not required. The study adheres to the law of China and the 2008 Declaration of Helsinki.

Study population

From March 27, 2018, to April 18, 2020, a total of 355 patients suffering from cancer have been receiving chemotherapy at the Department of Oncology of the First Affiliated Hospital of Soochow University (Suzhou, China) and the referring hospitals, and were under NUC or ONC. Patients with missing data were excluded. Data regarding cancer and chemotherapy-related symptoms and quality of life of 355 patients were collected from the institutional records. The flow diagram of the retrospective analysis is presented in Fig. 1.

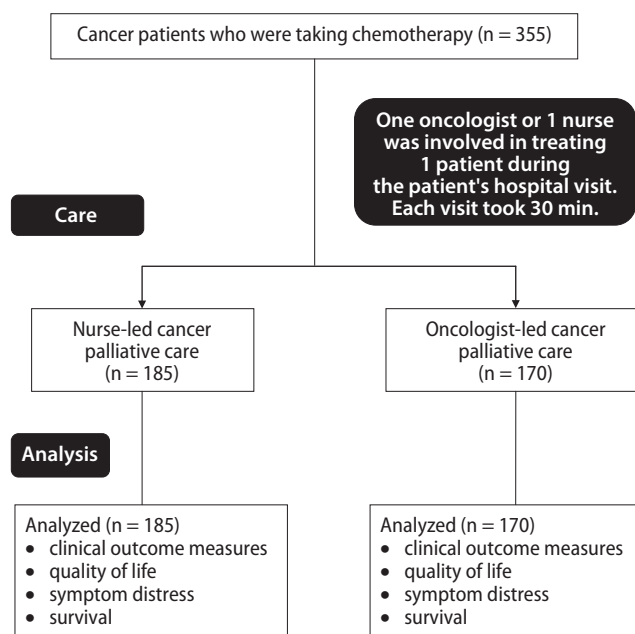


Fig. 1. Flow diagram of retrospective analysis

Cohorts

A total of 185 patients were subjected to NUC regarding physical check-ups, education, treatment adherence control, and counseling at the time of hospital visits because consulting oncologists were unavailable. These patients were included in the NUC cohort. A total of 170 patients were subjected to ONC regarding the same features at the time of hospital visits because their cases were difficult to manage due to history or comorbidities (e.g., respiratory or gastrointestinal disease) that were observed by a physician. These patients were included in the ONC cohort. One oncologist or 1 nurse was involved in treating one patient during the patient's hospital visit. Each visit took 30 min.

Clinical outcome measures

Physical measures

Pain was evaluated on a scale of 0–10, on which 0 indicates no pain and 10 indicates the worst possible pain. Dyspnea was evaluated on a scale of 0–10, where 0 indicates no dyspnea and 10 indicates the worst possible dyspnea. Constipation was evaluated on a scale of 0–10, where 0 indicates no constipation and 10 indicates the worst possible constipation.

Quality of life

The quality of life of patients was assessed by a trained instructor (3 years of experience) of First Affiliated Hospital of Soochow University, using the simplified Chinese version of the European Organization for Research and Treatment Quality of Life Questionnaire (the EORTC QLQ-C30) v. 3.0. It includes 32 items divided into 4 domains (physical, psychological, social, and adverse effects) and 9 facets. Each item is evaluated based on a 5-point Likert scale. The score ranges from 32 to 160. The higher the score, the better the quality of life.¹³

Symptom distress

The Chinese version of the Symptom Distress Scale was used for the evaluation of the degree of symptom distress of patients. A total of 24 common symptoms were included in the evaluation of the degree of symptom distress. Each item is scored based on a 5-point Likert scale. The score ranges from 0 to 120. The higher the score, the higher the degree of symptom distress.¹⁴

Progression free-survival

During treatment or follow-up, if patients were not subjected to extra chemotherapy and/or radiotherapy besides routine chemotherapy and/or radiotherapy (at the oncologist's discretion), it was considered progression-free survival. Patients visit the hospitals frequently during the course of treatment and clinical outcome measures were evaluated during such visits.

Statistical analyses

InStat v. 3.01 software (GraphPad Software, San Diego, USA) was used to perform statistical analyses. All eligible patients were included in the analysis. Continuous data are demonstrated as mean \pm standard deviation (SD) and constant data are demonstrated as frequency (percentages). The Fisher's exact test was used for constant data. Distribution of continuous data was checked visually whether they were distributed normally or not normally through frequency distribution. The continuous data were distributed

Table 1. The Brown–Forsythe test for the homogeneity of variance of continuous data

Parameter	p-value
Demographical conditions	
Age [years]	0.4521
Body mass index [kg/m ²]	0.6232
Outcome measures	
Pain	0.1336
Dyspnea	0.5543
Constipation	0.0108
EORTC QLQ-C30	0.0005
Symptom distress	0.0003

EORTC QLQ-C30 – the simplified Chinese version of the European Organization for Research and Treatment Quality of Life Questionnaire. A value of $p < 0.05$ was considered as showing not equal population variance.

normally. The homogeneity of variance of continuous data was checked using the Brown–Forsythe test (Table 1). If the population variance was not equal, unpaired t-test with Welch's correction was used for continuous data, and if the population variance was equal, unpaired t-test was used for continuous data. All results were considered significant if the p-value was lower than 0.05.

Results

Demographical and clinical conditions

Female patients preferred NUC ($p < 0.0001$). There is a distinct and significant difference in the types of cancer between the groups – for example, most prostate cancer patients received ONC ($p < 0.0001$). The other demographical and clinical conditions of patients before the start of chemotherapy presented no statistically significant differences between both cohorts ($p > 0.05$, Table 2).

Outcome measures

The pain intensity in patients who received ONC was higher than in those who had received NUC (4.13 ± 1.71 (minimum: 2, maximum: 8) compared to 3.35 ± 1.01 (minimum: 2, maximum: 8), $p < 0.0001$, degrees of freedom (df): 353, t-value: 5.271; t-test). Dyspnea was reported higher among patients who received ONC than in those who received NUC (3.89 ± 1.48 (minimum: 1, maximum: 8) compared to 2.82 ± 0.97 (minimum: 1, maximum: 8), $p < 0.0001$, df: 353, t-value: 8.189; t-test). Constipation was reported higher among patients who received ONC than in those who received NUC (3.56 ± 1.78 (minimum: 1, maximum: 9) compared to 3.06 ± 1.89 (minimum: 1, maximum: 8), $p = 0.0107$, df: 352, Welch's approximate t-value: 2.568; t-test with Welch's correction). Patients who received NUC had better quality of life than those who received ONC

Table 2. Demographical and clinical conditions of patients before the start of chemotherapy

Variables		Cohorts		Comparisons		
		NUC	ONC	p-value	df	t-value
Type of cancer palliative care		nurse-led	oncologist-led			
Number of patients		185	170	–	–	–
Gender	male	77 (42)	129 (76)	<0.0001 (Fisher's exact test)	N/A	N/A
	female	108 (58)*	41 (24)			
Age [years]	minimum	32	33	0.3392 (t-test)	353	0.9571
	maximum	67	67			
	mean \pm SD	39.51 \pm 7.14	40.45 \pm 11.09			
Body mass index [kg/m ²]	–	24.12 \pm 2.02	23.89 \pm 1.88	0.2687 (t-test)	353	1.108
ECOG Performance Status	1	139 (75)	129 (76)	0.902 (Fisher's exact test)	N/A	N/A
	2	46 (25)	41 (24)			
Morbidities	diabetes	21 (11)	21 (12)	0.869 (Fisher's exact test)	N/A	N/A
	hypertension	11 (6)	10 (6)	0.999 (Fisher's exact test)	N/A	N/A
	atherosclerosis	10 (5)	17 (10)	0.113 (Fisher's exact test)	N/A	N/A
	dyslipidemia	10 (5)	12 (7)	0.661 (Fisher's exact test)	N/A	N/A
Type of cancer	breast cancer	58 (31)*	5 (3)	<0.0001 (Fisher's exact test)	N/A	N/A
	prostate cancer	4 (2)	61 (36)	<0.0001 (Fisher's exact test)	N/A	N/A
	colorectal cancer	15 (8)	21 (12)	0.292 (Fisher's exact test)	N/A	N/A
	thyroid cancer	29 (16)*	3 (2)	<0.0001 (Fisher's exact test)	N/A	N/A
	oral cancer	47 (25)	51 (30)	0.344 (Fisher's exact test)	N/A	N/A
	lung cancer	3 (2)	5 (3)	0.487 (Fisher's exact test)	N/A	N/A
	liver cancer	9 (5)	13 (8)	0.379 (Fisher's exact test)	N/A	N/A
	cervical cancer	14 (8)*	2 (1)	0.004 (Fisher's exact test)	N/A	N/A
	brain cancer	1 (1)	2 (1)	0.610 (Fisher's exact test)	N/A	N/A
skin cancer	5 (3)	7 (4)	0.562 (Fisher's exact test)	N/A	N/A	

Continuous data are demonstrated as mean \pm standard deviation (SD) and constant data are demonstrated as frequency (percentages). Unpaired t-test was used for continuous data and Fisher's exact test was used for constant data. All results were considered significant if the p-value was less than 0.05.

* significantly higher value than that of the ONC cohort. NUC – nurse-led cancer palliative care; ONC – oncologist-led cancer palliative care; df – degrees of freedom; N/A – not applicable; ECOG – Eastern Cooperative Oncology Group.

(70.41 \pm 13.62 (minimum: 32, maximum: 90) compared to 45.63 \pm 7.94 (minimum: 33, maximum: 70), $p < 0.0001$, df: 300, Welch's approximate t-value: 21.145; t-test with Welch's correction). Patients who received ONC had a higher degree of symptom distress than those who received NUC (38.09 \pm 7.26 (minimum: 17, maximum: 50) compared to 35.05 \pm 7.92 (minimum: 15, maximum: 50), $p = 0.0002$, df: 352, Welch's approximate t-value: 3.806; t-test with Welch correction).

Survival

Eighteen months after the start of treatment, 11 (6%) patients from the NUC cohort and 10 (6%) patients from the ONC cohort have died ($p = 0.999$). A total of 174 (94%) patients from the NUC cohort and 160 (94%) patients from the ONC cohort survived 18 months from the start of treatment, irrespective of disease conditions. There was no statistically significant difference in overall survival 18 months from the start of treatment ($p = 0.999$). After

this period, 65 (35%) patients from the NUC cohort and 45 (26%) patients from the ONC cohort achieved progression-free survival. There was no statistically significant difference in progression-free survival 18 months after the start of treatment ($p = 0.086$). During the treatment and follow-up period, 1 (1%) patient from the NUC cohort and 2 (1%) patients from the ONC cohort developed distal metastasis ($p = 0.609$).

Discussion

The current study found that pain intensity, dyspnea, constipation, and symptom distress were lower, and the quality of life was higher among patients who received NUC than those who received ONC. The results of clinical outcome measures in the current study were consistent with those of a pilot study,¹ a randomized, parallel study,⁸ a meta-analysis,⁹ and some randomized trials^{11,15–17} but were not consistent with those of other

Table 3. Results of similar studies after follow-up care

Variable		Author, year							
		Zhang et al., 2020 ¹	Cheng et al., 2018 ⁹	Lin et al., 2016 ¹¹	Kim et al., 2018 ¹⁵	Beaver et al., 2017 ¹⁶	Malmström et al., 2016 ¹⁷	Kimman et al., 2011 ¹⁸	Verschuur et al., 2009 ¹⁹
Country		China	China	China	South Korea	UK	Sweden	the Netherlands	the Netherlands
Number of patients involved	nurse-led cancer palliative care	110	554	36	30	129	26	149	54
	consultant-led cancer palliative care	110	556	37	30	130	23	150	55
Pain (VAS)	nurse-led cancer palliative care	NV	NV	31%	20.6 ±19.4	21.5 ±29.8	25.6 ±26.8	NV	12%
	consultant-led cancer palliative care	NV	NV	19%	33.3 ±26.6	20.1 ±30.1	16.7 ±15.9	NV	14%
	p-value	>0.05	0.624	0.172	0.039*	0.56	0.303	N/A	0.24
Dyspnea	nurse-led cancer palliative care	NV	NV	5.0 ±3.2	20.0 ±22.5	17.5 ±28.5	35.9 ±29.7	NV	NV
	consultant-led cancer palliative care	NV	NV	5.6 ±2.9	25.6 ±28.6	13.2 ±23.7	18.8 ±16.9	NV	NV
	p-value	>0.05	0.509	0.404	0.403	0.5	0.041*	N/A	N/A
Constipation	nurse-led cancer palliative care	NV	NV	8.1 ±2.0	25.6 ±32.4	10.4 ±20.9	25.5 ±28.8	NV	NV
	consultant-led cancer palliative care	NV	NV	11.1 ±3.9	33.3 ±35.0	15.9 ±25.2	18.8 ±28.1	NV	NV
	p-value	>0.05	0.001*	0.001*	0.380	0.035*	0.288	N/A	N/A
Quality of life (EORTC QLQ-C30)	nurse-led cancer palliative care	NV	NV	79.6 ±21.0	64.4 ±15.6	71.6 ±19.8	47.8 ±14.4	78.9 ±15.8	74
	consultant-led cancer palliative care	NV	NV	63.2 ±18.1	51.4 ±22.4	73.2 ±21.5	40.2 ±15.4	77.2 ±16.6	69
	p-value	<0.05*	>0.05	0.009*	0.011*	0.31	<0.001*	0.42	0.13
Symptom distress (Symptom Distress Scale)	nurse-led cancer palliative care	NV	NV	NV	NV	NV	65.4 ±27.8	NV	NV
	consultant-led cancer palliative care	NV	NV	NV	NV	NV	64.9 ±21.8	NV	NV
	p-value	N/A	0.255	N/A	N/A	N/A	0.698	N/A	0.4
Metastasis	nurse-led cancer palliative care	NV	NV	NV	NV	4%	25%	2%	20%
	consultant-led cancer palliative care	NV	NV	NV	NV	4%	22%	2%	29%
	p-value	N/A	N/A	N/A	N/A	0.098	0.691	0.997	0.5
Death	nurse-led cancer palliative care	NV	NV	NV	NV	1%	NV	NV	13%
	consultant-led cancer palliative care	NV	NV	NV	NV	1%	NV	NV	13%
	p-value	N/A	N/A	N/A	N/A	0.096	N/A	N/A	0.998

NV – not available; N/A – not applicable; * significant difference. Dyspnea and constipation were evaluated on a scale of 0–10, where 0 indicates no event and 10 indicates the worst possible condition.

randomized trials.^{18,19} Heterogeneity of patient cohorts and short follow-up of the current study were responsible for results contradictory with those of randomized trials.^{18,19} The NUC results in better clinical outcome measures and quality of life than ONC.

Eighteen months after the start of treatment, there were statistically significant differences in the occurrence of death, progression-free survival, overall survival, and

occurrence of metastases between both cohorts. The survival rates of the current study were consistent with those of randomized trials.^{18,19} The cancer palliative care given by nurses or oncologists has no effects on chemotherapy outcomes. However, it can affect the quality of life, symptoms and mental strength of the patients.

Results of the different published studies are reported in Table 3.

All patients were offered either NUC or ONC. However, female patients preferred NUC. Female patients mostly suffered from breast, thyroid and/or cervical cancer. The NUC provides great effects in some areas of oncology, for example, in breast cancer treatment. Yet, there is usually a great imbalance of sexes in NUC and ONC cohorts that strongly influences the quality of life results.

Limitations

There are several limitations of the study that have to be reported. It is a retrospective study which lacks randomized trial and had a short (18-month) follow-up. There was a heterogeneity of patients among cohorts, which may create a bias in the analysis. There was also an imbalance in the types of cancer between groups – a lot of breast cancer patients in the NUC cohort and a lot of prostate cancer patients in the ONC cohort; these differences are statistically significant. Men and women patients suffered from different types of cancer and this imbalance influenced the study results.


Conclusions

The NUC results in better clinical outcome measures and higher quality of life than ONC in Chinese patients suffering from cancer, but this issue needs to be further examined using more sophisticated analytical methods. However, NUC did not change death, progression-free survival, overall survival, and metastasis rates. Female patients, especially those with breast cancer, preferred NUC. The present study provides evidence of the competence of nurses, and more studies like this will lead to the improvement of nurses' autonomy and professionalism.

ORCID iDs

Mengtian Xu  <https://orcid.org/0000-0002-0147-9960>

Li Zhu  <https://orcid.org/0000-0001-8220-7280>

Jingjuan Yang  <https://orcid.org/0000-0002-2941-2506>

References

- Zhang C, Guo H, Shen M, Chen G. Comparison of clinical effectiveness of nurse led care among Chinese patients with cancer: A prospective study evaluating effective patient care compared to consultant oncologist. *J Infect Public Health*. 2020;13(2):159–163. doi:10.1016/j.jiph.2019.07.010
- Ali A, Goffin JR, Arnold A, Ellis PM. Survival of patients with non-small-cell lung cancer after a diagnosis of brain metastases. *Curr Oncol*. 2013;20(4):300–306. doi:10.3747/co.20.1481
- Toftagen C, Visovsky C, Dominic S, McMillan S. Neuropathic symptoms, physical and emotional well-being, and quality of life at the end of life. *Support Care Cancer*. 2019;27(9):3357–3364. doi:10.1007/s00520-018-4627-x
- Tho PC, Ang E. The effectiveness of patient navigation programs for adult cancer patients undergoing treatment: A systematic review. *JBI Database System Rev Implement Rep*. 2016;14(2):295–321. doi:10.11124/jbisrir-2016-2324
- Lai X, Wong FKY, Leung CWY, et al. Development and assessment of the feasibility of a nurse-led care program for cancer patients in a chemotherapy day center: Results of the pilot study. *Cancer Nurs*. 2015;38(5):E1–E12. doi:10.1097/NCC.0000000000000192
- Brownhill S, Chang E, Bidewell J, Johnson A. A decision model for community nurses providing bereavement care. *Br J Commun Nurs*. 2013;18(3):133–139. doi:10.12968/bjcn.2013.18.3.133
- Schenker Y, Althouse AD, Rosenzweig M, et al. Effect of an oncology nurse-led primary palliative care intervention on patients with advanced cancer: The CONNECT cluster randomized clinical trial. *JAMA Intern Med*. 2021;181(11):1451. doi:10.1001/jamainternmed.2021.5185
- Wang J, Zou X, Cong L, Liu H. Clinical effectiveness and cost-effectiveness of nurse-led care in Chinese patients with rheumatoid arthritis: A randomized trial comparing with rheumatologist-led care. *Int J Nurs Pract*. 2018;24(1):e12605. doi:10.1111/ijn.12605
- Cheng X, Wei S, Zhang H, Xue S, Wang W, Zhang K. Nurse-led interventions on quality of life for patients with cancer: A meta-analysis. *Medicine (Baltimore)*. 2018;97(34):e12037. doi:10.1097/MD.00000000000012037
- Monterosso L, Platt V, Bulsara M, Berg M. Systematic review and meta-analysis of patient reported outcomes for nurse-led models of survivorship care for adult cancer patients. *Cancer Treat Rev*. 2019;73:62–72. doi:10.1016/j.ctrv.2018.12.007
- Lin H, Zhou S, Zhang D, Huang L. Evaluation of a nurse-led management program to complement the treatment of adolescent acute lymphoblastic leukemia patients. *Appl Nurs Res*. 2016;32:e1–e5. doi:10.1016/j.apnr.2016.08.001
- Kirkham AA, Van Patten CL, Gelmon KA, et al. Effectiveness of oncologist-referred exercise and healthy eating programming as a part of supportive adjuvant care for early breast cancer. *Oncologist*. 2018;23(1):105–115. doi:10.1634/theoncologist.2017-0141
- Wan C, Meng Q, Yang Z, et al. Validation of the simplified Chinese version of EORTC QLQ-C30 from the measurements of five types of inpatients with cancer. *Ann Oncol*. 2008;19(12):2053–2060. doi:10.1093/annonc/mdn417
- Tang PL, Wang C, Hung MF, Lin HS. Assessment of symptom distress in cancer patients before and after radiotherapy. *Cancer Nurs*. 2011;34(1):78–84. doi:10.1097/NCC.0b013e3181f04ac8
- Kim YH, Choi KS, Han K, Kim HW. A psychological intervention programme for patients with breast cancer under chemotherapy and at a high risk of depression: A randomised clinical trial. *J Clin Nurs*. 2018;27(3–4):572–581. doi:10.1111/jocn.13910
- Beaver K, Williamson S, Sutton C, et al. Comparing hospital and telephone follow-up for patients treated for stage-I endometrial cancer (ENDCAT trial): A randomised, multicentre, non-inferiority trial. *BJOG*. 2017;124(1):150–160. doi:10.1111/1471-0528.14000
- Malmström M, Ivarsson B, Klefsgård R, Persson K, Jakobsson U, Johansson J. The effect of a nurse led telephone supportive care programme on patients' quality of life, received information and health care contacts after oesophageal cancer surgery: A six month RCT-follow-up study. *Int J Nurs Stud*. 2016;64:86–95. doi:10.1016/j.ijnurstu.2016.09.009
- Kimman ML, Dirksen CD, Voogd AC, et al. Nurse-led telephone follow-up and an educational group programme after breast cancer treatment: Results of a 2x2 randomised controlled trial. *Eur J Cancer*. 2011;47(7):1027–1036. doi:10.1016/j.ejca.2010.12.003
- Verschuur EML, Steyerberg EW, Tilanus HW, et al. Nurse-led follow-up of patients after oesophageal or gastric cardia cancer surgery: A randomised trial. *Br J Cancer*. 2009;100(1):70–76. doi:10.1038/sj.bjc.6604811

Development and validation of a 4-lncRNA combined prediction model for patients with hepatocellular carcinoma

Cui Xu^{B,D}, Xiangxiu Qi^{A,F}

Department of General Surgery, Shengjing Hospital of China Medical University, Shenyang, China

A – research concept and design; B – collection and/or assembly of data; C – data analysis and interpretation; D – writing the article; E – critical revision of the article; F – final approval of the article

Advances in Clinical and Experimental Medicine, ISSN 1899–5276 (print), ISSN 2451–2680 (online)

Adv Clin Exp Med. 2022;31(10):1087–1097

Address for correspondence

Xiangxiu Qi
E-mail: lnszlyysurgeon@sohu.com

Funding sources

None declared

Conflict of interest

None declared

Received on October 24, 2021
Reviewed on December 12, 2021
Accepted on May 19, 2022

Published online on August 1, 2022

Abstract

Background. Hepatocellular carcinoma (HCC) is one of the most common and lethal cancers worldwide. Therefore, it is necessary to develop and validate a novel prognostic model for HCC patients.

Objectives. To establish an innovative and valuable prediction model of long non-coding RNAs (lncRNAs) for HCC.

Materials and methods. Transcriptome and clinical data from The Cancer Genome Atlas (TCGA) were analyzed globally using bioinformatic approaches. We used Cox and least absolute shrinkage and selection operator (LASSO) regression analyses to screen for prognostic lncRNAs, while receiver operating characteristic (ROC) and Kaplan–Meier curve analyses were used to evaluate the effectiveness of the models. Clinical data from our center were used as a validation set.

Results. In the training set, a prediction model was established based on the expression of AP000844.2, LINC00942, SRGAP3-AS2, and AC010280.2. Hepatocellular carcinoma patients were divided into 2 groups (high-risk group and low-risk group) according to their risk score, and differences in survival were compared between the groups. The clinical data from our center served as a validation set to re-evaluate the effectiveness of the predictive model. The model had an excellent performance. The area under the curve (AUC) of 3-year survival was 0.771, while for 5-year survival it was 0.741, and the concordance index (C-index) was 0.756 (standard error (SE) = 0.023, 95% confidence interval (95% CI) = 0.620–0.891).

Conclusions. The 4-lncRNA combination model is critically important in evaluating the prognosis of HCC. It is an effective independent prognostic factor, although prospective, multi-center studies are needed to validate our findings.

Key words: prognosis, survival analysis, hepatocellular carcinoma, least absolute shrinkage and selection operator

Cite as

Xu C, Qi X. Development and validation of a 4-lncRNA combined prediction model for patients with hepatocellular carcinoma. *Adv Clin Exp Med.* 2022;31(10):1087–1097. doi:10.17219/acem/150256

DOI

10.17219/acem/150256

Copyright

Copyright by Author(s)

This is an article distributed under the terms of the Creative Commons Attribution 3.0 Unported (CC BY 3.0) (<https://creativecommons.org/licenses/by/3.0/>)

Background

Hepatocellular carcinoma (HCC) is one of the most frequent malignancies globally and ranks 3rd for morbidity and mortality rates, respectively.¹ Although advances have been made in multidisciplinary treatment and targeted medicine, the 5-year survival rate of HCC patients remains relatively low due to the poor performance of diagnostic techniques and lack of comprehensive treatment.² Hepatocellular carcinoma diagnosis and treatment still pose a considerable challenge. Patients undergoing surgical treatment miss the opportunity for intervention due to the atypical recurrence of symptoms if there is no active postoperative follow-up.^{3,4} Therefore, a reasonable estimation of the patient's survival time and paying attention to the time window for possible recurrence are vital to improve the prognosis. Thus, it is critical to deepen our understanding of the pathogenesis of HCC development and to seek novel biological markers or therapeutic targets.⁵

Recently, it was detected that the abnormal expression of long non-coding RNAs (lncRNAs) correlate with the occurrence and development of tumors and other diseases.^{6,7} They are valuable in prognostic evaluation, early diagnosis and clinical treatment of many malignant tumors.⁸ More notably, lncRNAs have a critical impact on abnormal cellular regulation and tumorigenesis. At present, in the post-genomic era, lncRNAs are also a vital research hotspot. They regulate genes and play critical biological functions in cell development and multiple levels, such as transcription, post-transcription, translation, and post-translational modification.⁹ Therefore, it is crucial to characterize the structure and interaction of lncRNA for understanding its cellular mechanism of action.¹⁰ Some studies have found that lncRNAs are closely related to tumors, and their expression and regulation are found to be abnormal in breast cancer, colon cancer and stomach cancer.¹¹ Studies on the functions of lncRNAs have shown that the abnormal expression of lncRNAs may be used for the prognosis and treatment of HCC.¹² The lncRNA UPK1A-AS1 could work as a scaffold to reinforce the binding of EZH2 and SUZ12 in order to induce the chemoresistance of HCC cells.¹³ Furthermore, lncRNA LL22NC03-N14H11.1 promotes mitochondrial fission and induces the epithelial–mesenchymal transition of HCC through the MAPK pathway.¹⁴ These data indicate that the aberrant expression of lncRNAs may directly or indirectly adjust the malignant phenotype of HCC and affect its prognosis. In addition, as it is commonly known, genes are highly interactive. Therefore, it is necessary to select appropriate lncRNAs and establish multiple lncRNA prediction models. Such actions could play an essential role in assisting the evaluation of HCC prognosis.

Transcriptome data from the Cancer Genome Atlas (TCGA) and clinical data from Shengjing Hospital of China Medical University were analyzed. We have developed and

validated an effective multi-lncRNA combined survival prediction model using Cox regression and least absolute shrinkage and selection operator (LASSO) regression¹⁵; this model might be helpful in the prognosis of HCC patients.

Objectives

This study aims to establish a prediction model for HCC based on differentially expressed lncRNAs (DELs) and evaluate its effectiveness based on clinical data.

Materials and methods

Data acquisition

The raw RNA sequencing data were downloaded from TCGA (<https://portal.gdc.cancer.gov/>) through the RT-CGA Toolbox package (TCGA-Liver Hepatocellular Carcinoma (LIHC)) and matched survival data were obtained the same way. The LIHC data were used as the training set to build a predictive model, as described below. The training set consisted of 424 samples, including 374 cancer tissue samples and 50 normal tissue samples. The transcriptome data were captured using the Illumina HiSeq RNA-Seq platform (<https://portal.gdc.cancer.gov/projects/TCGA-LIHC>).

Bioinformatics analysis

We used the edgeR package (<https://bioconductor.org/packages/release/bioc/html/edgeR.html>) to obtain DELs based on the RNA expression profile data. First, we homogenized the expression of each lncRNA in each sample. Then, we compared the expression value of each lncRNA between the cancer tissue group and the normal tissue group, and the multiple of difference was expressed as fold change (FC) value, with $p < 0.05$ considered statistically different. The value of $p < 0.05$ and $|FC| \geq 4$ ($|\log_2 FC| \geq 2$) were determined as the cut-off values. Any lncRNA that met the above 2 conditions was classified as DEL. Then, the “survival” package was used to perform a univariate proportional hazards model (Cox) regression analysis. The meaningful DELs in univariate Cox regression analysis were enrolled to construct the LASSO (“glmnet” package) regression, and the “survminer” package was adopted for visualization. The effectiveness of lncRNA combined prediction model was evaluated in terms of receiver operating characteristic (ROC) and concordance index (C-index). Subjects were divided into the high-expression group and the low-expression group based on the prediction model, and the Kaplan–Meier survival curve described the clinical prognostic significance of the model. Subsequently, clinical data from our center were used as a validation set to evaluate the effectiveness of the model (the workflow process is described in Fig. 1A).

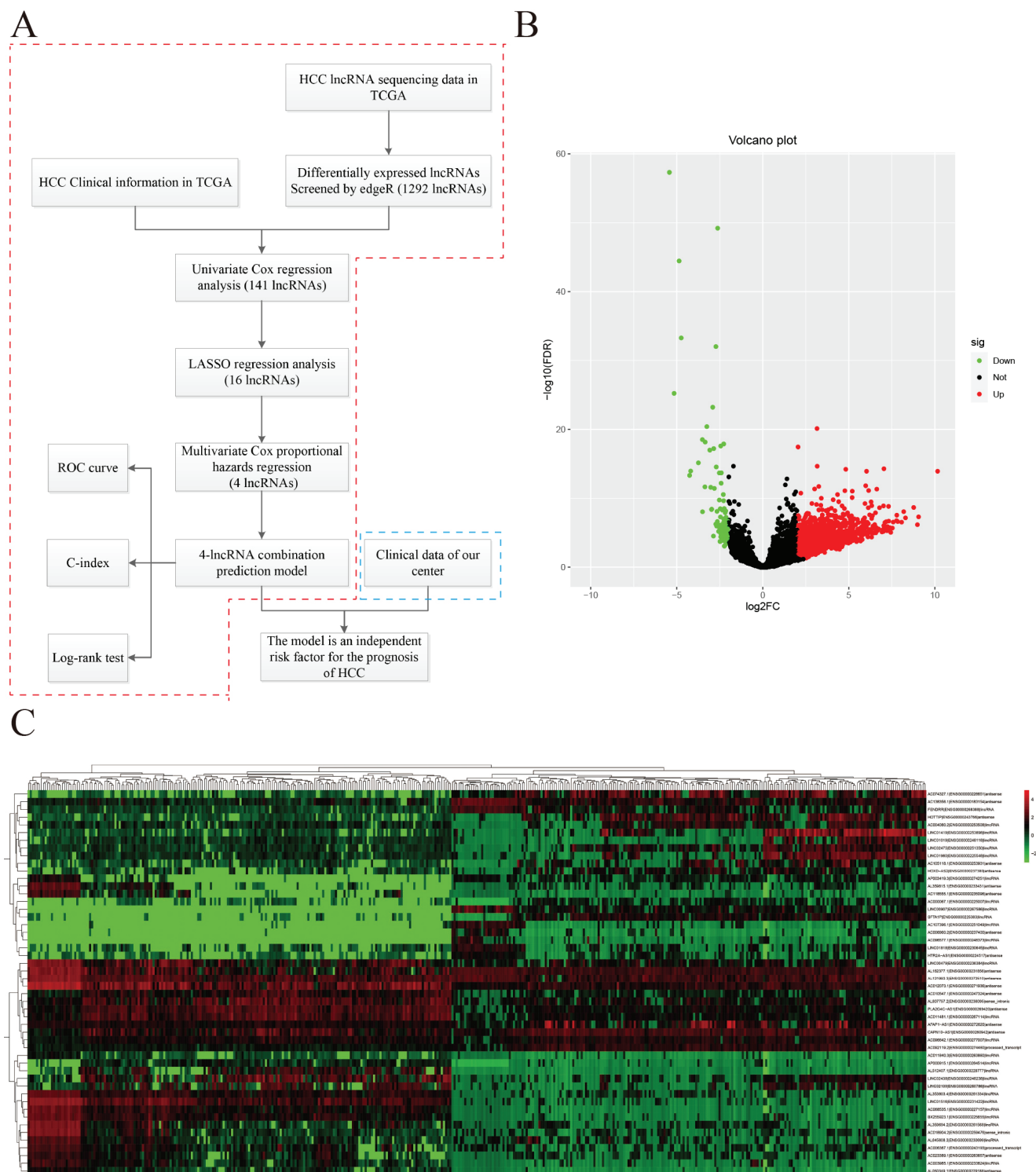


Fig. 1. Differentially expressed long non-coding RNAs (IncRNAs) (DELs) in The Cancer Genome Atlas-Liver Hepatocellular Carcinoma (TCGA-LIHC).

A. The workflow of the study. We obtained the hepatocellular carcinoma (HCC) transcriptome and survival data in TCGA as the training set, and from this we established the DELs prediction model. The clinical data from our center were used as a validation set to evaluate the effectiveness of the model (red box: training set; blue box: validation set); B. Volcano plots showing the expression of DELs screened using edgeR; C. Heatmap showing the expression of the top 50 DELs

LASSO – least absolute shrinkage and selection operator; ROC – receiver operating characteristic; C-index – concordance index.

Ethical statement and tissue samples

We obtained 100 tumor samples and matched non-tumor tissue samples from HCC patients undergoing surgical

resection at the Shengjing Hospital of China Medical University in 2010–2015. All specimens were pathologically confirmed as HCC. The Ethics Committee of Shengjing Hospital of China Medical University approved this study

(approval No. 20191215) and all patients signed informed consent prior to surgery. The follow-up deadline was January 31, 2020. These 100 patients were used as a validation set to evaluate the effectiveness of the model.

Cell culture

The human HCC cell lines (Huh7 and Hep3B) and a hepatocellular cell line (THLE-3) were acquired from China Medical University (Shenyang, China). Cell culture was performed using RPMI-1640 medium (Gibco, Carlsbad, USA) containing 10% fetal bovine serum (FBS) at 37°C with 5% CO₂.

Reverse transcription polymerase chain reaction (RT-PCR)

The TRIzol extraction kits (Invitrogen, Waltham, USA) were adopted for total RNA extraction, and optical density (OD) values were obtained at 260–280 nm using an ultraviolet spectrophotometer. The RNA was used for subsequent quantitative polymerase chain reaction (qPCR) quantification if its OD260/OD280 ratio was >1.8. Next, the reverse transcription of RNA into cDNA was performed using PrimeScript RT kits, with a system of 10 µL, according to the manufacturer's instruction. The reaction conditions

were 25°C for 30 min, 45°C for 30 min and 85°C for 5 min. Using cDNA as a template, quantitative fluorescence PCR was carried out with 2×TaqMan™ Universal PCR Master Mix (Thermo Fisher, Waltham, USA) under the reaction conditions of 95°C for 3 min, cycling 5 times (94°C for 20 s, 63°C for 30 s, 72°C for 30 s) and cycling 40 times (95°C for 15 s, 60°C for 30 s), with U6 being an internal reference. Three wells and negative controls without a template were set up for all reactions. The quantitative analysis was carried out using the 2^{-ΔΔCt} method. All primers were purchased from Sangon Biotech (Shanghai, China).

Statistical analyses

The IBM SPSS v. 21.0 statistical software (IBM Corp., Armonk, USA) and GraphPad Prism v. 8.0 (GraphPad, San Diego, USA) were used for data processing. Each experiment was repeated 3 times. Measurement data were expressed as mean ± standard deviation (SD). The Shapiro–Wilk test was used to check data normality. The expression of lncRNAs in cells conformed to a normal distribution, so an independent t-test was used to compare the expression of lncRNAs between cells. The expression of lncRNAs in tissues did not conform to a normal distribution, so the Mann–Whitney U test was performed to compare the expression of lncRNAs between tumor

Table 1. Results of Shapiro–Wilk test

Item	Statistic	dif	sig
lncRNAs expression in cells			
AP000844.2Huh7	0.996	3	0.878
AP000844.2Hep3B	0.990	3	0.806
AP000844.2THLE3	1.000	3	0.973
SRGAP3AS2Huh7	1.000	3	1.000
SRGAP3AS2Hep3B	0.997	3	0.902
SRGAP3AS2THLE3	1.000	3	0.972
LINC00942Huh7	1.000	3	0.960
LINC00942Hep3B	0.998	3	0.925
LINC00942THLE3	0.942	3	0.537
AC010280.2Huh7	0.997	3	0.900
AC010280.2Hep3B	1.000	3	1.000
AC010280.2THLE3	1.000	3	1.000
lncRNAs expression in tissues			
AP000844.2Cancer	0.971	100	0.025
AP000844.2Adj	0.916	100	0.000
SRGAP3AS2Cancer	0.968	100	0.016
SRGAP3AS2Adj	0.962	100	0.005
LINC00942Cancer	0.927	100	0.000
LINC00942Adj	0.961	100	0.005
AC010280.2Cancer	0.920	100	0.000
AC010280.2Adj	0.952	100	0.001

lncRNAs – long non-coding RNAs.

tissues and non-tumor tissues. Table 1 presents the results of the Shapiro–Wilk test. The Kaplan–Meier method and a log-rank test were used to measure overall survival (OS). Multivariate models of prognostic factors were carried out using Cox regression. The LASSO regression analysis was performed to reduce overfitting caused by univariate Cox regression. Getting the corresponding number of variables by the minimum lambda value of $p < 0.05$ was considered a statistically significant difference.

Results

lncRNAs have differential expression in HCC

The RNA transcriptome data were obtained from TCGA, including 374 HCC tissues and 50 normal tissues (TCGA-LIHC) as the training set. Then, treating the $p < 0.05$ and $|\log_2FC| \geq 2$ as the cut-off values, the edgeR package was performed to distinguish the DELs. A volcano plot of the distribution of DELs was drawn with the log values of FC and false discovery rate (FDR) as the horizontal and vertical axes, respectively. A total of 1212 up-regulated (in red) and 80 downregulated (in green) DELs were recognized (Fig. 1B). The DELs are listed in Supplementary Table 1 (available at: <https://doi.org/10.5281/zenodo.6794063>). Moreover, the top 50 DELs are displayed in a heatmap (Fig. 1C).

A prediction model based on the co-expression of 4-lncRNAs

It was necessary to evaluate the clinical significance of DELs in HCC. First, univariate Cox regression showed that a total of 141 DELs contributed to the survival of HCC (Supplementary Table 2 (available at: <https://doi.org/10.5281/zenodo.6794063>), $p < 0.05$). Subsequently, we extracted the expression data of DELs in HCC patients ($n = 141$) and obtained the corresponding clinical data. The LASSO regression analysis was performed to further evaluate these data; this analysis could reduce overfitting caused by univariate Cox regression. With a continuous lambda increase, the absolute value of the regression coefficient was correspondingly compressed, and some relatively unimportant variables were compressed to 0. This allowed an expression curve between regression coefficients and lambda values to be obtained (Fig. 2A). When the lambda value reached a specific size, increasing the number of model-independent variables and reducing the lambda value could not significantly improve the model performance. Therefore, we obtained the smallest lambda value using LASSO regression and got the corresponding number of variables. The analysis showed that 16 out of the 141 DELs may be associated with HCC prognosis (Fig. 2B). Furthermore, a multivariate regression analysis

was performed on these 16 DELs, and we discovered that only 4 DELs might be independent risk factors for HCC prognosis (Fig. 2C and Fig. 2D). We adopted these 4 DELs for modeling and assigned scores according to their respective weights in the multi-Cox analysis.

Then, each HCC sample got a risk score based on the expression level of the 4-DEL combination model. A cumulative distribution function (CDF) map was built based on the risk score value of each sample. With the risk score value = 1 as the cut-off value (\log_2 risk score = 0), we divided the samples into the high-risk (red) group and the low-risk (green) group (Fig. 3A). To assess the relationship between the risk score and patient survival, a scatter plot was drawn, with survival time measured in years (Fig. 3B; red: deceased, green: alive). With the increased risk score, the number of surviving patients decreased gradually and the number of deceased patients increased. We used a heatmap to demonstrate the score of 4 DELs in each sample (Fig. 3C).

Then, we evaluated the effectiveness of the model in predicting HCC prognosis. Traditionally, both ROC and C-index have been important indices for a prediction model. We applied these 2 indicators to evaluate the predictive ability of the 4-DEL prediction model. The area under the curve (AUC) of 3-year and 5-year survival were 0.771 and 0.741, respectively (Fig. 3D). In addition, the C-index was 0.756 (standard error (SE) = 0.023, 95% confidence interval (95% CI) = 0.620–0.891). As both indices were greater than 0.7, it suggested that this model was predictive for the prognosis of patients with HCC. The patients were divided into the high-risk group and the low-risk group, according to the risk score. The 5-year survival rate was significantly reduced in the high-risk group (Fig. 3E, $p = 0.0001$). Based on the above analysis, we obtained the 4-DEL combined prediction model for HCC: “Risk score = $1.14 \times AP000844.2 + 1.12 \times LINC00942 + 1.20 \times SRGAP3-AS2 - 0.84 \times AC010280.2$ ”, and prepared for further model validation (cut-off value = 0.945).

The expression of AP000844.2, LINC00942, SRGAP3-AS2, and AC010280.2 in HCC

We obtained a predictive model based on the molecular expression of 4 lncRNAs, namely AP000844.2, LINC00942, SRGAP3-AS2, and AC010280.2 using a bioinformatics analysis with a public database as the training set. To further demonstrate the authenticity and validity of the analysis, we confirmed the expression of these 4 molecules in HCC. The human HCC cell lines (Huh7 and Hep3B) and the hepatocellular cell line (THLE-3) were used to check the expression at the cell level using RT-PCR. We found that AP000844.2, LINC00942 and SRGAP3-AS2 were overexpressed in HCC cells, as compared with hepatocellular cells (Fig. 4A–C, $p < 0.05$). On the contrary, AC010280.2 was weakly expressed in HCC cells but it was upregulated in THLE-3

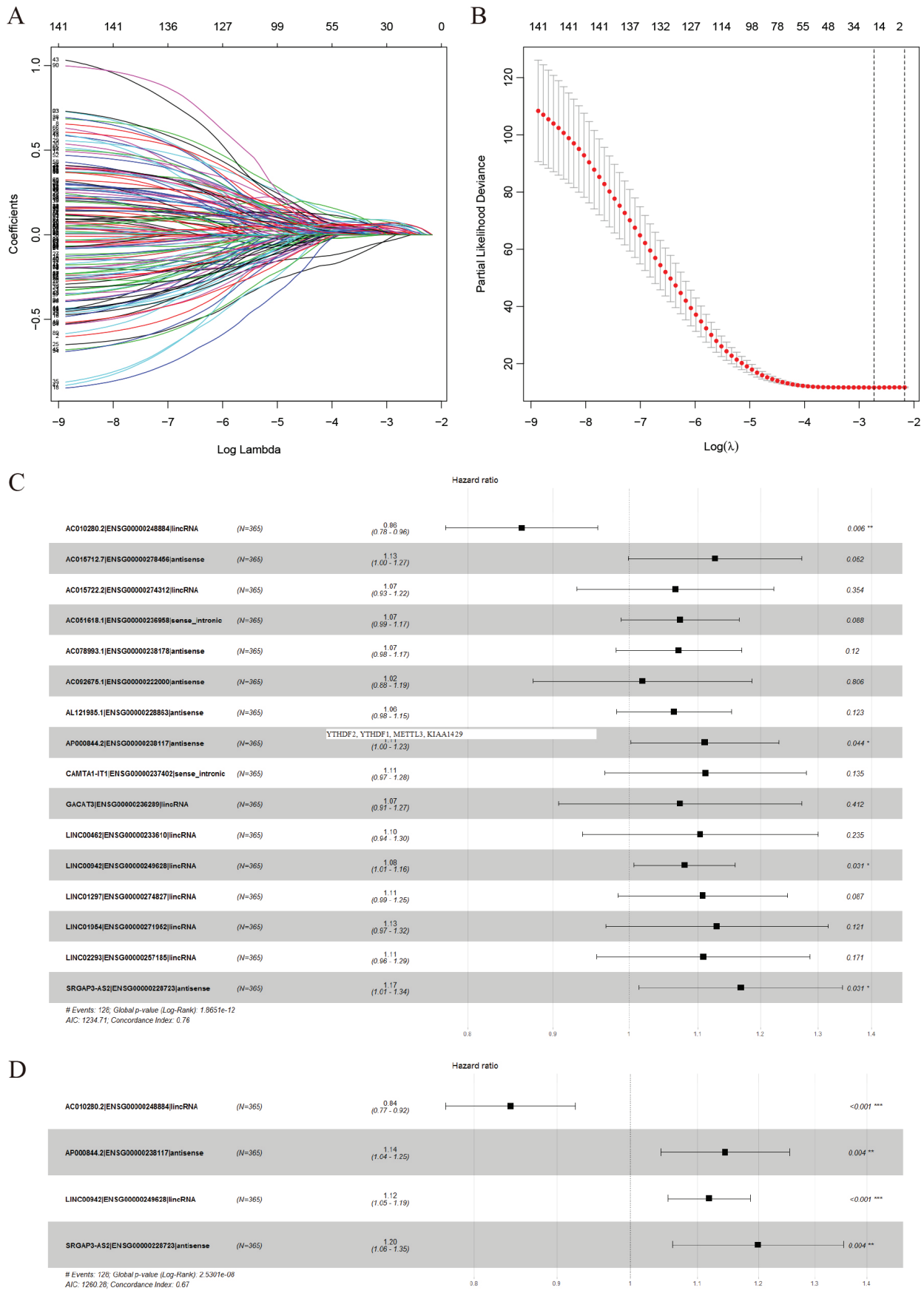


Fig. 2. Long non-coding RNAs (lncRNAs) screened by least absolute shrinkage and selection operator (LASSO) and Cox regression analyses. A. LASSO coefficient values of the 4 prognosis-related lncRNAs in hepatocellular carcinoma (HCC) cohort; B. L1-penalty of LASSO-Cox regression. The hatched vertical lines are at optimal log (lambda) value; C. Forest plot demonstrating the correlations between the 16 lncRNAs and survival; D. Forest plot showing the correlations between the 4 lncRNAs and survival

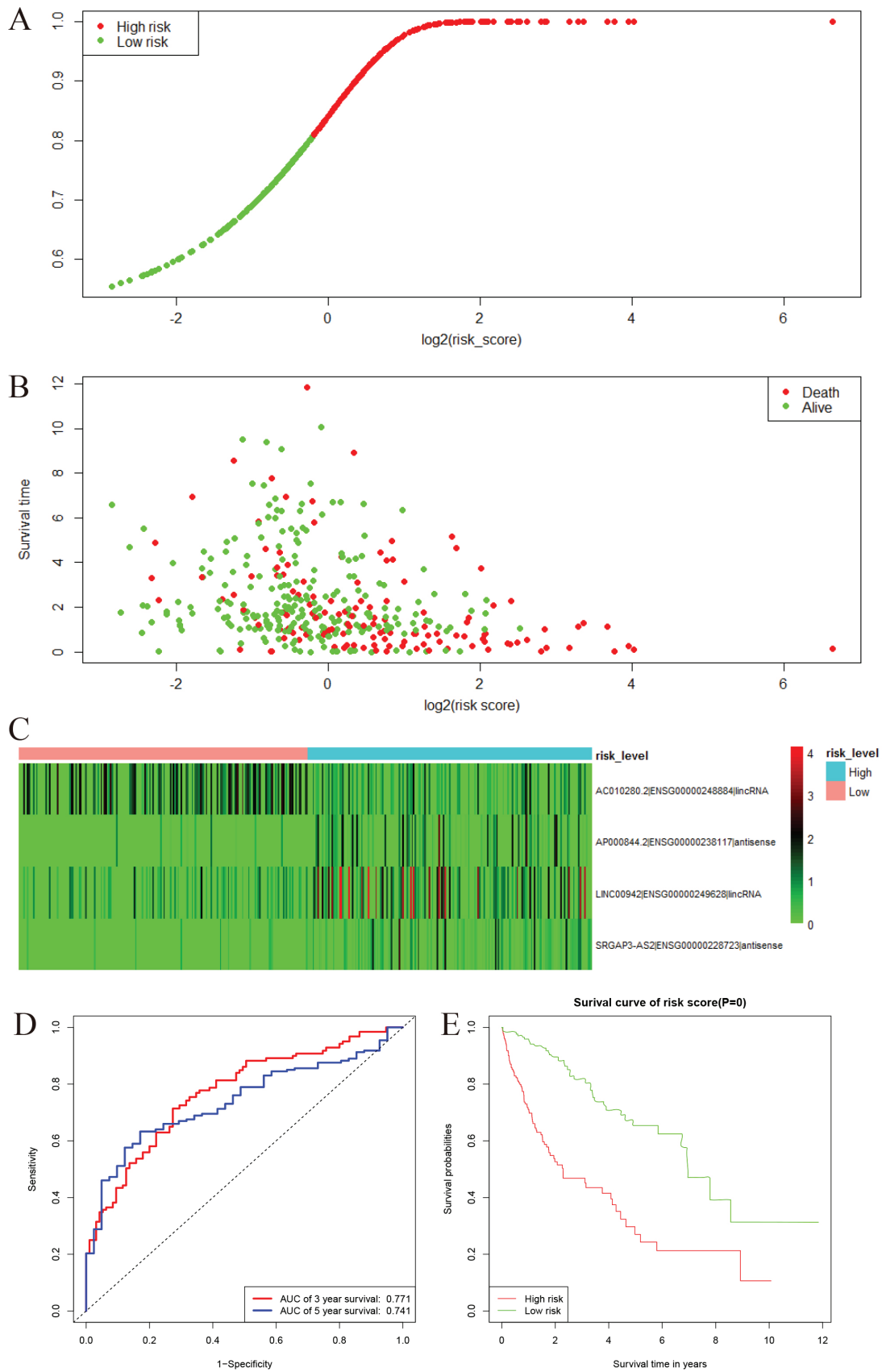


Fig. 3. Characteristics of the combination of 4 long non-coding RNAs (lncRNAs) in The Cancer Genome Atlas (TCGA) cohort. A. A cumulative distribution function (CDF) map built based on the risk score of each sample (the low-risk group: green; the high-risk group: red); B. Survival time in years of each sample (red: deceased; green: alive); C. The heatmap of the 4 lncRNAs expression (blue: high-risk group; pink: low-risk group); D. Receiver operating characteristic (ROC) curve evaluated the predictive effectiveness of the model; E. The high-risk group in this model had lower overall survival (OS)

AUC – area under the curve.

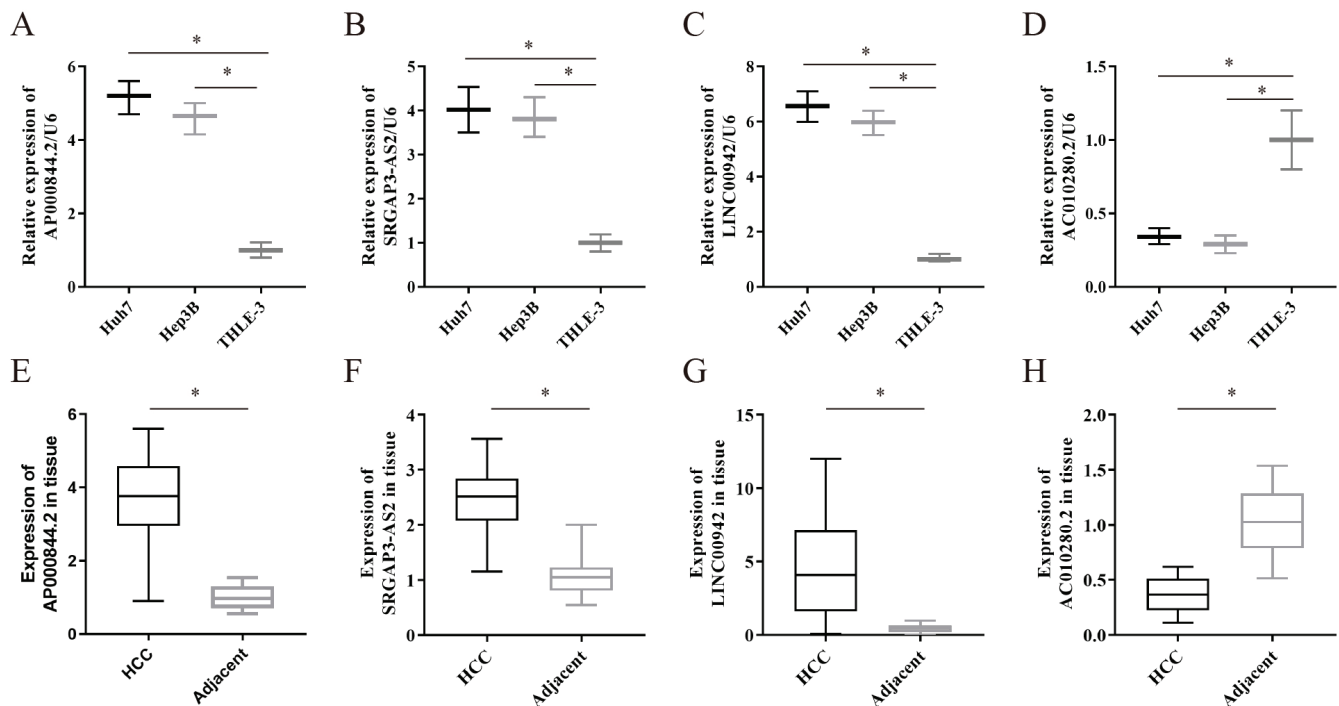


Fig. 4. The expression of AP000844.2, LINC00942, SRGAP3-AS2, and AC010280.2 in hepatocellular carcinoma (HCC) tissues and cells. All 4 long non-coding RNAs (lncRNAs) were overexpressed in both cells and tissues (AP000844.2: A and E; LINC00942: B and F; SRGAP3-AS2: C and G; AC010280.2: D and H)

(Fig. 4D, $p < 0.05$). The RT-PCR results were consistent with the data obtained in the previous bioinformatics analysis. Subsequently, we re-evaluated the expression of the 4 lncRNAs in HCC tissues and matched normal controls in our center ($n = 100$). As expected, AP000844.2, LINC00942 and SRGAP3-AS2 were all overexpressed in HCC tissues when compared to controls. The AC010280.2 was weakly expressed in HCC tissues but overexpressed in normal hepatic tissues (Fig. 4E–H, $p < 0.05$). Consistent results were also obtained for clinical samples and cell samples, which further corroborated the results of our bioinformatics analysis. It is worth emphasizing that LINC00942 showed the most significant difference at both cell and tissue levels.

Verification of the prognostic effect of the 4-lncRNA combination model

The disease-free survival (DFS) ranged from 5 to 90 months, and the OS ranged from 8 to 90 months. We found that 81 out of 100 patients died before the end of the follow-up in the validation set. The expressions of AP000844.2, LINC00942, SRGAP3-AS2, and AC010280.2 were tested in 100 tissue samples (Fig. 4E–H). Then, the correlation between the risk score and survival was assessed. The tumor number, tumor stage, vascular invasion, capsule, distant metastasis, and prediction model all contributed to the poor DFS and OS (Table 2, $p < 0.05$). The high-risk group in the 4-lncRNA combined prediction model demonstrated an unequivocally poor prognosis as evidenced by DFS (25.18 compared to 52.85, $p < 0.01$, Fig. 5A) and OS (31.42 compared to 57.31, $p < 0.01$, Fig. 5B) in the validation

set. The tumor stage and prediction model were independent prognostic risk factors for HCC (Table 3, $p < 0.05$).

Discussion

Hepatocellular carcinoma has high morbidity and mortality rates.¹⁶ Individual treatment and precision medicine are important ways of improving the prognosis. Through the use of genomics, proteomics and transcriptomics, and further development of related technologies, molecular stratification theory has become a powerful tool for the in-depth understanding of tumors. It brings oncology from a discipline that simply describes macro-information, such as size and quantity, to a more in-depth molecular analysis. Furthermore, the discovery of molecular therapies and prognostic biomarkers could bring hope to HCC treatment. Hence, it is necessary to explore novel therapeutic strategies and corresponding molecular targets. The lncRNAs, which have a limited protein-coding ability, play critical roles in cancer progression and metastasis.¹⁷ Clinical prediction tools based on lncRNAs have been rapidly developing, including diagnosis, prognostic biomarkers and potential therapeutic targets.⁸ The lncRNA UPK1A-AS1 promoted HCC development and indicated poor prognosis.¹³ Furthermore, lncRNA CASC9 is a potential diagnostic and prognostic biomarker for HCC.¹⁸ However, these studies only assessed the prognostic value of a single biomarker. Since genes are interactive, a single biomarker may not be enough to accurately predict the prognosis of HCC.

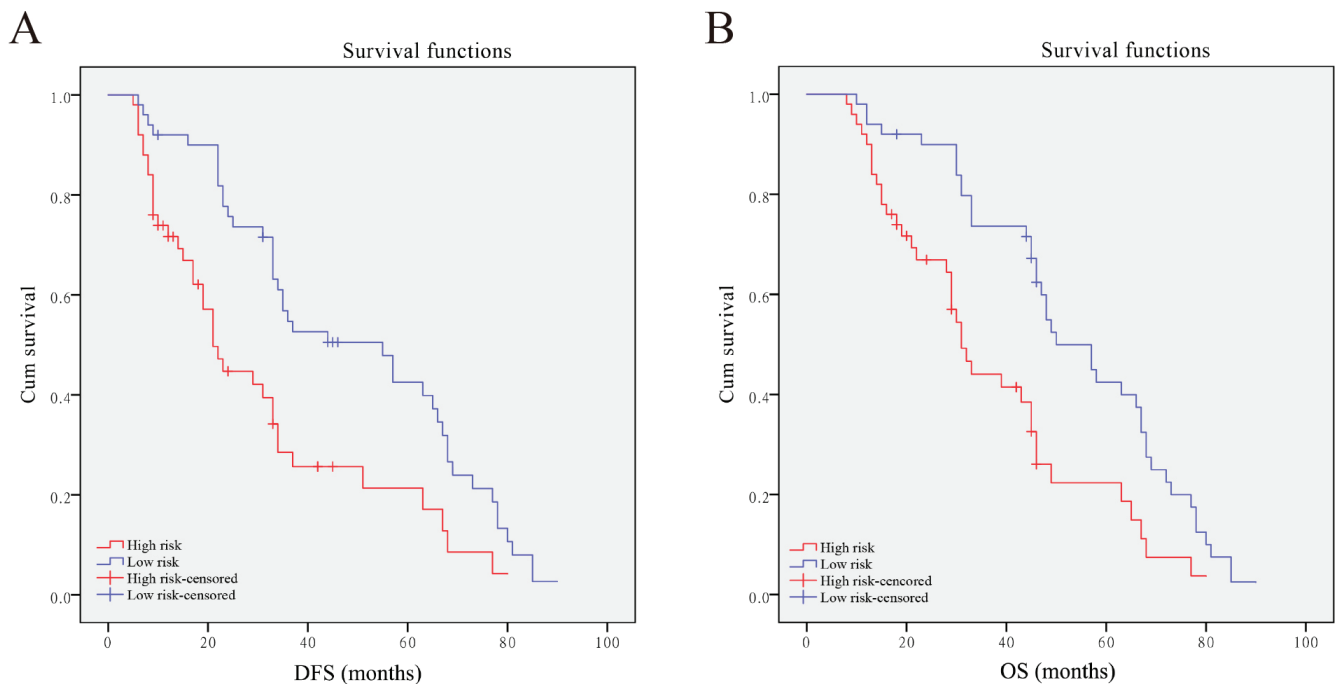


Fig. 5. Kaplan–Meier curves for disease-free survival (DFS) and overall survival (OS). A. DFS curves of 120 hepatocellular carcinoma (HCC) patients stratified by 4-long non-coding RNAs (lncRNAs) expression model ($p = 0.01$); B. OS curves of 120 HCC patients stratified by 4-lncRNA expression model ($p = 0.01$)

In this study, transcriptome and survival data of patients with HCC were obtained from TCGA and used as a training set. In order to improve the predictive accuracy of the regression model, Cox and LASSO regressions were used to evaluate the correlation between the expression of lncRNAs and survival of HCC patients. Finally, a 4-lncRNA combined prediction model was obtained, using lncRNAs AP000844.2, LINC00942, SRGAP3-AS2, and AC010280.2. Clinical data from patients in our hospital were used as a validation set. The AC010280.2 and LINC00942 are long intergenic non-coding RNAs. It has been previously reported that LINC00942 could act as an oncogene that promoted METTL14-mediated m⁶A methylation in breast cancer.¹⁹ The *LINC00942* gene had been recorded to be missing in an autism spectrum disorder patient.²⁰ It had been found that AC010280.2 could participate in establishing the HCC prognosis model.²¹ The AP000844.2 and SRGAP3-AS2 are antisense lncRNAs, and AP000844.2 might be the component of prostate cancer²² and hepatitis virus-positive HCC²³ prognostic models. The SRGAP3-AS2 is also expressed in lung adenocarcinoma²⁴ and could serve as a potential predictive biomarker for that disease.

Both the AUC and C-index demonstrated that our model has good predictive efficacy. The validation set also confirmed the prognostic validity of the model. Although some studies have used LASSO regression to analyze the prognosis of HCC data and obtained a prediction model, the predictive efficacy of this model has not been verified by a validation set.²¹ For the first time, we established a prediction model of HCC-related lncRNAs based on the LASSO analysis and verified its clinical efficacy. The LASSO analysis is a classic regression analysis method

related to statistics and machine learning^{25,26} aimed at improving the prediction accuracy and interpretability through variable selection and regularization compared with other regression methods. The evaluation process of LASSO regression includes the relation with ridge regression, the selection of optimal subset, and the relation between LASSO coefficient estimation and soft threshold.^{27,28} The validation set confirmed that the 4-lncRNA combined prediction model was an independent risk factor for HCC prognosis.

Limitations

This study has 3 limitations. First, it is limited to a single center, and it is still necessary to expand the sample size in order to verify our results in multiple centers. Second, our follow-up research goal was to integrate our model with clinical data to form a comprehensive quantitative index. Finally, the molecular mechanism of each lncRNA needs to be further explored in subsequent experiments.

Conclusions

Through the analysis of public databases and verification of clinical data from our center, we have obtained a 4-lncRNA combined prediction model. The model could effectively evaluate the prognosis of HCC patients. Currently, the TNM staging system is still the most important indicator for evaluating tumor malignancy and prognosis. However, the role of the molecular signature of tumors

Table 2. Patient characteristics and log-rank (Mantel–Cox) analysis

Characteristics	N	DFS			OS		
		month	p-value	F	month	p-value	F
Age							
≥55	57	38.36	0.436	0.606	44.64	0.417	0.59
<55	43	43.61			47.75		
Gender							
Male	57	38.89	0.654	0.201	44.46	0.534	0.386
Female	43	42.74			47.70		
AFP [μg/L]							
<20	52	46.29	0.144	2.130	50.15	0.200	1.644
≥20	48	35.36			42.47		
HbsAg							
Positive	64	38.49	0.316	1.005	44.56	0.308	1.039
Negative	36	44.72			48.68		
Cirrhosis							
Present	56	38.73	0.645	0.213	43.94	0.485	0.487
Absent	44	42.84			48.25		
Tumor size							
≥5 cm	53	34.93	0.015	5.939	40.42	0.013	6.123
<5 cm	47	46.12			51.32		
Tumor number							
Multiple	43	32.07	0.010	6.718	40.44	0.010	6.683
Solitary	57	44.99			48.90		
Tumor stage							
III–IV	62	28.23	<0.001	26.480	34.49	<0.001	30.534
I–II	38	56.60			60.83		
Vascular invasion							
Yes	41	32.14	0.019	5.511	37.71	0.010	6.556
No	59	46.55			51.56		
Capsule							
Absence	36	47.73	0.023	5.199	52.91	0.008	6.946
Presence	64	35.11			40.35		
Distant metastasis							
Absence	50	30.21	0.001	11.609	36.09	<0.001	14.364
Presence	50	49.10			54.07		
Model							
High risk	49	25.18	<0.001	30.760	31.42	<0.001	33.837
Low risk	51	52.85			57.31		

DFS – disease-free survival; OS – overall survival; AFP – alpha-fetoprotein; HbsAg – hepatitis B surface antigen.

Table 3. Multivariate Cox regression analysis of significant prognostic factor for survival in HCC patients

Variables	DFS			OS		
	p-value	HR	95% CI	p-value	HR	95% CI
Tumor number	0.939	0.979	0.572–1.77	0.547	1.189	0.678–2.085
Tumor stage	<0.001	0.330	0.179–0.607	<0.001	0.276	0.145–0.526
Vascular invasion	0.123	0.686	0.424–1.108	0.051	0.619	0.383–1.002
Capsule	0.571	1.169	0.681–2.009	0.385	1.274	0.737–2.202
Distant metastasis	0.085	0.615	0.354–1.069	0.029	0.540	0.311–0.940
Risk score	<0.001	0.359	0.209–0.616	<0.001	0.301	0.172–0.527

DFS – disease-free survival; OS – overall survival; HR – hazard ratio; 95% CI – 95% confidence interval; HCC – hepatocellular carcinoma.

cannot be ignored. For example, Ki-67 indicates proliferation and Her-2 indicates the degree of malignancy. Microsatellite instability (MSI) and tumor mutational burden (TMB) are also beacons for treatment options. We believe that a further improvement of molecular stratification and the application of prognostic markers can provide valuable information for tumor treatment. In addition, even though the expression of molecules still needs to be obtained from tissue samples, if, with the advancement of liquid biopsy technology, we can detect these molecules in the body fluid, their expression changes may indicate tumor recurrence and metastasis.

ORCID iDs

Xiangxiu Qi  <https://orcid.org/0000-0001-7569-165X>

Cui Xu  <https://orcid.org/0000-0002-2251-6150>

References

- Siegel RL, Miller KD, Jemal A. Cancer statistics, 2020. *CA Cancer J Clin*. 2020;70(1):7–30. doi:10.3322/caac.21590
- Tsuchiya N. Biomarkers for the early diagnosis of hepatocellular carcinoma. *World J Gastroenterol*. 2015;21(37):10573–10583. doi:10.3748/wjg.v21.i37.10573
- Pillai A, Ahn J, Kulik L. Integrating genomics into clinical practice in hepatocellular carcinoma: The challenges ahead. *Am J Gastroenterol*. 2020;115(12):1960–1969. doi:10.14309/ajg.0000000000000843
- Trevisan França de Lima L, Broszczak D, Zhang X, Bridle K, Crawford D, Punyadeera C. The use of minimally invasive biomarkers for the diagnosis and prognosis of hepatocellular carcinoma. *Biochim Biophys Acta Rev Cancer*. 2020;1874(2):188451. doi:10.1016/j.bbcan.2020.188451
- Singal AG, Lok AS, Feng Z, Kanwal F, Parikh ND. Conceptual model for the hepatocellular carcinoma screening continuum: Current status and research agenda. *Clin Gastroenterol Hepatol*. 2022;20(1):9–18. doi:10.1016/j.cgh.2020.09.036
- Xiao Y, Hu J, Yin W. Systematic identification of non-coding RNAs. In: Li X, Xu J, Xiao Y, Ning S, Zhang Y, eds. *Non-Coding RNAs in Complex Diseases*. Vol 1094. Advances in Experimental Medicine and Biology. Singapore, Singapore: Springer Singapore; 2018:9–18. doi:10.1007/978-981-13-0719-5_2
- Delaunay S, Frye M. RNA modifications regulating cell fate in cancer. *Nat Cell Biol*. 2019;21(5):552–559. doi:10.1038/s41556-019-0319-0
- Evans JR, Feng FY, Chinnaiyan AM. The bright side of dark matter: lncRNAs in cancer. *J Clin Invest*. 2016;126(8):2775–2782. doi:10.1172/JCI84421
- Chu C, Lei X, Li Y, et al. High expression of miR-222-3p in children with *Mycoplasma pneumoniae* pneumonia. *Ital J Pediatr*. 2019;45(1):163. doi:10.1186/s13052-019-0750-7
- Qian X, Zhao J, Yeung PY, Zhang QC, Kwok CK. Revealing lncRNA structures and interactions by sequencing-based approaches. *Trends Biochem Sci*. 2019;44(1):33–52. doi:10.1016/j.tibs.2018.09.012
- Peng WX, Koirala P, Mo YY. lncRNA-mediated regulation of cell signaling in cancer. *Oncogene*. 2017;36(41):5661–5667. doi:10.1038/nc.2017.184
- Xie C, Li SY, Fang JH, Zhu Y, Yang JE. Functional long non-coding RNAs in hepatocellular carcinoma. *Cancer Lett*. 2021;500:281–291. doi:10.1016/j.canlet.2020.10.042
- Zhang DY, Sun QC, Zou XJ, et al. Long noncoding RNA UPK1A-AS1 indicates poor prognosis of hepatocellular carcinoma and promotes cell proliferation through interaction with EZH2. *J Exp Clin Cancer Res*. 2020;39(1):229. doi:10.1186/s13046-020-01748-y
- Yi T, Luo H, Qin F, et al. lncRNA LL22NC03-N14H11.1 promoted hepatocellular carcinoma progression through activating MAPK pathway to induce mitochondrial fission. *Cell Death Dis*. 2020;11(10):832. doi:10.1038/s41419-020-2584-z
- Gao H, Li L, Xiao M, et al. Elevated DKK1 expression is an independent unfavorable prognostic indicator of survival in head and neck squamous cell carcinoma. *Cancer Manag Res*. 2018;10:5083–5089. doi:10.2147/CMAR.S177043
- Wu Q, Pi L, Le Trinh T, et al. A novel vaccine targeting glypican-3 as a treatment for hepatocellular carcinoma. *Mol Ther*. 2017;25(10):2299–2308. doi:10.1016/j.jymthe.2017.08.005
- Sahu A, Singhal U, Chinnaiyan AM. Long noncoding RNAs in cancer: From function to translation. *Trends Cancer*. 2015;1(2):93–109. doi:10.1016/j.trecan.2015.08.010
- Zeng YL, Guo ZY, Su HZ, Zhong FD, Jiang KQ, Yuan GD. Diagnostic and prognostic value of lncRNA cancer susceptibility candidate 9 in hepatocellular carcinoma. *World J Gastroenterol*. 2019;25(48):6902–6915. doi:10.3748/wjg.v25.i48.6902
- Sun T, Wu Z, Wang X, et al. LNC942 promoting METTL14-mediated m6A methylation in breast cancer cell proliferation and progression. *Oncogene*. 2020;39(31):5358–5372. doi:10.1038/s41388-020-1338-9
- Silva IMW, Rosenfeld J, Antoniuk SA, Raskin S, Sotomaior VS. A 1.5Mb terminal deletion of 12p associated with autism spectrum disorder. *Gene*. 2014;542(1):83–86. doi:10.1016/j.gene.2014.02.058
- Li W, Chen QF, Huang T, Wu P, Shen L, Huang ZL. Identification and validation of a prognostic lncRNA signature for hepatocellular carcinoma. *Front Oncol*. 2020;10:780. doi:10.3389/fonc.2020.00780
- Liu S, Wang W, Zhao Y, Liang K, Huang Y. Identification of potential key genes for pathogenesis and prognosis in prostate cancer by integrated analysis of gene expression profiles and the cancer genome atlas. *Front Oncol*. 2020;10:809. doi:10.3389/fonc.2020.00809
- Huang ZL, Li W, Chen QF, Wu PH, Shen LJ. Eight key long non-coding RNAs predict hepatitis virus positive hepatocellular carcinoma as prognostic targets. *World J Gastrointest Oncol*. 2019;11(11):983–997. doi:10.4251/wjgo.v11.i11.983
- Yang Z, Li H, Wang Z, et al. Microarray expression profile of long non-coding RNAs in human lung adenocarcinoma: lncRNA expression in LAD. *Thorac Cancer*. 2018;9(10):1312–1322. doi:10.1111/1759-7714.12845
- Santosa F, Symes WW. Linear inversion of band-limited reflection seismograms. *SIAM J Sci Stat Comput*. 1986;7(4):1307–1330. doi:10.1137/0907087
- Tibshirani R. Regression shrinkage and selection via the lasso: A retrospective. *J Royal Statist Soc B Statist Methodol*. 2011;73(3):273–282. doi:10.1111/j.1467-9868.2011.00771.x
- Tibshirani R. The Lasso method for variable selection in the Cox model. *Statist Med*. 1997;16(4):385–395. doi:10.1002/(SICI)1097-0258(19970228)16:4<385::AID-SIM380>3.0.CO;2-3
- Liu Y, Wu W, Hong S, et al. Lasso proteins: Modular design, cellular synthesis, and topological transformation. *Angew Chem Int Ed*. 2020;59(43):19153–19161. doi:10.1002/anie.202006727

A prognostic signature based on the expression profile of the ferroptosis-related long non-coding RNAs in hepatocellular carcinoma

Xixi Lin^{1,2,C,D}, Sijie Yang^{3,A–C,E,F}

¹ Division of Experimental Radiation Biology, Department of Radiation Therapy, University Hospital Essen, University of Duisburg-Essen, Germany

² Department of Radiotherapy, Second Affiliated Hospital of Guangxi Medical University, Nanning, China

³ Collaborative Innovation Centre of Regenerative Medicine and Medical BioResource Development and Application Co-constructed by the Province and Ministry, Guangxi Medical University, Nanning, China

A – research concept and design; B – collection and/or assembly of data; C – data analysis and interpretation; D – writing the article; E – critical revision of the article; F – final approval of the article

Advances in Clinical and Experimental Medicine, ISSN 1899–5276 (print), ISSN 2451–2680 (online)

Adv Clin Exp Med. 2022;31(10):1099–1109

Address for correspondence

Sijie Yang

E-mail: Yangsijiemdj@sina.com

Funding sources

None declared

Conflict of interest

None declared

Received on January 17, 2022

Reviewed on April 19, 2022

Accepted on April 28, 2022

Published online on May 18, 2022

Cite as

Lin X, Yang S. A prognostic signature based on the expression profile of the ferroptosis-related long non-coding RNAs in hepatocellular carcinoma *Adv Clin Exp Med.* 2022;31(10):1099–1109. doi:10.17219/acem/149566

DOI

10.17219/acem/149566

Copyright

Copyright by Author(s)

This is an article distributed under the terms of the Creative Commons Attribution 3.0 Unported (CC BY 3.0) (<https://creativecommons.org/licenses/by/3.0/>)

Abstract

Background. Ferroptosis is a special form of cell death with extensive biological associations with various cancers; however, the role of aberrantly expressed ferroptosis-related long non-coding RNAs (lncRNAs) in hepatocellular carcinoma (HCC) remains unclear.

Objectives. To explore the role and prognostic value of ferroptosis-related lncRNAs in HCC and to screen potential therapeutic targets.

Materials and methods. The RNA-seq data for 424 HCC patients and clinical data for 377 HCC patients were obtained from The Cancer Genome Atlas (TCGA) and evaluated using the Pearson's test to identify differentially expressed lncRNAs. The univariate analysis, least absolute shrinkage and selection operator Cox regression analysis were performed to construct and validate a prognostic risk-score model. The prognostic capacity was evaluated using the Kaplan–Meier method, univariate and multivariate Cox regression, and receiver operating characteristic (ROC) curve analyses. The enrichment analysis was performed to explore the functions of ferroptosis-related lncRNAs from the perspective of tumor immunology.

Results. Seventeen differentially expressed lncRNAs were identified (*AL139384.1*, *AL928654.1*, *MKLN1-AS*, *AC145207.8*, *LINC00205*, *ZFPM2-AS1*, *LINC00942*, *POLH-AS1*, *AC090772.3*, *AL603839.3*, *AC012073.1*, *AC099850.1*, *AC026401.3*, *AP001469.3*, *AL031985.3*, *SNHG10*, *SNHG21*) to establish the risk-score model. Survival analyses demonstrated poorer survival in high-risk patients, and the risk score was shown to be a better independent prognostic factor than conventional clinical characteristics. Additionally, we found close correlations between the risk score and immune cell subpopulation functions, as well as between the expression of immune checkpoint and carcinogenic N6-methyladenosine (m6A)-related mRNAs.

Conclusions. The novel ferroptosis-related lncRNA signature may serve as an individualized prognostic prediction tool for patients with HCC.

Key words: immune response, hepatocellular carcinoma, long non-coding RNA, ferroptosis, genes

Background

Hepatocellular carcinoma (HCC) is the main subtype of primary liver cancer and the 4th most common cause of cancer-related deaths worldwide.¹ The incidence of HCC in USA increased from 4.4/100,000 in 2000 to 6.7/100,000 in 2012.² Multidisciplinary treatment strategies have greatly improved the efficacy of HCC treatment, while novel immunotherapy and molecular targeted therapies, such as programmed cell death protein 1 inhibitors, have shown promising results in selected patients.^{3,4} However, the survival outcomes of patients with advanced HCC remain poor, with a 5-year overall survival (OS) rate <30%.^{5,6} Thus, there is a need to identify novel potential therapeutic targets and accurate prognostic biomarkers at the gene level.

Mounting evidence has indicated the involvement of ferroptosis, a special mode of programmed cell death, in several pathophysiological processes of HCC.⁷ Ferroptosis is characterized by the over-accumulation of lethal reactive oxygen species (ROS) and production of lipid peroxides,⁸ and has shown suppressive effects in head and neck, colorectal and ovarian cancer.^{9–11} In the context of HCC, ferroptosis induced by the multikinase inhibitor sorafenib and its potential targets has attracted the attention of researchers. Louandre et al. demonstrated that the deactivation of retinoblastoma protein has increased the efficacy of sorafenib in HCC by exacerbating ferroptosis, both in vitro and in vivo.¹² Additionally, Sun et al. found that the expression of metallothionein-1G after sorafenib treatment contributed to drug resistance and negatively regulated ferroptosis.¹³ The increasing appreciation of the importance of ferroptosis in terms of the pathogenesis and treatment of HCC highlights the need to understand the mechanisms underlying ferroptosis-related genetic alterations in HCC.

Long non-coding RNAs (lncRNAs) perform a wide range of regulatory functions at the gene expression level. They have been shown to play a vital role in promoting the progression of HCC through the involvement in proliferative signaling, invasion and metastasis, angiogenesis, as well as immune escape.¹⁴ Recent studies have indicated the potential role of lncRNAs in regulating ferroptotic cell death in relation to cancer biology. For example, the overexpression of lncRNA *H19* was reported to function as a competing endogenous RNA to enhance the activity of ferroptosis.¹⁵ These findings suggest that the ferroptosis–lncRNA relationship may have relevant and important functions in terms of prognostic prediction and treatment in patients with HCC.

Objectives

The role of ferroptosis-related lncRNAs is currently not fully understood and sequence-based systematic evaluations has been limited. We therefore aimed to explore

the role and prognostic value of ferroptosis-related lncRNAs in HCC by constructing a lncRNA signature based on the Cancer Genome Atlas (TCGA), thereby screening potential targets for HCC treatment.

Materials and methods

Data collection

Transcriptome data for 424 HCC patients (374 tumor and 50 non-cancerous (normally differentiated)) and clinicopathological data for 377 HCC patients (age, sex, tumor grade, TNM stage, follow-up time, and survival outcome) were obtained from the TCGA-HCC database up to October 1, 2021. The clinical characteristics of patients are shown in Table 1. The corresponding ferroptosis-related genes were downloaded from FerrDb database (<http://www.zhounan.org/ferrdb/>; the first database dedicated to ferroptosis regulators and ferroptosis-disease associations).¹⁶ Free data on gene regulators, including drivers, suppressors and markers, could be downloaded for further management and investigation. We identified a total of 382 genes (drivers: 150; suppressors: 109; markers: 123; detailed data given in Supplementary Table 1). The correlations between lncRNAs and HCC were analyzed using the Pearson's test. We first evaluated the functions of the ferroptosis-related differentially expressed genes (DEGs), and then assessed the related biological pathways with Gene Ontology analysis, and analyzed biological processes (BP), molecular functions (MF), and cellular components (CC) regulated by the DEGs using Kyoto Encyclopedia of Genes and Genomes (KEGG) analysis, using R software (ggplot2 package; R Foundation for Statistical Computing, Vienna, Austria).

Table 1. Clinical characteristics of patients in The Cancer Genome Atlas (TCGA) dataset

Variable	Number of samples
Gender (male/female)	255/122
Age [years] (<=65/>65/NA)	235/141/1
Grade (G1/G2/G3/G4/NA)	55/180/124/13/5
Stage (I/II/III/IV/NA)	175/87/86/5/24
T (T1/T2/T3/T4/NA)	185/95/81/13/3
M (M0/M1/NA)	272/4/101
N (N0/N1/NA)	257/4/116

NA – not applicable.

Construction of ferroptosis-related lncRNA prognostic signature

We identified the ferroptosis-related lncRNA signature using univariate Cox regression analyses, least absolute shrinkage and selection-penalized Cox regression.

The risk scores were calculated as the sum of coefficient lncRNA \times expression of lncRNA. The HCC patients were divided into high-risk and low-risk group according to the median risk score, and we compared the OS between the 2 groups using the Kaplan–Meier analysis, and evaluated the prognostic capacity of the risk-score model using receiver operating characteristic (ROC) curves.

Gene set enrichment analysis and predictive nomogram

We performed gene set enrichment analysis (GSEA) to assess the enriched pathways and to define the lncRNA signature with the KEGG gene set. A nomogram combining the prognostic signatures was created to predict the 1-, 3- and 5-year OS of HCC patients.

Gene expression and immunity analysis

We compared the TMER, CIBERSORT, CIBERSORT-ABS, QUANTISEQ, MCPOUNTER, XCELL, EPIC, and single-sample GSEA (ssGSEA) algorithms (<http://timer.comp-genomics.org/>) to estimate cellular immune responses and cellular components between the low-risk and high-risk group according to the risk score. The tumor-infiltrating immune cell subgroups were quantified using ssGSEA and the immunological functions were assessed. A box diagram was used to assess the differential expression of N6-methyladenosine (m6A)-related genes.

Statistical analyses

Data were analyzed using Bioconductor packages (R software v. 4.1.0; R Foundation for Statistical Computing). Gene expression was compared between normal and HCC tissues using the Wilcoxon test, and correlations between lncRNAs and HCC were analyzed using the Pearson's test (correlation coefficient $R^2 > 0.4$ at $p < 0.01$). We identified the differential expression of lncRNAs using the Benjamini–Hochberg method, with the criteria of a false discovery rate <0.05 and \log^2 fold change ≥ 1 . We compared the ssGSEA-normalized HCC DEGs with a genome using the Gene Set Variation Analysis (GSVA) R-package. The sensitivity and specificity of the prognostic signature were assessed using ROC and decision curve analyses,¹⁷ and the associations between lncRNAs and clinical characteristics were evaluated with logistic regression analyses and a heatmap graph. The survival of HCC patients based on the ferroptosis-related signature was evaluated using Kaplan–Meier survival analysis with a 2-sided log-rank test. Additionally, immune cell infiltration, immune checkpoint and m6A-related gene expression were compared between the groups using Wilcoxon test. Statistical significance was set at $p < 0.05$ unless otherwise noted.

Results

Enrichment analysis of ferroptosis-related genes

We identified 84 ferroptosis-related DEGs, including 71 upregulated and 13 downregulated genes, using KEGG-based analysis. Among these, BP-related genes were involved with organic acid transport and oxidative stress reaction, as well as changes in nutrient levels, toxic substances and extracellular stimuli. The CC-related genes were primarily related to the nicotinamide adenine dinucleotide phosphate hydrate (NADPH) oxidase complex, apical plasma membrane synthesis pathway, lysosomes, and melanin granules, while the MF were connected to the regulation of NADPH production, along with the binding of molecular oxygen and ferric iron (Supplementary Figure 1A). The KEGG-based analysis indicated that the overexpressed genes were commonly involved in ferroptosis, hypoxia-inducible factor-1 (HIF-1) signaling pathway, multiple cancers, synthesis of microRNAs in cancer cells, diabetes, atherosclerosis, viral infection, endocrine system, cell senescence, leukemia, and the mechanistic target of rapamycin signaling pathway (Supplementary Figure 1B).

Prognostic signature of ferroptosis-based lncRNAs

A total of 781 ferroptosis-related lncRNAs, including 17 downregulated and 764 upregulated lncRNAs, were found. Sixty-six significant ferroptosis-related lncRNAs that were incorporated into the multivariate Cox analysis were also analyzed using the univariate Cox analysis. Seventeen differentially expressed lncRNAs were finally confirmed as independent prognosis predictors of HCC: *AL139384.1*, *AL928654.1*, *MKLN1-AS*, *AC145207.8*, *LINC00205*, *ZFPM2-AS1*, *LINC00942*, *POLH-AS1*, *AC090772.3*, *AL603839.3*, *AC012073.1*, *AC099850.1*, *AC026401.3*, *AP001469.3*, *AL031985.3*, *SNHG10*, and *SNHG21* (Supplementary Table 2). The network diagram shows the relationship between mRNAs and lncRNAs (Supplementary Figure 1C). On the basis of these findings, we established risk scores and prognostic signatures for the lncRNAs.

Survival results and multivariate analysis

The Kaplan–Meier analysis indicated that the expression of a high-risk lncRNA signature was related to lower survival outcomes ($p < 0.001$; Fig. 1A). Similar results were obtained in a subgroup analysis according to tumor stage (Supplementary Figure 2A). The area under the ROC curve for the lncRNA signature was higher than those for the clinical indices (Fig. 1B) in all patients, and in subgroups according to tumor stage (Supplementary Figure 2B). The risk survival status plot (Fig. 1C) verified

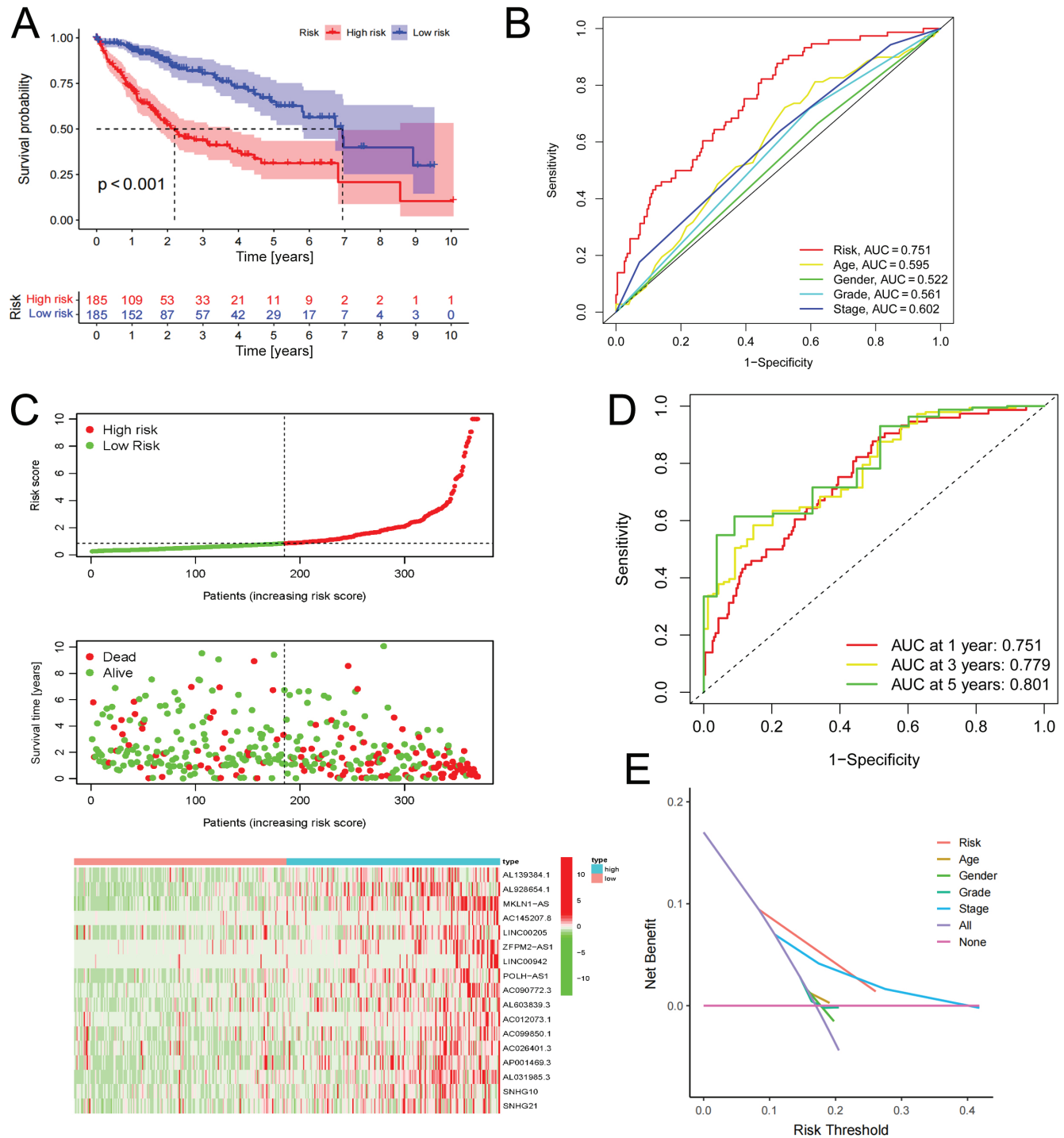


Fig. 1. Ferroptosis-related long non-coding RNAs (lncRNAs) signature based on The Cancer Genome Atlas (TCGA). A. Kaplan–Meier curves result. Curves were compared using the log-rank test, hazard ratio (HR) = 3.187 (95% confidence interval (95% CI): 2.245–4.523), $p = 5.621 \times 10^{-11}$; B. The area under the curve (AUC) values of the risk factors in predicting 1-year survival of hepatocellular carcinoma (HCC); C. Risk survival status plot. The high-risk group was related to low survival, and the novel lncRNAs are positively correlated with the risk score; D. The AUC of predicting 1-, 3- and 5-year OS of HCC patients; E. The decision curve analysis (DCA) of the risk factors

that patients with high-risk scores were prone to low survival outcomes. Additionally, the heatmap demonstrated that most candidate lncRNAs were strongly expressed in the high-risk group (Fig. 1C). Taken together, the current risk model demonstrated that specific ferroptosis-associated lncRNAs provided a useful prognostic signature for HCC.

The areas under the curve for 1-, 3- and 5-year OS rates predicted by the novel lncRNA signature were 0.751, 0.779 and 0.801, respectively (Fig. 1D). The signature still exhibited good specificity and sensitivity when analyzed in relation to HCC stage (Supplementary Figure 2C). The decision curve analysis confirmed that the lncRNA signature performed better predictive

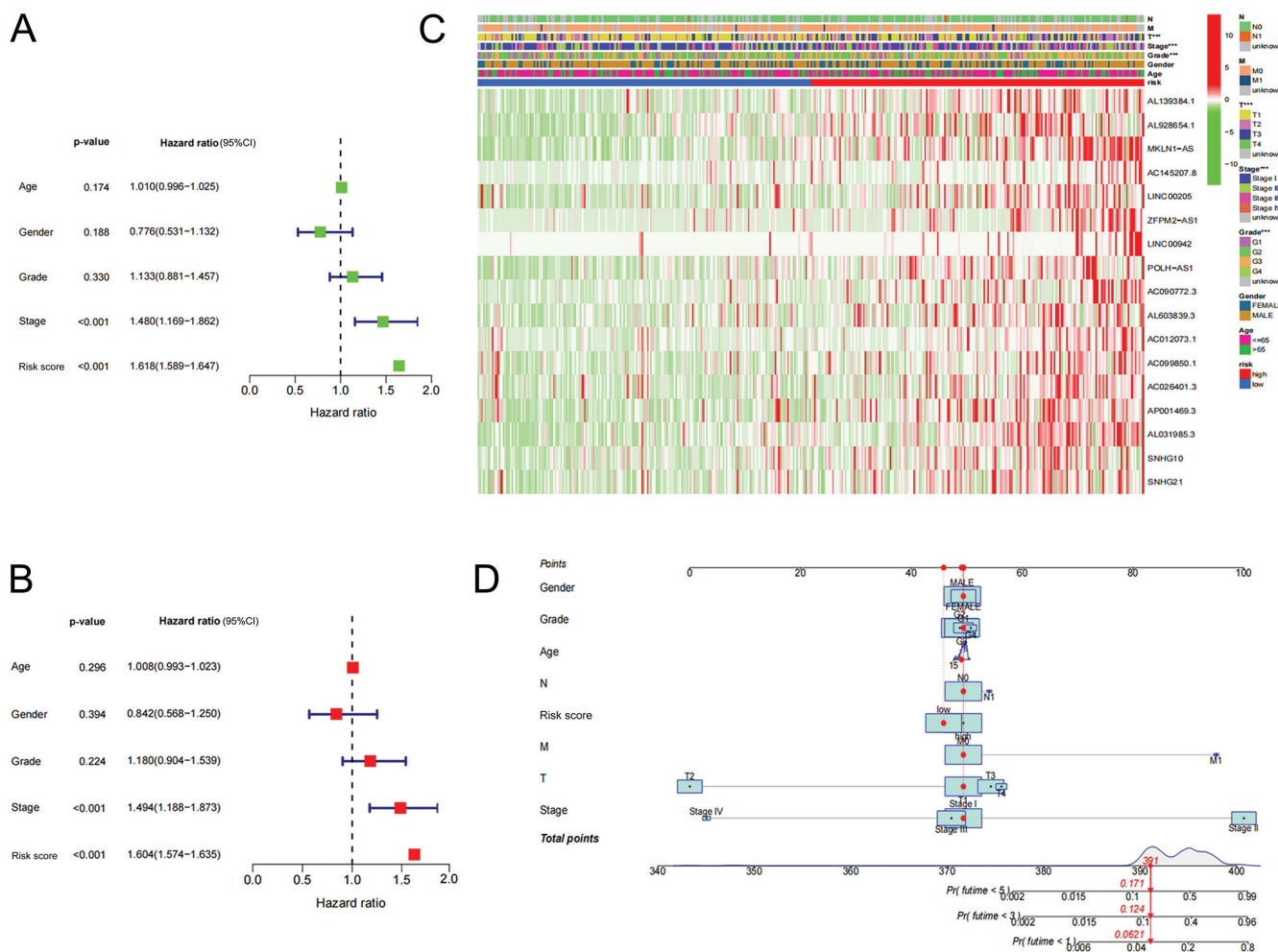


Fig. 2. Univariate (A) and multivariate Cox (B) analyses for the expression of ferroptosis-related long non-coding RNAs (lncRNAs; 95% confidence interval (95% CI)); C. Heatmap for ferroptosis-related lncRNAs prognostic signature and clinical manifestations; D. Nomogram for both clinical manifestations and prognostic ferroptosis-related lncRNAs. The points for each of the 8 variables are obtained by drawing a line upwards from the value of each variable to the points line. The sum of points for the 8 variables is marked in the total points line, and the line drawn perpendicularly downward indicates the probability of survival at 1 year, 3 years and 5 years

ability than other conventional clinical and pathological characteristics (Fig. 1E).

The univariate analysis revealed that lncRNA-based signature (hazard ratio (HR): 1.618, 95% confidence interval (95% CI): 1.589–1.647) together with tumor stage (HR: 1.480, 95% CI: 1.169–1.862) were independent prognostic factors for HCC (Fig. 2A, Supplementary Table 3). The multivariate Cox analysis confirmed that the lncRNA signature was an independent prognostic risk factor for HCC (Fig. 2B, Supplementary Table 3).

Heatmap analyses illustrated the association between the prognostic signature of ferroptosis-related lncRNA and clinical manifestations (Fig. 2C). Predictors in the hybrid nomogram incorporated the risk-score model and clinicopathological characteristics (Fig. 2D).

GSEA

The GSEA revealed that most of the prognostic signatures played roles in metabolism and tumor-related

pathways, including the metabolism of amino acids, salts and drugs (such as β -alanine), butanoate, fatty acids, propanoate, pyruvate, and tryptophan, as well as being involved in the citrate cycle, tricarboxylic acid cycle, complement and coagulation cascades, and the peroxisome proliferator-activated receptor signaling pathway (Supplementary Figure 3).

Immunity and gene expression

We evaluated the immune response using the MCP-COUNTER, XCELL, EPIC, TIMER, CIBERSORT, CIBERSORT-ABS, and QUANTISEQ algorithms to determine the association between the ferroptosis-related lncRNA signature and tumor immunity (Fig. 3A). The heatmap demonstrated that macrophage and T cell functions were relatively active in the high-risk group. We further investigated the association between immune cell subpopulations and their related functions, and found that the immune cell functions of antigen-presenting cell (APC) co-inhibition, chemokine

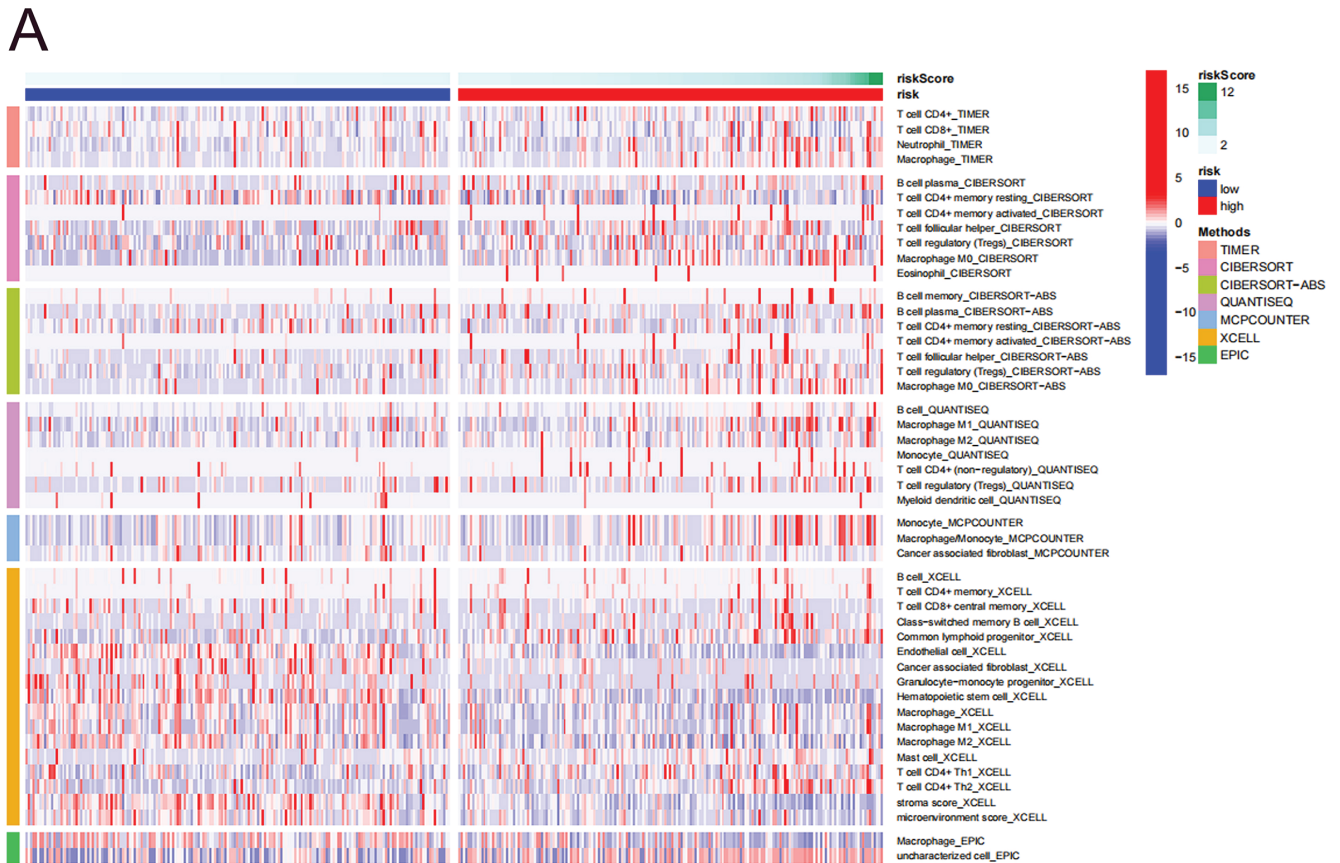


Fig. 3. A. Heatmap for immune responses in the high-risk and low-risk group; B. Single sample gene set enrichment analysis (ssGSEA) for the association between immune cell subpopulations and related functions

* $p < 0.05$, ** $p < 0.01$, *** $p < 0.001$. The boxes show the middle scores ranging between the 25th and 75th percentile. The upper and lower whiskers represent scores outside the middle 50% (i.e., the lower 25% of scores and the upper 25% of scores). Values outside this range are considered to be outliers and are represented by dots; APC – antigen-presenting cell; CCR – chemokine receptor; HLA – human leukocyte antigen; MHC – major histocompatibility complex.

receptor (CCR), checkpoint, cytolytic activity, inflammation-promoting, T cell co-inhibition/stimulation, and type II interferon response differed significantly between the high-risk and low-risk group (Fig. 3B, Supplementary Table 4).

Because immune checkpoint inhibition is an important clinical therapeutic strategy in HCC, we also compared the expression of immune checkpoints between the 2 groups.^{3,4} All selected immune checkpoints showed

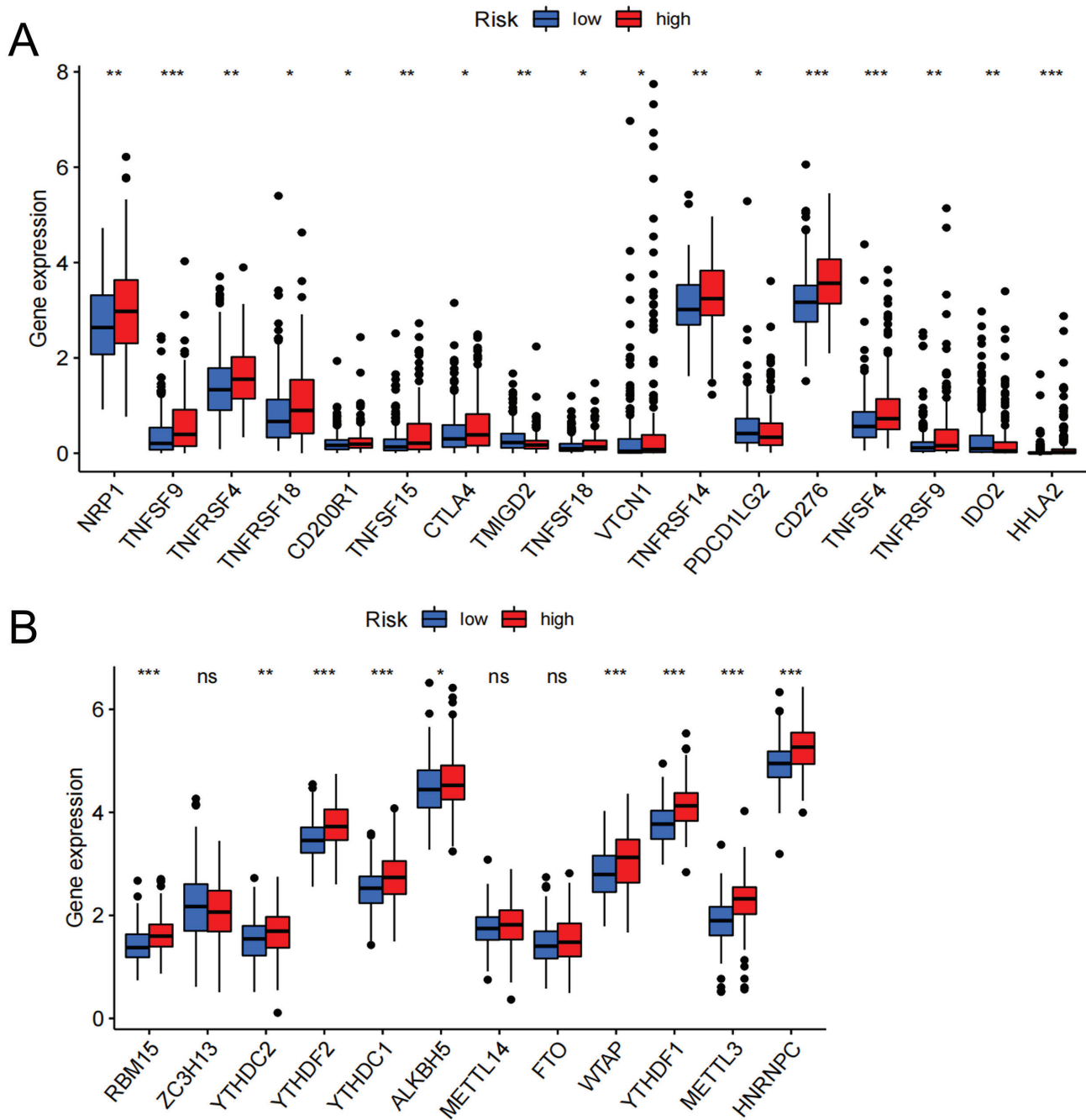


Fig. 4. A. Expression of immune checkpoints in the high-risk and low-risk group; B. The expression of N6-methyladenosine (m6A)-related genes in the high-risk and low-risk group

* $p < 0.05$, ** $p < 0.01$, *** $p < 0.001$. The boxes show the middle scores ranging between the 25th and 75th percentile. The upper and lower whiskers represent scores outside the middle 50%. Values outside this range are considered to be outliers and are represented by dots.

a significantly differential expression between the 2 groups (Fig. 4A, Supplementary Table 5). Notably, the expression levels of the tumor necrosis factor superfamily (TNFSF)/TNF receptor superfamily (TNFRSF) signaling pathways were all higher in the high-risk group, as compared with the low-risk group.

The m6A as the cofactor of lncRNAs in regulating post-transcriptional modifications has recently come to the spotlight in lncRNA studies.¹⁸ We compared the m6A-related mRNA status between the 2 groups and

found that the expression levels of *RBM15*, *YTHDF1/2*, *ALKBH5*, *WTAP*, *METTL3*, *HNRNPC*, and *YTHDC1/2* were all significantly higher in the high-risk group (Fig. 4B, Supplementary Table 6).

Discussion

The poor survival and high recurrence rate of HCC have highlighted the need for effective prognostic biomarkers

and therapeutic targets. In this study, we constructed a novel ferroptosis-related lncRNA prognostic risk model and explored the roles of the relevant lncRNAs in the immune response and checkpoint regulation in HCC. These findings allowed us to screen possible ferroptosis-related biomarkers and treatment targets, which might inform the development of new therapeutic approaches.

The prognostic model in our study integrated 17 ferroptosis-related lncRNAs. A subset of lncRNAs (*MKLN1-AS*, *LINC00205*, *ZFPM2-AS1*) was reported to be involved in several HCC cellular activities, including cell proliferation, migration and invasion, cell cycle progression, and apoptosis, through microRNAs, signaling pathways and other biological components or proteins (Table 2). Notably, the biological functions of some of the identified lncRNAs

(*LINC00205*, *ZFPM2-AS1*, *LINC00942*) have also been associated with other malignancies and might thus be non-specific to HCC.^{22–24,27–30,33,34} However, numerous other lncRNAs (*AL139384.1*, *AL928654.1*, *AC145207.8*, *POLH-AS1*, *AC090772.3*, *AL603839.3*, *AC012073.1*, *AC099850.1*, *AC026401.3*, *AP001469.3*, *AL031985.3*, *SNHG10*, *SNHG21*) lack corresponding basic studies to validate their prognostic roles in the development of HCC. Further studies are therefore needed to establish the associations of these identified lncRNAs with ferroptosis and their contribution to the regulation of HCC pathogenesis through ferroptosis.

Based on the risk-score method, the ferroptosis-related lncRNA signature classified HCC patients into high-risk and low-risk groups, with significantly different OS rates. Both univariate and multivariate Cox regression analyses

Table 2. Biological functions of identified long non-coding RNAs (lncRNAs) in ferroptosis, hepatocellular carcinoma (HCC) and other cancer pathologies

Identified lncRNAs	In other cancer pathology	In HCC pathology
MKLN1-AS	–	<ul style="list-style-type: none"> mediates the effects of SOX9 on the proliferation and EMT of HCC cells¹⁹; enhances tumor growth in vivo through regulating miR-22-3p/ETS1 axis²⁰; positively modulates YAP1 expression and intensifies the proliferation, migration and invasion of HCC cells.²¹
LINC00205	<ul style="list-style-type: none"> enhances hepatoblastoma progression by regulating <i>ROCK1</i> expression via sponging miR-154-3p through MAPK signaling²²; promotes tumorigenesis and metastasis by competitively suppressing miRNA-26a in gastric cancer²³; facilitates malignant phenotypes in lung cancer by recruiting FUS to stabilize CSDE1.²⁴ 	<ul style="list-style-type: none"> activated by YY-1, facilitates the proliferation of HCC cells through YY1/miR-26a-5p/CDK6²⁵; enhances tumorigenicity of HCC cells through modulating EPHX1 and inhibiting miR-184.²⁶
ZFPM2-AS1	<ul style="list-style-type: none"> promotes retinoblastoma progression by targeting miR-511-3p/PAX6 axis²⁷; exerts oncogenic effect in cutaneous malignant melanoma progression via targeting miR-650/NOTCH1 signaling²⁸; promotes esophageal squamous cell carcinoma (ESCC) cell growth and upregulates TRAF4 to trigger NF-κB pathway by sequestering miR-3612²⁹; regulates gastric cancer progression via protecting the degradation of MIF and destabilizing p53.³⁰ 	<ul style="list-style-type: none"> promotes proliferation, migration and invasion by adsorbing miR-576-3p and upregulating HIF-1α³¹; enhances the progression of HCC by competitively binding to miR-139 and downregulating the expression of <i>GDF10</i>.³²
LINC00942	<ul style="list-style-type: none"> recruits METTL14 to stabilize CXCR4 and CYP1B1 through methylation modification in breast cancer cell proliferation and progression³³; accelerates chemoresistance in gastric cancer by suppressing MSI2 degradation to stabilize c-Myc mRNA.³⁴ 	–
AL139384.1	–	–
AL928654.1	–	–
AC145207.8	–	–
POLH-AS1	–	–
AC090772.3	–	–
AL603839.3	–	–
AC012073.1	–	–
AC099850.1	–	–
AC026401.3	–	–
AP001469.3	–	–
AL031985.3	–	–
SNHG10	–	–
SNHG21	–	–

EMT – epithelial–mesenchymal transition; MIF – macrophage migration inhibitory factor.

identified the risk score as an independent prognostic factor. Additionally, ROC curve and nomogram analyses showed that the risk score had higher sensitivity and better clinical applicability than traditional standards for predicting HCC survival. Furthermore, stratification analyses by stage confirmed the prognostic predictive value of the risk score signature for each tumor stage.

Numerous studies have established the role of the lncRNA prognostic signature for HCC using bioinformatics analysis. The biological processes related to the lncRNAs in the signatures in these studies included pyroptosis,³⁵ hypoxia,³⁶ metabolism,³⁷ and epithelial–mesenchymal transition.³⁸ Chen et al. recently reported a ferroptosis-related signature model that integrated both mRNAs and lncRNAs,³⁹ with outstanding HCC predictive efficiency. Notably, lncRNA *ZFPM2-AS1* was also included in this signature, indicating its strong connection with the development and progression of HCC. In the current study, we focused solely on ferroptosis-related lncRNAs and attempted to explore their role from the perspective of the immune response, immune checkpoints and m6A status.

Mounting evidence has revealed that crosstalk between lncRNAs and immune cells modulates the tumor immune response. However, both immune response and enrichment analyses revealed no significant differences in activities of any immune cell species between the high-risk and low-risk groups. Moreover, levels of all examined immune cell subpopulations were relatively lower in the high-risk group, suggesting a possible regulatory role for lncRNAs in escape from tumor immunity.

Notably, the expression levels of all the immune checkpoints examined in this study were significantly higher in the high-risk group. Among these, TNFSF/TNFRSF signaling pathways showed potential as immunotherapy targets in combination with ferroptosis induction. Interactions among TNFSF/TNFRSF mediate signaling that controls immune cell survival, proliferation and differentiation.⁴⁰ As the most important superfamily member, the function of tumor necrosis factor alpha (TNF- α) in promoting tumor growth and its association with a poor prognosis of HCC have been widely demonstrated, and TNF- α inhibition has accordingly demonstrated appreciable anti-tumor effects in various studies.^{41–44} Therefore, the relationship between ferroptosis and TNF- α signaling, as well as the combined efficacy of TNF- α inhibition and ferroptosis in HCC, warrant further investigation.

The importance of reversible chemical modifications of RNA, particularly methylation, has recently gained a renewed interest. The m6A is the most prevalent form of internal mRNA modification and has been implicated in HCC carcinogenesis.⁴⁵ Accordingly, the current study showed that several m6A-related genes were highly expressed in the high-risk group (*RBM15*, *YTHDF1/2*, *ALKBH5*, *WTAP*, *METTL3*, *HNRNPC*, and *YTHDC1/2*). The *METTL3* was reported to process oncogenic functions

in HCC by promoting m6A modification of the tumor suppressor gene *SOCS2* in a *YTHDF2*-dependent pathway.⁴⁶ At the same time, *METTL3* was shown to work collaboratively with *YTHDF1* to activate the protein translation of Snail, leading to increased epithelial–mesenchymal transition and metastasis of HCC.⁴⁷ The investigation of the biological links between m6A and lncRNAs suggests that the modification of m6A might affect the structure, stability, expression, and subcellular distribution of lncRNAs, thereby promoting tumor growth.^{48–50} From this perspective, we hope that these findings might identify feasible targets for HCC intervention.

Limitations

This study had some limitations. It was based mainly on integrative bioinformatics, and histological examination of corresponding tissue samples, follow-up clinical data and experimental validation of the findings are currently lacking. Additionally, the biological functions of the signature components might be nonspecific to HCC, given that they have also been associated with other malignancies. Therefore, further validation of the clinical applicability and clarification of the exact role of ferroptosis in HCC based on our risk score are needed.

Conclusions

In summary, we constructed a ferroptosis-related lncRNA signature to predict the prognosis of HCC. These results might provide new indications for understanding the mechanisms of ferroptosis-related lncRNAs in regulating the immune response, and for the development of individualized treatments.

Supplementary materials

The supplementary tables and figures are available at <https://doi.org/10.5281/zenodo.6492096>. The package contains the following files:

Supplementary Figure 1. Gene Ontology (GO), KEGG analysis of DEGs, and the relationship between identified lncRNAs and mRNAs expression.

Supplementary Figure 2. Kaplan–Meier analysis and the area under the curve (AUC) predicting value results of HCC patients in TNM stage I, II and III.

Supplementary Figure 3. GSEA for ferroptosis-related lncRNAs based on TCGA.

Supplementary Table 1. Information of driver, marker and suppressor.

Supplementary Table 2. Statistical information on univariate and multivariate Cox analysis of identified lncRNAs.

Supplementary Table 3. Statistical information on univariate and multivariate Cox analysis of clinical characteristics and the risk score.


Supplementary Table 4. Statistical information on immune function between the high-risk and low-risk group.

Supplementary Table 5. Statistical information on immune checkpoint between the high-risk and low-risk group.

Supplementary Table 6. Statistical information on m6A-related gene expression between the high-risk and low-risk group.

ORCID iDs

Xixi Lin  <https://orcid.org/0000-0002-3161-0253>

Sijie Yang  <http://orcid.org/0000-0002-4856-8717>

References

- Yang JD, Hainaut P, Gores GJ, Amadou A, Plymoth A, Roberts LR. A global view of hepatocellular carcinoma: Trends, risk, prevention and management. *Nat Rev Gastroenterol Hepatol*. 2019;16(10):589–604. doi:10.1038/s41575-019-0186-y
- White DL, Thrift AP, Kanwal F, Davila J, El-Serag HB. Incidence of hepatocellular carcinoma in all 50 United States, from 2000 through 2012. *Gastroenterology*. 2017;152(4):812–820.e5. doi:10.1053/j.gastro.2016.11.020
- Pinato DJ, Cortellini A, Sukumaran A, et al. PRIME-HCC: Phase Ib study of neoadjuvant ipilimumab and nivolumab prior to liver resection for hepatocellular carcinoma. *BMC Cancer*. 2021;21(1):301. doi:10.1186/s12885-021-08033-x
- Bang YJ, Golan T, Dahan L, et al. Ramucirumab and durvalumab for previously treated, advanced non-small-cell lung cancer, gastric/gastro-oesophageal junction adenocarcinoma, or hepatocellular carcinoma: An open-label, phase Ia/b study (JVDJ). *Eur J Cancer*. 2020;137:272–284. doi:10.1016/j.ejca.2020.06.007
- Rahimi RS, Trotter JF. Liver transplantation for hepatocellular carcinoma: Outcomes and treatment options for recurrence. *Ann Gastroenterol*. 2015;28(3):323–330. PMID:26130250. PMID:PMCID:4480168.
- Koh YX, Tan HL, Lye WK, et al. Systematic review of the outcomes of surgical resection for intermediate and advanced Barcelona Clinic Liver Cancer stage hepatocellular carcinoma: A critical appraisal of the evidence. *World J Hepatol*. 2018;10(6):433–447. doi:10.4254/wjh.v10.i6.433
- Sun X, Ou Z, Chen R, et al. Activation of the p62-Keap1-NRF2 pathway protects against ferroptosis in hepatocellular carcinoma cells: Hepatobiliary malignancies. *Hepatology*. 2016;63(1):173–184. doi:10.1002/hep.28251
- Yang WS, Stockwell BR. Ferroptosis: Death by lipid peroxidation. *Trends Cell Biol*. 2016;26(3):165–176. doi:10.1016/j.tcb.2015.10.014
- Sui X, Zhang R, Liu S, et al. RSL3 drives ferroptosis through GPX4 inactivation and ROS production in colorectal cancer. *Front Pharmacol*. 2018;9:1371. doi:10.3389/fphar.2018.01371
- Carbone M, Melino G. Stearoyl CoA desaturase regulates ferroptosis in ovarian cancer offering new therapeutic perspectives. *Cancer Res*. 2019;79(20):5149–5150. doi:10.1158/0008-5472.CAN-19-2453
- Shin D, Kim EH, Lee J, Roh JL. Nrf2 inhibition reverses resistance to GPX4 inhibitor-induced ferroptosis in head and neck cancer. *Free Radic Biol Med*. 2018;129:454–462. doi:10.1016/j.freeradbiomed.2018.10.426
- Louandre C, Marcq I, Bouhhal H, et al. The retinoblastoma (Rb) protein regulates ferroptosis induced by sorafenib in human hepatocellular carcinoma cells. *Cancer Lett*. 2015;356(2):971–977. doi:10.1016/j.canlet.2014.11.014
- Sun X, Niu X, Chen R, et al. Metallothionein-1G facilitates sorafenib resistance through inhibition of ferroptosis. *Hepatology*. 2016;64(2):488–500. doi:10.1002/hep.28574
- Wong LS, Wong CM. Decoding the roles of long noncoding RNAs in hepatocellular carcinoma. *Int J Mol Sci*. 2021;22(6):3137. doi:10.3390/ijms22063137
- Zhang R, Pan T, Xiang Y, et al. Curcumenol triggered ferroptosis in lung cancer cells via lncRNA H19/miR-19b-3p/FTH1 axis. *Bioact Mater*. 2022;13:23–36. doi:10.1016/j.bioactmat.2021.11.013
- Zhou N, Bao J. FerrDb: A manually curated resource for regulators and markers of ferroptosis and ferroptosis-disease associations. *Database (Oxford)*. 2020;2020:baaa021. doi:10.1093/database/baaa021
- Vickers AJ, Elkin EB. Decision curve analysis: A novel method for evaluating prediction models. *Med Decis Making*. 2006;26(6):565–574. doi:10.1177/0272989X06295361
- Chen M, Wong CM. The emerging roles of N6-methyladenosine (m6A) deregulation in liver carcinogenesis. *Mol Cancer*. 2020;19(1):44. doi:10.1186/s12943-020-01172-y
- Guo C, Zhou S, Yi W, et al. SOX9/MKL1-AS axis induces hepatocellular carcinoma proliferation and epithelial-mesenchymal transition [published online ahead of print on February 9, 2022]. *Biochem Genet*. 2022. doi:10.1007/s10528-022-10196-6
- Pan G, Zhang J, You F, et al. ETS Proto-oncogene 1-activated muskellin 1 antisense RNA drives the malignant progression of hepatocellular carcinoma by targeting miR-22-3p to upregulate ETS proto-oncogene 1. *Bioengineered*. 2022;13(1):1346–1358. doi:10.1080/21655979.2021.2017565
- Guo C, Zhou S, Yi W, et al. Long non-coding RNA muskellin 1 antisense RNA (MKLN1-AS) is a potential diagnostic and prognostic biomarker and therapeutic target for hepatocellular carcinoma. *Exp Mol Pathol*. 2021;120:104638. doi:10.1016/j.yexmp.2021.104638
- Liu Q, Zhu Q, Wang H, Zhou J, Jiang B. Long non-coding RNA Linc00205 promotes hepatoblastoma progression through regulating microRNA-154-3p/Rho-associated coiled-coil Kinase 1 axis via mitogen-activated protein kinase signaling. *Aging*. 2022;14(4):1782–1796. doi:10.18632/aging.203902
- Huangfu L, Fan B, Wang G, et al. Novel prognostic marker LINC00205 promotes tumorigenesis and metastasis by competitively suppressing miRNA-26a in gastric cancer. *Cell Death Discov*. 2022;8(1):5. doi:10.1038/s41420-021-00802-8
- Xie P, Guo Y. LINC00205 promotes malignancy in lung cancer by recruiting FUS and stabilizing CSDE1. *Biosci Rep*. 2020;40(10):BSR20190701. doi:10.1042/BSR20190701
- Cheng T, Yao Y, Zhang S, et al. LINC00205, a YY1-modulated lncRNA, serves as a sponge for miR-26a-5p facilitating the proliferation of hepatocellular carcinoma cells by elevating CDK6. *Eur Rev Med Pharmacol Sci*. 2021;25(20):6208–6219. doi:10.26355/eurrev_202110_26991
- Long X, Li Q, Zhi L, Li J, Wang Z. LINC00205 modulates the expression of EPHX1 through the inhibition of miR-184 in hepatocellular carcinoma as a ceRNA. *J Cell Physiol*. 2020;235(3):3013–3021. doi:10.1002/jcp.29206
- Ni W, Li Z, Ai K. lncRNA ZFPM2-AS1 promotes retinoblastoma progression by targeting microRNA miR-511-3p/paired box protein 6 (PAX6) axis. *Bioengineered*. 2022;13(1):1637–1649. doi:10.1080/21655979.2021.2021346
- Liu W, Hu X, Mu X, et al. ZFPM2-AS1 facilitates cell proliferation and migration in cutaneous malignant melanoma through modulating miR-650/NOTCH1 signaling. *Dermatol Ther*. 2021;34(2):e14751. doi:10.1111/dth.14751
- Sun G, Wu C. ZFPM2-AS1 facilitates cell growth in esophageal squamous cell carcinoma via up-regulating TRAF4. *Biosci Rep*. 2020;40(4):BSR20194352. doi:10.1042/BSR20194352
- Kong F, Deng X, Kong X, et al. ZFPM2-AS1, a novel lncRNA, attenuates the p53 pathway and promotes gastric carcinogenesis by stabilizing MIF. *Oncogene*. 2018;37(45):5982–5996. doi:10.1038/s41388-018-0387-9
- Song Y, Jin X, Liu Y, et al. Long noncoding RNA ZFPM2-AS1 promotes the proliferation, migration, and invasion of hepatocellular carcinoma cells by regulating the miR-576-3p/HIF-1 α axis. *Anticancer Drugs*. 2021;32(8):812–821. doi:10.1097/CAD.0000000000001070
- He H, Wang Y, Ye P, et al. Long noncoding RNA ZFPM2-AS1 acts as a miRNA sponge and promotes cell invasion through regulation of miR-139/GDF10 in hepatocellular carcinoma. *J Exp Clin Cancer Res*. 2020;39(1):159. doi:10.1186/s13046-020-01664-1
- Sun T, Wu Z, Wang X, et al. Correction to: LNC942 promoting MET- TL14 -mediated m6A methylation in breast cancer cell proliferation and progression. *Oncogene*. 2022;41(11):1677–1677. doi:10.1038/s41388-022-02194-0
- Zhu Y, Zhou B, Hu X, et al. lncRNA LINC00942 promotes chemoresistance in gastric cancer by suppressing MSI2 degradation to enhance c-Myc mRNA stability. *Clin Transl Med*. 2022;12(1):e703. doi:10.1002/ctm2.703
- Liu ZK, Wu KF, Zhang RY, et al. Pyroptosis-related lncRNA signature predicts prognosis and is associated with immune infiltration in hepatocellular carcinoma. *Front Oncol*. 2022;12:794034. doi:10.3389/fonc.2022.794034

36. Cheng M, Zhang J, Cao PB, Zhou GQ. Prognostic and predictive value of the hypoxia-associated long non-coding RNA signature in hepatocellular carcinoma. *Yi Chuan*. 2022;44(2):153–167. doi:10.16288/j.ycz.21-416
37. Wang W, Deng Z, Jin Z, et al. Bioinformatics analysis and experimental verification of five metabolism-related lncRNAs as prognostic models for hepatocellular carcinoma. *Medicine (Baltimore)*. 2022;101(4):e28694. doi:10.1097/MD.00000000000028694
38. Tao H, Zhang Y, Yuan T, et al. Identification of an EMT-related lncRNA signature and LINC01116 as an immune-related oncogene in hepatocellular carcinoma. *Aging*. 2022;14(3):1473–1491. doi:10.18632/aging.203888
39. Chen ZA, Tian H, Yao DM, Zhang Y, Feng ZJ, Yang CJ. Identification of a ferroptosis-related signature model including mRNAs and lncRNAs for predicting prognosis and immune activity in hepatocellular carcinoma. *Front Oncol*. 2021;11:738477. doi:10.3389/fonc.2021.738477
40. Dostert C, Grusdat M, Letellier E, Brenner D. The TNF family of ligands and receptors: Communication modules in the immune system and beyond. *Physiol Rev*. 2019;99(1):115–160. doi:10.1152/physrev.00045.2017
41. Jing Y, Sun K, Liu W, et al. Tumor necrosis factor- α promotes hepatocellular carcinogenesis through the activation of hepatic progenitor cells. *Cancer Lett*. 2018;434:22–32. doi:10.1016/j.canlet.2018.07.001
42. Xu ZW, Yan SX, Wu HX, Zhang Y, Wei W. Angiotensin II and tumor necrosis factor- α stimulate the growth, migration and invasion of BEL-7402 cells via down-regulation of GRK2 expression. *Digest Liver Dis*. 2019;51(2):263–274. doi:10.1016/j.dld.2018.06.007
43. Wang H, Liu J, Hu X, Liu S, He B. Prognostic and therapeutic values of tumor necrosis factor- α in hepatocellular carcinoma. *Med Sci Monit*. 2016;22:3694–3704. doi:10.12659/MSM.899773
44. Xiao Y, Huang S, Qiu F, et al. Tumor necrosis factor α -induced protein 1 as a novel tumor suppressor through selective downregulation of CSNK2B blocks nuclear factor- κ B activation in hepatocellular carcinoma. *EBioMedicine*. 2020;51:102603. doi:10.1016/j.ebiom.2019.102603
45. Chen M, Wong CM. The emerging roles of N6-methyladenosine (m6A) deregulation in liver carcinogenesis. *Mol Cancer*. 2020;19(1):44. doi:10.1186/s12943-020-01172-y
46. Chen M, Wei L, Law CT, et al. RNA N6-methyladenosine methyltransferase-like 3 promotes liver cancer progression through YTHDF2-dependent posttranscriptional silencing of SOCS2. *Hepatology*. 2018;67(6):2254–2270. doi:10.1002/hep.29683
47. Lin X, Chai G, Wu Y, et al. RNA m6A methylation regulates the epithelial mesenchymal transition of cancer cells and translation of Snail. *Nat Commun*. 2019;10(1):2065. doi:10.1038/s41467-019-09865-9
48. Brown JA, Kinzig CG, DeGregorio SJ, Steitz JA. Methyltransferase-like protein 16 binds the 3'-terminal triple helix of MALAT1 long noncoding RNA. *Proc Natl Acad Sci U S A*. 2016;113(49):14013–14018. doi:10.1073/pnas.1614759113
49. Zuo X, Chen Z, Gao W, et al. M6A-mediated upregulation of LINC00958 increases lipogenesis and acts as a nanotherapeutic target in hepatocellular carcinoma. *J Hematol Oncol*. 2020;13(1):5. doi:10.1186/s13045-019-0839-x
50. Wu Y, Yang X, Chen Z, et al. m6A-induced lncRNA RP11 triggers the dissemination of colorectal cancer cells via upregulation of Zeb1. *Mol Cancer*. 2019;18(1):87. doi:10.1186/s12943-019-1014-2

Artery-first microwave ablation in the treatment of benign thyroid nodules

Gulşah Yildirim^{A–F}, Hakki Muammer Karakas^{A,C,E,F}

Department of Radiology, Istanbul Fatih Sultan Mehmet Training and Research Hospital, Turkey

A – research concept and design; B – collection and/or assembly of data; C – data analysis and interpretation; D – writing the article; E – critical revision of the article; F – final approval of the article

Advances in Clinical and Experimental Medicine, ISSN 1899–5276 (print), ISSN 2451–2680 (online)

Adv Clin Exp Med. 2022;31(10):1111–1119

Address for correspondence

Gulşah Yildirim
E-mail: dr.gulsah.yildirim@gmail.com

Funding sources

None declared

Conflict of interest

None declared

Received on November 24, 2021

Reviewed on February 4, 2022

Accepted on June 9, 2022

Published online on June 29, 2022

Abstract

Background. Microwave ablation (MWA) is a safe and effective procedure for the treatment of benign thyroid nodules. The MWA causes progressive nodule shrinkage as well as the improvement of the symptoms and cosmesis. Some basic techniques have been described to further increase the efficacy and safety of this procedure.

Objectives. To evaluate the efficacy of artery-first MWA as an advanced technique in the treatment of benign thyroid nodules.

Materials and methods. A total of 40 patients treated with MWA were enrolled in the study. Nineteen patients who underwent artery-first MWA were selected for the study group and 21 patients who underwent MWA alone were included in the control group. Nodular vascularization was assessed using a new Doppler technique (Superb Microvascular Imaging (SMI)) and characterized using a 3-point scale. All patients were evaluated in terms of volume, symptoms, cosmetic scores, and laboratory findings before the procedure as well as 3 months (early-term follow-up) and 6 months (intermediate-term follow-up) after the procedure.

Results. Both groups were comparable with respect to the baseline volume ($p=0.135$). Nevertheless, the nodular volume reduction rate was significantly different at 3-month follow-up (study group: $56.97 \pm 11.39\%$, control group: $47.07 \pm 7.93\%$; $p=0.003$) and 6-month follow-up (study group: $78.38 \pm 8.91\%$, control group: $69.54 \pm 9.41\%$; $p=0.004$). In both groups, cosmetic and symptom scores decreased progressively ($p < 0.005$) and there were no major complications. Thyroid hormones and antibodies were within normal limits before the procedure, and no significant change was observed during follow-up after the ablation.

Conclusions. The artery-first MWA technique can be used in the treatment of benign thyroid nodules as a method of increasing the effectiveness of MWA.

Key words: thyroid nodule, microwave/therapeutic use, ablation techniques, ultrasonography/interventional

Cite as

Yildirim G, Karakas HM. Artery-first microwave ablation in the treatment of benign thyroid nodules. *Adv Clin Exp Med.* 2022;31(10):1111–1119. doi:10.17219/acem/150829

DOI

10.17219/acem/150829

Copyright

Copyright by Author(s)

This is an article distributed under the terms of the Creative Commons Attribution 3.0 Unported (CC BY 3.0) (<https://creativecommons.org/licenses/by/3.0/>)

Background

Thyroid nodules are common in the adult population and their prevalence depends on the diagnostic method used (ultrasound (US): 20–70%, physical examination: 4–7%, autopsy: 8–65%). A widespread use of imaging techniques has revealed an epidemic of incidental nonpalpable thyroid nodules. Most nodules are cytologically benign and do not warrant treatment. However, the nodules may grow, leading to symptoms by compressing the surrounding anatomical structures as well as causing cosmetic problems. Previously, the standard treatments of choice for benign thyroid nodules were total thyroidectomy and levothyroxine therapy.¹ However, for patients with benign nodules that cause pressure symptoms and/or cosmetic concerns, current guidelines recommend thermal ablation as a cost- and risk-effective alternative to surgery or observation alone, without causing hypothyroidism or surgical complications.²

Among thermal ablation methods, microwave ablation (MWA) has been proven to be a safe and effective option for the treatment of thyroid nodules.³ It uses electromagnetic radiation to heat the tissue and dielectric hysteresis to produce the heat. The MWA provides several advantages in comparison to the other heat-based modalities. It is less susceptible to local differences in impedance and vascular cooling by the heat sink effect, and produces faster heating and higher temperatures, resulting in a larger ablation volume in contrast to radiofrequency ablation (RFA).⁴

Several studies compare MWA with other methods; there are also studies comparing different MWA devices (i.e., cooled, uncooled).^{2–4} In these studies, the efficacy was determined by a reduction in nodular volume after treatment. There are many predictive factors that affect volume reduction rates (VRRs), such as initial nodule volume, functional autonomy, components of the nodules, and energy delivery. In order to increase the efficacy and safety of the ablation procedure, some basic techniques have been proven to be efficacious, including the trans-isthmus approach, the moving shot technique and the overlapping technique. In addition, the artery-first nodular ablation technique, which was developed for RFA and has had efficacy studies conducted, is used as an advanced technique in the treatment of benign thyroid nodules. However, to our knowledge, there have not been any reports validating the efficacy of this technique in MWA.

Objectives

The objective of this study was to investigate the effects of intra-arterial MWA before nodular ablation on volume reduction and clinical improvement in the treatment of benign thyroid nodules.

Materials and methods

Patients

The study was approved by the Institutional Review Board of the Istanbul Fatih Sultan Mehmet Training and Research Hospital, Turkey (approval No. 17073117_050.06_050.06). Informed consent was obtained prior to the study and all patients were informed about the procedure.

In this retrospective study, 40 patients who underwent 1 session of nodular MWA or artery-first nodular MWA from September 2019 to June 2021 were included, and a total of 40 benign thyroid nodules were evaluated. The cohort was divided into 2 groups: a study group, which consisted of 19 patients who were treated with artery-first MWA, and a control group of 21 patients who underwent MWA alone. The artery-first MWA technique was performed on hypervascularized nodules when the feeding artery could be clearly identified. The baseline characteristics of the patients in both groups are summarized in Table 1.

Table 1. Comparison of demographic and clinical characteristics of patients

Parameter	Control group (n = 21)	Study group (n = 19)	p-value
Age, mean ±SD	46.05 ±10.43	43.47 ±10.24	0.437 ^a
Gender, n (%)			
Male	9 (42.9)	9 (47.4)	0.774 ^b
Female	12 (57.1)	10 (52.6)	
Location of nodule, n (%)			
Right	9 (42.9)	8 (42.1)	0.631 ^b
Left	10 (47.6)	7 (36.8)	
Isthmus	2 (9.5)	4 (21.1)	
Composition of nodule, n (%)			
Solid	18 (85.7)	17 (89.5)	1.000 ^b
Mainly solid	3 (14.3)	2 (10.5)	

^a t-test for independent samples; ^b Fisher's exact test; SD – standard deviation.

The inclusion criteria included: 1) over 18 years of age and not pregnant; 2) benign thyroid nodules proven after 2 different US-guided fine-needle aspiration biopsies (according to the American Bethesda System for Reporting Thyroid Cytopathology); 3) solid or mainly solid nodules (solid component >80%) on US; 4) presence of subjective compressive symptoms (dysphagia, dysphonia, dyspnea, foreign body sensation, etc.) or cosmetic concerns; and 5) normal thyroid function. The exclusion criteria were: 1) retrosternal excessive growth; 2) presence of US findings indicating a malignant nodule despite benign results of biopsies; 3) incomplete US or laboratory data; and 4) follow-up time shorter than 6 months.

Equipment and pre-ablative assessment

Sonograms of all nodules were performed using the Aplio 500 ultrasound system (Toshiba Medical Systems, Tokyo, Japan) with a broad bandwidth linear array transducer (imaging frequency: 14 MHz). First, a grayscale US was performed to evaluate the size, volume, composition, and characteristics (echogenicity, shape, margin, etc.) of the nodules. The maximum diameter (A) and 2 vertical diameters (B and C) were measured and the nodular volume was calculated using the following equation:

$$\text{volume} = (A \times B \times C)/2$$

Next, color Doppler (CD), power Doppler (PD), and monochrome and color Superb Microvascular Imaging (SMI) were performed to evaluate the vascularity of the nodules. Monochrome and color SMI were included in the pre-procedural vascular examination because the microvascular flow was provided in greater detail compared to CD and PD.⁵ This new Doppler technique has recently been developed to improve microvascular flow imaging. Intranodular blood flow was assessed subjectively using SMI and identified using a 3-point scale (1 – no vascularization, 2 – slight vascularization, 3 – marked vascularization) in all patients.⁵ If the nodules were demonstrated to have slight or marked intranodular vascularization, the arterial flow was evaluated to determine which ablation procedure should be used. The artery-first MWA technique was performed in patients where the feeding artery could be clearly identified using SMI and whose intranodular vascularity index was 2 or 3. All examinations were performed by the same interventional radiologist who also performed the ablation procedure.

The MWA system used in this study was a 2.45 GHz microwave generator (TATO; Terumo, Rome, Italy) and an uncooled 18 G antenna. The indicated probe used during thyroid ablation had 8 cm in length and 50 g in weight.

It had a teflon (PTTFE) coating to prevent adhesions and a metal tip for soft and precise targeting of thyroid nodules.

Before the ablation, all patients underwent laboratory examination. Laboratory tests included a complete blood count, blood coagulation test and complete thyroid function tests (triiodothyronine (T3), free thyroxine (T4), and thyroid-stimulating hormone (TSH) levels). In addition, anti-thyroid peroxidase (anti-TPO) and anti-thyroglobulin (anti-TG) antibody levels were evaluated. Clinical examination was performed using symptom and cosmetic scores. Clinical symptoms were scored using a 10-cm visual analog scale, and a 4-point subjective scale (I – no palpable mass, II – an invisible but palpable mass, III – a visible mass during neck extension or swallowing, and IV – easily visible mass) was used for cosmetic scoring.

Procedure

All MWA treatment procedures were performed as outpatient procedures. Local anesthesia (2% prilocaine) was injected subcutaneously into the puncture site in a supine cervical extension position. Ultrasound-guided hydrodissection procedures were performed around the capsule using a 1:1 concentration of 0.5% bupivacaine and 0.9% isotonic NaCl in order to protect neighbor structures from thermal damage and subcapsular anesthesia (Fig. 1). Then, the feeding artery was imaged with monochrome (Fig. 2A) and color SMI (Fig. 2B) and the antennas were inserted into the center of the feeding artery in the study group (Fig. 2C,D). After ablation of the artery, the following nodular ablation steps were performed in the same manner in both groups. The MWA antenna was placed into the nodule along its short axis using a trans-isthmus approach, which is preferred to minimize the risk of injury to vital structures and allow visualization of the entire length of the antenna on the transverse US. During the session, 15-Watt power output was used and the procedures were conducted using

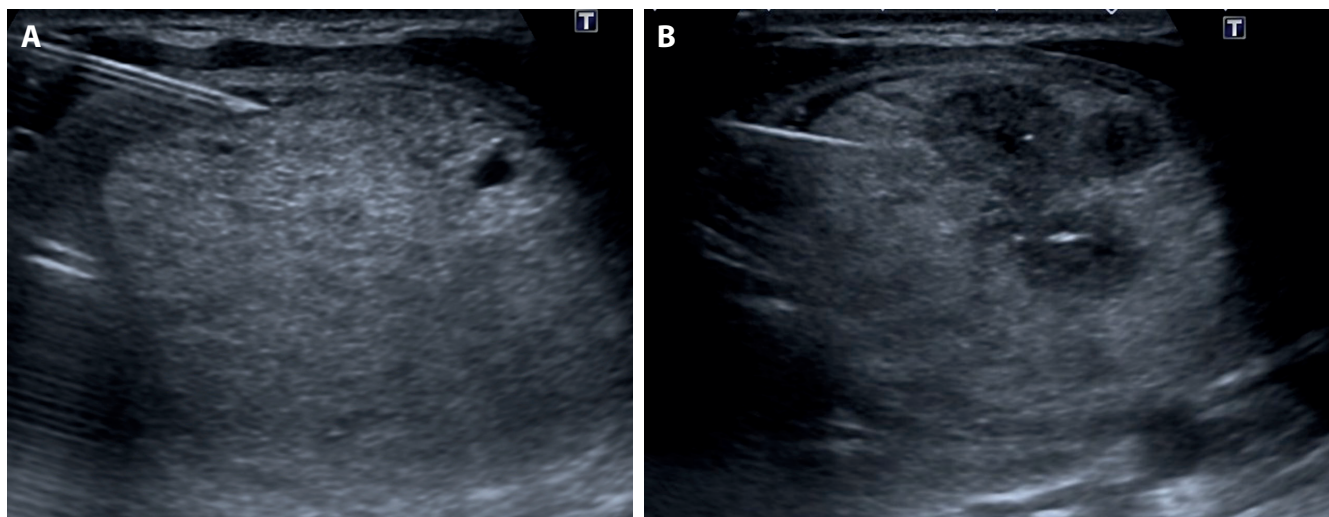


Fig. 1. Trans-isthmus approach (A,B), hydrodissection (A) and multiple overlapping (B) techniques, which are basic microwave ablation (MWA) techniques

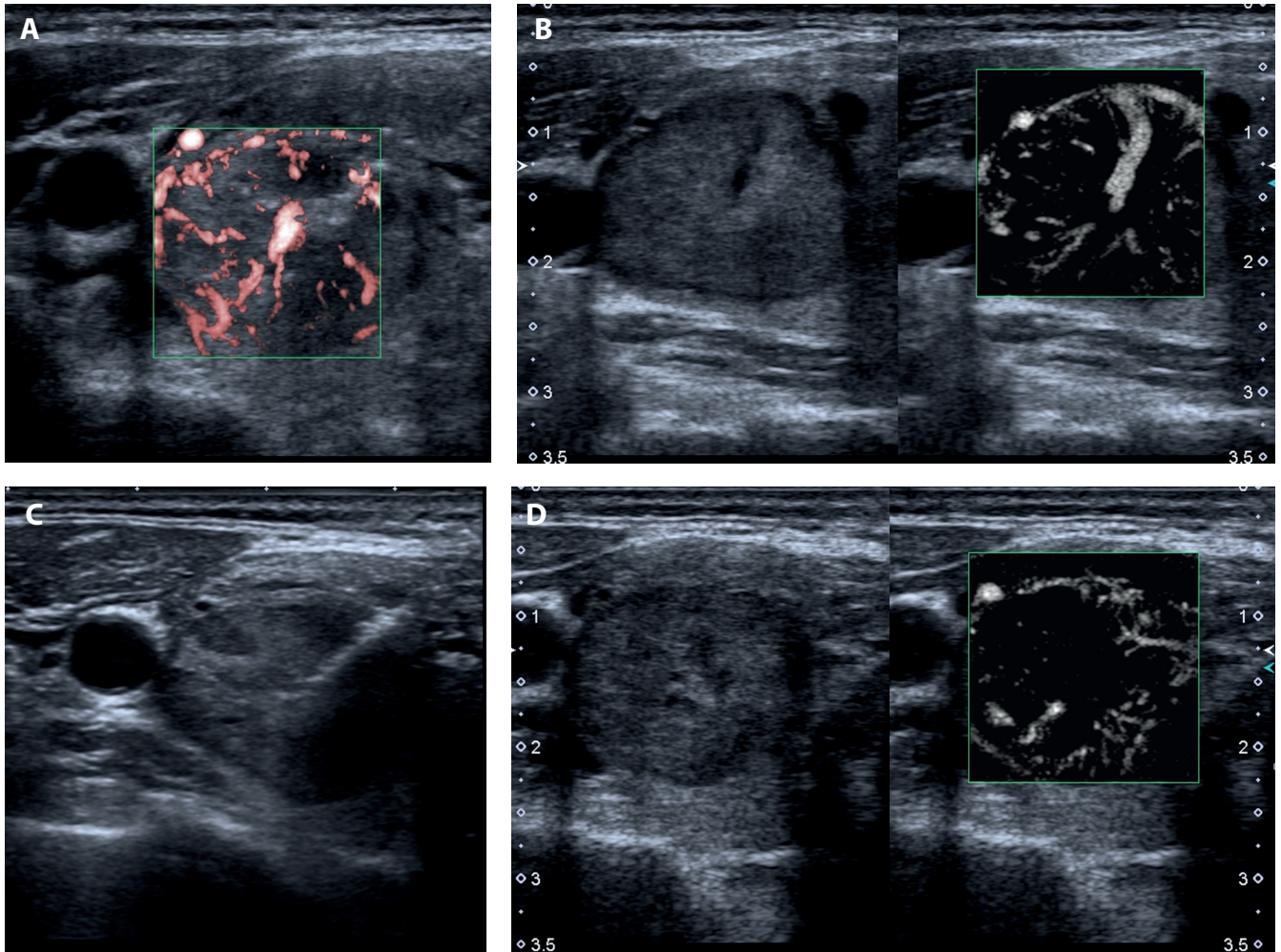


Fig. 2. A 52-year-old female patient who underwent artery-first microwave ablation (MWA). The feeding artery was detected with the color (A) and monochrome (B) Superb Microvascular Imaging (SMI) methods. Prior to nodular ablation, the probe was localized into the feeding artery (C). No flow was observed after artery ablation (D)

the multiple overlapping technique. Each overlapping ablation area was visualized with real-time US and satisfactory volume coverage was obtained. If the patient could not tolerate the pain and discomfort during the session, the procedure was interrupted for a short period. The extent of ablation was estimated taking into account the echogenic changes around the MWA probe, and the session was terminated when the hyper-echo area covered the entire nodule. Phonatory control was performed during and after the ablation procedure in order to exclude a recurrent laryngeal nerve injury. The complete procedure was performed under aseptic conditions. At the end of the procedure, mild cold compression was applied to the neck, and patients were observed in the hospital for 2 h. Before discharge, US was performed to exclude any possible complications.

Follow-up

Both groups were evaluated in terms of US examination, clinical symptoms and laboratory data 3 months (early-term follow-up) and 6 months (intermediate-term

follow-up) after the procedure. The US examination was performed to assess the characteristics of the nodule. We determined the VRRs as a primary outcome. Other efficacy outcomes included improvements in a patient's symptoms and cosmetic scores in the early- and intermediate-term follow-up. The percentage of volume reduction was calculated using the following formula:

$$\text{VRR} = \frac{[(\text{Pre-procedural volume} - \text{follow-up volume}) \times 100]}{(\text{Pre-procedural volume})}$$

Statistical analyses

Nominal and ordinal parameters were described with frequencies. Mean and standard deviation (SD) were used for the description of scale parameters. Median and interquartile range (IQR) were used for skewed parameters. The Kolmogorov–Smirnov test was used to test for the normality distribution of scale parameters. For normally distributed parameters, independent samples *t*-tests were used. For non-normally distributed parameters, Mann–Whitney *U* tests were used.

The Fisher’s exact test and χ^2 likelihood ratio tests were used for differences in nominal and ordinal parameters. Repeated measures analysis of variance (ANOVA) tests were performed to evaluate the group and time effects on variables. The SPSS v. 17.0 for Windows (SPSS Inc., Chicago, USA) software was used with a 95% confidence interval (95% CI) and a p-value of 0.05 as the significance level.

Results

Both groups were compared regarding age, gender, location, and nodule composition (difference between the solid and mainly solid structure percentage), and the differences between the groups were not statistically significant ($p > 0.05$) (Table 1). Baseline nodular blood flow scores were 2.08 ± 0.51 in the study group compared to 1.30 ± 0.63 in the control group ($p = 0.03$). The SMI allowed for choosing the artery-first MWA technique for nodules demonstrating high nodular blood flow.

The mean baseline volume was 20.94 ± 15.38 mL in the whole cohort and did not significantly differ between groups ($p = 0.135$). Volumes decreased progressively after ablation in the whole cohort and were found to be 10.13 ± 8.39 mL ($p = 0.001$) and 5.41 ± 4.41 mL ($p = 0.001$) at 3-month and 6-month follow-up, respectively. When the 2 groups were evaluated separately, the mean baseline volume of the study group was 17.10 ± 14.65 mL, and it decreased to 5.90 ± 4.4 mL at the 3-month follow-up and to 3.72 ± 3.92 mL at the 6-month follow-up. The mean nodular volume of control group was 24.23 ± 15.55 mL at baseline, and decreased to 11.30 ± 5.4 mL at the 3-month follow-up and 6.94 ± 4.34 mL at the 6-month follow-up (Table 2). In addition, the longest baseline diameter was 37.41 ± 11.26 mm in the study group and 43.94 ± 9.10 mm in the control group ($p = 0.053$). In the study group, it decreased to 27.63 ± 8.37 mm and 22.25 ± 7.87 mm, and in the control group it decreased to 36.68 ± 7.87 mm and 31.75 ± 7.90 mm at 3-month and 6-month follow-up, respectively. Although the pre-procedural volumes ($p = 0.135$) and longest diameters ($p = 0.053$) were statistically similar in both groups, both parameters were significantly higher in the control group at 3-month and 6-month follow-up ($p < 0.05$) (Table 2).

As a primary endpoint, VRR in the cohort was $52.53 \pm 10.56\%$ at the 3-month follow-up and $73.91 \pm 10.11\%$ at the 6-month follow-up. The mean VRRs were higher in the study group at the 3-month follow-up (study group: $56.97 \pm 11.39\%$, control group: $47.07 \pm 7.93\%$, $p = 0.003$). This significant difference between the groups remained unchanged at the 6-month follow-up, registering a greater volume reduction percentage in patients treated with artery-first MWA than in patients treated with MWA only (study group: $78.38 \pm 8.91\%$, control group: $69.54 \pm 9.41\%$; $p = 0.004$) (Fig. 3A,B).

Table 2. Clinical and physical examination properties and difference analysis results of patient groups (study and control groups)

Mean \pm SD	Control group (n = 21)	Study group (n = 19)	p-value
Volume			
Preprocedural	24.41 \pm 15.55	17.10 \pm 14.65	0.135 ^a
3 rd month, median (IQR)	11.30 (5.4)	5.90 (4.4)	0.000 ^b
6 th month	6.94 \pm 4.34	3.72 \pm 3.92	0.019 ^a
Volume reduction ratio			
3 rd month	47.07 \pm 7.93	56.97 \pm 11.39	0.003 ^a
6 th month	69.54 \pm 9.41	78.38 \pm 8.91	0.004 ^a
Longest diameter			
Preprocedural	43.94 \pm 9.10	37.41 \pm 11.26	0.053 ^a
3 rd month	36.68 \pm 7.87	27.63 \pm 8.37	0.001 ^a
6 th month	31.75 \pm 7.90	22.25 \pm 7.87	0.001 ^a
Cosmetic score			
Preprocedural, median (IQR)	4.00 (0)	3.00 (1)	0.006 ^b
3 rd month, median (IQR)	3.00 (2)	2.00 (1)	0.069 ^b
6 th month, median (IQR)	2.00 (1)	2.00 (1)	0.153 ^b
Symptom score			
Preprocedural, median (IQR)	6.00 (1)	6.00 (1)	0.668 ^b
3 rd month	2.71 \pm 1.06	2.16 \pm 1.30	0.144 ^a
6 th month, median (IQR)	1.00 (2)	1.00 (2)	0.830 ^b
TSH			
Preprocedural	1.33 \pm 0.58	1.21 \pm 0.57	0.543 ^a
3 rd month	1.55 \pm 0.84	1.47 \pm 0.90	0.783 ^a
6 th month	1.63 \pm 1.02	1.34 \pm 0.77	0.309 ^a
fT4			
Preprocedural, median (IQR)	1.02 (0.12)	1.02 (0.23)	0.979 ^b
3 rd month	1.11 \pm 0.20	1.03 \pm 0.19	0.214 ^a
6 th month	1.21 \pm 0.26	1.08 \pm 0.17	0.081 ^a
T3			
Preprocedural	3.18 \pm 0.31	3.23 \pm 0.42	0.726 ^a
3 rd month	3.29 \pm 0.32	3.23 \pm 0.48	0.658 ^a
6 th month	3.32 \pm 0.43	3.16 \pm 0.29	0.197 ^a
Anti-TG			
Preprocedural	4.55 \pm 7.68	9.30 \pm 12.55	0.294 ^b
3 rd month	11.16 \pm 19.68	6.98 \pm 6.17	0.999 ^b
6 th month	9.84 \pm 9.98	9.22 \pm 7.47	0.828 ^a
Anti-TPO			
Preprocedural	9.00 \pm 19.72	6.97 \pm 7.94	0.573 ^b
3 rd month	10.60 \pm 20.69	7.01 \pm 7.63	0.768 ^b
6 th month	8.82 \pm 5.09	8.19 \pm 6.87	0.520 ^b

^a independent samples t-test; ^b Mann–Whitney U test. Data are presented as mean \pm standard deviation (SD). Median and interquartile range (IQR) were added for skewed parameters. TSH – thyroid-stimulating hormone; fT4 – free thyroxine; T3 – triiodothyronine; anti-TG – anti-thyroglobulin; anti-TPO – anti-thyroid peroxidase antibody.

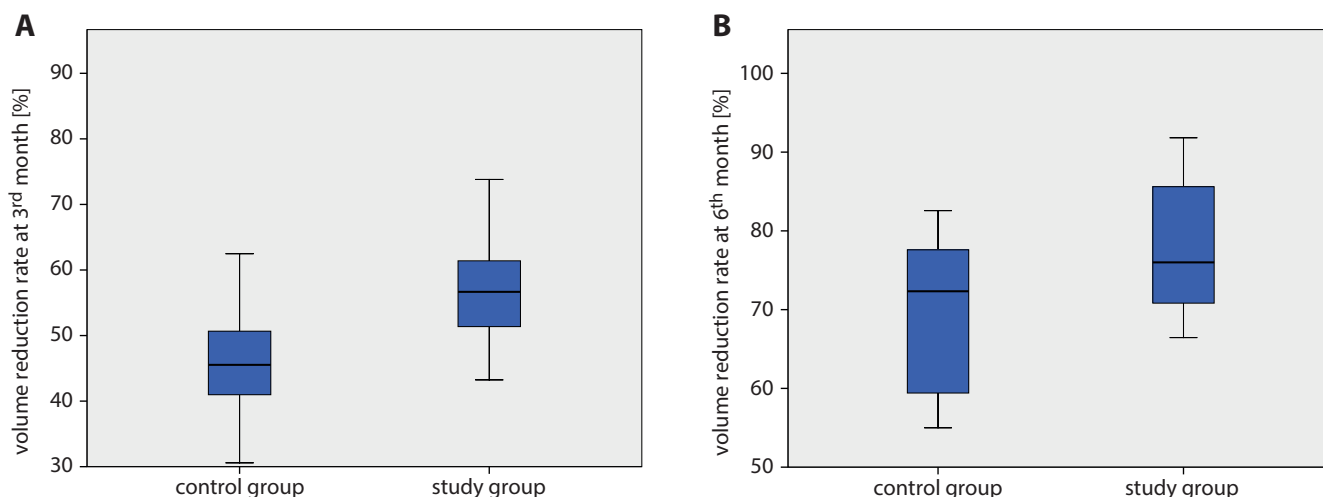


Fig. 3. Box-plot (ranges, 1st quartile (Q1), 3rd quartile (Q3), medians) of the volume reduction rate (VRR) compression at 3-month (A) and 6-month (B) follow-up in respective groups

In the study group, symptom scores decreased from 6.00 ± 1 at baseline to 2.16 ± 1.30 at the 3-month follow-up and 1.00 ± 2 at the 6-month follow-up. In the control group, symptom scores decreased from 6.00 ± 1 at baseline to 2.71 ± 1.06 at the 3-month follow-up and 1.00 ± 2 at the 6-month follow-up. Thus, we observed that these scores decreased rapidly at 3-month follow-up in both groups. There were no significant differences between the groups in terms of symptom scores before ablation ($p = 0.668$) and at 3-month ($p = 0.144$) and 6-month ($p = 0.830$) follow-up.

In addition, cosmetic score decreased from 3.00 ± 1 to 2.00 ± 1 , 2.00 ± 1 in the study group and from 4.00 ± 0 to 3.00 ± 2 and to 2.00 ± 1 in the control group at 3- and 6-month follow-up, respectively. Pre-procedural cosmetic scores were significantly higher in the control group ($p = 0.006$) (Table 2).

Patients had normal thyroid laboratory values at baseline and 3-month and 6-month follow-up. There were no significant differences between groups in terms of thyroid hormone levels (TSH, fT4, T3) and thyroid antibodies (anti-TG, anti-TPO) at baseline and both follow-up assessments (Table 2).

The results of repeated measures ANOVA showed that the differences in volume, longest diameter and cosmetic scores between the groups were statistically significant ($p < 0.05$). However, time (3-month and 6-month follow-up) and group effect among subjects did not reach statistical significance ($p > 0.05$) (Table 3).

Although the treatment was well-tolerated, mild pain was reported by 2 patients during the ablation and was easily managed by reducing the energy. One patient in the study group developed first-degree burns to the skin at the puncture site, which did not require any specific treatment and resolved within days. There were no major complications in either group during the session and at post-procedural follow-up assessments.

Discussion

Minimally invasive thermal ablation has been used to successfully treat benign thyroid nodules, with MWA being a more recently developed ablation technique. Microwaves create an ablation area with thermal and nonthermal effects. Coagulation necrosis is a thermal effect, while electroporation, ion acceleration, collision, and dipole rotation are nonthermal effects.^{6–8} This explains the main mechanisms in which MWA causes significant volume reductions in thyroid nodules.⁹ These 2 different mechanisms of ablation provide some advantages to MWA, as compared to RFA and percutaneous laser ablation (LA). Several reports have shown that MWA has a lower complication rate and similar efficacy when compared to RFA.^{10,11} Recent studies have recognized the efficacy and safety of MWA in the treatment of benign thyroid nodules.^{12,13} However, the VRRs of nodules have wide variations of approx. 40–80% after 3 months, 48–86% after 6 months and 75–90% after 12 months.^{12–17} As stated above, this situation may be due to certain factors and the type of system may be one of the important determinants. Uncooled systems that provide real-time temperature control may have a different effect on the nodular tissue surrounding the ablated area during the procedure, which may affect the success of the treatment.¹⁵ In this study, we performed the procedures with an uncooled system. Because the properties of the system are dedicated to the thyroid, it is 18 G in size and has an 8-cm shaft that provides safe and ergonomic use. Furthermore, literature studies and our recent study have shown that the tumor volume, clinical scores and symptom scores significantly improve after treatment with an uncooled MWA system with low complication rates.^{14,16,17} In the present study, the findings in both groups were consistent with the literature and the overall mean VRR of the treated nodules reached 53% and 74% at 3 and 6 months after ablation, respectively.

Table 3. Repeated measures results for research parameters based on time and group

Parameter	F and p-value	Source			
		Intercept	Group	Time	Group * Time
Volume	F	6.923	20.956	58.489	0.414
	p-value	0.119	0.045	0.017	0.662
Longest diameter	F	69.683	82.416	74.945	0.329
	p-value	0.014	0.012	0.013	0.720
Cosmetic score	F	39.150	98.880	312.189	0.133
	p-value	0.025	0.010	0.003	0.876
Symptom score	F	4.520	2.883	414.366	0.745
	p-value	0.167	0.232	0.002	0.477
TSH	F	352.967	5.618	4.895	0.218
	p-value	0.003	0.141	0.170	0.804
ft4	F	1563.772	9.043	4.362	0.469
	p-value	0.001	0.095	0.187	0.627
T3	F	37152.998	1.012	0.352	0.661
	p-value	0.000	0.420	0.740	0.518
Anti-TG	F	112.197	0.000	0.384	1.485
	p-value	0.009	0.996	0.723	0.231
Anti-TPO	F	1238.864	6.001	0.316	0.124
	p-value	0.001	0.134	0.760	0.883

Group * Time – effect of both group and time on the parameters; T3 – triiodothyronine; ft4 – free thyroxine; TSH – thyroid-stimulating hormone; anti-TG – anti-thyroglobulin; anti-TPO – anti-thyroid peroxidase antibody. The p-values in bold are statistically significant.

Thermoablative treatment was performed on an afferent artery of the nodule in the artery-first approach in order to obtain a better ablation of the nodular tissue and increase the volume of the induced necrosis. Intranodal prominent vascularity is less than 15% in small benign thyroid nodules, but can be more than 50% in large benign thyroid nodules.¹⁸ Artery-first MWA is an advanced technique and, to the best of our knowledge, no other studies have demonstrated a difference in the efficacy (VRRs) of artery-first MWA. In our study, the efficacy of artery-first ablation was demonstrated and the VRR showed a significant difference at the 3-month (p = 0.000) and 6-month (p = 0.003) follow-up. In our study, 3-month and 6-month follow-up were assessed because, as mentioned by Cui et al., the changes in VRR become evident with the removal of necrotic tissue during the 3rd to 6th month post-procedure, due to a delay in the immune system.¹⁹

Many benign thyroid nodules are hypervascularized and the artery-first ablation technique can be performed in hypervascularized nodules when a prominent feeding artery can be identified.²⁰ The nodules in the upper pole of the thyroid are usually vascularized from the superior thyroid artery, while those in the lower pole are vascularized by the inferior thyroid artery.¹⁸ In recent studies, the feeding artery was detected using CD and PD.^{21,22} However, we have assessed the nodular microvascular architecture using SMI, which provided greater detail compared to other Doppler techniques. This newly developed Doppler technique uses advanced clutter suppression to extract

flow signals from large to small vessels and depicts this information at high-frame rates as a color overlay image or as a grayscale flow map.²² In recent studies, the artery-first technique was used to reduce the dispersion of generated heat in the RFA of thyroid nodules, and has increased the efficacy of the procedure during follow-up.²³ Offi et al. pointed out that the differences between RFA and artery-first RFA techniques were seen in nodular volume at follow-up. At the 3-month follow-up, the mean VRR was 72.7 ±8.99% in the study group and 56.28 ±14.55% in the control group (p = 0.003). Moreover, at the 6-month follow-up, the mean VRR was 83.01 ±5.04% in the study group and 70.0 ±15.04% in the control group (p = 0.013).²⁴ Similarly, in our study, a significant difference was found between the 2 techniques in VRR at the 3-month (p = 0.000) and 6-month (p = 0.012) follow-up. These data lead us to hypothesize that artery-first ablation may increase the efficacy of the procedure and allow a more rapid reduction in volume. Furthermore, this study detected a significant improvement in clinical findings between baseline and the 3-month and 6-month follow-up, but there was no significant difference between the 2 groups.

The MWA-associated complications are classified as major and minor. Major complications include transient or permanent voice change, hypoparathyroidism, esophageal injury, dysphagia, infection, and nodule rupture. Minor complications include severe pain requiring medication for relief, skin burns, hematoma, and vomiting. Thermal ablation procedures have significantly lower

complication rates, and recent studies have reported that the complications of MWA are mostly minor, although it was reported that both MWA methods (cooled and uncooled) had similar incidence of major complications (4.9% compared to 5.0%, $p = 0.49$). Pain and skin burns were reported as the most common minor complications and were significantly higher in the uncooled MWA group ($p < 0.01$).¹⁴ In our study, 2.5% of treated patients had minor complications and there were no major complications. The low complication rate achieved using the uncooled system compared to previous studies may be due to artificial liquid isolation-assisted ablation, real-time US guidance, phonatory control during the procedure, the overlapping technique, and the trans-isthmic approach. In addition, as an advanced technique, arterial ablation may have reduced the risk of procedure-related hemorrhage.²³

Limitations


This study has some limitations. First, it was a retrospective in design single-center study with a small sample size. Second, follow-up longer than 6 months may be necessary to further observe nodular behavior, since nodule regrowth may occur and the decision to undergo repeat thermal ablation or surgery may be needed. Some studies have suggested supplementary treatment 3–6 months after ablation.^{25,26} Regardless, in our study, we achieved a 79% VRR with a single session using artery-first MWA, and this result is consistent with the current literature. In addition, in this retrospective study, we did not collect any data on elastography for nodular stiffness. In the literature, some measurements with elastography have been found to positively correlate with better results in thermal ablation, but these were not clearly defined factors to predict success.²⁷

Conclusions

In conclusion, MWA devices and techniques continue to evolve amidst minimally invasive treatment of thyroid nodules. The use of basic and advanced technical strategies is critical to ensure treatment efficacy and patient safety. Therefore, additional prospective studies with large-scale and long-term follow-up are necessary to validate our findings.

ORCID iDs

Gulşah Yildirim  <https://orcid.org/0000-0002-5971-7079>

Hakki Muammer Karakas  <https://orcid.org/0000-0002-1328-8520>

References

- Efremidou EI, Papageorgiou MS, Liratzopoulos N, Manolas KJ. The efficacy and safety of total thyroidectomy in the management of benign thyroid disease: A review of 932 cases. *Can J Surg*. 2009; 52(1):39–44. PMID:19234650. PMID:PMC2637645.
- Papini E, Monpeyssen H, Frasoldati A, Hegedüs L. 2020 European Thyroid Association Clinical Practice Guideline for the Use of Image-Guided Ablation in Benign Thyroid Nodules. *Eur Thyroid J*. 2020;9(4): 172–185. doi:10.1159/000508484
- Wu W, Gong X, Zhou Q, Chen X, Chen X, Shi B. US-guided percutaneous microwave ablation for the treatment of benign thyroid nodules. *Endocr J*. 2017;64(11):1079–1085. doi:10.1507/endocrj.EJ17-0152
- Klein JA, Lee Jr FT, Hinshaw L, Lubner MG, Brace CL. Overview of thermal ablation devices: Microwave. In: Clark T, Sabharwal T, eds. *Interventional Radiology Techniques in Ablation*. London, UK: Springer; 2013:21–28. doi:10.1007/978-0-85729-094-6
- Cappelli C, Pirola I, Gandossi E, et al. Ultrasound microvascular blood flow evaluation: A new tool for the management of thyroid nodule? *Int J Endocrinol*. 2019;2019:1–6. doi:10.1155/2019/7874890
- Simon CJ, Dupuy DE, Mayo-Smith WW. Microwave ablation: Principles and applications. *RadioGraphics*. 2005;25(Suppl 1):S69–S83. doi:10.1148/rg.25si055501
- Ward RC, Healey TT, Dupuy DE. Microwave ablation devices for interventional oncology. *Exp Rev Med Devices*. 2013;10(2):225–238. doi:10.1586/erd.12.77
- Banik S, Bandyopadhyay S, Ganguly S. Bioeffects of microwave: A brief review. *Bioresour Technol*. 2003;87(2):155–159. doi:10.1016/S0960-8524(02)00169-4
- Brace CL. Microwave ablation technology: What every user should know. *Curr Probl Diagn Radiol*. 2009;38(2):61–67. doi:10.1067/j.cpradiol.2007.08.011
- Yang YL, Chen CZ, Zhang XH. Microwave ablation of benign thyroid nodules. *Future Oncol*. 2014;10(6):1007–1014. doi:10.2217/fon.13.260
- Yue WW, Wang SR, Lu F, et al. Radiofrequency ablation vs. microwave ablation for patients with benign thyroid nodules: A propensity score matching study. *Endocrine*. 2017;55(2):485–495. doi:10.1007/s12020-016-1173-5
- Korkusuz H, Happel C, Heck K, Ackermann H, Grünwald F. Percutaneous thermal microwave ablation of thyroid nodules: Preparation, feasibility, efficiency. *Nuklearmedizin*. 2014;53(04):123–130. doi:10.3413/Nukmed-0631-13-10
- Feng B, Liang P, Cheng Z, et al. Ultrasound-guided percutaneous microwave ablation of benign thyroid nodules: Experimental and clinical studies. *Eur J Endocrinol*. 2012;166(6):1031–1037. doi:10.1530/EJE-11-0966
- Zheng BW, Wang JF, Ju JX, Wu T, Tong G, Ren J. Efficacy and safety of cooled and uncooled microwave ablation for the treatment of benign thyroid nodules: A systematic review and meta-analysis. *Endocrine*. 2018;62(2):307–317. doi:10.1007/s12020-018-1693-2
- Mader OM, Tanha NF, Mader A, Happel C, Korkusuz Y, Grünwald F. Comparative study evaluating the efficiency of cooled and uncooled single-treatment MWA in thyroid nodules after a 3-month follow up. *Eur J Radiol Open*. 2017;4:4–8. doi:10.1016/j.ejro.2017.01.004
- Yildirim G. Uncooled microwave ablation method for thyroid nodules: Our early-term results. *Bosphorus Med J*. 2021;8(1):13–20. doi:10.14744/bmj.2020.62681
- Korkusuz H, Nimsdorf F, Happel C, Ackermann H, Grünwald F. Percutaneous microwave ablation of benign thyroid nodules: Functional imaging in comparison to nodular volume reduction at a 3-month follow-up. *Nuklearmedizin*. 2015;54(01):13–19. doi:10.3413/Nukmed-0678-14-06
- Lyshchik A, Moses R, Barnes SL, et al. Quantitative analysis of tumor vascularity in benign and malignant solid thyroid nodules. *J Ultrasound Med*. 2007;26(6):837–846. doi:10.7863/jum.2007.26.6.837
- Cui T, Jin C, Jiao D, Teng D, Sui G. Safety and efficacy of microwave ablation for benign thyroid nodules and papillary thyroid microcarcinomas: A systematic review and meta-analysis. *Eur J Radiol*. 2019; 118:58–64. doi:10.1016/j.ejrad.2019.06.027
- Shin JH, Baek JH, Chung J, et al. Ultrasonography diagnosis and imaging-based management of thyroid nodules: Revised Korean Society of Thyroid Radiology Consensus Statement and Recommendations. *Korean J Radiol*. 2016;17(3):370. doi:10.3348/kjr.2016.17.3.370
- Kong J, Li JC, Wang HY, et al. Role of Superb Microvascular Imaging in the preoperative evaluation of thyroid nodules: Comparison with power Doppler flow imaging. *J Ultrasound Med*. 2017;36(7):1329–1337. doi:10.7863/ultra.16.07004
- Machado P, Segal S, Lyshchik A, Forsberg F. A novel microvascular flow technique: Initial results in thyroids. *Ultrasound Q*. 2016;32(1):67–74. doi:10.1097/RUQ.0000000000000156
- Park HS, Baek JH, Park AW, Chung SR, Choi YJ, Lee JH. Thyroid radiofrequency ablation: Updates on innovative devices and techniques. *Korean J Radiol*. 2017;18(4):615. doi:10.3348/kjr.2017.18.4.615

24. Offi C, Garberoglio S, Antonelli G, et al. The ablation of thyroid nodule's afferent arteries before radiofrequency ablation: Preliminary data. *Front Endocrinol.* 2021;11:565000. doi:10.3389/fendo.2020.565000
25. Jeong WK, Baek JH, Rhim H, et al. Radiofrequency ablation of benign thyroid nodules: Safety and imaging follow-up in 236 patients. *Eur Radiol.* 2008;18(6):1244–1250. doi:10.1007/s00330-008-0880-6
26. Liu YJ, Qian LX, Liu D, Zhao JF. Ultrasound-guided microwave ablation in the treatment of benign thyroid nodules in 435 patients. *Exp Biol Med (Maywood).* 2017;242(15):1515–1523. doi:10.1177/1535370217727477
27. Bisceglia A, Rossetto R, Garberoglio S, et al. Predictor analysis in radiofrequency ablation of benign thyroid nodules: A single center experience. *Front Endocrinol.* 2021;12:638880. doi:10.3389/fendo.2021.638880

Citrulline and long-term mortality in patients with cardiovascular disease

Radosław Andrzej Konieczny^{1,A–F}, Ewa Żurawska-Płaksej^{2,B–D,F}, Konrad Kaaz^{3,B,C,F},
Hanna Czapor-Irzabek^{4,B,C,F}, Wojciech Bombała^{5,C,E,F}, Andrzej Mysiak^{3,A,C,F}, Wiktor Kuliczkowski^{3,A,C,D,F}

¹ Jan Mikulicz-Radecki University Teaching Hospital, Clinic of Gastroenterology and Hepatology, Wrocław, Poland

² Department of Toxicology, Wrocław Medical University, Poland

³ Institute of Heart Diseases, Wrocław Medical University, Poland

⁴ Laboratory of Elemental Analysis and Structural Research, Wrocław Medical University, Poland

⁵ Statistical Analysis Centre, Wrocław Medical University, Poland

A – research concept and design; B – collection and/or assembly of data; C – data analysis and interpretation;

D – writing the article; E – critical revision of the article; F – final approval of the article

Advances in Clinical and Experimental Medicine, ISSN 1899–5276 (print), ISSN 2451–2680 (online)

Adv Clin Exp Med. 2022;31(10):1121–1128

Address for correspondence

Radosław Andrzej Konieczny
E-mail: rkonieczny.med@gmail.com

Funding sources

The study was funded by a statutory grant from the Institute of Heart Diseases, Wrocław Medical University, Poland.

Conflict of interest

None declared

Acknowledgements

The samples were provided by the Biobank of Łukasiewicz Research Network – PORT Polish Center for Technology Development in Wrocław, Poland.

Received on March 25, 2022

Reviewed on May 19, 2022

Accepted on May 26, 2022

Published online on June 14, 2022

Cite as

Konieczny RA, Żurawska-Płaksej E, Kaaz K, et al. Citrulline and long-term mortality in patients with cardiovascular disease. *Adv Clin Exp Med.* 2022;31(10):1121–1128. doi:10.17219/acem/150475

DOI

10.17219/acem/150475

Copyright

Copyright by Author(s)

This is an article distributed under the terms of the Creative Commons Attribution 3.0 Unported (CC BY 3.0) (<https://creativecommons.org/licenses/by/3.0/>)

Abstract

Background. Cardiovascular disease (CVD) is associated with intestinal barrier dysfunction and increased intestinal permeability. Increased intestinal permeability to gut microbial metabolites may accelerate the progression of CVD. Plasma citrulline levels are a marker of functional enterocyte mass, and reduced citrulline levels indicate intestinal epithelial damage. Citrulline was reported as a useful prognostic marker in critically ill patients. However, data are lacking on the association of citrulline with long-term mortality in patients with CVD and with the levels of trimethylamine N-oxide (TMAO), a microbiota-derived metabolite which has been implicated in the pathogenesis of CVD.

Objectives. To assess the effect of citrulline levels, a marker of intestinal barrier disruption, on long-term mortality in patients with CVD. Moreover, the relationship between the concentrations of 2 biomarkers – citrulline and TMAO – was assessed.

Materials and methods. Serum citrulline levels were retrospectively assessed in 1036 consecutive patients with CVD (median age: 62 years; 61% men) hospitalized between 2013 and 2015. Associations of citrulline levels with 5-year mortality rates as well as anthropometric and biochemical parameters were evaluated for the entire study group and in subgroups of patients with acute coronary syndrome (ACS), chronic coronary syndrome, chronic heart failure (chronic HF), and atrial fibrillation (AF). Correlations between serum citrulline and TMAO levels were assessed.

Results. The median citrulline level in the study population was 22.5 μM (interquartile range (IQR): 17.8–27.9). Citrulline levels were not associated with 5-year mortality in patients with CVD (hazard ratio (HR) = 0.99; 95% confidence interval (95% CI): 0.97–1.00; $p = 0.49$). Median citrulline levels differed significantly between deceased patients and survivors at 5 years in patients with ACS ($p = 0.025$). There were no significant correlations between citrulline and TMAO levels (Kendall's tau = 0.027).

Conclusions. Decreasing citrulline levels do not predict long-term mortality of hospitalized patients with CVD. Moreover, they are not associated with the serum levels of TMAO in these patients.

Key words: cardiovascular diseases, intestinal barrier, citrulline, gut permeability, TMAO

Background

Cardiovascular disease (CVD) has been reported to be associated with intestinal barrier dysfunction and increased intestinal permeability.¹ Initial studies focused on altered intestinal function in patients with chronic heart failure (chronic HF).^{2–4} However, a link between intestinal barrier dysfunction and coronary artery disease,^{5,6} ST-segment elevation myocardial infarction^{7,8} and arterial hypertension^{9,10} has also been reported. A vicious cycle has been described wherein CVD impairs the intestinal barrier, making it more permeable to toxic substances that favor the progression of cardiovascular abnormalities.¹

The assessment of the intestinal barrier competency is a complex task which can be achieved using a number of approaches.¹¹ One approach is to use biomarkers such as bacterial lipopolysaccharide (LPS),¹¹ zonulin,¹² claudins,¹³ and intestinal fatty acid binding protein.¹⁴ There are also tools for evaluating the function of intestinal barrier samples such as the Ussing chamber.¹⁵ Depending on the method used, various structural and functional parameters can be measured. One available biomarker of intestinal barrier function is serum citrulline level, which allows for an indirect assessment of absorptive enterocyte mass.^{1,16–18} Citrulline is an amino acid synthesized mainly by enterocytes in the proximal small bowel, in the middle and upper parts of intestinal villi.¹⁷ Citrulline measurements have been reported to be a useful marker of acute mesenteric ischemia.¹⁹ Moreover, their use as a marker of epithelial lining damage in a human model of small intestinal ischemia and reperfusion has been described.²⁰ Reduced citrulline levels also serve as a biomarker of intestinal barrier failure and are an independent prognostic factor in critically ill patients.^{21–24}

A recent meta-analysis of 26 randomized controlled studies found that long-term citrulline supplementation significantly improves vascular endothelial function and reduces arterial stiffness.²⁵ As the authors point out, these effects are associated with a reduced risk of cardiovascular events. Other beneficial effects of citrulline supplementation include improved blood pressure, glucose and lipid profile, and the bioavailability of arginine and nitric oxide.²⁶

So far, no studies have assessed the use of citrulline levels as a predictor of long-term mortality in patients with CVD. Moreover, data are lacking on the association between levels of citrulline and the microbiota-derived metabolite trimethylamine N-oxide (TMAO).^{27,28} It was postulated that intestinal permeability can significantly affect the absorption of TMAO and its precursors.²⁹ The current study is a continuation of our previous research on the same population of patients (unpublished data). The previous study did not reveal a significant association between TMAO levels and long-term mortality in CVD patients. The assessment of intestinal permeability may shine a new light on our previous findings and guide the direction of future research.

Objectives

This study aimed to assess the effects of citrulline levels, a marker of enterocyte functional mass, on the long-term mortality of CVD patients. Moreover, the relationship between 2 biomarkers – citrulline and TMAO levels – was evaluated.

Materials and methods

Patients

The study included 1036 consecutive patients hospitalized between March 2013 and November 2015 in the Department of Cardiology at Wrocław Medical University in Wrocław, Poland. All patients provided written informed consent to participate in the study and submitted blood samples for laboratory testing.

The exclusion criterion was the lack of patient's informed consent. Patients who did not want to consent or were unable to consent due to their clinical condition (i.e., unconscious or intubated) were excluded from the study. We routinely included patients on days 1 or 2 of the hospital stay in order to enroll patients with stable conditions who were willing to participate in the study.

Specimen characteristics

Blood samples were stored at a temperature of -80°C at the BioBank of the Łukasiewicz Research Network – PORT Polish Center for Technology Development in Wrocław, Poland.

Assay methods

Liquid chromatography with tandem mass spectrometry was used to determine serum L-citrulline and TMAO levels. Briefly, samples were thawed on ice and extracted by adding a mix of d4-citrulline and d9-TMAO (Cambridge Isotope Laboratories, Tewksbury, USA) in acetonitrile (final concentration 10 μM) at a ratio of 1:3 (v/v). The chromatographic separation was performed using a Luna Silica analytical column (3 μm , 100 \AA , 150 \times 2 mm; Phenomenex, Torrance, USA) and the UltiMateTM 3000 UPLC system (Dionex, Sunnyvale, USA). An isocratic elution of the mobile phase consisting of 0.1% formic acid in acetonitrile and water at a ratio of 60:40 (v/v) was applied at a flow rate of 0.3 mL/min (total run time: 5 min). A multiple reaction monitoring mode was selected for mass spectrometric detection using ESI-Q-TOF (Bruker Daltonics, Bremen, Germany) in a positive ion mode. A calibration curve was constructed at a range of 0.5–100 μM for L-citrulline (Sigma-Aldrich, St. Louis, USA) and 0.125–25 μM for TMAO.

This method has been validated according to the Food and Drug Administration (FDA) guidelines.³⁰ The linearity

was determined by using correlation coefficients (R^2) which were 0.9997 for both citrulline and TMAO levels. The sensitivity of the laboratory analysis was assessed based on the limit of detection and limit of quantification. These were 0.221 μM and 0.662 μM , respectively, for citrulline and 0.236 μM and 0.708 μM , respectively, for TMAO. The precision and accuracy of the measurements were assessed with the use of quality control samples and standard solutions of various concentrations. The calculated inter- and intra-assay coefficients of variation did not exceed 8% for any of the tested levels, and the accuracy was in the range of 95–105%. This is in line with the limits proposed for the validation of assay methods for biological samples.

All samples were measured in 2 biological and 2 technical replicates. The peak area ratio (analyte/internal standard) was used for the calculation of mean L-citrulline and TMAO levels in samples. Data on current diagnosis, comorbidities, anthropometric parameters, laboratory test results, and medication use were obtained from the medical records of the index hospitalization.

Study design

This is a retrospective observational study.

At the time of hospitalization, patients donated blood samples for future research. The protocol of sampling and biobank creation was approved by the local ethics committee of Wrocław Medical University on February 9, 2011 (approval No. 73/2012). All patients consented to the storage and processing of samples for future studies.

The concentrations of the selected biomarkers were assessed retrospectively in collected samples. Mortality was analyzed using the registry of the Polish National Health Fund (as of February 19, 2020).

Statistical analyses were performed to assess the correlation of biomarker concentrations with mortality and the available clinical data obtained during the hospitalization of each patient.

The study protocol was approved by the local ethics committee of Wrocław Medical University on February 28, 2019 (approval No. 163/2019). The study was conducted in accordance with the Declaration of Helsinki. All patients provided written informed consent to participate in the study.

Statistical analyses

The statistical analyses were performed on the whole population. Subgroups of patients were classified according to the main clinical diagnosis of CVD: 1) patients with acute coronary syndrome (ACS) during the index hospitalization; 2) patients with chronic coronary syndrome; 3) patients with chronic HF without ACS; and 4) patients with atrial fibrillation (AF).

Additionally, patients were classified according to the occurrence of death during the follow-up period, as shown

in Table 1 for the whole study group, and within subpopulations, as shown in Table 2. Depending on data distribution, quantitative data were presented as means with standard deviations (SDs) and medians with interquartile ranges (IQRs). The rates of CVD and medication use were presented as percentages of patients. The normality of data distribution was assessed using the Kolmogorov–Smirnov and Lilliefors tests. The Kendall's tau test was used to assess the correlation between variables. The mean values of 2 independent variables were compared using the non-parametric Mann–Whitney test, while the Kruskal–Wallis analysis of variance (ANOVA) was used to compare more than 2 independent variables. The effect of continuous variables on mortality in subgroups was assessed using the Cox proportional hazards model. The proportional hazards assumptions were tested with proportional tests and presented graphically using the plots of scaled Schoenfeld residuals. The goodness-of-fit was tested by calculating the coefficient of determination (R^2). The Cox proportional hazards model with interactions was used to assess the independence of variables on mortality prediction. Survival curves for individual variables were generated using the Kaplan–Meier estimator. A value of $p < 0.05$ was considered statistically significant. All analyses were performed using STATISTICA v. 13 software (TIBCO Software Inc., Palo Alto, USA; <https://www.tibco.com/>).

Results

The characteristics of the study population are presented in Table 1. The study included a total of 1036 patients, including 177 (11.3%) patients with ACS, 441 (42.6%) patients with chronic coronary syndrome, 292 (28.2%) patients with chronic HF, and 277 (26.7%) patients with AF. The mean follow-up for the study group was 58.4 months. The 5-year mortality rate for the whole population was 16.5% (171 deaths). Most of the clinical and biochemical parameters differed between the deceased patients and the survivors (Table 1).

There were no significant differences in citrulline levels between subgroups divided according to survival (Table 1). Moreover, the univariate Cox proportional hazards analysis revealed no association between citrulline levels and death at 5 years (hazard ratio (HR) = 0.99; 95% confidence interval (95% CI): 0.97–1.00; $p = 0.49$). Therefore, a multivariate analysis was not performed.

For a more detailed analysis, citrulline levels were divided into quartiles. However, no differences were noted between the quartiles in terms of their effect on survival at 5 years (χ^2 test = 3.53; $p = 0.31$) (Fig. 1).

To obtain a more detailed insight into the effect of citrulline levels on mortality in patients with CVD, we performed a subgroup analysis of citrulline levels. The differences in citrulline levels in subgroups divided according to survival at 5 years are presented in Table 2. Significantly

Table 1. Study population characteristics

Parameter	Study population (n = 1036)	Death at 5 years		p-value*	
		yes (n = 171)	no (n = 865)		
Age [years], mean (SD)	62.0 (14.1)	68.9 (11.1)	60.7 (14.3)	<0.0001	
Male sex [%]	61.1	73.0	58.8	<0.001	
TMAO [$\mu\text{mol/L}$]	4.06 (2.79–6.01)	5.65 (3.48–8.94)	3.86 (2.70–5.62)	<0.0001	
Citrulline [$\mu\text{mol/L}$]	22.5 (17.8–27.9)	21.5 (16.5–27.6)	22.8 (18.0–28.0)	0.18	
Acute coronary syndrome [%]	17.0	32.7	19.4	<0.001	
Chronic coronary syndrome [%]	42.5	57.1	40.0	<0.0001	
Chronic HF [%]	28.1	54.7	23.4	<0.0001	
Atrial fibrillation [%]	26.7	43.2	23.4	<0.0001	
Other types of arrhythmia [%]	16.4	14.7	85.2	0.48	
Conduction disorders [%]	44.0	13.1	86.8	0.01	
PCI during hospitalization [%]	21.0	31.1	23.3	0.051	
Previous PCI [%]	14.4	25.7	16.9	0.017	
Previous CABG [%]	7.6	12.2	6.7	0.012	
Diabetes [%]	24.7	35.2	22.6	<0.001	
Chronic kidney disease [%]	14.58	28.5	71.5	0.002	
Dialysis patients [%]	1.45	27.67	73.33	0.001	
Hypertension [%]	71.7	81.8	69.7	0.001	
Smoking (current) [%]	23.2	30.0	21.9	0.026	
NYHA (% of patients with chronic HF)	I	7.0	8.7	6.3	0.16
	II	55.5	48.3	58.8	
	III	34.0	37.7	32.3	
	IV	3.3	5.3	2.6	
CCS (% of patients with chronic coronary syndrome)	I	10.2	6.0	11.3	0.65
	II	54.3	57.5	53.5	
	III	32.2	33.3	32.0	
	IV	3.1	3.0	3.1	
LVEF [%]	60 (50–65)	50 (37–65)	65 (55–66)	<0.0001	
eGFR [mL/min/1.73 m^2]	68 (55–80)	58 (44–72)	69 (58–81)	<0.0001	
hsCRP [mg/L]	3.47 (1.33–13.3)	7.79 (2.64–30.8)	3.11 (1.24–10.1)	<0.0001	
HbA _{1c} [%]	5.70 (5.40–6.20)	5.90 (5.50–6.65)	5.70 (5.40–6.10)	0.018	
TC [mg/dL]	182 (149–216)	171 (135–207)	184 (151–218)	0.003	
LDL-C [mg/dL]	104 (80–136)	97 (33–249)	106 (83–136)	0.094	
HDL-C [mg/dL]	45 (37–55)	42 (34–51)	46 (38–55)	<0.001	
Triglycerides [mg/dL]	124 (95–169)	115 (89–155)	127 (96–172)	0.018	
ASA [%]	54.8	64.0	52.9	0.009	
Clopidogrel [%]	29.4	28.1	35.1	0.075	
OAC [%]	28.9	43.4	26.0	<0.0001	
ACEIs [%]	70.2	76.1	69.0	0.066	
ARBs [%]	7.19	3.01	8.02	0.022	
β -blockers [%]	81.2	92.2	79.0	<0.0001	
Statins [%]	79.1	89.2	77.0	<0.001	
Loop diuretics [%]	19.1	43.4	14.3	<0.0001	

Data are presented as median and interquartile range (IQR) unless indicated otherwise. ACEI – angiotensin-converting enzyme inhibitor; ARB – angiotensin receptor blocker; ASA – acetylsalicylic acid; CABG – coronary artery bypass grafting; CCS – Canadian Cardiovascular Society grading of angina pectoris; eGFR – estimated glomerular filtration rate; HbA_{1c} – glycated hemoglobin A_{1c}; HDL-C – high-density lipoprotein cholesterol; HF – heart failure; hsCRP – high-sensitivity C-reactive protein; LDL-C – low-density lipoprotein cholesterol; LVEF – left ventricular ejection fraction; NYHA – New York Heart Association Functional Classification; OAC – oral anticoagulation; PCI – percutaneous coronary intervention; SD – standard deviation; TC – total cholesterol; TMAO – trimethylamine N-oxide.

Table 2. Citrulline levels in subgroups of deceased patients compared to survivors at 5 years

Subgroup	Whole subgroup [$\mu\text{mol/L}$]	Death at 5 years		p-value
		yes (n =)	no (n =)	
Acute coronary syndrome (n = 177)	23.3 (18.3–29.1)	yes (n = 37)	no (n = 140)	0.025
		20.9 (15.2–25.8)	24.0 (18.5–30.1)	
Chronic coronary syndrome (n = 441)	22.2 (17.5–28.1)	yes (n = 96)	no (n = 345)	0.12
		21.0 (15.7–21.3)	22.4 (18.0–28.4)	
Chronic HF (n = 292)	22.2 (17.9–28.2)	yes (n = 93)	no (n = 199)	0.50
		21.7 (16.6–28.2)	22.3 (18.3–28.3)	
Atrial fibrillation (n = 277)	22.2 (17.7–28.5)	yes (n = 74)	no (n = 203)	0.89
		22.9 (16.5–30.1)	22.1 (18.1–28.4)	

Data are presented as median and interquartile range (IQR). HF – heart failure.

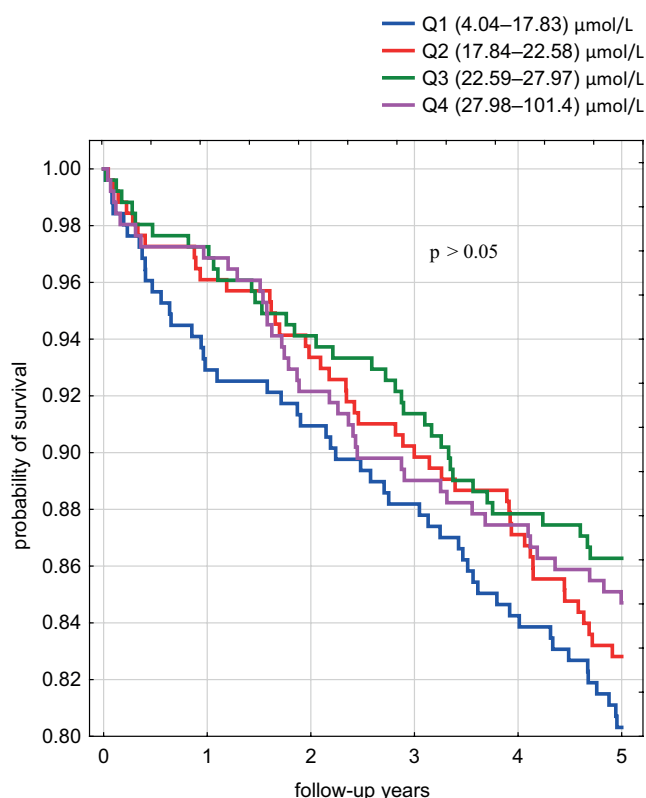


Fig. 1. Kaplan–Meier survival curves in subgroups divided according to quartiles of citrulline levels (Q1, Q2, Q3, and Q4 – quartiles 1, 2, 3, and 4, respectively).

lower citrulline levels were observed in deceased patients compared to survivors at 5 years in patients with ACS. However, the univariate Cox proportional hazards analysis did not reveal any significant associations between citrulline levels and the risk of death at 5 years in any of the subgroups, including patients with ACS. Therefore, multivariate analysis was not performed.

Our analysis revealed no significant correlations between citrulline levels and any of the recorded clinical parameters. Additionally, there were no significant correlations between citrulline levels and multimorbidity, defined as the number of comorbidities present in 1 patient, including ACS, stable coronary syndrome (SCS),

chronic HF, AF, arterial hypertension, arrhythmias, and/or conduction disorders. Finally, no significant correlations were noted between TMAO and citrulline levels (Kendall’s tau = 0.027).

Discussion

Our study indicates that serum citrulline levels are not correlated with long-term mortality in patients hospitalized due to CVD. While several markers of intestinal barrier dysfunction are available, this study was constructed to assess a single parameter. We decided on citrulline because there is limited research available on the association between citrulline levels and long-term outcomes in CVD patients.

When investigating a single marker of intestinal permeability, the interpretation of the results must account for some inherent limitations. One of the most common markers of an impaired intestinal barrier is LPS.¹¹ However, LPS assessment in peripheral blood is relatively difficult and often produces false positive results. Moreover, similarly to anti-endotoxin antibodies, it serves only as an indirect marker of increased intestinal permeability.¹¹ Another known biomarker is intestinal fatty acid-binding protein. However, there are limited data supporting its use in the assessment of chronic intestinal barrier disruption.³¹ As for zonulin, previous studies have used commercial enzyme-linked immunosorbent assays (ELISAs) for zonulin measurements. However, these assays do not reflect the actual levels of zonulin but rather the levels of a structurally similar haptoglobin.¹² The reliability of studies on zonulin is further limited by the fact that zonulin is not expressed in mice. Thus, the results obtained actually reflect the levels of unknown proteins rather than zonulin.¹² Finally, claudins are a highly diverse class of 27 proteins present in numerous tissues.¹³ They have not only low tissue specificity but also opposing functions, making it difficult to choose a specific protein and interpret the results.¹³

The usefulness of citrulline for the direct functional assessment of enterocyte mass has been confirmed in previous research studies.^{16,32} According to the literature, citrulline cutoff values have a sensitivity of 80% and

a specificity of 84% for diagnosing intestinal dysfunction. The most commonly used threshold for low citrulline levels is 20 $\mu\text{mol/L}$,¹⁶ which is in line with our findings. According to other investigators, a citrulline threshold of 10 $\mu\text{mol/L}$ indicates a significant loss of enterocyte mass.³² Finally, it has been reported that citrulline levels ranging from 10 $\mu\text{mol/L}$ to 20 $\mu\text{mol/L}$ are a grey zone for interpretation in critically ill patients.³³ Citrulline level of 40 ± 10 $\mu\text{mol/L}$ is considered normal.³² The abnormal citrulline levels in our population may indirectly suggest intestinal epithelial damage. However, several other factors need to be considered when interpreting these results.

Despite high susceptibility to blood supply disorders, high regenerative capacity of the intestinal epithelial lining after ischemia and reperfusion has been reported.²⁰ So far, citrulline assays have been used mainly for the assessment of critically ill patients.^{22–24,34,35} Changes in citrulline levels have been associated with patient prognosis²⁴ and enteral nutrition.³⁵ However, these studies were limited by a shorter duration of follow-up compared with our current research.

Considering the currently available literature, the fact that the diagnostic and prognostic values of citrulline are higher in acute states than in chronic ones cannot be excluded. At the same time, reduced citrulline levels are typically observed in chronic diseases associated with intestinal epithelial loss, such as Crohn's disease, celiac disease and short bowel syndrome.¹⁶ It is possible that changes in citrulline levels during the course of chronic CVD result in different dynamics and are induced by different mechanisms. This seems to be supported by the lack of correlation between citrulline levels and multimorbidity in our study. A significant difference in citrulline levels between deceased patients and survivors was noted only in patients with ACS, the only subgroup with an acute cardiovascular condition in our study. Previous studies on patients with myocardial infarctions reported abnormal levels of other markers indicating impaired intestinal barrier, such as LPS, D-lactate, zonulin, and endotoxin.^{7,8,36} Moreover, Zhou et al. reported that LPS and D-lactate were associated with a higher risk of mortality at 3 years.⁸ In our study, citrulline was not related to mortality risk at 5 years even in patients with ACS. The discrepancy between our study and the study by Zhou et al. may result from differences in the type of biomarkers and frequency of measurements. Zhou et al. assessed the levels of LPS and D-lactate at 2 time points over consecutive days.⁸ Our study, on the other hand, involved a single measurement of citrulline levels.

Serial measurements have advantages over a single assessment. Previous studies assessing changes in citrulline levels have revealed correlations between citrulline and the clinical status of patients.^{24,35} In an experimental study by Park et al., serial measurements reduced the potential confounding effect of circadian variation and fluctuations in citrulline levels.³⁷

Our study did not reveal any correlation between citrulline levels and clinical parameters such as estimated glomerular filtration rate (eGFR) or C-reactive protein (CRP) levels. This is surprising because kidney disorders and enhanced inflammatory processes may induce changes in citrulline levels.³² Citrulline is converted to arginine in the kidneys. Arginine is then used in nitric oxide synthesis, for example, in response to inflammation.³² Rare metabolic disorders and partial small bowel resections resulting in short bowel syndrome can affect citrulline levels, but these conditions were excluded from our study population. Only 2 patients had Crohn's disease and there were no cases of celiac disease or short bowel syndrome in the population examined in our study. Therefore, citrulline levels were not affected by these factors in our patients.

In our opinion, this study increases the current knowledge on the absorption of gut microbial metabolites. A previous prospective study by Kitai et al. revealed a significant association between worse prognosis and increased intestinal permeability assessed using the lactulose/rhamnose permeability test.³⁸ However, the sample size was relatively small (29 patients with HF) and the follow-up was shorter than in our study (median: 56 days). The increased intestinal permeability was not associated with levels of TMAO and intestinal fatty acid binding protein.³⁸ The lack of correlation between citrulline and TMAO levels may be explained by a yet unknown mechanism of TMAO uptake through the intestinal wall, independent of the number of enterocytes. However, this would be surprising because enterocyte mass reduction should result in the disruption of organic cation transporters mediating TMAO uptake.^{39,40}

Limitations

The major limitation of our study is that only a single measurement of citrulline was performed due to the retrospective study design and available biologic material. Optimally, the assessment of several different markers indicating intestinal barrier function performed at different timepoints depending on the duration of short-term and long-term follow-up needs to be conducted. A histopathological examination of an intestinal mucosa biopsy or the functional assessment of gastrointestinal absorption might also provide additional valuable data.

The strength of our study was its large sample size, the use of multiple clinical parameters, and the long-term follow-up. Additionally, the samples were obtained in a daily clinical practice setting and the citrulline levels were assessed using validated and reproducible methods.

Conclusions

Despite the limitations inherent to its retrospective design, our study provides novel insights into intestinal barrier dysfunction and fills the existing gap in the literature.

Decreased citrulline levels do not predict long-term mortality of hospitalized patients with CVD. Moreover, they are not associated with serum TMAO levels in these patients. We believe that these findings will provide a basis for future research into the links between intestinal permeability and the prognosis of CVD patients. The use of citrulline levels in conjunction with morphological and functional assessments of intestinal biopsies in CVD patients would allow for the assessment of potential new correlations. Perhaps serial measurements of citrulline concentrations during hospitalization and shorter follow-up will allow to capture the dynamics of the processes affecting the intestinal barrier and prognosis of patients with CVD.

ORCID iDs

Radosław Andrzej Konieczny  <https://orcid.org/0000-0002-0949-4364>
 Ewa Żurawska-Plaksej  <https://orcid.org/0000-0001-8566-3943>
 Konrad Kaaz  <https://orcid.org/0000-0001-5227-0027>
 Hanna Czapor-Irzabek  <https://orcid.org/0000-0001-8689-8314>
 Andrzej Mysiak  <https://orcid.org/0000-0002-4728-2565>
 Wiktor Kuliczkowski  <https://orcid.org/0000-0001-6284-0820>

References

- Lewis CV, Taylor WR. Intestinal barrier dysfunction as a therapeutic target for cardiovascular disease. *Am J Physiol Heart Circ Physiol*. 2020; 319(6):H1227–H1233. doi:10.1152/ajpheart.00612.2020
- Sandek A, Bauditz J, Swidsinski A, et al. Altered intestinal function in patients with chronic heart failure. *J Am Coll Cardiol*. 2007;50(16): 1561–1569. doi:10.1016/j.jacc.2007.07.016
- Sandek A, Bjarnason I, Volk HD, et al. Studies on bacterial endotoxin and intestinal absorption function in patients with chronic heart failure. *Int J Cardiol*. 2012;157(1):80–85. doi:10.1016/j.ijcard.2010.12.016
- Sandek A, Swidsinski A, Schroedl W, et al. Intestinal blood flow in patients with chronic heart failure: A link with bacterial growth, gastrointestinal symptoms, and cachexia. *J Am Coll Cardiol*. 2014; 64(11):1092–1102. doi:10.1016/j.jacc.2014.06.1179
- Li C, Gao M, Zhang W, et al. Zonulin regulates intestinal permeability and facilitates enteric bacteria permeation in coronary artery disease. *Sci Rep*. 2016;6:29142. doi:10.1038/srep29142
- Sanchez-Alcoholado L, Castellano-Castillo D, Jordán-Martínez L, et al. Role of gut microbiota on cardio-metabolic parameters and immunity in coronary artery disease patients with and without type-2 diabetes mellitus. *Front Microbiol*. 2017;8:1936. doi:10.3389/fmicb.2017.01936
- Carrera-Bastos P, Picazo Ó, Fontes-Villalba M, et al. Serum zonulin and endotoxin levels in exceptional longevity versus precocious myocardial infarction. *Aging Dis*. 2018;9(2):317–321. doi:10.14336/AD.2017.0630
- Zhou X, Li J, Guo J, et al. Gut-dependent microbial translocation induces inflammation and cardiovascular events after ST-elevation myocardial infarction. *Microbiome*. 2018;6(1):66. doi:10.1186/s40168-018-0441-4
- Kim S, Goel R, Kumar A, et al. Imbalance of gut microbiome and intestinal epithelial barrier dysfunction in patients with high blood pressure. *Clin Sci (Lond)*. 2018;132(6):701–718. doi:10.1042/CS20180087
- Santisteban MM, Qi Y, Zubcevic J, et al. Hypertension-linked pathophysiological alterations in the gut. *Circ Res*. 2017;120(2):312–323. doi:10.1161/CIRCRESAHA.116.309006
- Galipeau HJ, Verdu EF. The complex task of measuring intestinal permeability in basic and clinical science. *Neurogastroenterol Motil*. 2016;28(7):957–965. doi:10.1111/nmo.12871
- Massier L, Chakaroun R, Kovacs P, Heiker JT. Blurring the picture in leaky gut research: How shortcomings of zonulin as a biomarker mislead the field of intestinal permeability. *Gut*. 2021;70(9):1801–1802. doi:10.1136/gutjnl-2020-323026
- Scalise AA, Kakogiannis N, Zanardi F, Iannelli F, Giannotta M. The blood-brain and gut–vascular barriers: From the perspective of claudins. *Tissue Barriers*. 2021;9(3):1926190. doi:10.1080/21688370.2021.1926190
- Kastl SP, Krychtiuk KA, Lenz M, et al. Intestinal fatty acid binding protein is associated with mortality in patients with acute heart failure or cardiogenic shock. *Shock*. 2019;51(4):410–415. doi:10.1097/SHK.0000000000001195
- Hempstock W, Ishizuka N, Hayashi H. Functional assessment of intestinal tight junction barrier and ion permeability in native tissue by using chamber technique. *J Vis Exp*. 2021;2021:71. doi:10.3791/62468
- Fragkos KC, Forbes A. Citrulline as a marker of intestinal function and absorption in clinical settings: A systematic review and meta-analysis. *United European Gastroenterol J*. 2018;6(2):181–191. doi:10.1177/2050640617737632
- Crenn P, Messing B, Cynober L. Citrulline as a biomarker of intestinal failure due to enterocyte mass reduction. *Clin Nutr*. 2008;27(3):328–339. doi:10.1016/j.clnu.2008.02.005
- Vancamelbeke M, Vermeire S. The intestinal barrier: A fundamental role in health and disease. *Expert Rev Gastroenterol Hepatol*. 2017; 11(9):821–834. doi:10.1080/17474124.2017.1343143
- Kulu R, Akyildiz H, Akcan A, Oztürk A, Sozuer E. Plasma citrulline measurement in the diagnosis of acute mesenteric ischaemia. *ANZ J Surg*. 2017;87(9):E57–E60. doi:10.1111/ans.13524
- Schellekens DH, Hundscheid IH, Leenarts CA, et al. Human small intestine is capable of restoring barrier function after short ischemic periods. *World J Gastroenterol*. 2017;23(48):8452–8464. doi:10.3748/wjg.v23.i48.8452
- Piton G, Capellier G. Biomarkers of gut barrier failure in the ICU. *Curr Opin Crit Care*. 2016;22(2):152–160. doi:10.1097/MCC.0000000000000283
- Fagoni N, Piva S, Marino R, et al. The IN-PANCIA study: Clinical evaluation of gastrointestinal dysfunction and failure, multiple organ failure, and levels of citrulline in critically ill patients. *J Intensive Care Med*. 2020;35(3):279–283. doi:10.1177/0885066617742594
- Blaser A, Padar M, Tang J, Dutton J, Forbes A. Citrulline and intestinal fatty acid-binding protein as biomarkers for gastrointestinal dysfunction in the critically ill. *Anaesthesiol Intensive Ther*. 2019;51(3):230–239. doi:10.5114/ait.2019.86049
- Piton G, Manzoni C, Monnet E, et al. Plasma citrulline kinetics and prognostic value in critically ill patients. *Intensive Care Med*. 2010; 36(4):702–706. doi:10.1007/s00134-010-1751-6
- Smeets ETHC, Mensink RP, Joris PJ. Effects of L-citrulline supplementation and watermelon consumption on longer-term and postprandial vascular function and cardiometabolic risk markers: A meta-analysis of randomized controlled trials in adults. *Br J Nutr*. 2021;2021:1–34. doi:10.1017/S0007114521004803
- Flores-Ramírez AG, Tovar-Villegas VI, Maharaj A, Garay-Sevilla ME, Figueroa A. Effects of L-citrulline supplementation and aerobic training on vascular function in individuals with obesity across the lifespan. *Nutrients*. 2021;13(9):2991. doi:10.3390/nu13092991
- Stremmel W, Schmidt KV, Schuhmann V, et al. Blood trimethylamine-N-oxide originates from microbiota mediated breakdown of phosphatidylcholine and absorption from small intestine. *PLoS One*. 2017; 12(1):e0170742. doi:10.1371/journal.pone.0170742
- Farhangi MA. Gut microbiota-dependent trimethylamine N-oxide and all-cause mortality: Findings from an updated systematic review and meta-analysis. *Nutrition*. 2020;78:110856. doi:10.1016/j.nut.2020.110856
- Ufnal M, Pham K. The gut–blood barrier permeability: A new marker in cardiovascular and metabolic diseases? *Med Hypotheses*. 2017; 98:35–37. doi:10.1016/j.mehy.2016.11.012
- United States Department of Health and Human Services – Food and Drug Administration (FDA) and Center for Drug Evaluation and Research (CDER). *Bioanalytical Method Validation Guidance for Industry Biopharmaceuticals*. *Bioanalytical Method*. <https://www.fda.gov/files/drugs/published/Bioanalytical-Method-Validation-Guidance-for-Industry.pdf>.
- Bischoff SC, Barbara G, Buurman W, et al. Intestinal permeability: A new target for disease prevention and therapy. *BMC Gastroenterol*. 2014;14:189. doi:10.1186/s12876-014-0189-7
- Maric S, Restin T, Muff JL, et al. Citrulline, biomarker of enterocyte functional mass and dietary supplement: Metabolism, transport, and current evidence for clinical use. *Nutrients*. 2021;13(8):2794. doi:10.3390/nu13082794

33. Piton G, Capellier G. Plasma citrulline in the critically ill: Intriguing biomarker, cautious interpretation. *Crit Care*. 2015;19:204. doi:10.1186/s13054-015-0881-1
34. Reintam Blaser A, Padar M, Mändul M, et al. Development of the Gastrointestinal Dysfunction Score (GIDS) for critically ill patients: A prospective multicenter observational study (iSOFA study). *Clin Nutr*. 2021;40(8):4932–4940. doi:10.1016/j.clnu.2021.07.015
35. Padar M, Starkopf J, Starkopf L, et al. Enteral nutrition and dynamics of citrulline and intestinal fatty acid-binding protein in adult ICU patients. *Clin Nutr ESPEN*. 2021;45:322–332. doi:10.1016/j.clnesp.2021.07.026
36. Carnevale R, Sciarretta S, Valenti V, et al. Low-grade endotoxaemia enhances artery thrombus growth via Toll-like receptor 4: Implication for myocardial infarction. *Eur Heart J*. 2020;41(33):3156–3165. doi:10.1093/eurheartj/ehz893
37. Park CJ, Shaughnessy MP, Armenia SJ, Cowles RA. Serum citrulline levels exhibit circadian variation and fluctuations in relation to food intake in mice. *Gastroenterology Res*. 2019;12(2):88–92. doi:10.14740/gr1146
38. Kitai T, Nemet I, Engelman T, et al. Intestinal barrier dysfunction is associated with elevated right atrial pressure in patients with advanced decompensated heart failure. *Am Heart J*. 2022;245:78–80. doi:10.1016/j.ahj.2021.11.014
39. Samodelov SL, Kullak-Ublick GA, Gai Z, Visentin M. Organic cation transporters in human physiology, pharmacology, and toxicology. *Int J Mol Sci*. 2020;21(21):E7890. doi:10.3390/ijms21217890
40. Teft WA, Morse BL, Leake BF, et al. Identification and characterization of trimethylamine-N-oxide uptake and efflux transporters. *Mol Pharm*. 2017;14(1):310–318. doi:10.1021/acs.molpharmaceut.6b00937

Effects of exposure to air pollution on acute cardiovascular and respiratory admissions to the hospital and early mortality at emergency department

Dawid Żyrek^{A–D,F}, Anastasija Krzemińska^{B,C}, Nina Żyrek^{A,B,E}, Andrzej Wajda^{B,C},
Wojciech Pabian^{B,C}, Michał Pacholski^{B,C}, Mateusz Sokolski^{E,F}, Robert Zymlński^{E,F}

Institute of Heart Diseases, Wrocław Medical University, Poland

A – research concept and design; B – collection and/or assembly of data; C – data analysis and interpretation;
D – writing the article; E – critical revision of the article; F – final approval of the article

Advances in Clinical and Experimental Medicine, ISSN 1899–5276 (print), ISSN 2451–2680 (online)

Adv Clin Exp Med. 2022;31(10):1129–1138

Address for correspondence

Dawid Żyrek
E-mail: dawid.zyrek96@gmail.com

Funding sources

None declared

Conflict of interest

None declared

Acknowledgements

We are greatly indebted to J. Sokołowski, PhD, G. Gogolewski, PhD and W. Sycz, MD, from the Department of Emergency Medicine, Wrocław Medical University, Poland, for helping to obtain clinical data on emergency department admissions.

Received on December 28, 2021

Reviewed on April 4, 2022

Accepted on April 22, 2022

Published online on May 11, 2022

Abstract

Background. Particulate matter (PM) and NO₂ induce pathophysiological changes which contribute to an increased incidence of acute cardiovascular (CV) and respiratory (Rp) events.

Objectives. To analyze the relationship between air quality and the frequency of admissions to the emergency department (ED) due to the CV diseases and Rp causes.

Materials and methods. The study analyzed the reasons for admissions to the ED during the cold periods from January 2017 to January 2020. These data were combined with the average daily concentrations of NO₂, PM_{2.5} and PM₁₀, and the individual air quality indexes (IAQIs) for these pollutants.

Results. Our analyses have shown that 3468 (11.4%) and 1053 (3.46%) of all 30,419 analyzed patients were admitted to the ED for CV and Rp reasons, respectively. Cardiovascular patients were significantly more often admitted to the ED when the IAQI for NO₂ was worse than very good, and the IAQI for PM_{2.5} or PM₁₀ was worse than good. In such periods, diagnoses such as ischemic heart disease (IHD) or syncope were statistically more common and the risk of admission of a patient with a diagnosis such as IHD, heart failure (HF), syncope, stroke, or transient ischemic attack (TIA) was increased. Registered deaths occurred significantly more often among patients admitted on days with moderate or worse than moderate air quality determined in relation to PM₁₀ in comparison to days with very good or good air quality (0.35% and 0.23%, respectively, $p = 0.04$).

Conclusions. Air quality significantly affects the admissions to the ED for CV and Rp reasons and has an impact on mortality.

Key words: cardiovascular diseases, air pollution, emergency department, particulate matter, respiratory tract diseases

Cite as

Żyrek D, Krzemińska A, Żyrek N, et al. Effects of exposure to air pollution on acute cardiovascular and respiratory admissions to the hospital and early mortality at emergency department. *Adv Clin Exp Med.* 2022;31(10):1129–1138. doi:10.17219/acem/149400

DOI

10.17219/acem/149400

Copyright

Copyright by Author(s)

This is an article distributed under the terms of the Creative Commons Attribution 3.0 Unported (CC BY 3.0) (<https://creativecommons.org/licenses/by/3.0/>)

Background

Industrial progress leads to an uncontrolled increase in air pollution. The most toxic component of smog is particulate matter (PM) containing PM₁₀, PM_{2.5} and PM_{0.1} fractions. In urban conditions, combustion of fossil fuels remains the primary source of PM and is complemented by products of weathering and decomposition that contain both inorganic (e.g., Pb, Cr, Ni) and organic (e.g., endotoxins, fungal spores, plant debris) compounds.^{1–5}

At the cellular level, PM increases oxidative stress, generates free radicals, causes tissue damage, and triggers an inflammatory response.^{6–8} These noxious pathophysiological changes exacerbate the impact of air pollution on the human body. They are reflected through an increase of heart rate and blood pressure, deterioration of left ventricular diastolic function, induction of myocardial remodeling, progression of atherosclerosis, and activation of platelets and coagulation system; the overall greater risk of thromboembolism and myocardial ischemia is increased. Inflammation accounts for the majority of these changes through damage and dysfunction of blood vessel endothelium.^{9–14} Consequently, all factors contribute to an increased incidence of acute cardiovascular (CV) events.¹⁵

Although air quality in Poland is one of the worst in Europe, data on the impact of air pollution on health remain limited.^{16,17} Albeit a handful of studies conducted on the Polish population have investigated the relationship of air pollution to overall mortality and the incidence of respiratory (Rp) diseases, its impact on CV causes was rarely addressed.

Objectives

To the best of our knowledge, this is the first such analysis carried out in one of the most polluted parts of Poland (Lower Silesia). Our primary goal was to analyze the relationship between the quality of local air and the frequency of all admissions to the emergency department (ED) of the regional tertiary referral center, including hospitalization due to CV or Rp causes and early ED mortality.¹⁷ For this purpose, we tested the correlation between the abovementioned variables and determined the relative risk of admission to the ED for a given reason.

Materials and methods

Study design and setting

Our primary focus was to analyze the causes of admissions and reports to the ED of the University Teaching Hospital in Wrocław, Poland, during the cold months (December–February), from January 1, 2017, to December 31, 2020. The choice of such observation period was dictated

by the peak of the heating season when the concentration of airborne toxins reaches its highest levels in year.¹ We compared the data on hospital admissions and air quality retrospectively. The study design is depicted in Fig. 1.

We analyzed data collected from the observation of 30,419 admissions, which accounted for all ED admissions in the studied period.

Variables and data sources

The primary reason for ED visit, along with any additional diagnoses, was established on the basis of medical records obtained from the ED and, if required, other departments to which the patients were referred in the course of the diagnostic and therapeutic processes. The final reason for the report was determined at the patient's discharge. Respiratory causes included the following diagnoses: asthma (exacerbation or symptomatic dyspnea), chronic obstructive pulmonary disease (COPD; exacerbation or symptomatic dyspnea), pneumonia, bronchitis, other lower respiratory tract inflammations, cough, and (unless, on the basis of documentation, it could be attributed to a known cardiogenic cause) shortness of breath. If at least 1 diagnosis on admission to the ED was one of the following, the patient classified as a CV patient: ischemic heart disease (IHD; including symptomatic chronic IHD), unstable angina or myocardial infarction (MI; along with ST/non-ST-elevation MI and unspecified MI), heart failure (HF; exacerbated or symptomatic HF), arrhythmia (Arrh.; atrial flutter, atrial fibrillation (AF), other types of supraventricular tachycardia, ventricular tachycardia, and symptomatic atrioventricular block), elevated blood pressure (EBP; symptomatic or systolic ≥ 180 mm Hg or diastolic ≥ 110 mm Hg), stroke or transient ischemic attack (TIA), syncope, venous thromboembolism (VTE; including deep vein thrombosis and pulmonary embolism), or sudden cardiac arrest (SCA). All deaths that occurred within 24 h of reporting to the ED were recorded regardless of the cause.

The mean values of NO₂, PM₁₀ and PM_{2.5} used in calculations were obtained from the arithmetic mean of daily automatic measurements performed by the representative air quality monitoring stations at Wiśniowa Street and Korzeniowskiego Street (NO₂, PM₁₀ and PM_{2.5}), and Bartnicza

Table 1. Individual air quality index (IAQI) for each pollutant

IAQI	Daily average		
	NO ₂ [$\mu\text{g}/\text{m}^3$]	PM _{2.5} [$\mu\text{g}/\text{m}^3$]	PM ₁₀ [$\mu\text{g}/\text{m}^3$]
Very good	0–40	0–13	0–20
Good	40.1–100	13.1–35	20.1–50
Moderate	100.1–150	35.1–55	50.1–80
Sufficient	150.1–230	55.1–75	80.1–110
Bad	230.1–400	75.1–110	110.1–150
Very bad	>400	>110	>150

PM – particulate matter.

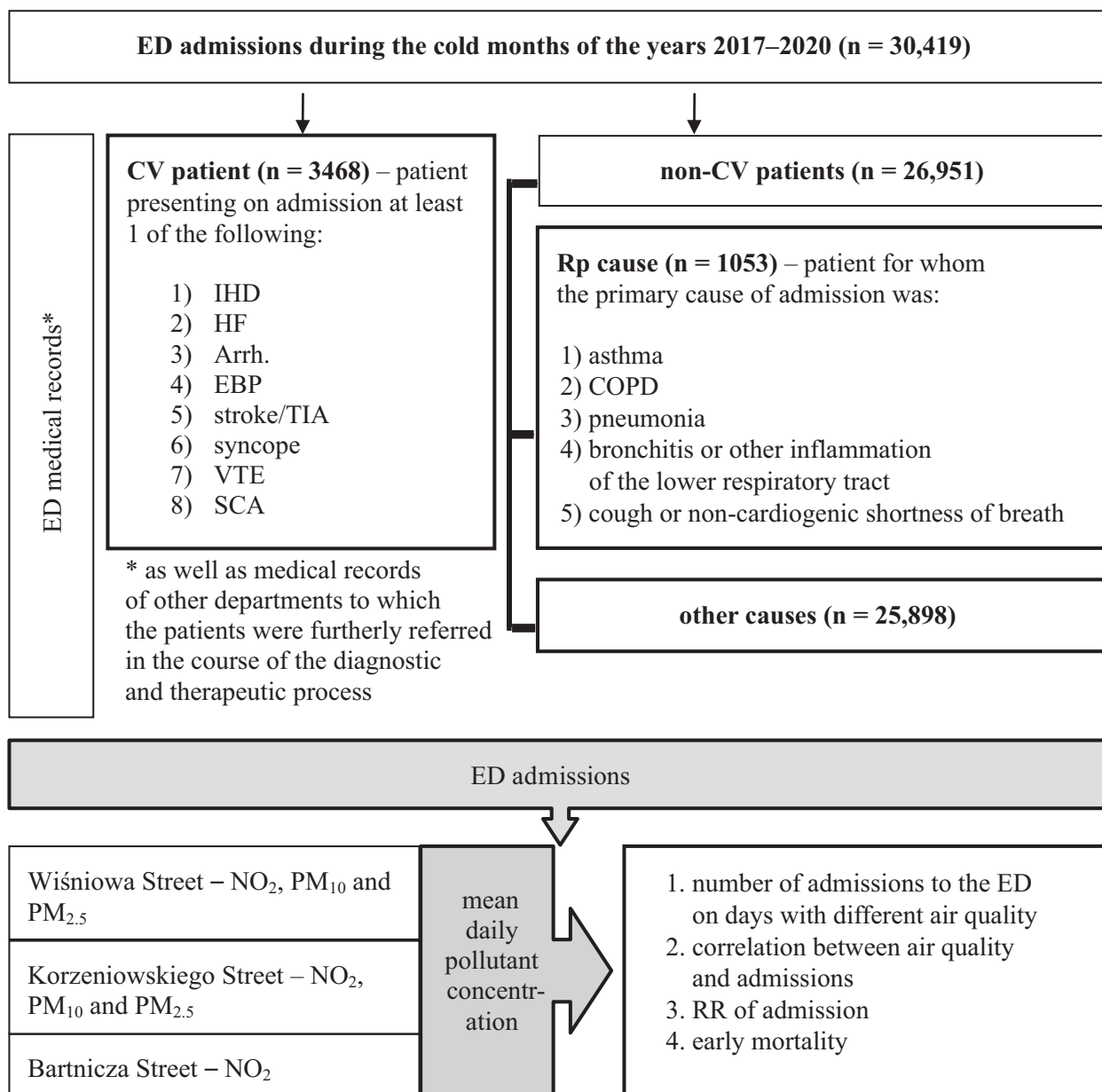


Fig. 1. Flowchart of study design

COPD – chronic obstructive pulmonary disease; ED – emergency department; CV – cardiovascular; Rp – respiratory; IHD – ischemic heart disease; HF – heart failure; Arrh. – arrhythmia; EBP – elevated blood pressure; TIA – transient ischemic attack; VTE – venous thromboembolism; SCA – sudden cardiac arrest; PM – particulate matter; RR – relative risk.

Street (NO₂ only) in Wrocław. In the calculations, the individual air quality index (IAQI), described as air quality index determined on the basis of a single pollutant (NO₂, PM₁₀ or PM_{2.5}), were referred to as presented below (Table 1). The IAQI is compliant with the standards used to calculate the air quality index established by the Polish General Directorate for Environmental Protection.¹⁸

Statistical analyses

We analyzed the relationship between the number of reports due to CV and Rp reasons and factors causing air pollution (PM_{2.5}, PM₁₀ and NO₂). The explanatory variables

were continuous variables. We used the Shapiro–Wilk test to check the normal distribution of the compared variables, out of which only the NO₂ variable approximated a normal distribution. The analysis of Kendall rank correlation coefficient (r) between all the reasons for registration to the ED on individual days and the average level of NO₂, PM_{2.5} and PM₁₀ on the day of admission (lag = 0) was performed, considering the time delay up to 3 days (lag = 1, lag = 2, lag = 3).

The Mann–Whitney U (M–W) test was performed to compare deaths and admissions on days belonging to 2 different categories of days grouped based on IAQIs. The admissions on days with very good or good IAQIs for PM_{2.5} or PM₁₀ were compared with admissions on days

with moderate or worse air quality. In the analyzed period, the IAQI for NO₂ did not qualify to moderate or worse air quality; therefore, the admissions on days with very good IAQI were compared to the admissions on days with good IAQI for this pollutant. The mortality on days with particular air quality was compared in an identical manner.

In the groups of days with specific IAQI, we determined an average daily number of admissions to the ED due to particular reasons. To calculate the relative risk (RR) of hospitalization for a reported reason in relation to the average daily concentration of NO₂, PM_{2.5} or PM₁₀ on the day of admission (lag = 0), a generally accepted formula was used. Baseline risk (RR = 1) was derived from the risk of registration to the ED for a particular cause in “very good” air quality conditions, defined as the average daily concentration of an individual pollutant (NO₂ ≤ 40 µg/m³, PM_{2.5} ≤ 13 µg/m³ or PM₁₀ ≤ 20 µg/m³). For these calculations, the following categories: sufficient, bad and very bad – were combined to characterize air quality worse than moderate (PM_{2.5} > 55 µg/m³ and PM₁₀ > 80 µg/m³). Separately, they described only a few days.

The results of the research were analyzed statistically using the STATISTICA v. 13.3 software (StatSoft Inc., Tulsa, USA). The result was considered statistically significant if p ≤ 0.05. A retrospective study protocol was approved by the Bioethical Committee of the Wrocław Medical University, Poland (approval No. KB-722/2019 provided on October 30, 2019).

Results

In the analyzed period, the air quality, determined separately by the average daily concentration of PM₁₀, PM_{2.5} or NO₂ was most often very good or good (Fig. 2). The highest recorded average daily concentrations of NO₂, PM_{2.5} and PM₁₀ were 74 µg/m³, 208 µg/m³ and 240 µg/m³, respectively. The average daily level of PM₁₀ exceeded the informing level (100 µg/m³) specified in the ordinance of the Polish Minister of the Environment 9 times, and it exceeded twice the alarming level (150 µg/m³) set in the same ordinance.¹⁹

Out of 30,419 analyzed patients, 3468 (11.4%) were admitted to the ED for CV reasons (Table 2). If all admissions for CV reasons are taken as 100%, the most common CV diagnoses were as follows: EBP – 1127 (32.50%), Arrh. – 975 (28.11%), AF – 633 (18.25%), stroke or TIA – 786 (22.66%), HF – 395 (11.39%), and IHD – 330 (9.52%), and MI – 204 (5.88%) (Fig. 3). Apart from CV reasons for admission, respiratory causes as the reason for admission were reported 1053 times (3.46%).

The correlation coefficients between the number of daily admissions and the concentration of tested pollutants are presented in Table 3. The average daily number of admissions for the majority of registered CV and Rp causes is greater in periods of higher daily concentrations of pollutants (Table 4). The RR of reporting to the ED for Rp causes under conditions of different air quality based on IAQIs for the selected pollutant is presented in Table 5.

Table 2. Number of patients registered in the emergency department (ED) in individual months, percentage of CV cases and characteristics of monthly levels of pollutants

Month	All patients	CV patients (% of all patients)	NO ₂ [µg/m ³] monthly median (±SD); IQR	PM _{2.5} [µg/m ³] monthly median (±SD); IQR	PM ₁₀ [µg/m ³] monthly median (±SD); IQR
January 2017	3162	440 (13.92)	36.33 (±10.48); 14.33	51.50 (±33.53); 57.50	62.00 (±34.41); 59.00
February 2017	2740	233 (8.62)	29.17 (±14.18); 17.17	51.50 (±44.36); 51.25	56.00 (±48.23); 54.50
December 2017	3189	327 (11.39)	29.33 (±8.33); 11.00	17.00 (±9.66); 15.00	21.00 (±9.27); 11.00
January 2018	2917	359 (13.10)	28.67 (±8.80); 15.00	21.00 (±14.68); 25.00	25.00 (±14.17); 22.00
February 2018	2703	312 (8.54)	33.67 (±10.51); 15.50	37.50 (±26.00); 19.75	44.50 (±27.29); 23.00
December 2018	3270	325 (9.95)	23.33 (±8.84); 12.33	17.00 (±15.61); 22.50	20.00 (±17.11); 24.00
January 2019	3159	444 (13.92)	27.67 (±9.54); 17.34	19.00 (±25.96); 27.00	17.00 (±26.38); 27.00
February 2019	2870	337 (10.67)	32.00 (±9.66); 12.33	29.75 (±17.60); 17.50	30.50 (±17.27); 23.00
December 2019	3267	290 (9.23)	29.33 (±9.86); 15.00	22.00 (±12.58); 21.00	27.50 (±16.25); 28.00
January 2020	3142	401 (13.75)	30.67 (±7.98); 10.67	23.50 (±20.20); 21.00	27.00 (±23.06); 25.00
Total	30,149	3468 (11.50)	30.00 (±10.38); 13.67	26.00 (±26.59); 29.50	30.00 (±28.83); 30.00

CV – cardiovascular; SD – standard deviation; IQR – interquartile range; PM – particulate matter.

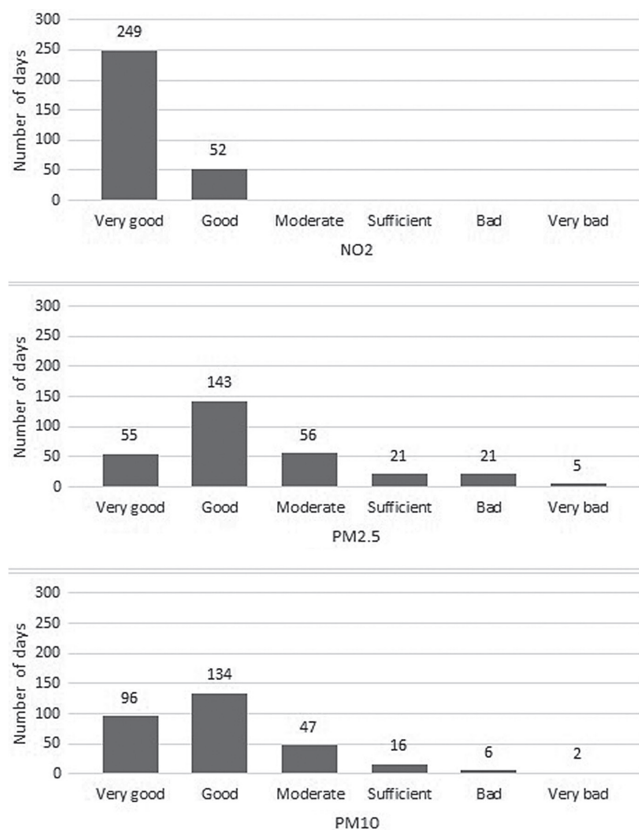


Fig. 2. The number of days in the analyzed period belonging to a given category of the individual air quality index (AQI)

PM – particulate matter.

In the analyzed period, there were 79 (0.26% of all admitted patients) registered deaths which occurred within 24 h of admission to the ED. These deaths happened significantly more often among patients admitted to the ED on days with moderate or worse than moderate air quality, determined by PM₁₀, in comparison to days with very good or good air quality (0.35% and 0.23%, respectively, M–W test; p = 0.039; Z = 2.06). This relationship, however, did not occur in the case of other pollutants and IAQI categories. Figure 4 depicts the number of deaths per 100 patients admitted to the ED under different air quality conditions for individual pollutants.

Discussion

The main finding of our study is that CV patients were significantly more often admitted to the ED when the IAQI for NO₂ was worse than very good, and the IAQI for PM_{2.5} or PM₁₀ was worse than good. In those periods, diagnoses such as IHD and syncope were statistically more common. Moreover, the risk of admission to the ED due to a CV cause was increased for patients diagnosed with IHD, MI, HF, EBP, syncope, stroke, or TIA. Additionally, the negative impact of air pollution below the alarming level (PM₁₀ = 150 µg/m³) and the informing level (PM₁₀ = 100 µg/m³) on the frequency of CV reports is particularly noteworthy.¹⁹

In our study, the average daily number of admissions due to IHD was higher during periods with worse air quality. Likewise, the RR of reporting due to IHD including MI was increased in each analyzed category of the IAQI, regardless of the selected pollutant, reaching statistical significance

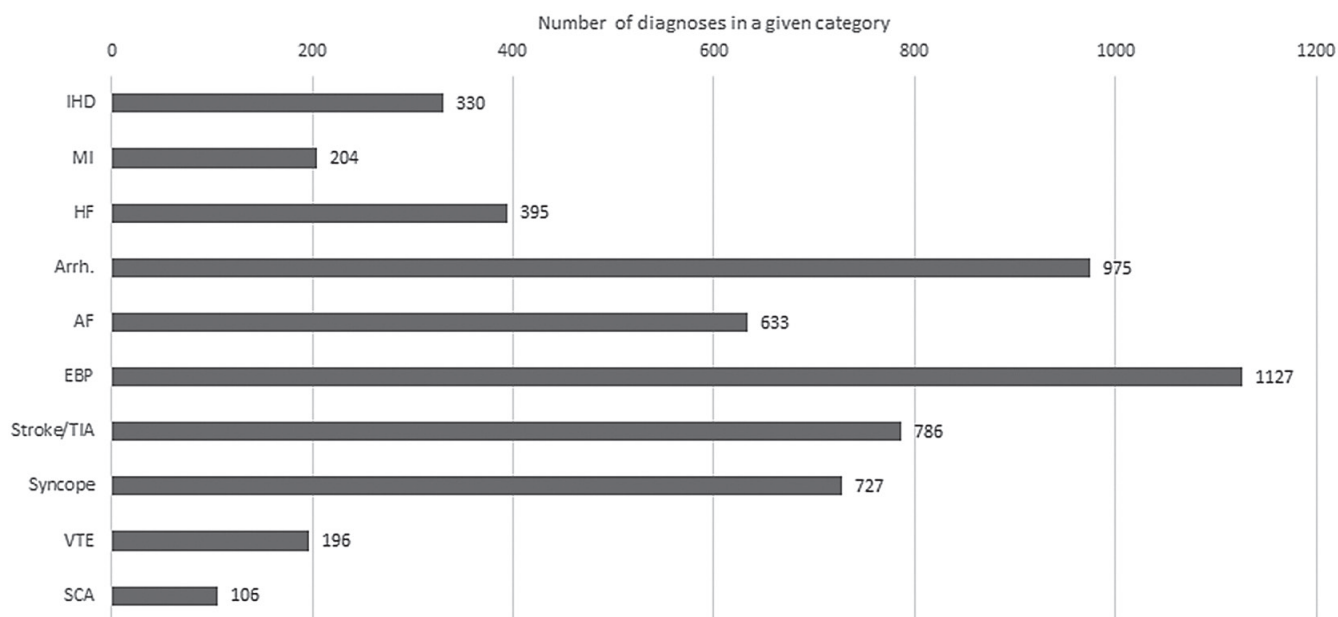


Fig. 3. The number of diagnoses in a given category among all patients registered in the ED for CV reasons. A patient on admission might have had more than 1 diagnosis

ED – emergency department; CV – cardiovascular; EBP – elevated blood pressure; Arrh. – arrhythmia; AF – atrial fibrillation; TIA – transient ischemic attack; HF – heart failure; IHD – ischemic heart disease; MI – myocardial infarction; VTE – venous thromboembolism; SCA – sudden cardiac arrest.

Table 3. Correlation of the daily number of admissions with a given diagnosis with the average daily concentration of NO₂, PM_{2.5} and PM₁₀ on the day of admission (lag = 0) and on the day preceding admission by 1, 2 or 3 days (lag = 1/2/3).

Cause of admission	Delay time [days]	NO ₂ r; (p-value); [n]	PM _{2.5} r; (p-value); [n]	PM ₁₀ r; (p-value); [n]
CV patients	lag = 0	0.179; (<0.001); [301]	0.122; (0.002); [301]	0.095; (0.014); [300]
	lag = 1	0.067; (0.084); [300]	0.082; (0.033); [300]	0.056; (0.151); [300]
	lag = 2	0.028; (0.464); [299]	0.052; (0.180); [299]	0.019; (0.617); [298]
	lag = 3	0.048; (0.220); [298]	0.059; (0.132); [298]	0.021; (0.593); [297]
IHD	lag = 0	0.131; (<0.001); [301]	0.135; (<0.001); [301]	0.142; (<0.001); [300]
	lag = 1	0.096; (0.013); [300]	0.117; (0.002); [300]	0.096; (0.013); [299]
	lag = 2	0.059; (0.129); [299]	0.103; (0.008); [299]	0.078; (0.044); [298]
	lag = 3	0.077; (0.048); [298]	0.099; (0.011); [298]	0.090; (0.021); [297]
MI	lag = 0	0.065; (0.094); [301]	0.107; (0.006); [301]	0.126; (0.001); [300]
	lag = 1	0.059; (0.124); [300]	0.102; (0.008); [300]	0.088; (0.024); [299]
	lag = 2	0.039; (0.319); [299]	0.095; (0.014); [299]	0.074; (0.055); [298]
	lag = 3	0.056; (0.153); [298]	0.065; (0.095); [298]	0.051; (0.189); [297]
HF	lag = 0	0.113; (0.003); [301]	0.108; (0.005); [301]	0.104; (0.007); [300]
	lag = 1	0.095; (0.014); [300]	0.091; (0.019); [300]	0.081; (0.038); [299]
	lag = 2	0.018; (0.641); [299]	0.042; (0.281); [299]	0.029; (0.448); [298]
	lag = 3	0.020; (0.602); [298]	0.056; (0.148); [298]	0.037; (0.341); [297]
Arrh.	lag = 0	0.082; (0.033); [301]	0.029; (0.450); [301]	0.018; (0.642); [300]
	lag = 1	0.020; (0.598); [300]	0.021; (0.580); [300]	0.023; (0.545); [299]
	lag = 2	-0.031; (0.417); [299]	-0.037; (0.337); [299]	-0.039; (0.322); [298]
	lag = 3	-0.017; (0.666); [298]	-0.017; (0.668); [298]	-0.015; (0.709); [297]
AF	lag = 0	0.089; (0.022); [301]	0.066; (0.089); [301]	0.067; (0.082); [300]
	lag = 1	0.034; (0.374); [300]	0.057; (0.143); [300]	0.069; (0.075); [299]
	lag = 2	-0.007; (0.848); [299]	-0.010; (0.803); [299]	0.003; (0.947); [298]
	lag = 3	-0.002; (0.965); [298]	-0.013; (0.731); [298]	-0.006; (0.868); [297]
EBP	lag = 0	0.084; (0.031); [301]	0.075; (0.052); [301]	0.014; (0.722); [300]
	lag = 1	-0.012; (0.761); [300]	0.044; (0.261); [300]	-0.024; (0.543); [299]
	lag = 2	-0.010; (0.794); [299]	0.039; (0.319); [299]	-0.024; (0.544); [298]
	lag = 3	0.033; (0.392); [298]	0.075; (0.053); [298]	0.005; (0.904); [297]
Stroke/TIA	lag = 0	0.142; (<0.001); [301]	0.116; (0.003); [301]	0.115; (0.003); [300]
	lag = 1	0.090; (0.020); [300]	0.092; (0.017); [300]	0.101; (0.009); [299]
	lag = 2	0.043; (0.264); [299]	0.055; (0.153); [299]	0.069; (0.074); [298]
	lag = 3	0.047; (0.223); [298]	0.078; (0.046); [298]	0.072; (0.063); [297]
Syncope	lag = 0	0.151; (<0.001); [301]	0.109; (0.005); [301]	0.109; (0.005); [300]
	lag = 1	0.059; (0.127); [300]	0.069; (0.075); [300]	0.059; (0.129); [299]
	lag = 2	0.033; (0.400); [299]	0.047; (0.229); [299]	0.033; (0.391); [298]
	lag = 3	-0.008; (0.830); [298]	-0.007; (0.852); [298]	-0.013; (0.731); [297]
VTE	lag = 0	0.058; (0.136); [301]	0.015; (0.691); [301]	0.013; (0.733); [300]
	lag = 1	0.016; (0.684); [300]	-0.001; (0.979); [300]	-0.003; (0.947); [299]
	lag = 2	-0.007; (0.867); [299]	0.013; (0.730); [299]	0.024; (0.529); [298]
	lag = 3	0.002; (0.953); [298]	0.015; (0.698); [298]	0.009; (0.823); [297]
SCA	lag = 0	-0.015; (0.696); [301]	0.017; (0.656); [301]	0.025; (0.696); [300]
	lag = 1	0.047; (0.221); [300]	0.081; (0.036); [300]	0.081; (0.037); [299]
	lag = 2	0.033; (0.390); [299]	0.060; (0.123); [299]	0.033; (0.397); [298]
	lag = 3	0.009; (0.825); [298]	0.037; (0.343); [298]	0.024; (0.540); [297]
Rp causes	lag = 0	0.227; (<0.001); [301]	0.192; (<0.001); [301]	0.162; (<0.001); [300]
	lag = 1	0.191; (<0.001); [300]	0.191; (<0.001); [300]	0.158; (<0.001); [300]
	lag = 2	0.147; (<0.001); [299]	0.150; (<0.001); [299]	0.115; (0.003); [298]
	lag = 3	0.069; (0.075); [298]	0.080; (0.039); [298]	0.042; (0.284); [297]

The values of Kendall rank correlation coefficient (r) in bold show statistical significance (p < 0.05). CV – cardiovascular; IHD – ischemic heart disease; MI – myocardial infarction; HF – heart failure; Arrh. – arrhythmia; AF – atrial fibrillation; EBP – elevated blood pressure; TIA – transient ischemic attack; VTE – venous thromboembolism; SCA – sudden cardiac arrest; Rp – respiratory; PM – particulate matter.

in most cases. As shown in Table 5, the RR of reporting due to MI was significantly increased even on days with very good air quality defined by the IAQI for PM₁₀ (good IAQI for PM₁₀ occurred in almost 45% of days in the analyzed period). Data supporting our observations can be found in numerous studies from various parts of the world; however, the specific values often differ significantly regarding

the strength of the studied relationships.^{15,20–22} Recently, 2 studies conducted in Poland have investigated the relationship between air pollution and hospitalization for acute coronary syndromes. In one of them, carried out in Białystok, PM₁₀ concentrations exceeding 50 µg/m³ corresponded with a higher number of hospitalizations on the day of exposure.²³ Those findings aligned with

Table 4. Average and median daily number of particular diagnoses depending on the individual air quality index on the day of admission (lag = 0)

Daily average (median)	Individual air quality index								
	NO ₂			PM _{2.5}			PM ₁₀		
	very good	good	p-value (Z value)	very good or good	moderate or worse	p-value (Z value)	very good or good	moderate or worse	p-value (Z value)
Number of days	249	52	–	198	103	–	230	71	–
CV patients	11.06 (11.00)	13.75 (13.00)	<0.001 (3.75)	10.97 (10.00)	12.58 (12.00)	0.003 (2.95)	11.01 (10.00)	13.17 (13.00)	<0.001 (3.43)
IHD	1.01 (1.00)	1.50 (1.00)	0.028 (2.19)	0.98 (1.00)	1.31 (1.00)	0.022 (2.28)	0.99 (1.00)	1.44 (1.00)	0.022 (2.29)
MI	0.63 (0.00)	0.88 (0.50)	0.187 (1.32)	0.63 (0.00)	0.78 (0.00)	0.169 (1.38)	0.62 (0.00)	0.86 (1.00)	0.086 (1.71)
HF	1.23 (1.00)	1.69 (1.00)	0.051 (1.95)	1.13 (1.00)	1.66 (1.00)	0.003 (2.93)	1.21 (1.00)	1.65 (1.00)	0.013 (2.48)
Arrh.	3.18 (3.00)	3.50 (3.00)	0.538 (0.62)	3.14 (3.00)	3.44 (3.00)	0.283 (1.07)	3.10 (3.00)	3.70 (3.00)	0.037 (2.08)
AF	2.08 (2.00)	2.23 (2.00)	0.528 (0.63)	2.01 (2.00)	2.28 (2.00)	0.179 (1.34)	1.98 (2.00)	2.49 (2.00)	0.024 (2.56)
EBP	3.61 (3.00)	4.38 (4.00)	0.031 (2.16)	3.64 (3.00)	3.95 (4.00)	0.126 (1.53)	3.67 (3.00)	3.97 (3.00)	0.202 (1.28)
Stroke/TIA	2.53 (2.00)	3.02 (3.00)	0.063 (1.86)	2.45 (2.00)	2.92 (3.00)	0.023 (2.28)	2.42 (2.00)	3.23 (3.00)	<0.001 (3.52)
Syncope	2.27 (2.00)	3.10 (3.00)	<0.001 (3.45)	2.25 (2.00)	2.73 (3.00)	0.008 (2.67)	2.31 (2.00)	2.76 (3.00)	0.028 (2.19)
VTE	0.65 (0.00)	0.67 (0.00)	0.895 (–0.13)	0.66 (0.00)	0.64 (0.00)	0.621 (0.49)	0.65 (0.00)	0.66 (1.00)	0.580 (0.55)
SCA	0.35 (0.00)	0.37 (0.00)	0.790 (–0.27)	0.33 (0.00)	0.39 (0.00)	0.505 (0.67)	0.32 (0.00)	0.45 (0.00)	0.114 (1.58)
Rp causes	3.27 (3.00)	4.79 (4.00)	<0.001 (4.34)	3.14 (3.00)	4.27 (4.00)	<0.001 (3.74)	3.12 (3.00)	4.85 (4.00)	<0.001 (5.02)

The categories „moderate or worse” include days when the individual air quality index was moderate, sufficient, bad, or very bad. The fields containing categories in which admissions for a given reason occur significantly more often (Mann–Whitney test; $p < 0.05$) than on days when the individual air quality index is very good (in case of NO₂) or not better than good (in case of PM_{2.5} and PM₁₀) are in bold. CV – cardiovascular; IHD – ischemic heart disease; MI – myocardial infarction; HF – heart failure; Arrh. – arrhythmia; AF – atrial fibrillation; EBP – elevated blood pressure; TIA – transient ischemic attack; VTE – venous thromboembolism; SCA – sudden cardiac arrest; Rp – respiratory; PM – particulate matter.

Table 5. The RR of registering the given diagnosis on days with different air quality

RR	Individual air quality index													
	NO ₂		PM _{2.5}						PM ₁₀					
	good NO ₂ = 40–100 µg/m ³		good PM _{2.5} = 13–35 µg/m ³		moderate PM _{2.5} = 35–55 µg/m ³		worse than moderate PM _{2.5} > 55 µg/m ³		good PM ₁₀ = 20–50 µg/m ³		moderate PM ₁₀ = 50–80 µg/m ³		worse than moderate PM ₁₀ > 80 µg/m ³	
	RR	95% CI	RR	95% CI	RR	95% CI	RR	95% CI	RR	95% CI	RR	95% CI	RR	95% CI
CV patients	1.24	1.15–1.34	1.04	0.95–1.14	1.11	1.00–1.24	1.31	1.18–1.46	1.02	0.95–1.10	1.17	1.06–1.28	1.29	1.15–1.45
IHD	1.48	1.15–1.90	1.05	0.77–1.44	1.17	0.81–1.69	1.69	1.19–2.41	1.31	1.00–1.71	1.50	1.07–2.09	2.15	1.49–3.10
MI	1.39	1.00–1.93	1.20	0.80–1.81	1.20	0.74–1.94	1.74	1.10–2.77	1.67	1.17–2.38	1.72	1.11–2.68	2.35	1.44–3.84
HF	1.37	1.08–1.73	1.27	0.93–1.72	1.79	1.28–2.51	1.78	1.26–2.53	1.11	0.87–1.41	1.40	1.05–1.88	1.54	1.08–2.20
Arrh.	1.10	0.94–1.28	0.94	0.79–1.11	1.02	0.83–1.24	1.13	0.92–1.39	0.93	0.80–1.07	1.12	0.93–1.34	1.22	0.97–1.53
AF	1.07	0.88–1.31	1.11	0.89–1.39	1.23	0.95–1.60	1.27	0.97–1.66	1.02	0.84–1.22	1.27	1.01–1.60	1.28	0.96–1.71
EBP	1.21	1.05–1.40	1.07	0.91–1.27	1.09	0.90–1.33	1.26	1.03–1.53	0.99	0.86–1.13	1.09	0.92–1.30	1.04	0.83–1.30
Stroke/TIA	1.19	1.00–1.42	1.11	0.91–1.36	1.16	0.92–1.47	1.50	1.19–1.90	1.08	0.92–1.28	1.36	1.11–1.67	1.49	1.16–1.91
Syncope	1.36	1.14–1.61	1.09	0.88–1.34	1.33	1.05–1.68	1.30	1.01–1.67	1.11	0.93–1.32	1.18	0.95–1.48	1.50	1.16–1.95
VTE	1.04	0.72–1.49	1.04	0.71–1.53	0.94	0.59–1.51	1.12	1.70–1.80	0.91	0.66–1.26	1.03	0.68–1.56	0.86	0.48–1.52
SCA	1.04	0.64–1.71	0.95	0.56–1.61	0.95	0.50–1.80	1.38	0.75–2.54	0.95	0.60–1.51	1.42	0.82–2.43	1.26	0.62–2.57
Rp causes	1.46	1.27–1.68	1.15	0.96–1.38	1.40	1.14–1.71	1.71	1.40–2.09	1.04	0.90–1.20	1.62	1.37–1.92	1.54	1.24–1.90

RR = 1 for admission with a given diagnosis in conditions of „very good” air quality. The categories: „PM_{2.5} > 55 µg/m³” and „PM₁₀ > 80 µg/m³” include days when the individual air quality index was sufficient, bad or very bad. The values in bold show statistical significance ($p < 0.05$). RR – relative risk; 95% CI – 95% confidence interval; CV – cardiovascular; IHD – ischemic heart disease; MI – myocardial infarction; HF – heart failure; Arrh. – arrhythmia; AF – atrial fibrillation; EBP – elevated blood pressure; TIA – transient ischemic attack; VTE – venous thromboembolism; SCA – sudden cardiac arrest; Rp – respiratory; PM – particulate matter

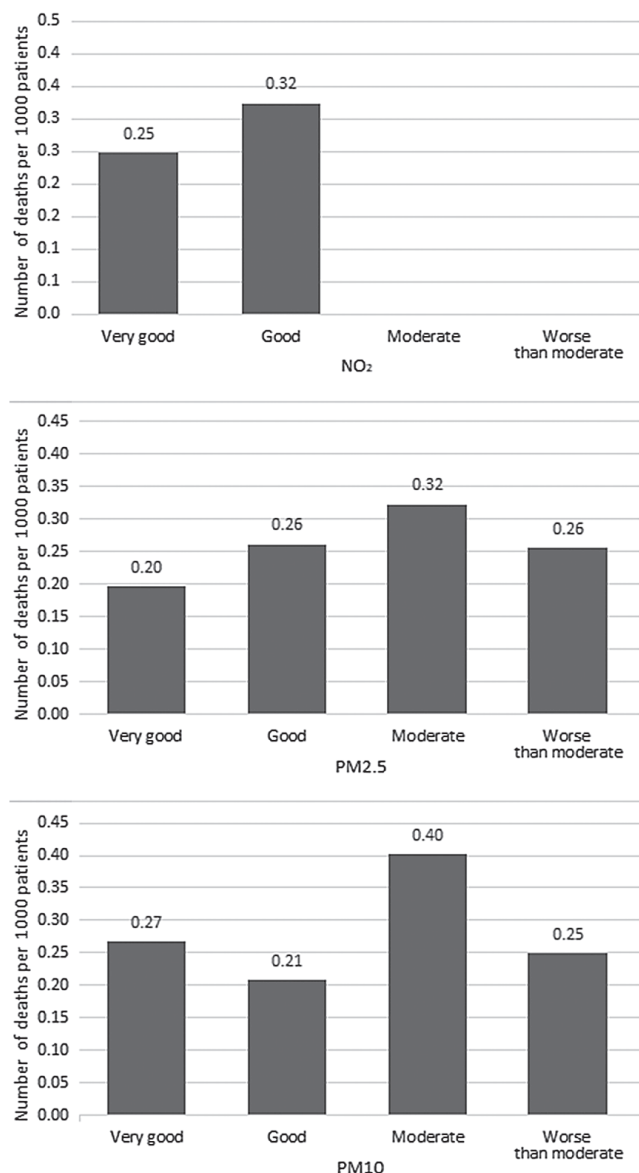


Fig. 4. Number of deaths per 1000 registered patients in a given category of the individual air quality index (IAQ)

PM – particulate matter.

the study conducted in Kraków, where a short-term increase in PM_{2.5} concentration was associated with a higher number of daily hospital admissions due to MI, while for PM₁₀, the effect was statistically significant only with a concomitant decrease in temperature.²⁴ It should not be forgotten that our work was based on the records from cold periods, hence the temperature differences are undoubtedly responsible for part of the observed effect.

Furthermore, we have shown that the number of patients who reported to the ED resulting from HF was higher on days with poorer air quality, regardless of the pollutant (Table 4). The observed relationship of exposure to polluted air with the diagnosis of HF is stronger in comparison to the results obtained by the majority of researchers. A meta-analysis published in 2013 revealed the negative impact of short-term exposure to polluted

air on hospitalization or deaths due to HF.²⁵ The RR of admission or death from HF due to increase in NO₂ [ppb], PM_{2.5} and PM₁₀ [µg/m³] concentrations by 10 units on the exposure day (lag = 0) rose by about 1% for each of these pollutants, although these relationships became more pronounced when the exposure lasted longer.^{25,26}

We observed a significantly higher RR of admission due to the EBP in the conditions of good air quality determined in relation to the average daily NO₂ concentration and worse than moderate air quality determined in relation to PM₁₀. The admissions due to EBP showed a correlation of a weak significance with the concentration of NO₂ on the day of admission, and no correlation with any of the tested pollutants on the preceding days. Nevertheless, literature provides a solid basis that both short-term and chronic exposure to polluted air increase the risk of hospitalization due to EBP and further promote the development of chronic hypertension in exposed individuals.^{27–29} It should be noted, however, that a particularly common cause of an increase in blood pressure is the omission of an antihypertensive drug dose, which appears unrelated to atmospheric pollution.^{30,31}

The exposure to polluted air or lead is estimated to account for approx. 33% of strokes worldwide.³² In our study, the risk of stroke or TIA increased significantly (RR = 1.5; 95% confidence interval (95% CI): 1.19–1.90) either when PM_{2.5} exceeded the level of 55 µg/m³ or when the mean daily PM₁₀ was in the moderate air quality category (RR = 1.36; 95% CI: 1.11–1.67). Most likely, this could also be observed at much lower concentrations of PM.²² Other researchers have noted a significant increase in the risk of admission for these reasons, even at the level of 15 µg/m³, 24 h before the admission.²⁰ Both long-term and short-term exposure to polluted air increased the risk of stroke, with the effects being more pronounced for ischemic strokes than hemorrhagic strokes.^{32,33} Our findings indicate that the effect is the strongest on the day of stroke occurrence (lag = 0) and decreases over time (Table 3), which aligns with the literature.^{32,34}

We found limited data on the relationship between air pollution and the occurrence of syncope. In a study which investigated the reasons for reports to emergency medical services, a significant correlation was established between the reported syncope/loss of consciousness and the concentration of PM_{2.5} on the day of reporting, with a moving average of 2–5 days.³⁵ In our study, this relationship was among the strongest observed (Table 3,5). However, it seems like this effect could be partly explained by the arrhythmic potential of some pollutants. Fainting could also be a symptom of many other CV diseases, well documented as associated with polluted air. It is also worth noting that the exposure to PM_{2.5} leads to an increased cerebral vascular resistance and, hence, decreased cerebral blood flow.³⁶ It is possible that some of the reports classified as syncope might have been an episode of TIA. The difficulty in distinguishing syncope from loss of consciousness for

any other reason (when based mainly on patient history) increases the likelihood of analytic bias of the frequency of such reports. Given the limited literature on the subject and the single-center nature of our study, the indications for further research are to analyze the relationship between air pollution and the occurrence of syncope, and to investigate the etiopathogenesis of this phenomenon.

Limitations

Our study has several limitations. The manual method of collecting medical records and creating databases is relatively susceptible to human error, e.g., incorrect interpretation of the disease history or misclassification of cases as individual categories due to ambiguous descriptions. We did not record the location where main symptoms occurred; therefore, some patients admitted to the University Teaching Hospital might have arrived from other, sometimes distant, regions of Poland. In addition, it is noteworthy that weekday and weather corrections were not taken into account and the impact of pollutants other than NO₂, PM_{2.5} and PM₁₀ was not assessed. Although this study analyses average daily concentrations of NO₂ and PM, it does not allow to distinguish the effect of short-term from chronic exposure to polluted air. The obtained data are an approximation of how polluted air impacts human health, covering the period of at least a few days before admission, which could explain why the relationships we observed, albeit generally consistent with the available literature, seem stronger than in most of the studies examining short-term exposure to polluted air, and better correspond with the results of long-term exposure. Nevertheless, due to differences in the methodology and presentation of results, a precise comparison of the quoted data was not possible.

Conclusions

Air pollution significantly affects the frequency of admissions to ED for CV and Rp reasons. This impact is observable below the alarming or informing level, and in the case of MI, remains significant even with good air quality in relation to daily PM₁₀ concentration. Due to the potentially serious health consequences of aspirating air pollutants, it is crucial to immediately take extensive measures in order to reduce anthropogenic emissions of NO₂, PM_{2.5} and PM₁₀, educate particularly vulnerable patients and limit their exposure to polluted air.

ORCID iDs

Dawid Żyrek  <https://orcid.org/0000-0002-9921-0811>
 Nina Żyrek  <https://orcid.org/0000-0002-8178-0322>
 Andrzej Wajda  <https://orcid.org/0000-0001-8832-3565>
 Wojciech Pabian  <https://orcid.org/0000-0001-5721-9458>
 Mateusz Sokolski  <https://orcid.org/0000-0001-9925-3566>
 Robert Zymlński  <https://orcid.org/0000-0003-1483-7381>

References

- Chlebowska-Styś A, Sówka I, Kobus D, Pachurka Ł. Analysis of concentrations trends and origins of PM₁₀ in selected European cities. Kaźmierczak B, Kutylowska M, Piekarska K, Trusz-Zdybek A, eds. *E3S Web Conf.* 2017;17:00013. doi:10.1051/e3sconf/20171700013
- Celis JE, Morales JR, Zaror CA, Inzunza JC. A study of the particulate matter PM₁₀ composition in the atmosphere of Chillán, Chile. *Chemosphere.* 2004;54(4):541–550. doi:10.1016/S0045-6535(03)00711-2
- Majewski G, Łykowski B. Chemical composition of particulate matter PM₁₀ in Warsaw conurbation. *Acta Scientiarum Polonorum Formatio Circumiectus.* 2008;7(1):81–96.
- Chow JC, Yang X, Wang X, et al. Characterization of ambient PM₁₀ bioaerosols in a California agricultural town. *Aerosol Air Qual Res.* 2015;15(4):1433–1447. doi:10.4209/aaqr.2014.12.0313
- Chirino YI, Sánchez-Pérez Y, Osornio-Vargas ÁR, Rosas I, García-Cuellar CM. Sampling and composition of airborne particulate matter (PM₁₀) from two locations of Mexico City. *Data in Brief.* 2015;4:353–356. doi:10.1016/j.dib.2015.06.017
- Cong X, Xu X, Xu L, et al. Elevated biomarkers of sympatho-adrenomedullary activity linked to e-waste air pollutant exposure in preschool children. *Environ Int.* 2018;115:117–126. doi:10.1016/j.envint.2018.03.011
- Ying Z, Xu X, Bai Y, et al. Long-term exposure to concentrated ambient PM_{2.5} increases mouse blood pressure through abnormal activation of the sympathetic nervous system: A role for hypothalamic inflammation. *Environ Health Perspect.* 2014;122(1):79–86. doi:10.1289/ehp.1307151
- Hoffmann B, Moebus S, Dragano N, et al. Chronic residential exposure to particulate matter air pollution and systemic inflammatory markers. *Environ Health Perspect.* 2009;117(8):1302–1308. doi:10.1289/ehp.0800362
- Huang F, Chen R, Shen Y, Kan H, Kuang X. The impact of the 2013 Eastern China smog on outpatient visits for coronary heart disease in Shanghai, China. *Int J Environ Res Public Health.* 2016;13(7):627. doi:10.3390/ijerph13070627
- Brook RD, Franklin B, Cascio W, et al. Air pollution and cardiovascular disease: A statement for healthcare professionals from the expert panel on population and prevention science of the American Heart Association. *Circulation.* 2004;109(21):2655–2671. doi:10.1161/01.CIR.0000128587.30041.C8
- Mishra S. Is smog innocuous? Air pollution and cardiovascular disease. *Indian Heart J.* 2017;69(4):425–429. doi:10.1016/j.ihj.2017.07.016
- Ohlwein S, Klümper C, Vossoughi M, et al. Air pollution and diastolic function in elderly women: Results from the SALIA study cohort. *Int J Hyg Environ Health.* 2016;219(4–5):356–363. doi:10.1016/j.ijheh.2016.02.006
- Bonnefont-Rousselot D, Mahmoudi A, Mougnot N, et al. Catecholamine effects on cardiac remodelling, oxidative stress and fibrosis in experimental heart failure. *Redox Rep.* 2002;7(3):145–151. doi:10.1179/135100002125000389
- Lanki T, Hoek G, Timonen KL, et al. Hourly variation in fine particle exposure is associated with transiently increased risk of ST segment depression. *Occup Environ Med.* 2008;65(11):782–786. doi:10.1136/oem.2007.037531
- Gluszek J, Losicka TM. Effects of air pollution on cardiovascular diseases. *Choroby Serca i Naczyni.* 2019;16(3):201–209. https://journals.viamedica.pl/choroby_serca_i_naczyni/article/view/ChSiN.2019.0030/49229
- European Environment Agency. Healthy Environment, Healthy Lives: How the Environment Influences Health and Well Being in Europe. Copenhagen, Denmark: European Environment Agency; 2020. <https://data.europa.eu/doi/10.2800/53670>. Accessed March 21, 2021. doi:10.2800/53670
- European Environment Agency. Air Quality in Europe: 2020 Report. Denmark: European Environment Agency; 2020. <https://data.europa.eu/doi/10.2800/786656>. Accessed September 8, 2021. doi:10.2800/786656
- General Directorate for Environmental Protection. Air Quality Index. https://powietrze.gios.gov.pl/pjp/content/health_informations. Accessed April 10, 2021.
- Dziennik Ustaw. Rozporządzenie ministra środowiska z dnia 24 sierpnia 2012 r. w sprawie poziomów niektórych substancji w powietrzu. <https://isap.sejm.gov.pl/isap.nsf/DocDetails.xsp?id=WDU20120001031>. Accessed September 18, 2021.

20. Wellenius GA. Ambient air pollution and the risk of acute ischemic stroke. *Arch Intern Med.* 2012;172(3):229. doi:10.1001/archinternmed.2011.732
21. Beelen R, Raaschou-Nielsen O, Stafoggia M, et al. Effects of long-term exposure to air pollution on natural-cause mortality: An analysis of 22 European cohorts within the multicentre ESCAPE project. *Lancet.* 2014;383(9919):785–795. doi:10.1016/S0140-6736(13)62158-3
22. Pope CA, Muhlestein JB, Anderson JL, et al. Short-term exposure to fine particulate matter air pollution is preferentially associated with the risk of ST-segment elevation acute coronary events. *J Am Heart Assoc.* 2015;4(12):e002506. doi:10.1161/JAHA.115.002506
23. Kuźma Ł, Pogorzelski S, Struniawski K, Dobrzycki S, Bachórzewska-Gajewska H. Evaluation of the influence of air pollution on the number of hospital admissions for acute coronary syndrome in elderly patients (BIA-ACS Registry). *Pol Arch Intern Med.* 2020;130(1):38–46. doi:10.20452/pamw.15064
24. Konduracka E, Niewiara Ł, Guzik B, et al. Effect of short-term fluctuations in outdoor air pollution on the number of hospital admissions due to acute myocardial infarction among inhabitants of Krakow, Poland. *Pol Arch Intern Med.* 2019;129(2):88–96. doi:10.20452/pamw.4424
25. Shah AS, Langrish JP, Nair H, et al. Global association of air pollution and heart failure: A systematic review and meta-analysis. *Lancet.* 2013;382(9897):1039–1048. doi:10.1016/S0140-6736(13)60898-3
26. Pope CA, Renlund DG, Kfoury AG, May HT, Horne BD. Relation of heart failure hospitalization to exposure to fine particulate air pollution. *Am J Cardiol.* 2008;102(9):1230–1234. doi:10.1016/j.amjcard.2008.06.044
27. Honda T, Pun VC, Manjourides J, Suh H. Associations of long-term fine particulate matter exposure with prevalent hypertension and increased blood pressure in older Americans. *Environ Res.* 2018;164:1–8. doi:10.1016/j.envres.2018.02.008
28. Xie X, Wang Y, Yang Y, et al. Long-term effects of ambient particulate matter (with an aerodynamic diameter $\leq 2.5 \mu\text{m}$) on hypertension and blood pressure and attributable risk among reproductive-age adults in China. *J Am Heart Assoc.* 2018;7(9):e008553. doi:10.1161/JAHA.118.008553
29. Gluszek J, Kosicka TM. Effect of short and long exposure to ambient air pollution on blood pressure. *Arter Hypertens.* 2020;24(1):10–15. https://journals.viamedica.pl/arterial_hypertension/article/view/AH.a2019.0009/62626. Accessed August 20, 2021
30. Heaton PC, Tundia NL, Luder HR. U.S. emergency departments visits resulting from poor medication adherence: 2005–07. *J Am Pharm Assoc.* 2013;53(5):513–519. doi:10.1331/JAPhA.2013.12213
31. Pittman DG, Tao Z, Chen W, Stettin GD. Antihypertensive medication adherence and subsequent healthcare utilization and costs. *Am J Manag Care.* 2010;16(8):568–576. PMID:20712390.
32. Feigin VL, Roth GA, Naghavi M, et al. Global burden of stroke and risk factors in 188 countries, during 1990–2013: A systematic analysis for the Global Burden of Disease Study 2013. *Lancet Neurol.* 2016;15(9):913–924. doi:10.1016/S1474-4422(16)30073-4
33. Yuan S, Wang J, Jiang Q, et al. Long-term exposure to $\text{PM}_{2.5}$ and stroke: A systematic review and meta-analysis of cohort studies. *Environ Res.* 2019;177:108587. doi:10.1016/j.envres.2019.108587
34. Samoli E, Stafoggia M, Rodopoulou S, et al. Associations between fine and coarse particles and mortality in Mediterranean cities: Results from the MED-PARTICLES project. *Environ Health Perspect.* 2013;121(8):932–938. doi:10.1289/ehp.1206124
35. Youngquist ST, Hood CH, Hales NM, Barton CC, Madsen TE, Arden Pope C. Association between EMS calls and fine particulate air pollution in Utah. *Air Qual Atmos Health.* 2016;9(8):887–897. doi:10.1007/s11869-016-0392-5
36. Wellenius GA, Boyle LD, Wilker EH, et al. Ambient fine particulate matter alters cerebral hemodynamics in the elderly. *Stroke.* 2013;44(6):1532–1536. doi:10.1161/STROKEAHA.111.000395

Association between the long-term exposure to air pollution and depression

Anna Gładka^{1,A–D}, Tomasz Zatoński^{2,D–F}, Joanna Rymaszewska^{1,D–F}

¹ Department of Psychiatry, Wrocław Medical University, Poland

² Department of Otolaryngology, Head and Neck Surgery, Wrocław Medical University, Poland

A – research concept and design; B – collection and/or assembly of data; C – data analysis and interpretation; D – writing the article; E – critical revision of the article; F – final approval of the article

Advances in Clinical and Experimental Medicine, ISSN 1899–5276 (print), ISSN 2451–2680 (online)

Adv Clin Exp Med. 2022;31(10):1139–1152

Address for correspondence

Anna Gładka
E-mail: agladka@gmail.com

Funding sources

None declared

Conflict of interest

None declared

Received on October 25, 2021
Reviewed on January 26, 2022
Accepted on May 11, 2022

Published online on June 2, 2022

Abstract

Background. Air pollution has a negative influence on neurological and psychiatric disorders. However, findings concerning the impact of air pollution on depression remain inconclusive. A deeper insight into these associations is warranted.

Objectives. To evaluate the impact of long-term exposure to air pollution on the incidence of depression among residents of 13 counties in the Lower Silesia region of Poland.

Materials and methods. We used data on cases of depression from the National Health Fund (Narodowy Fundusz Zdrowia – NFZ) from 13 counties of Lower Silesia between January 1, 2010, and December 31, 2015. Patients with a confirmed diagnosis of depression were included. Data on air pollution levels were extracted from the Chief Inspectorate of Environmental Protection (Główny Inspektorat Ochrony Środowiska – GIOŚ), and demographic data were extracted from Statistics Poland (Główny Urząd Statystyczny – GUS).

Results. The percentage of people diagnosed with depression over the 6-year study period depended on the group of counties homogeneous in terms of air pollution exposure ($p < 0.001$). We showed statistically significant correlations between different depression diagnoses and exposure to air pollutants. Elevated concentration of airborne fine particles with a diameter less than $2.5 \mu\text{m}$ ($\text{PM}_{2.5}$) and carbon monoxide (CO), and low benzo(a)pyrene (BaP), sulfur dioxide (SO_2) and cadmium (Cd) levels were independent risk factors for major depressive episodes with psychotic symptoms (F32.3). There was a significant negative correlation between ozone (O_3) levels and depression incidence.

Conclusions. Regions with heavy air pollution had a higher incidence of depression. There is a significant association between the exposure to air pollutants and different depression diagnoses.

Key words: depression, air pollution, particulate matter, ozone, nitrogen oxides

Cite as

Gładka A, Zatoński T, Rymaszewska J. Association between the long-term exposure to air pollution and depression. *Adv Clin Exp Med.* 2022;31(10):1139–1152. doi:10.17219/acem/149988

DOI

10.17219/acem/149988

Copyright

Copyright by Author(s)

This is an article distributed under the terms of the Creative Commons Attribution 3.0 Unported (CC BY 3.0) (<https://creativecommons.org/licenses/by/3.0/>)

Background

Depression is a mental disorder that affects 264 million people worldwide, and is a major cause of disability.¹ Beck described depression as a combination of disturbed thinking, low mood and a negative perception of self, the surrounding world and the future.² Depression is associated with excess mortality³ and increased suicide risk.⁴ There are many risk factors for depression,⁵ such as female gender, chronic illness, traumatic life events,⁶ unemployment, lower education, a lack of physical activity, and limited social support.⁷

In recent years, there has been an increasing interest in the environmental risk factors for depression.⁸ Lack of green spaces, poor quality of housing, chronic noise exposure, and air pollution are all strongly associated with risk of depression.⁹ Both chronic stress¹⁰ and gene–environment interactions¹¹ contribute to risk for psychiatric illnesses, such as depression. Neuroinflammation is one of the main pathogenic mechanisms implicated in depression.¹² A prominent environmental risk factor associated with neuroinflammation is air pollution.¹³ The exposure to intense air pollution may disrupt metabolic processes and thus lead to inflammation.¹⁴ For example, experimental studies have shown that high concentrations of air pollutants are associated with systemic inflammation and insulin resistance.^{15,16}

Long-term exposure to certain air pollutants leads to low-grade inflammation.¹⁷ In response, more anti-inflammatory cytokines are released, in turn causing immune tolerance. Chronic inflammation is also linked to the activation of the kynurenine (KYN) metabolic pathway of tryptophan, leading to the synthesis of various oxidant and immunomodulating molecules at the expense of the serotonin production.¹⁸ These metabolites modulate the immune system towards low-grade inflammation, strengthening the vicious cycle of the immune response.¹⁹ The KYN pathway plays a role in the pathogenesis of neurodegenerative and psychiatric diseases.¹⁸ The levels of quinolinic acid (a toxin produced by KYN pathway) are increased in patients with major depression.²⁰ Moreover, experimental data indicate that one compound of air pollution, ozone (O₃), causes increased concentration of kynurenine.²¹ These mechanisms could explain the adverse impact of air pollution on neuroinflammation and risk for mental illnesses.

Air pollution is a mixture of various particles and gases suspended in the air, such as particulate matter (coarse particles with an aerodynamic diameter between 2.5 µm and 10 µm (PM₁₀), fine particles with a diameter less than 2.5 µm (PM_{2.5}), and ultrafine particles with a diameter less than 0.1 µm (PM_{0.1})), e.g., O₃, carbon monoxide (CO), sulfur dioxide (SO₂), nitrogen oxides (NO_x), nitrogen dioxide (NO₂), and polycyclic aromatic hydrocarbons (PAHs). Their main sources are anthropogenic emissions from traffic, industry and coal stoves.²² The Lancet Commission highlighted that air pollution is one of the main environmental causes of disease and premature death.²³ It is estimated that 8.79 million people worldwide died prematurely in 2019.²⁴

Studies consistently indicate that increased mortality associated with exposure to air pollutants is largely due to cardiovascular and respiratory diseases.¹⁴ The health impact of air pollutants has been broadened to include neurological and psychiatric disorders such as anxiety, depression and dementia.²⁵ Research on these associations is extremely important, since mental and neurological conditions are among the main causes of disability, including 30% of all strokes being related to air pollution.²⁶

There are some proposed mechanisms whereby air pollutants can negatively affect the brain. For instance, particulate matter can reach the systemic circulation through the lungs or through olfactory neurons,²⁷ and directly interact with the brain.²⁸ Especially dangerous are ultrafine particles which, due to their small size and the toxic compounds bound to them, can cause pathophysiological alterations in the central nervous system.²⁸ Another mechanism is alveolar inflammation, which leads to the production of cytokines²⁹ that can penetrate the blood–brain barrier.³⁰ The exposure to air pollutants triggers the activation of the hypothalamic–pituitary–adrenal (HPA) axis and the release of stress hormones,³¹ which is commonly associated with cardiovascular disease (CVD), type II diabetes mellitus, dementia, and depression.³² These mechanisms can explain the negative effect of air pollution on the central nervous system and mental health.³³

Findings on the impact of air pollution on depression remain inconclusive. Two meta-analyses confirmed that a long-term exposure to fine particles is associated with increased incidence of depression³⁴ and suicide risk.³⁵ Another study showed that PM_{2.5} is significantly associated with the occurrence of depression for both long, and short-term exposure.³⁶ Long-term exposure to PM_{2.5} and short-term exposure to PM₁₀, NO₂, SO₂, and CO, are risk factors for depression.³⁷ On the other hand, a meta-analysis of 22 studies showed a weaker relationship between air pollution and depression risk. This includes long-term exposure to PM_{2.5}, PM₁₀ and NO₂, as well as short-term exposure to PM_{2.5}, PM₁₀, SO₂, O₃, and NO₂.³⁸ Moreover, current studies are based mostly on self-reports, and they do not specify the association between air pollution and the sub-diagnoses of depression.^{34,37} No studies have examined the relationship between the exposure to air pollution and risk for depression with psychotic symptoms. There is also not enough evidence on long-term exposure to many different air pollutants and its impact on depression, especially at the sub-diagnosis level. Therefore, a deeper insight into these associations is important, and more data are needed to clarify the impact of air pollutants on depression risk.

Objectives

The aim of this study was to evaluate the impact of long-term exposure to air pollution on depression risk among residents of 13 counties in Lower Silesia (Poland).

Materials and methods

Data on depression cases used in the study were derived from the National Health Fund (Narodowy Fundusz Zdrowia – NFZ) from counties (Polish: powiat; Głogów, Jelenia Góra, Kłodzko, Legnica, Lubań, Oława, Oleśnica, Polkowice, Złotoryja, Zgorzelec, Wałbrzych, Świdnica, and Wrocław) pertaining the period between January 1, 2010, and December 31, 2015. The inclusion criteria were based on the International Classification of Diseases, 10th Revision (ICD-10) code diagnosis: F32 (depressive episode), F32.0 (mild depressive episode), F32.1 (moderate depressive episode), F32.2 (severe depressive episode without psychotic symptoms), F32.3 (severe depressive episode with psychotic symptoms), F33 (recurrent depressive disorder), F33.0 (recurrent depressive disorder, current episode mild), F33.1 (recurrent depressive disorder, current episode moderate), F33.2 (recurrent depressive disorder, current episode severe without psychotic symptoms), and F33.3 (recurrent depressive disorder, current episode severe with psychotic symptoms). In total, data on depression diagnoses were available for 318,779 individuals per study year. Data on air pollution levels were extracted from the Chief Inspectorate of Environmental Protection (Główny Inspektorat Ochrony Środowiska – GIOŚ) and covered the period from 2010 to 2015. Considered pollutants included: PM₁₀, PM_{2.5}, SO₂, NO_x, benzo(a)pyrene (BaP)(PM₁₀), O₃, CO, and NO₂. We used demographic data for the period 2010–2015 from Statistics Poland (Główny Urząd Statystyczny – GUS), including marriage and divorce rate, feminization rate, non-working population, working people, people >65 years old, medical help accessibility, beneficiaries of social welfare, unemployment, average salary, and

total pollution emissions. Two statistical methods were used. Cluster analysis was used to distinguish between counties homogeneous in terms of air pollution. The 2nd method utilized all county data to perform univariate and multivariate regression analyses, and an analysis of variance (ANOVA). For multivariate and ANOVA analyses, data on marriage and divorce rate, feminization rate, non-working population, working people, people >65 years old, medical help accessibility, beneficiaries of social welfare, unemployment, average salary, total pollution emissions, and PM₁₀, PM_{2.5}, SO₂, NO_x, BaP(PM₁₀), O₃, CO, and NO₂ concentrations were used. For univariate analyses, we used depression rate and its associations with PM₁₀, PM_{2.5}, SO₂, NO_x, BaP(PM₁₀), O₃, CO, and NO₂ concentrations. The homogeneity of variance in the groups was verified using the Levene's test. In the case of unequal variances in the compared groups, the Welch's correction was applied. Normality of distribution was determined using the Kolmogorov–Smirnov and Shapiro–Wilk tests. For the construction of multivariate linear regression models, non-normal data were transformed using the Box–Cox method.

Results

Air pollution

Table 1 presents data on air pollutant levels. Cluster analysis was used to distinguish homogeneous counties in terms of air pollution. It was possible to reduce a whole set to the average of individual groups. The Euclidean distance was used as a dissimilarity measure. Based

Table 1. Average air pollutant levels (2010–2015) in 13 counties of Lower Silesia (Me (IQR))

County	PM _{2.5} [µm/m ³]	PM ₁₀ [µm/m ³]	NO ₂ [µm/m ³]	CO [µm/m ³]	Pb [µm/m ³]	SO ₂ [µm/m ³]
Głogów	27.5 (1.1)	30.0 (7.5)	11.3 (2.3)	0.36 (0.10)	0.052 (0.021)	5.8 (1.5)
Jelenia Góra	27.2 (1.5)	44.8 (21.0)	15.7 (4.4)	0.45 (0.20)	0.033 (0.017)	10.4 (3.6)
Kłodzko	29.2 (1.4)	32.0 (5.6)	19.1 (4.6)	0.47 (0.02)	0.032 (0.007)	10.0 (2.7)
Legnica	26.7 (4.3)	34.1 (6.7)	22.6 (4.1)	0.47 (0.03)	0.049 (0.008)	7.6 (1.6)
Lubań	17.2 (1.6)	22.4 (4.4)	5.9 (1.8)	0.32 (0.00)	0.009 (0.008)	5.6 (2.1)
Oława	23.9 (1.1)	35.0 (6.7)	17.7 (2.0)	0.41 (0.04)	0.023 (0.004)	7.8 (0.2)
Oleśnica	24.2 (1.6)	31.3 (3.4)	18.8 (0.2)	0.41 (0.02)	0.030 (0.002)	7.1 (1.5)
Polkowice	22.4 (1.6)	29.4 (5.2)	10.4 (7.7)	0.38 (0.01)	0.025 (0.011)	6.5 (2.6)
Złotoryja	25.7 (1.8)	33.7 (3.5)	10.8 (3.7)	0.44 (0.05)	0.032 (0.002)	7.1 (1.2)
Zgorzelec	21.6 (4.8)	23.9 (12.3)	15.8 (9.8)	0.39 (0.05)	0.024 (0.005)	7.5 (1.8)
Wałbrzych	23.9 (2.0)	27.0 (5.1)	15.4 (2.4)	0.39 (0.08)	0.033 (0.015)	8.5 (3.0)
Świdnica	25.7 (2.6)	18.4 (12.2)	16.8 (1.8)	0.41 (0.07)	0.035 (0.004)	11.8 (1.9)
Wrocław	30.6 (1.6)	39.0 (9.5)	55.1 (10.6)	0.61 (0.15)	0.025 (0.009)	6.1 (0.9)
All	25.2 (4.7)	31.1 (8.7)	16.5 (7.6)	0.41 (0.09)	0.030 (0.014)	7.5 (2.9)

Me (IQR) – median and interquartile range; PM_{2.5} – atmospheric aerosols with a diameter of not more than 2.5 µm (the average daily dust standard ≤25 µg/m³ and average annual standard ≤10 µg/m³); PM₁₀ – a mixture of suspended dusts with a diameter ≤10 µm (the average daily dust standard ≤200 µg/m³ and average annual standard ≤20 µg/m³); NO₂ – nitrogen dioxide; CO – carbon monoxide; Pb – lead; SO₂ – sulfur dioxide.

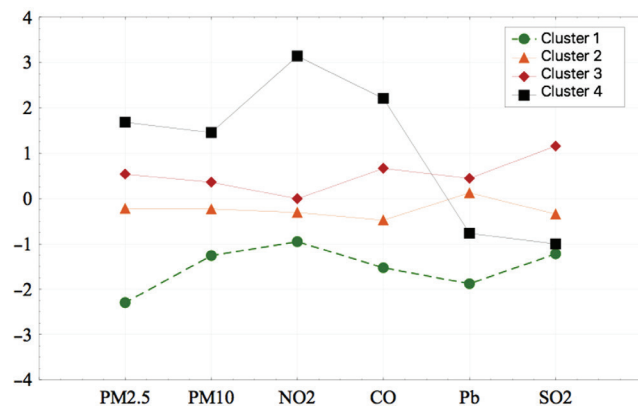


Fig. 1. Average values of pollution in 4 groups of counties (cluster 1 – Lubań county; cluster 2 – Głogów, Oława, Oleśnica, Polkowice, Złotoryja, Zgorzelec, and Wałbrzych counties; cluster 3 – Jelenia Góra, Kłodzko, Legnica, and Świdnica counties; cluster 4 – Wrocław county)

PM_{2.5} – atmospheric aerosols with a diameter of not more than 2.5 µm (the average daily dust standard ≤25 µg/m³ and average annual standard ≤10 µg/m³); PM₁₀ – a mixture of suspended dusts with a diameter ≤10 µm (the average daily dust standard ≤200 µg/m³ and average annual standard ≤20 µg/m³); NO₂ – nitrogen dioxide; CO – carbon monoxide; Pb – lead; SO₂ – sulfur dioxide.

on the hierarchical structure of the set of counties, they were divided into 4 clusters homogeneous in terms of air pollution:

- cluster 1: Lubań county;
- cluster 2: Głogów, Oława, Oleśnica, Polkowice, Złotoryja, Zgorzelec, and Wałbrzych counties;
- cluster 3: Jelenia Góra, Kłodzko, Legnica, and Świdnica counties;
- cluster 4: Wrocław county.

A graph of average values (Fig. 1) for standardized air pollution parameters showed that the highest level of air pollution, except for lead (Pb) and SO₂, was recorded in the Wrocław county (cluster 4). The next most affected counties in terms of the level of air pollution were Jelenia Góra, Kłodzko, Legnica, and Świdnica (cluster 3). The lowest level of pollution was recorded in the Lubań county (cluster 1).

Depression cases

The number of people diagnosed with depression in 2010–2015 was compared between individual counties (Table 2). The structure index (percentage) of people diagnosed with depression in the next 6 years of observation did not change significantly ($p > 0.05$). However, this depended significantly ($p = 0.003$) on the group of counties homogeneous in terms of air pollution (Fig. 2). The average structure index of people diagnosed with depression between 2010 and 2015 across the 13 counties was $2.72 \pm 1.78\%$ (women: $2.04 \pm 1.30\%$; men: $0.67 \pm 0.50\%$).

The linear relationships between depression diagnoses and air pollutant levels measured between 2010 and 2015

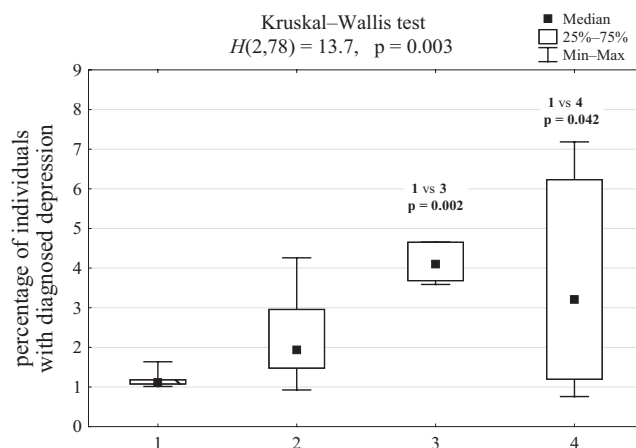


Fig. 2. Percentage of individuals with diagnosed depression in 4 groups of counties homogeneous in terms of air pollution, and results of the analysis of variance (ANOVA)

for all counties are summarized in Table 3. Since there were statistically significant correlations between the independent variables (predictors), the variance inflation factor (VIF) was estimated for each of them (Table 4). The strongest collinearity with PM₁₀ was observed for NO₂ and NO_x ($VIF > 10$). Variables NO₂ and NO_x were excluded from the predictive model for estimating the depression rate. The concentration of PM₁₀ ($r = 0.385$) and CO ($r = 0.344$) were significantly positively correlated with the frequency of severe depressive episodes with psychotic symptoms (F32.3). The concentration of O₃ was significantly negatively correlated with depression risk ($r = -0.283$). There were statistically significant correlations between different depression diagnoses and the following pollutants: PM_{2.5} and F32 (B = 0.303), PM₁₀ and F32, F32.0, F32.2, and F33; CO and F32, F32.0, F32.1, F32.2, F32.3, and F33; Pb(PM₁₀) and F32, F32.0, and F32.2; BaP(PM₁₀) and F32.0; arsenic (As)(PM₁₀) and F32, F32.0 and F32.2; and cadmium (Cd) (PM₁₀) and F32, F32.0 and F32.2. The O₃ levels were significantly negatively correlated with all depression diagnoses except F33.

Mathematical model of the occurrence of major depressive episodes with psychotic symptoms (F32.3)

The percentage of people diagnosed with a F32.3 in all counties was $0.23 \pm 0.19\%$. Table 5 presents the results of uni- and multivariate regression analyses of predictors associated with the risk for F32.3. The PM_{2.5}, CO, BaP, SO₂, and Cd levels were independently associated with the occurrence of F32.3. The formula for evaluating the structure index of F32.3 can be expressed as:

$$F32.3 = -403.4 + 10.8 \times PM_{2.5} + 379.8 \times CO + 24.1 \times Ni - 5.33 \times BaP - 6.44 \times SO_2 + 25.8 \times Cd$$

$$R = 0.803; F (\text{degrees of freedom (df)}: 7,70) = 18.2; p < 0.001$$

Table 2. Basic statistics (IQR) of the structure (%) of depression diagnosis in 13 counties in 2010–2015

County	Percentage of people diagnosed with depression (ICD-10)					
	F32.0	F32.1	F32.2	F32.3	F33	F34
Głogów	6.1 (1.5)	1.2 (0.6)	4.2 (1.6)	0.2 (0.2)	0.1 (0.1)	10.6 (4.2)
Jelenia Góra	11.8 (5.4)	5.0 (3.4)	8.9 (4.9)	0.4 (0.4)	0.3 (0.3)	10.4 (2.2)
Kłodzko	2.8 (0.7)	0.5 (0.1)	0.6 (0.1)	0.1 (0.1)	0.1 (0.1)	1.4 (0.6)
Legnica	5.9 (1.1)	6.5 (1.8)	15.4 (6.2)	0.4 (0.1)	0.6 (0.3)	6.1 (1.5)
Lubań	2.0 (1.3)	0.7 (0.6)	1.8 (1.6)	0.2 (0.1)	0.1 (0.1)	2.3 (0.3)
Oława	1.2 (0.3)	1.0 (0.2)	1.2 (0.8)	0.1 (0.1)	0.2 (0.2)	3.5 (2.8)
Oleśnica	0.9 (0.7)	0.7 (0.2)	0.7 (0.3)	0.1 (0.0)	0.0 (0.0)	2.6 (0.7)
Polkowice	1.1 (0.4)	3.9 (1.2)	3.9 (2.7)	0.1 (0.1)	0.0 (0.0)	3.3 (2.3)
Złotoryja	1.3 (1.0)	0.9 (0.4)	4.0 (1.3)	0.1 (0.2)	0.1 (0.0)	3.4 (1.1)
Zgorzelec	5.9 (1.8)	1.1 (0.5)	1.5 (0.9)	0.2 (0.1)	0.2 (0.1)	3.6 (0.7)
Wałbrzych	4.4 (0.3)	4.8 (0.5)	5.4 (1.0)	0.5 (0.1)	0.4 (0.0)	4.5 (0.3)
Świdnica	2.3 (1.2)	0.7 (0.6)	1.3 (0.3)	0.1 (0.0)	0.0 (0.0)	3.8 (0.5)
Wrocław	3.3 (1.4)	4.6 (1.7)	4.4 (2.2)	0.4 (0.1)	0.4 (0.2)	4.9 (0.3)
Cluster 1	2.0 (1.3)	0.7 (0.6)	1.8 (1.6)	0.2 (0.1)	0.1 (0.1)	2.3 (0.3)
Cluster 2	1.6 (4.0)	1.1 (2.4)	2.9 (3.3)	0.2 (0.2)	0.1 (0.2)	3.7 (1.9)
Cluster 3	3.3 (1.4)	4.6 (1.7)	4.4 (2.2)	0.4 (0.1)	0.4 (0.2)	4.9 (0.3)
Cluster 4	4.9 (4.1)	2.1 (5.5)	3.6 (11.3)	0.2 (0.3)	0.1 (0.4)	4.8 (5.7)
All	3.1 (3.9)	1.3 (3.5)	3.1 (4.1)	0.2 (0.3)	0.1 (0.3)	4.0 (2.4)

IQR – interquartile range; ICD-10 – International Classification of Diseases, 10th Revision; F32.0 – mild depressive episode; F32.1 – moderate depressive episode; F32.2 – severe depressive episode without psychotic symptoms; F32.3 – severe depressive episode with psychotic symptoms; F33 – recurrent depressive disorders; F34 – persistent mood disorders.

Table 3. Values of Pearson’s correlation coefficients between air pollution and indices of the structure of depressive episodes in all 13 analyzed counties

Air pollutants	F32	F32.0	F32.1	F32.2	F32.3	F33	F34
PM _{2.5}	0.303	0.204	0.198	0.152	0.222	0.197	0.281
PM ₁₀	0.341	0.277	0.198	0.211	0.385	0.328	0.291
CO	0.326	0.226	0.260	0.234	0.344	0.330	0.102
Pb	0.327	0.270	0.213	0.352	0.117	0.157	0.431
SO ₂	−0.040	0.171	−0.093	−0.064	−0.057	0.013	0.032
BaP	0.039	0.269	−0.060	−0.004	0.067	−0.052	0.071
O ₃	−0.412	−0.264	−0.296	−0.288	−0.283	−0.166	−0.375
As	0.433	0.295	0.215	0.513	0.158	0.218	0.491
Cd	0.241	0.237	0.124	0.267	0.073	0.218	0.293
Ni	0.091	0.065	0.017	0.004	0.091	0.163	0.092

Values in bold are statistically significant. BaP – benzo(a)pyrene; PM_{2.5} – atmospheric aerosols with a diameter of not more than 2.5 µm (the average daily dust standard ≤25 µg/m³ and average annual standard ≤10 µg/m³); PM₁₀ – a mixture of suspended dusts with a diameter ≤10 µm (the average daily dust standard ≤200 µg/m³ and average annual standard ≤20 µg/m³); CO – carbon monoxide; Pb – lead; SO₂ – sulfur dioxide; O₃ – ozone; As – arsenic; Cd – cadmium; Ni – nickel.

Table 4. Results of the collinearity analysis (variance inflation factor (VIF) values) of independent variables

Predictors	PM _{2.5}	PM ₁₀	NO ₂	CO	Pb	SO ₂	NO _x	BaP	O ₃	As	Cd	Ni
VIF	8.44	3.21	27.55	4.26	2.99	2.73	20.81	3.07	8.62	3.36	4.57	3.41

Values in bold are statistically significant. BaP – benzo(a)pyrene; NO_x – nitrogen oxides; PM_{2.5} – atmospheric aerosols with a diameter of not more than 2.5 µm (the average daily dust standard ≤25 µg/m³ and average annual standard ≤10 µg/m³); PM₁₀ – a mixture of suspended dusts with a diameter ≤10 µm (the average daily dust standard ≤200 µg/m³ and average annual standard ≤20 µg/m³); NO₂ – nitrogen dioxide; CO – carbon monoxide; Pb – lead; SO₂ – sulfur dioxide; O₃ – ozone; As – arsenic; Cd – cadmium; Ni – nickel.

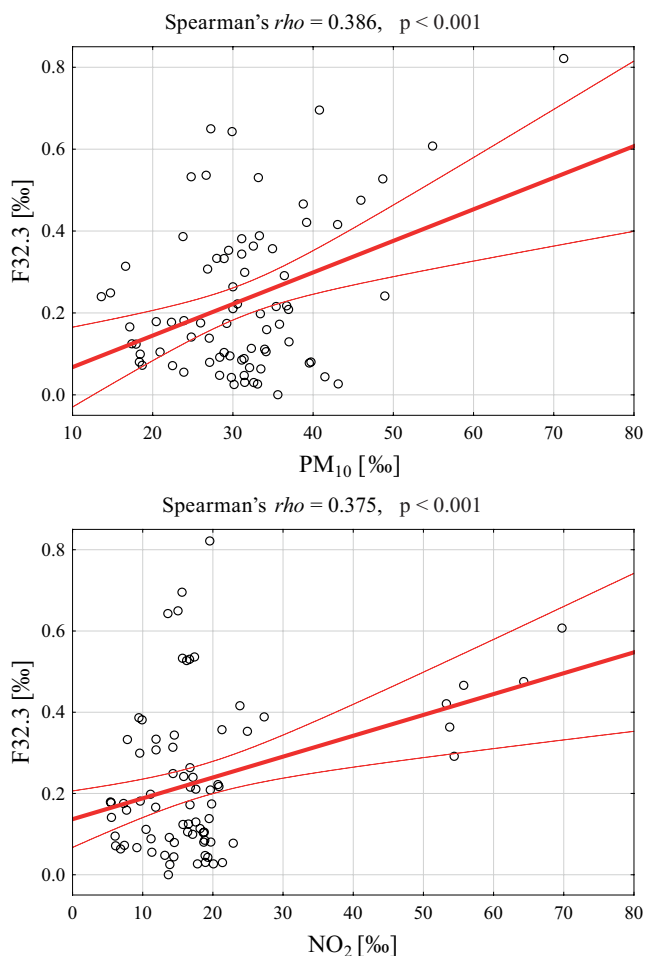


Fig. 3. Scatterplots showing reported cases of depression with psychotic symptoms (F32.3) and coarse particles with an aerodynamic diameter between 2.5 μm and 10 μm (PM_{10}) and nitrogen dioxide (NO_2) concentrations

Table 5. Values of univariate and multivariate regression analyses between air pollution and the occurrence of severe depressive episodes with psychotic symptoms (F32.3)

Risk factors (F32.3 occurrence predictors)	Univariate analysis		Multivariate analysis	
	b	p-value	β	p-value
$\text{PM}_{2.5}$	11.04	<0.001	10.8	<0.001
PM_{10}	-0.42	0.614	0.06	0.918
CO	409.0	<0.001	379.8	<0.001
Pb	154.7	0.775	538.2	0.775
SO_2	-7.36	0.014	-6.44	0.019
BaP	-5.42	0.002	-5.33	0.002
O_3	2.09	0.188	1.95	0.160
As	-0.85	0.702	-0.01	0.682
Cd	-47.2	0.192	-54.4	0.039
Ni	25.7	0.089	24.1	0.040

Multivariate regression statistics: $R^2_{\text{adj.}} = 0.609$, $F(7, 70) = 18.2$, $p < 0.001$, $\text{SE} = 38.3$. SE – standard error; b – linear regression coefficient; β – standardized regression coefficient. Values in bold are statistically significant. BaP – benzo(a)pyrene; $\text{PM}_{2.5}$ – atmospheric aerosols with a diameter of not more than 2.5 μm (the average daily dust standard $\leq 25 \mu\text{g}/\text{m}^3$ and average annual standard $\leq 10 \mu\text{g}/\text{m}^3$); PM_{10} – a mixture of suspended dusts with a diameter $\leq 10 \mu\text{m}$ (the average daily dust standard $\leq 200 \mu\text{g}/\text{m}^3$ and average annual standard $\leq 20 \mu\text{g}/\text{m}^3$); CO – carbon monoxide; Pb – lead; SO_2 – sulfur dioxide; O_3 – ozone; As – arsenic; Cd – cadmium; Ni – nickel.

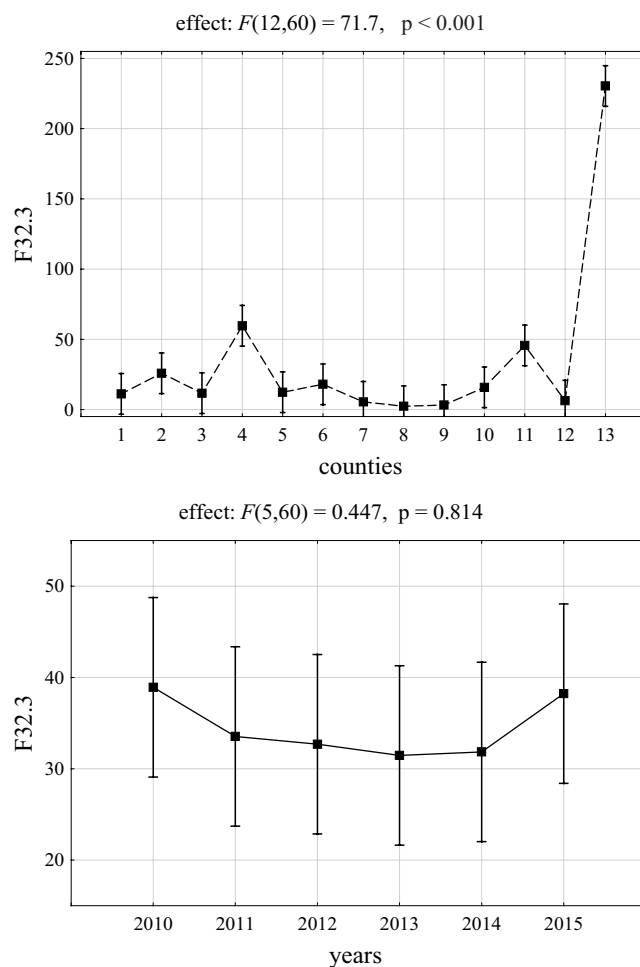


Fig. 4. F-ratio of the analysis of variance (ANOVA) concerning depression with psychotic symptoms (F32.3) ratio

The positive values of the regression coefficients indicated the effects of increased $\text{PM}_{2.5}$, CO, Ni, and Cd on the occurrence of F32.3. All structural parameters of the model were statistically significant ($p < 0.05$), and the model fit was satisfactory ($p < 0.001$). In order to avoid the pseudo-replication problem, and since the measurements of depression rates were taken in each county annually, the correlation analysis in consecutive individual years between air pollution and the occurrence of F32.3 was performed. The PM_{10} correlated significantly with the F32.3 diagnosis in 2010 ($\rho = 0.560$, $p < 0.05$), and both PM_{10} and NO_2 concentrations were linked to this diagnosis across all years ($\rho = 0.386$, $p < 0.001$; $\rho = 0.375$, $p < 0.001$; Table 6; Fig. 3,4).

Analysis including demographic and social data

Over the entire analyzed period, the percentage of diagnosed cases of depression was stable at a level of $2.7 \pm 1.8\%$. The analyzed database lacked information on the depression incidence in the Wałbrzych county in 2010–2012. The missing data were supplemented with average values.

Table 6. Correlation analysis in consecutive individual years between air pollution and the occurrence of severe depressive episodes with psychotic symptoms (F32.3)

Year	PM ₁₀ compared to F32.3	NO ₂ compared to F32.2
2010	rho = 0.560 p < 0.05	rho = 0.407 p > 0.05
2011	rho = -0.044 p > 0.05	rho = -0.077 p > 0.05
2012	rho = 0.440 p > 0.05	rho = 0.198 p > 0.05
2013	rho = 0.104 p > 0.05	rho = 0.473 p > 0.05
2014	rho = 0.544 p > 0.05	rho = 0.401 p > 0.05
2015	rho = 0.429 p > 0.05	rho = 0.099 p > 0.05
All	rho = 0.386 p < 0.001	rho = 0.375 p < 0.001

Values in bold are statistically significant. PM₁₀ – a mixture of suspended dusts with a diameter ≤10 µg (the average daily used standard ≤200 µg/m³ and average annual standard ≤20 µg/m³); NO₂ – nitrogen dioxide.

Basic demographic data concerning depression cases (2010–2015) across the 13 counties of Lower Silesia are summarized in Table 6 and Table 7. Statistically significant differences were observed between depression incidence in individual counties (Fig. 5) (p < 0.001). The highest incidence of depression was recorded in Jelenia Góra (2) and Legnica (4) counties (6.1%), while the lowest in Kłodzko (0.9%) and Oleśnica (1.1%) counties.. Table 8 shows the results of ANOVA concerning depression cases and Table 9 displays the results of post-hoc test (Turkey’s test).

The distribution of depression cases was non-normal (Fig. 6). The analyzed counties were classified into 3 groups: group A – depression rate below 1.5% (Kłodzko, Lubań, Oleśnica, and Świdnica counties); group B – depression rate of 1.5–3.1% (Oława, Polkowice, Złotoryja, and Zgorzelec counties); group C – depression rate over 3.1% (Głogów, Jelenia Góra, Legnica, Wałbrzych, and Wrocław counties) (Fig. 7). In group C, a high percentage of diagnosed depression cases was associated with higher concentrations of PM₁₀ and PM_{2.5}, as well as lower O₃ concentrations. The level of BaP did not differ significantly between

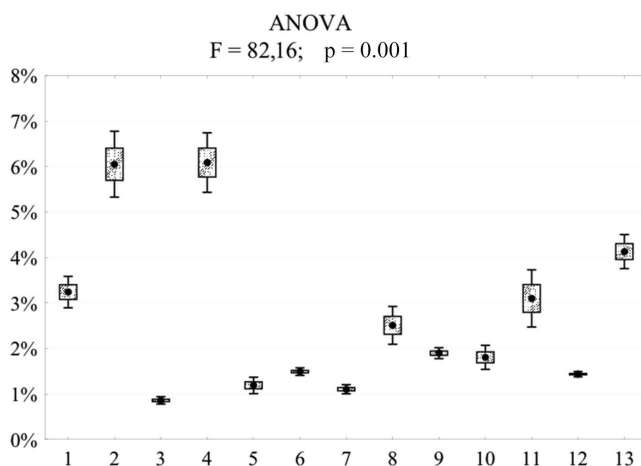


Fig. 5. Percentage of diagnosed depression cases in 2010–2015 in 13 counties of Lower Silesia and the result of the analysis of variance (ANOVA)

Table 7. Statistics of the percentage of diagnosed depression cases in 2010–2015 in 13 counties of Lower Silesia and the results of ANOVA

Years	Mean ±SD	Me (Q1–Q3)	Min–Max	Result of the test
2010	2.5 ±1.5	1.8 (1.5–3.7)	0.8–7.2	F = 0.29 df = 5 p = 0.868
2011	2.4 ±1.5	1.6 (1.4–3.6)	0.8–5.1	
2012	2.7 ±1.8	1.8 (1.4–3.9)	0.8–6.2	
2013	2.8 ±2.0	2.1 (1.5–3.5)	0.9–6.9	
2014	3.0 ±2.1	2.1 (1.5–4.3)	0.8–7.2	
2015	3.0 ±2.0	2.2 (1.3–3.9)	1.0–6.9	
Counties				
Głogów	3.2 ±0.4	3.3 (3.0–3.6)	2.5–3.6	F = 88.6 df = 12 p < 0.001
Jelenia Góra	6.1 ±0.9	6.0 (5.3–6.9)	4.9–7.2	
Kłodzko	0.9 ±0.1	0.8 (0.8–0.9)	0.8–1.0	
Legnica	6.1 ±0.8	6.4 (5.1–6.7)	5.1–6.9	
Lubań	1.2 ±0.2	1.1 (1.1–1.2)	1.0–1.6	
Oława	1.5 ±0.1	1.5 (1.4–1.5)	1.4–1.7	
Oleśnica	1.1 ±0.1	1.1 (1.0–1.2)	0.9–1.3	
Polkowice	2.5 ±0.5	2.8 (1.9–2.9)	1.8–3.0	
Złotoryja	1.9 ±0.2	1.9 (1.8–2.0)	1.6–2.1	
Zgorzelec	1.8 ±0.3	1.8 (1.5–2.1)	1.5–2.2	
Wałbrzych*	3.5 ±0.7	3.9 (3.9–4.0)	2.4–4.3	
Świdnica	1.4 ±0.1	1.4 (1.4–1.5)	1.3–1.5	
Wrocław	4.1 ±0.5	4.1 (3.7–4.7)	3.6–4.7	
All (n = 78)	2.7 ±1.8	1.9 (1.4–3.9)	0.8–7.2	–

* missing data for 2010–2012 have been replaced with averages; ANOVA – analysis of variance; M – arithmetic mean; SD – standard deviation; Me – median (50%); Q1 – lower quartile (25%); Q3 – upper quartile (75%); df – degrees of freedom; Min – the smallest value; Max – the largest value. The differences between the percentages of diagnosed depression cases in 2010–2015 in all counties turned out to be statistically insignificant (Fig. 1; p > 0.05).

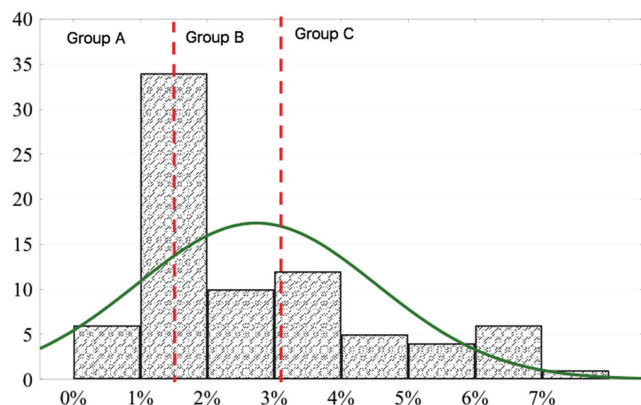


Fig. 6. Histogram of the percentage of depression cases against the normal distribution, the results of normality tests, and the adopted division. Kolmogorov–Smirnov test: d = 0.193, p < 0.01; Lilliefors test: p < 0.01; Shapiro–Wilk test: W = 0.866, p < 0.00001

Table 8. The results of ANOVA concerning depression cases

Effect	SS	df	MS	F	p-value
Constant	52563	1	92564	295	<0.001
Years	701	5	140	0.45	0.814
Countries	270075	12	22506	71.7	<0.001
Error	18821	60	314	–	–

R²adj. = 0.917, F(17, 60) = 50.8, p < 0.001. ANOVA – analysis of variance; SS – sums of squares; df – degrees of freedom; MS – mean squares. Values in bold are statistically significant.

the individual counties. The average values of pollutants in groups of counties differing in the severity of diagnosed depression are summarized in Table 10 and Table 11, as well as Fig. 8.

In counties with the highest percentage of diagnosed depression, there were significantly higher emissions of gaseous pollutants (1000 t/year/km²) (p = 0.003), SO₂ (p = 0.011), NO_x (p = 0.002), CO (p = 0.001), and CO₂ (p = 0.003), as well as concentrations of PM₁₀ (p = 0.039), PM_{2.5} (p = 0.008) and NO_x (p = 0.025). The O₃ levels were significantly inversely correlated with depression (p < 0.001; Table 10,11, Fig. 8).

In order to determine the independent predictors of depression incidence, univariate and multivariate linear regression analyses were performed (Table 12). Univariate regression analysis showed that PM₁₀ and PM_{2.5} concentrations, as well as divorces (per 1000 inhabitants), demographic burden, demographic dependency rate for the elderly, percentage of people >65 years old, feminization rate, outpatient clinics per 1000 population, doctors (total working staff) per 10,000 population, number of beds

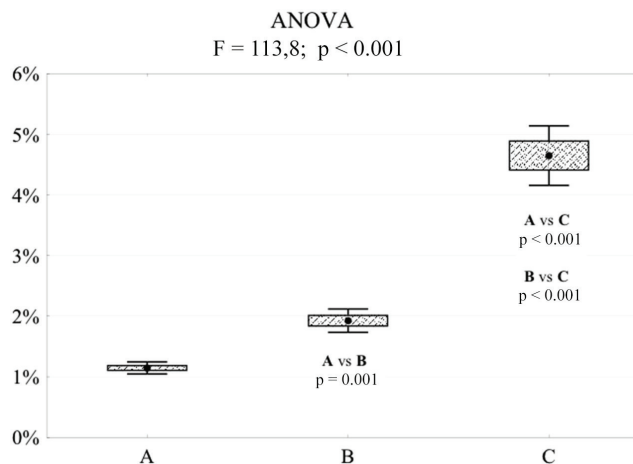


Fig. 7. Percentage of depression diagnosed in 2010–2015 in 3 groups of counties and the result of the analysis of variance (ANOVA) and post hoc tests (Tukey’s test)

in hospitals in relation to the population, working people rate, emission of gaseous pollutants, and average monthly gross salary were significantly positively correlated with the incidence of depression. On the other hand, O₃ concentration, the number of marriages and the number of beneficiaries of social welfare were significantly negatively correlated with depression risk. Multivariate regression analysis showed that O₃ concentration, demographic burden, feminization rate, number of doctors, number of hospital beds in relation to the population, number of employed people per 1000 population, and average monthly gross salary were independent predictors of the depression rate. Increased O₃ concentrations were significantly associated with a lower depression risk (p = 0.004).

Table 9. Results of multiple comparisons (post hoc) with Tukey’s test: Głogów compared to Jelenia Góra (3.2% compared to 6.1%; p < 0.001) and Głogów compared to Polkowice (3.2% compared to 2.5%; p = 0.261)

Counties	Multiple comparison results (Tukey’s test)												
	Głogów M = 3.2	Jelenia Góra M = 6.1	Kłodzko M = 0.9	Legnica M = 6.1	Lubań M = 1.2	Oława M = 1.5	Oleśnica M = 1.1	Polkowice M = 2.5	Złotoryja M = 1.9	Zgorzelec M = 1.8	Wałbrzych M = 3.5	Świdnica M = 1.4	Wrocław M = 4.1
Głogów	–	0.000	0.000	0.000	0.000	0.000	0.000	0.261	0.000	0.000	0.998	0.000	0.068
Jelenia Góra	0.000	–	0.000	1.000	0.000	0.000	0.000	0.000	0.000	0.000	0.000	0.000	0.000
Kłodzko	0.000	0.000	–	0.000	0.989	0.478	0.999	0.000	0.014	0.038	0.000	0.623	0.000
Legnica	0.000	1.000	0.000	–	0.000	0.000	0.000	0.000	0.000	0.000	0.000	0.000	0.000
Lubań	0.000	0.000	0.989	0.000	–	0.995	1.000	0.001	0.305	0.525	0.000	0.999	0.000
Oława	0.000	0.000	0.478	0.000	0.995	–	0.962	0.018	0.947	0.993	0.000	1.000	0.000
Oleśnica	0.000	0.000	0.999	0.000	1.000	0.962	–	0.000	0.161	0.322	0.000	0.989	0.000
Polkowice	0.261	0.000	0.000	0.000	0.001	0.018	0.000	–	0.536	0.314	0.020	0.009	0.000
Złotoryja	0.000	0.000	0.014	0.000	0.305	0.947	0.161	0.536	–	1.000	0.000	0.877	0.000
Zgorzelec	0.000	0.000	0.038	0.000	0.525	0.993	0.322	0.314	1.000	–	0.000	0.974	0.000
Wałbrzych	0.998	0.000	0.000	0.000	0.000	0.000	0.000	0.020	0.000	0.000	–	0.000	0.538
Świdnica	0.000	0.000	0.623	0.000	0.999	1.000	0.989	0.009	0.877	0.974	0.000	–	0.000
Wrocław	0.068	0.000	0.000	0.000	0.000	0.000	0.000	0.000	0.000	0.000	0.538	0.000	–

M – arithmetic mean. Values in bold are statistically significant.

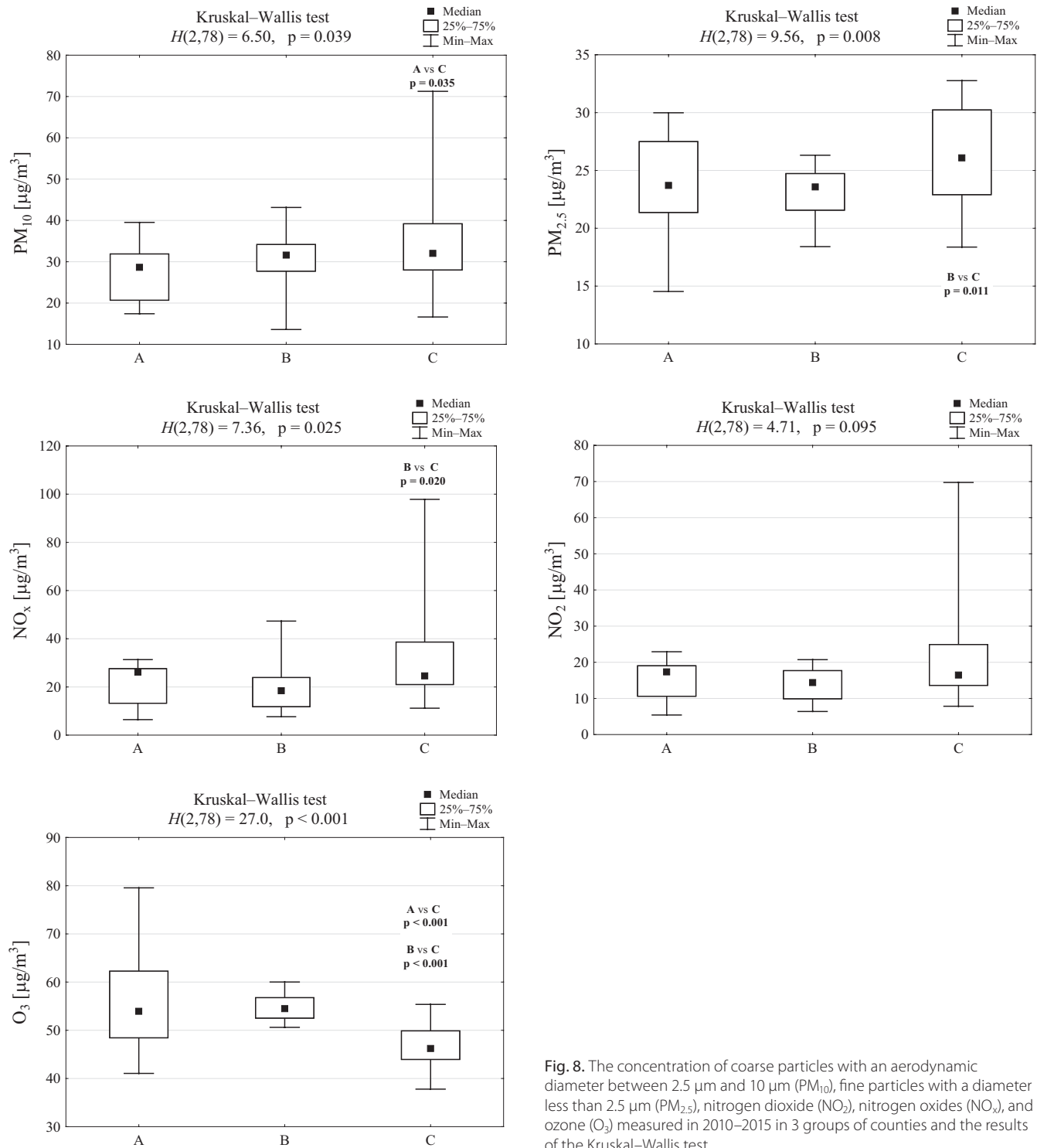


Fig. 8. The concentration of coarse particles with an aerodynamic diameter between 2.5 μm and 10 μm (PM₁₀), fine particles with a diameter less than 2.5 μm (PM_{2.5}), nitrogen dioxide (NO₂), nitrogen oxides (NO_x), and ozone (O₃) measured in 2010–2015 in 3 groups of counties and the results of the Kruskal–Wallis test

Discussion

We showed that depression is associated with long-term exposure to higher concentrations of PM₁₀, PM_{2.5} and NO_x, and high emissions of SO₂, NO_x, CO, and CO₂. Other studies have reported similar results. For example, research using the National Health Insurance Database demonstrated a positive association between PM_{2.5} and depression risk for both 1-year and 4-year exposure.³⁹ Other studies also

found this relationship for periods of 1 year,⁴⁰ 2 years and 5 years.⁴¹ In terms of PM₁₀ long-term exposure, a positive relationship was found over a 1-year time period.⁴² A study by Vert et al. supports these results for both PM fractions.⁴³ However, there was also a negative association for PM₁₀.⁴⁴ Furthermore, only a few studies evaluated the relationship between depression and NO_x. These studies consistently suggest a positive correlation between depression and long-term exposure to NO₂ and NO_x.^{43,45}

Table 10. Comparison of the features characterizing the counties of Lower Silesia in groups differing in the occurrence of depression

Parameter	Group A	Group B	Group C	p-value
Percentage of depression [%]	1.1 (0.4)	1.9 (0.5)	4.3 (2.0)	<0.001^a
PM ₁₀ [µg/m ³]	28.6 (11.2)	31.6 (6.5)	32.0 (11.2)	0.010^b
BaP [µg/m ³]	7.9 (10.7)	4.8 (3.6)	5.6 (3.4)	0.229 ^b
O ₃ [µg/m ³]	54.0 (13.8)	54.5 (4.3)	46.2 (5.9)	<0.001^b
PM _{2.5} [µg/m ³]	23.7 (6.1)	23.6 (3.2)	26.1 (7.3)	0.002^b
D1. Marriages (per 1000 inhabitants)	5.1 (0.7)	5.2 (0.9)	4.7 (1.0)	0.009^b
D2. Divorces (per 1000 inhabitants)	2.0 (0.4)	1.8 (0.3)	2.3 (0.3)	<0.001^b
D3. Demographic burden: non-working age population per 100 working age population	55.3 (3.4)	53.6 (3.4)	57.5 (5.1)	<0.001^b
D4. Demographic dependency rate for the elderly	19.8 (3.2)	17.6 (3.3)	23.2 (6.1)	<0.001^b
D5. Percentage of people aged 65 and over in the total population	14.2 (2.1)	12.7 (2.2)	16.6 (3.8)	<0.001^b
D6. Feminization rate	107 (2)	104 (2)	112 (3)	<0.001^b
D7. Outpatient clinics for 10,000 population	4.0 (1.0)	4.0 (1.0)	5.0 (1.0)	<0.001^b
D8. Medical advice to the population	4.3 (0.9)	4.2 (0.8)	4.0 (0.5)	0.008^b
D9. Total advice (in thousands)	536 (345)	288 (160)	413 (112)	0.004^b
D10. Beneficiaries of social welfare per 10,000 population	744 (192)	784 (276)	584 (250)	<0.001^b
D11. Doctors working according to the basic workplace per 10,000 population	13.4 (4.4)	12.7 (7.4)	24.4 (6.9)	<0.001^b
D12. Doctors (total working staff) per 10,000 population	31.2 (15.5)	26.8 (11.5)	50.4 (16.4)	<0.001^b
D13. Social welfare homes	2.0 (3.5)	1.0 (1.0)	2.0 (2.0)	0.014^b
D14. Inhabitants of social welfare homes (including branches) per 1000 population	3.0 (2.0)	1.0 (2.5)	2.0 (1.0)	<0.001^b
D15. Hospital beds to population (%)	0.0 (0.0)	0.0 (0.0)	0.0 (0.0)	<0.001^b
D16. Registered unemployment rate	16.1 (9.6)	12.0 (9.0)	10.2 (6.3)	<0.001^b
D17. Working people per 1000 population	167 (45)	250 (198)	284 (74)	<0.001^b
D18. Average monthly gross salaries	3187 (374)	3487 (401)	3580 (639)	<0.001^b
D19. Average monthly gross salaries in relation to the national average (Poland = 100)	82 (6)	91 (6)	88 (12)	<0.001^b

^a – significance level of the Pearson χ^2 test, ^b – significance level of the Kruskal–Wallis test. Values in bold are statistically significant. BaP – benzo(a) pyrene; PM_{2.5} – atmospheric aerosols with a diameter of not more than 2.5 µm (the average daily dust standard ≤ 25 µg/m³ and average annual standard ≤ 10 µg/m³); PM₁₀ – a mixture of suspended dusts with a diameter ≤ 10 µm (the average daily dust standard ≤ 200 µg/m³ and average annual standard ≤ 20 µg/m³); O₃ – ozone.

Table 11. Comparison of the characteristics of the groups of counties in Lower Silesia in terms of pollutant emissions per 1 km² of land in counties with different rates of depression

Parameter	Group A	Group B	Group C	p-value
Percentage of depression	1.1 (0.4)	1.9 (0.5)	4.3 (2.0)	
Z1. Emission of gaseous pollutants (1000 t/year/km ²)	4530 (8864)	14732 (483176)	64755 (58043)	0.003
Z2. SO ₂	0.14 (0.32)	0.27 (7.14)	1.22 (3.46)	0.011
Z3. NO _x	0.06 (0.11)	0.32 (4.61)	0.65 (1.46)	0.002
Z4. CO	0.19 (0.11)	0.42 (0.68)	0.57 (0.56)	0.001
Z5. CO ₂	45.0 (88.1)	146.5 (4820.8)	644.5 (576.1)	0.003

p-value is significance level of the Kruskal–Wallis test. Values in bold are statistically significant. NO_x – nitrogen oxides; SO₂ – sulfur dioxide; CO – carbon monoxide; CO₂ – carbon dioxide.

We have observed a negative association between long-term exposure to O₃ and depression, which contradicts some of the previous results.⁴¹ However, some studies found no relationship between O₃ levels and depressive symptoms.⁴⁶ Volatile organic compounds and NO_x are precursors to O₃ formation,⁴⁷ and photochemical processes which depend on sunlight play a key role.⁴⁸ This can explain our results, since sunlight exposure⁴⁹ and vitamin D₃ production⁵⁰ have a preventive impact on depression. The O₃ exposure

and its health effects are more complicated, and possibly threshold-like.⁵¹ Finally, our study showed the important correlation between NO_x, NO₂ and depression risk, and these pollutants are known to decrease O₃ production.⁵²

We showed that high levels of PM_{2.5}, CO, and low BaP, SO₂ and Cd concentrations are independent risk factors for depressive episodes with psychotic symptoms (F32.3). To the best of our knowledge, there is no available research on this topic. However, some researchers

Table 12. Values of univariate and multivariate regression coefficients between the depression rate and risk factors

Risk factor	Univariate analysis		Multivariate analysis	
	b	p-value	β	p-value
PM ₁₀ [μg/m ³]	0.065	0.002	0.005	0.739
PM _{2.5} [μg/m ³]	0.140	0.007	−0.115	0.080
O ₃ [μg/m ³]	−0.089	<0.001	−0.082	0.004
BaP [μg/m ³]	0.017	0.738	–	–
D1. Marriages (per 1000 inhabitants)	−0.821	0.013	−0.027	0.932
D2. Divorces (per 1000 inhabitants)	3.023	<0.001	0.305	0.580
D3. Demographic burden: non-working age population per 100 working age population	0.208	<0.001	−0.213	0.004
D4. Demographic dependency rate for the elderly	0.234	<0.001	0.123	0.302
D5. Percentage of people aged 65 and over in the total population	0.365	<0.001	0.458	0.718
D6. Feminization rate	0.328	<0.001	0.378	<0.001
D7. Outpatient clinics per 10,000 population	0.384	0.027	−0.054	0.758
D8. Medical advice to the population	0.001	0.127	–	–
D9. Total advice (in thousands)	0.004	0.054	–	–
D10. Beneficiaries of social welfare per 10,000 population	−0.003	0.002	−0.001	0.588
D11. Doctors working according to the basic workplace per 10,000 population	0.091	<0.001	0.158	0.014
D12. Doctors (total working staff) per 10,000 population	0.039	<0.001	−0.043	0.130
D13. Social welfare homes	0.030	0.668	–	–
D14. Inhabitants of social welfare homes (including branches) per 1000 population	−0.294	0.094	–	–
D15. Hospital beds to population (%)	0.001	0.019	−0.001	<0.001
D16. Registered unemployment rate	−0.001	0.434	–	–
D17. Working people per 1000 population	0.010	<0.001	0.007	0.001
D18. Average monthly gross salaries	0.001	0.013	0.003	0.001
D19. Average monthly gross salaries in relation to the national average (Poland = 100)	0.054	0.026	−0.130	0.008
Z1. Emission of gaseous pollutants (1000 t/year/km ²)	0.860	<0.001	0.001	0.324
Z2. SO ₂	−0.001	0.429	–	–
Z3. NO _x	−0.001	0.489	–	–
Z4. CO	0.001	0.120	–	–
Z5. CO ₂	0.001	0.475	–	–

b – linear regression coefficient; β – standardized regression coefficient. Values in bold are statistically significant. BaP – benzo(a)pyrene; PM_{2.5} – atmospheric aerosols with a diameter of not more than 2.5 μm (the average daily dust standard ≤25 μg/m³ and average annual standard ≤10 μg/m³); PM₁₀ – a mixture of suspended dusts with a diameter ≤10 μm (the average daily dust standard ≤200 μg/m³ and average annual standard ≤20 μg/m³); O₃ – ozone; NO_x – nitrogen oxides; SO₂ – sulfur dioxide; CO – carbon monoxide; CO₂ – carbon dioxide.

attempted to find a connection between air pollution and depression severity. Pun et al. showed that PM_{2.5} levels are positively associated with depressive symptom severity.³⁶ On the other hand, Wang et al. found no relationship between depressive symptoms and both long- and short-term exposure to air pollutants.¹³ Similarly, there is very little evidence regarding psychotic symptoms and air pollution. An analysis using machine learning found a connection between schizophrenia emergency room admissions and ambient PM_{2.5},⁵³ which was confirmed by Gao et al.⁵⁴

A multivariate analysis of demographic and pollution data showed that the number of hospital beds, number of welfare recipients, number of employed people, and the average monthly gross salary were all related

to the incidence of depression. These results are inconsistent with other studies, which demonstrated that welfare recipients are more likely to suffer from depression.⁵⁵ However, our results could represent reverse causality. For instance, we showed a positive correlation between depression and the number of hospital beds in the region, which could result from the fact that people with depression are more frequently hospitalized.¹³ Similarly, employment status and depression rates could be related to workplace conditions, burnout, stress, and bullying,⁵⁶ which also translate into monthly salary. Depression accounts for up to 46% of days lost due to illness; therefore, it is more often diagnosed among the working population.^{56,57} However, in our study, data concerning employment were not available.

Limitations

Results of our analyses based on 318,779 cases showed that there is a positive association between air pollutant levels and the risk of depression. However, these results should be interpreted cautiously, because, as an observational study, despite being useful in explaining the exposure to an outcome, they carry out the risk of possible reverse causality or undetected bias.⁵⁸ Other limitations are related to the use of semi-individual data, and potential underestimation of the prevalence of depression due to social stigmatization related to this diagnosis.⁵⁹ Nevertheless, because of the large and standardized sample size, our study provides new insights into the relationship between air pollutant exposure and depression.

The analyzed database lacked information on depression incidence for the Wałbrzych county in 2010–2012. Since regression analysis was used, even if a strong correlation is evident, it does not imply causation. Moreover, some risk factors found in our study could simply reflect the indirect effects of other risk factors. Finally, it is crucial to remember that air pollutant concentrations depend on many variables, such as the direction and speed of the wind, atmospheric stability, solar radiation, or geography.⁶⁰ This can cause spatial and temporal variations of pollutants levels, reaching dramatic changes, even over the course of several hours. Moreover, the stress response in the human population is extremely heterogeneous.⁶¹ Age, gender, existing disease status, and psychosocial stressors play a potential role in the biological response to air pollutants. Given the numerous risk factors of depression, demonstrating the impact of air pollution on depressive disorders is difficult. Therefore, obtaining large-scale data on depression cases, and relating this to demographic and pollution information can help in identifying environmental risk factors, which could be potentially modifiable.

Conclusions

Heavy air pollution is associated with a higher incidence of depression, while O₃ levels were linked to the lower rate of depression. Elevated concentration of airborne PM_{2.5}, as well as CO, and low BaP, SO₂ and Cd levels are independent risk factors for the occurrence of major depressive episodes with psychotic symptoms (F32.3). A high percentage of people with depression could be related to higher concentrations of PM₁₀ and PM_{2.5}, lower O₃ concentrations and higher emissions of gaseous pollutants, such as SO₂, NO_x, CO, and CO₂.

The incidence of depression was associated with high concentrations of PM₁₀ and PM_{2.5}, as well as divorce rate per 1000 inhabitants, demographic burden, demographic dependency rate for the elderly, percentage of people >65 years old, feminization rate, outpatient clinics per


1000 population, doctors (total working staff) per 10,000 population, the number of hospital beds in relation to the population, working people rate, emission of gaseous pollutants, and average monthly gross salary. On the other hand, O₃ concentration, the number of marriages, and the number of welfare beneficiaries were negatively correlated with depression risk. The independent predictors of depression were: O₃ concentration, demographic burden, feminization rate, number of doctors, number of hospital beds in relation to the population, number of employed people per 1000 population, and the average monthly gross salary.


Availability of data and material

Data on air pollution are available on the website of the Chief Inspectorate of Environmental Protection: <http://powietrze.gios.gov.pl/pjp/current>. Demographic data are available on the website of the Statistics Poland: <https://stat.gov.pl/>.

ORCID iDs

Anna Gładka  <https://orcid.org/0000-0002-7392-1244>

Tomasz Zatoński  <https://orcid.org/0000-0003-3043-4806>

Joanna Rymaszewska  <https://orcid.org/0000-0001-8985-3592>

References

1. World Health Organization. Depression. <https://www.who.int/news-room/fact-sheets/detail/depression>. Accessed January 3, 2021.
2. King R. Book Review: *Cognitive Therapy of Depression*. Aaon Beck, John Rush, Brian Shaw, Gary Emery. New York: Guilford, 1979. *Aust NZ J Psychiatry*. 2002;36(2):272–275. doi:10.1046/j.1440-1614.2002.t01-4-01015.x
3. Walker ER, McGee RE, Druss BG. Mortality in mental disorders and global disease burden implications: A systematic review and meta-analysis [published correction appears in: *JAMA Psychiatry*. 2015;72(7):736] [published correction appears in: *JAMA Psychiatry*. 2015;72(12):1259]. *JAMA Psychiatry*. 2015;72(4):334. doi:10.1001/jama-psychiatry.2014.2502
4. Briley M, Lépine JP. The increasing burden of depression. *Neuropsychiatr Dis Treat*. 2011;7(Suppl 1):3–7. doi:10.2147/NDT.S19617
5. Otte C, Gold SM, Penninx BW, et al. Major depressive disorder. *Nat Rev Dis Primers*. 2016;2(1):16065. doi:10.1038/nrdp.2016.65
6. Jackson JC, Pandharipande PP, Girard TD, et al. Depression, post-traumatic stress disorder, and functional disability in survivors of critical illness in the BRAIN-ICU study: A longitudinal cohort study. *Lancet Respir Med*. 2014;2(5):369–379. doi:10.1016/S2213-2600(14)70051-7
7. Köhler CA, Evangelou E, Stubbs B, et al. Mapping risk factors for depression across the lifespan: An umbrella review of evidence from meta-analyses and Mendelian randomization studies. *J Psychiatr Res*. 2018;103:189–207. doi:10.1016/j.jpsychires.2018.05.020
8. Li F, Liu X, Zhang D. Fish consumption and risk of depression: A meta-analysis. *J Epidemiol Community Health*. 2016;70(3):299–304. doi:10.1136/jech-2015-206278
9. Rautio N, Filatova S, Lehtiniemi H, Miettunen J. Living environment and its relationship to depressive mood: A systematic review. *Int J Soc Psychiatry*. 2018;64(1):92–103. doi:10.1177/0020764017744582
10. Ross JA, Glibus G, Van Bockstaele EJ. Stress induced neural reorganization: A conceptual framework linking depression and Alzheimer's disease. *Prog Neuropsychopharmacol Biol Psychiatry*. 2018;85:136–151. doi:10.1016/j.pnpbp.2017.08.004
11. Januar V, Saffery R, Ryan J. Epigenetics and depressive disorders: A review of current progress and future directions. *Int J Epidemiol*. 2015;44(4):1364–1387. doi:10.1093/ije/dyu273
12. Campos ACP, Antunes GF, Matsumoto M, Pagano RL, Martinez RCR. Neuroinflammation, pain and depression: An overview of the main findings. *Front Psychol*. 2020;11:1825. doi:10.3389/fpsyg.2020.01825

13. Wang Y, Eliot MN, Koutrakis P, et al. Ambient air pollution and depressive symptoms in older adults: Results from the MOBILIZE Boston study. *Environ Health Perspect.* 2014;122(6):553–558. doi:10.1289/ehp.1205909
14. Brook RD, Newby DE, Rajagopalan S. Air pollution and cardiometabolic disease: An update and call for clinical trials. *Am J Hypertens.* 2018;31(1):1–10. doi:10.1093/ajh/hpx109
15. Sun Q, Yue P, Deiuliis JA, et al. Ambient air pollution exaggerates adipose inflammation and insulin resistance in a mouse model of diet-induced obesity. *Circulation.* 2009;119(4):538–546. doi:10.1161/CIRCULATIONAHA.108.799015
16. Lodovici M, Bigagli E. Oxidative stress and air pollution exposure. *J Toxicol.* 2011;2011:1–9. doi:10.1155/2011/487074
17. Liu K, Cao H, Li B, et al. Long-term exposure to ambient nitrogen dioxide and ozone modifies systematic low-grade inflammation: The CHCN-BTH study. *Int J Hyg Environ Health.* 2022;239:113875. doi:10.1016/j.ijheh.2021.113875
18. Tanaka M, Vécsei L. Monitoring the kynurenine system: Concentrations, ratios or what else? *Adv Clin Exp Med.* 2021;30(8):775–778. doi:10.17219/acem/139572
19. Tanaka M, Tóth F, Polyák H, Szabó Á, Mándi Y, Vécsei L. Immune influencers in action: Metabolites and enzymes of the tryptophan–kynurenine metabolic pathway. *Biomedicines.* 2021;9(7):734. doi:10.3390/biomedicines9070734
20. Ogyu K, Kubo K, Noda Y, et al. Kynurenine pathway in depression: A systematic review and meta-analysis. *Neurosci Behav Rev.* 2018; 90:16–25. doi:10.1016/j.neubiorev.2018.03.023
21. Rose M, Filiatreault A, Guénette J, Williams A, Thomson EM. Ozone increases plasma kynurenine–tryptophan ratio and impacts hippocampal serotonin receptor and neurotrophic factor expression: Role of stress hormones. *Environ Res.* 2020;185:109483. doi:10.1016/j.envres.2020.109483
22. Thomson EM, Breznan D, Karthikeyan S, et al. Contrasting biological potency of particulate matter collected at sites impacted by distinct industrial sources. *Part Fibre Toxicol.* 2016;13(1):65. doi:10.1186/s12989-016-0176-y
23. Landrigan PJ, Fuller R, Acosta NJR, et al. The Lancet Commission on pollution and health [published correction appears in: *Lancet.* 2018;391(10119):430]. *Lancet.* 2018;391(10119):462–512. doi:10.1016/S0140-6736(17)32345-0
24. Lelieveld J, Klingmüller K, Pozzer A, et al. Cardiovascular disease burden from ambient air pollution in Europe reassessed using novel hazard ratio functions. *Eur Heart J.* 2019;40(20):1590–1596. doi:10.1093/eurheartj/ehz135
25. Thomson EM. Air pollution, stress, and allostatic load: Linking systemic and central nervous system impacts. *J Alzheimers Dis.* 2019; 69(3):597–614. doi:10.3233/JAD-190015
26. Feigin VL, Roth GA, Naghavi M, et al. Global burden of stroke and risk factors in 188 countries, during 1990–2013: A systematic analysis for the Global Burden of Disease Study 2013. *Lancet Neurol.* 2016; 15(9):913–924. doi:10.1016/S1474-4422(16)30073-4
27. Doty RL. The olfactory vector hypothesis of neurodegenerative disease: Is it viable? *Ann Neurol.* 2008;63(1):7–15. doi:10.1002/ana.21327
28. Elder A, Gelein R, Silva V, et al. Translocation of inhaled ultrafine manganese oxide particles to the central nervous system [published correction appears in: *Environ Health Perspect.* 2006;114(8):1178]. *Environ Health Perspect.* 2006;114(8):1172–1178. doi:10.1289/ehp.9030
29. Nel A. Air pollution-related illness: Effects of particles [published correction appears in: *Science.* 2005;309(5739):1326]. *Science.* 2005; 308(5723):804–806. doi:10.1126/science.1108752
30. Genc S, Zadeoglulari Z, Fuss SH, Genc K. The adverse effects of air pollution on the nervous system. *J Toxicol.* 2012;2012:1–23. doi:10.1155/2012/782462
31. Hajat A, Diez Roux AV, Castro-Diehl C, et al. The association between long-term air pollution and urinary catecholamines: Evidence from the multi-ethnic study of atherosclerosis. *Environ Health Perspect.* 2019;127(5):057007. doi:10.1289/EHP3286
32. Thomson EM. Air pollution, stress, and allostatic load: Linking systemic and central nervous system impacts. *J Alzheimers Dis.* 2019;69(3): 597–614. doi:10.3233/JAD-190015
33. Chen C, Nakagawa S. Planetary health and the future of human capacity: The increasing impact of planetary distress on the human brain. *Challenges.* 2018;9(2):41. doi:10.3390/challe9020041
34. Braithwaite I, Zhang S, Kirkbride JB, Osborn DPJ, Hayes JF. Air pollution (particulate matter) exposure and associations with depression, anxiety, bipolar, psychosis and suicide risk: A systematic review and meta-analysis. *Environ Health Perspect.* 2019;127(12):126002. doi:10.1289/EHP4595
35. Davoudi M, Barjasteh-Askari F, Amini H, et al. Association of suicide with short-term exposure to air pollution at different lag times: A systematic review and meta-analysis. *Sci Total Environ.* 2021;771:144882. doi:10.1016/j.scitotenv.2020.144882
36. Pun VC, Manjourides J, Suh H. Association of ambient air pollution with depressive and anxiety symptoms in older adults: Results from the NSHAP Study. *Environ Health Perspect.* 2017;125(3):342–348. doi:10.1289/EHP494
37. Zeng Y, Lin R, Liu L, Liu Y, Li Y. Ambient air pollution exposure and risk of depression: A systematic review and meta-analysis of observational studies. *Psychiatry Res.* 2019;276:69–78. doi:10.1016/j.psychres.2019.04.019
38. Fan SJ, Heinrich J, Bloom MS, et al. Ambient air pollution and depression: A systematic review with meta-analysis up to 2019. *Sci Total Environ.* 2020;701:134721. doi:10.1016/j.scitotenv.2019.134721
39. Kim KN, Lim YH, Bae HJ, Kim M, Jung K, Hong YC. Long-term fine particulate matter exposure and major depressive disorder in a community-based urban cohort. *Environ Health Perspect.* 2016;124(10):1547–1553. doi:10.1289/EHP192
40. Lin H, Guo Y, Kowal P, et al. Exposure to air pollution and tobacco smoking and their combined effects on depression in six low- and middle-income countries. *Br J Psychiatry.* 2017;211(3):157–162. doi:10.1192/bjp.bp.117.202325
41. Kioumourtoglou MA, Power MC, Hart JE, et al. The association between air pollution and onset of depression among middle-aged and older women. *Am J Epidemiol.* 2017;185(9):801–809. doi:10.1093/aje/kww163
42. Kim J, Kim H. Demographic and environmental factors associated with mental health: A cross-sectional study. *Int J Environ Res Public Health.* 2017;14(4):431. doi:10.3390/ijerph14040431
43. Vert C, Sánchez-Benavides G, Martínez D, et al. Effect of long-term exposure to air pollution on anxiety and depression in adults: A cross-sectional study. *Int J Hyg Environ Health.* 2017;220(6):1074–1080. doi:10.1016/j.ijheh.2017.06.009
44. Zijlema WL, Wolf K, Emery R, et al. The association of air pollution and depressed mood in 70,928 individuals from four European cohorts. *Int J Hyg Environ Health.* 2016;219(2):212–219. doi:10.1016/j.ijheh.2015.11.006
45. Altuğ H, Fuks KB, Hüls A, et al. Air pollution is associated with depressive symptoms in elderly women with cognitive impairment. *Environ Int.* 2020;136:105448. doi:10.1016/j.envint.2019.105448
46. Szyszkowicz M, Rowe B, Colman I. Air pollution and daily emergency department visits for depression. *Int J Occup Med Environ Health.* 2009;22(4):355–362. doi:10.2478/v10001-009-0031-6
47. Pollack IB, Ryerson TB, Trainer M, et al. Airborne and ground-based observations of a weekend effect in ozone, precursors, and oxidation products in the California South Coast Air Basin. *J Geophys Res Atmos.* 2012;117(D21):D00V05. doi:10.1029/2011JD016772
48. Tan Z, Lu K, Jiang M, et al. Exploring ozone pollution in Chengdu, south-western China: A case study from radical chemistry to O₃-VOC-NO_x sensitivity. *Sci Total Environ.* 2018;636:775–786. doi:10.1016/j.scitotenv.2018.04.286
49. Kim SY, Bang M, Wee JH, et al. Short- and long-term exposure to air pollution and lack of sunlight are associated with an increased risk of depression: A nested case-control study using meteorological data and national sample cohort data. *Sci Total Environ.* 2021;757:143960. doi:10.1016/j.scitotenv.2020.143960
50. Penckofer S, Kouba J, Byrn M, Estwing Ferrans C. Vitamin D and depression: Where is all the sunshine? *Issues Ment Health Nurs.* 2010; 31(6):385–393. doi:10.3109/01612840903437657
51. Zhao T, Markevych I, Standl M, et al. Short-term exposure to ambient ozone and inflammatory biomarkers in cross-sectional studies of children and adolescents: Results of the GINIplus and LISA birth cohorts. *Environ Pollut.* 2019;255:113264. doi:10.1016/j.envpol.2019.113264
52. Gao W, Tie X, Xu J, et al. Long-term trend of O₃ in a mega City (Shanghai), China: Characteristics, causes, and interactions with precursors. *Sci Total Environ.* 2017;603–604:425–433. doi:10.1016/j.scitotenv.2017.06.099

53. Lary DJ, Lary T, Sattler B. Using machine learning to estimate global $PM_{2.5}$ for environmental health studies. *Environ Health Insights*. 2015; 9(Suppl 1):41–52. doi:10.4137/EHI.S15664
54. Gao Q, Xu Q, Guo X, Fan H, Zhu H. Particulate matter air pollution associated with hospital admissions for mental disorders: A time-series study in Beijing, China. *Eur Psychiatry*. 2017;44:68–75. doi:10.1016/j.eurpsy.2017.02.492
55. Lennon MC, Blome J, English K. Depression among women on welfare: A review of the literature. *J Am Med Womens Assoc (1972)*. 2002; 57(1):27–31,40. PMID:11905486.
56. Heinz AJ, Meffert BN, Halvorson MA, Blonigen D, Timko C, Cronkite R. Employment characteristics, work environment, and the course of depression over 23 years: Does employment help foster resilience? *Depress Anxiety*. 2018;35(9):861–867. doi:10.1002/da.22782
57. Gray P, Senabe S, Naicker N, Kgalamono S, Yassi A, Spiegel JM. Workplace-based organizational interventions promoting mental health and happiness among healthcare workers: A realist review. *Int J Environ Res Public Health*. 2019;16(22):4396. doi:10.3390/ijerph16224396
58. Salanti G, Ioannidis JPA. Synthesis of observational studies should consider credibility ceilings. *J Clin Epidemiol*. 2009;62(2):115–122. doi:10.1016/j.jclinepi.2008.05.014
59. Kane JC, Elafros MA, Murray SM, et al. A scoping review of health-related stigma outcomes for high-burden diseases in low- and middle-income countries. *BMC Med*. 2019;17(1):17. doi:10.1186/s12916-019-1250-8
60. Pöschl U, Shiraiwa M. Multiphase chemistry at the atmosphere-biosphere interface influencing climate and public health in the Anthropocene. *Chem Rev*. 2015;115(10):4440–4475. doi:10.1021/cr500487s
61. Thomas J, Guénette J, Thomson EM. Stress axis variability is associated with differential ozone-induced lung inflammatory signaling and injury biomarker response. *Environ Res*. 2018;167:751–758. doi:10.1016/j.envres.2018.09.007

New insights into the neural network of the nongravid uterus

Vasilios Tanos^{1,2,A–F}, Jennifer Laidlaw^{3,B,D,E}, Panayiotis Tanos^{4,C–E}, Anna Papadopoulou^{5,C–E}

¹ Department of Obstetrics and Gynecology, Aretaio Hospital, Nicosia, Cyprus

² University of Nicosia Medical School, Team Lead ObGyn, Cyprus

³ St George's University of London MBBS program at University of Nicosia, Cyprus

⁴ Institute of Applied Health Sciences, University of Aberdeen Medical School, United Kingdom

⁵ Department of Anatomy, University of Nicosia Medical School, Cyprus

A – research concept and design; B – collection and/or assembly of data; C – data analysis and interpretation;

D – writing the article; E – critical revision of the article; F – final approval of the article

Advances in Clinical and Experimental Medicine, ISSN 1899–5276 (print), ISSN 2451–2680 (online)

Adv Clin Exp Med. 2022;31(10):1153–1162

Address for correspondence

Vasilios Tanos

E-mail: v.tanos@aretaio.com

Funding sources

None declared

Conflict of interest

None declared

Acknowledgements

We would like to thank Ms. Maria Trakoshi for the graphic design of the image in Figure 2.

Received on October 12, 2021

Accepted on May 9, 2022

Published online on June 29, 2022

Abstract

The human uterus is exposed to epigenetic factors during maturation, which might influence its neural network. The mesh muscle is formed from the circular muscle during development and maturation, and it coordinates the longitudinal and circular muscle function. The uterus has an autonomous neural network with contractility and propagation patterns that determine its reproductive potential and health during pregnancy and delivery. Emerging knowledge on the uterine neural network and mesh muscle ultrastructure contributes to new ideas and solutions on the role of intrauterine pressure and distending fluid intravasation during hysteroscopy, and even allows for improving the operative techniques of myomectomy, adenoma cytoreductive surgery and metroplasty. Good health and well-being start from the in utero stage of life. Prenatal and antenatal care are of paramount importance to minimize the risks of malnutrition and pollutants, and foster a healthy uterus. Research regarding the neural network, function and contractility of the nongravid uterus is a new chapter in gynecology that provides significant information for a better understanding and early diagnosis and treatment of uterine pathologies and early pregnancy support.

Key words: uterus, myometrium, neurotransmitter, estrogen, progesterone

Cite as

Tanos V, Laidlaw J, Tanos P, Papadopoulou A. New insights into the neural network of the nongravid uterus.

Adv Clin Exp Med. 2022;31(10):1153–1162.

doi:10.17219/acem/149913

DOI

10.17219/acem/149913

Copyright

Copyright by Author(s)

This is an article distributed under the terms of the Creative Commons Attribution 3.0 Unported (CC BY 3.0)

(<https://creativecommons.org/licenses/by/3.0/>)

Background

The single uterine body is shaped through fusion of the bilateral Müllerian ducts during the embryological development. The thick muscular layers of the uterus derive from mesenchymal cells, while the inner part (the junctional zone and endometrium) derives from the Müllerian duct. During maturation, the outer and inner mesenchymal layers of the body of the fetal uterus give rise to the myometrium and the endometrial stroma of the adult uterus, respectively.¹

Konishi et al. studied the prenatal development of uterine smooth muscle using light and electron microscopy in specimens obtained from 10 human fetuses between 12- and 40-week gestation period in order to establish whether the smooth muscle of the fetal uterus develops into both smooth muscle cells and endometrial stromal cells in the mature uterus.¹ Smooth muscle differentiation takes place at 18–31 weeks of gestation, with differentiation beginning at 18 weeks and the myometrium being clearly distinguishable from the inner layer corresponding to the endometrial stroma at 31 weeks.

The myometrium has muscle layers of different orientation, the innermost muscle layer being circular and the outermost muscle layer being longitudinal. These layers contribute to peristaltic contractions while the uterus is both gravid and nongravid. The middle layer, also referred to as the mesh muscle layer, corresponds to the fusion area of the 3rd muscle layer in the Müllerian ducts. This mesh-like structure with relatively scarce muscle fibers is a vascular-enriched layer, which can be affected by sex hormones, and which contributes to the autonomic uterine contraction control.^{2,3} Telocytes (TCs) in the mesh muscle express receptors for progesterone and estrogen, and respond to stimulation by steroids in order to form homo- and heterocellular junctions consisting of bundles of nerves and muscle fibers.⁴ The abundance of these TCs implies that they act as local pace-making cells.^{5,6} In addition, TCs contact with capillaries controls myometrial blood flow.^{3,7} The mesh muscle provides the communication between the longitudinal and circular muscles.³ These primary results should be confirmed using electrophysiological studies and calcium imaging.

In a nongravid uterus, the innermost layer of the myometrium is called the junctional zone endometrium (JZE). It is the main source of peristaltic activity across the menstrual cycle. The endometrial stem/progenitor cells lie in the basalis layer of the endometrium, next to the myometrium and JZE. Myometrial cells signal to regulate endometrial mesenchymal stem-like cells (eMSCs) with self-renewal activity influenced by cyclic estrogens and progesterone secretion.⁸ The uterus derives its innervation from the lumbar plexus. The lumbar plexus is formed from L1–L4 nerve roots and gives rise to the iliohypogastric, ilioinguinal, genitofemoral, femoral, and obturator nerves. As such, these nerves are important to consider when

describing the contractility, neurophysiology and possible pain pathology of the uterus.⁹ Endometrial waves are initiated in the sub-endometrial myometrium, but the link between the innervation of the uterus and its contractility mechanisms remain unclear. Estrogens affect the central nervous system (CNS) and, together with progesterone, play a role in neurotransmission in the uterus by acting as neuromodulators. Estrogens accelerate the frequency and intensity of uterine contractions, while progesterone decelerates them.^{10,11}

Objectives

In this literature review, we analyzed and indicated the importance of available information on the uterine neural network, and its anatomical localization of the uterus, within the uterus. The relation of uterine neurophysiology to uterine contractility, and the hormonal control of neurotransmission is also discussed. The presented data enable a better understanding of how: a) the uterus responds to menstrual cycle; b) pain emerges from uterus; c) myometrium compensates intrauterine pressure during a hysteroscopic procedure; d) to diminish complications due to prolonged hysteroscopic surgery, and; e) to further improve hysteroscopic surgery and its outcomes.

Materials and methods

The initial search for the data collected for this review was conducted in March 2020. The search strategy involved searching the National Center for Biotechnology Information (NCBI) and PubMed databases using the keywords ‘uterus’, ‘uterine innervation’, ‘sensory nerve

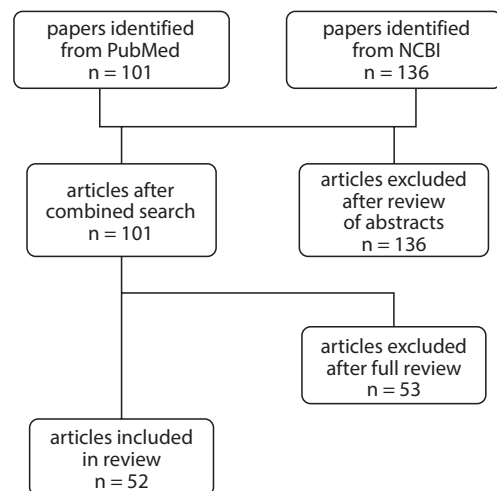


Fig. 1. Diagrammatic presentation of the methodology used for the collection of articles, and exclusion and inclusion process of the relevant papers

NCBI – National Center for Biotechnology Information.

fibers’, and ‘neural transmitters in the endometrium and myometrium’, which revealed 101 papers. During the 2nd round of data collection, more precise keywords were used: ‘endometrium’, ‘myometrium’, ‘uterine’, ‘adrenergic receptors’, ‘purinergic receptors’, ‘estrogen receptor (ER)’, ‘estrogen receptor-related proteins (ERRs)’, ‘substance P (SP)’, ‘protein gene product 9.5 (PGP9.5)’, ‘vasoactive intestinal polypeptide (VIP)’, ‘nerve growth factor (NGF)’, ‘TCs’, ‘tropomyosin receptor kinase A (TrkA)’, and ‘neurotrinin (NTM)’. This more focused search yielded 237 articles. Papers were selected based on their relevance to our objective, particularly excluding those that dealt with animal models or the gravid uterus, except if they held relevance to the neurophysiology and neuroanatomy of the nongravid human uterus. Figure 1 summarizes the procedure followed during data collection.

Results

Uterine innervation

Two main components form the uterine innervation, i.e., the efferent (autonomic) and afferent (interoceptive) nerves. Normal myometrium consists of autonomic innervation with TCs, which are long, thin interstitial cells with long extensions, called telopodes. The presence of extracellular vesicles along the telopodes suggests active

intercellular signalling.⁴ Additionally, uterine TCs express progesterone and ERs. Since estrogen influences the development of uterine innervation, it has been suggested to affect the regulation of uterine innervation and contractility.¹² Furthermore, nitric oxide-synthesizing nerves are abundant in the uterus, and can be sensory or autonomic. Neurotransmitters are secreted into the perifascicular space, and their axonal ends are not in close contact with the myocytes. The development of the sympathetic branch of the uterine autonomic nervous system can be suppressed by estrogen. The TCs express progesterone and ERs specific to their location.¹³ Blood vessels and the innervation of the uterus are closely related. Despite this, multiple fibers are found lying freely within the connective tissue and muscles of the mesometrium, and in the myometrial layer of the uterine body. They are also found, to a lesser extent, in the endometrial layer of the uterine body.

The regional distribution of these nerve fibers as well as their type has been identified with the use of selective markers of sympathetic innervation. The density of autonomic nerve fibers is higher in the cervix and the tubal ampule than in the main tubal part, and is moderate in both the longitudinal and circular smooth muscle layers. However, within the vascular zone, this density is high and interposed amongst the 2 smooth muscle layers in the mesh muscle, as portrayed in Fig. 2.¹⁴ Endometrial innervation is significantly less dense than the innervation of other

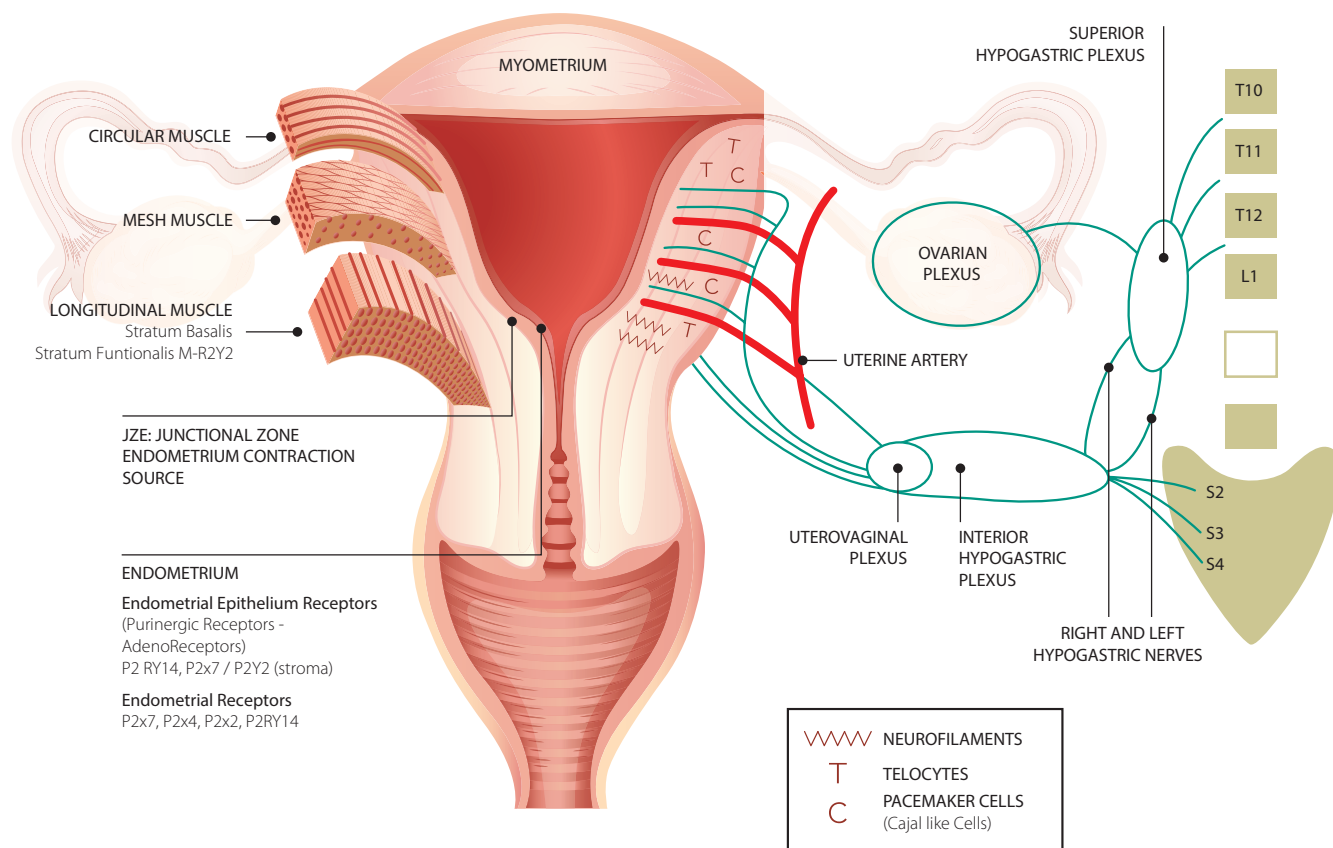


Fig. 2. Graphical representation of nerve and cell distribution

zones of the myometrium. The endometrium fibers that are present are mainly related with blood vessels of the myometrial border. This distribution may indicate that estrogens alter uterine neuritogenic properties via regulating

the synthesis of brain-derived neurotrophic factor (BDNF), and thus inhibiting the outgrowth of sympathetic neurite.¹⁵ The summary of key function cells and receptors involved in uterine neural network is presented in Table 1.

Table 1. Summary of key function cells, hormones and receptors involved in uterine neural network and contractility

References	Structure	Location	Function	Physiological response	Comments
Gibson et al. 2012 ¹⁶ Bengtsson 1973 ¹⁷	ER	ER α and ER β expressed in myometrium	ER α mRNA expression is higher than that of ER β	estrogens produce small, frequent, local, and non-propagated contractions of the myometrium	affect development and function
Burnstock et al. 2014 ¹⁸ Bottari et al. 1985 ¹⁹ Hayashida et al. 1982 ²⁰	adreno-receptor	α and β adrenergic receptors are found in myometrium using radioligand binding	regulatory mechanisms involved in contractility	α -adrenergic stimulation increases the frequency and intensity of uterine contractions, while β -adrenergic binds to epinephrine	α/β -adrenergic stimulation decreases both spontaneous and induced uterine contractility
Burnstock et al. 2014 ¹⁸	P2X1	myometrial SMCs	mediate contraction of smooth muscle	α,β -meATP induced receptor-mediated contractions associated with Cx 43	may be involved in gap junction formation
Burnstock et al. 2014 ¹⁸	P2X2/3	myometrial SMCs	mediates contraction of smooth muscle	differentiation and apoptosis of endometrial cells	changes of P2X R subtypes-related cells can cause differentiation and apoptosis
Burnstock et al. 2014 ¹⁸	P2X7	endometrial, endocervical and ectocervical epithelial cells	regulation of differentiation and control apoptosis	modulated vasodilatation; proapoptotic receptor plays a role in the development of endometrial cancers	these receptors shown to be immunoreactive
Chang et al. 2008 ²¹	P2X4	apical surface of endometrial epithelial cells	controls cervical mucous secretions	activation induces slower and prolonged junctional resistance	decreased transepithelial fluid secretion
Burnstock et al. 2014 ¹⁸	P2Y2	endometrial stromal cells	in vascular smooth muscle cause vasoconstriction, hypertension, hypertrophy	ATP acts through this receptor to inhibit cellular viability and induce early growth response 1	related to immunological impact of tissue highly occupied with neurofibers
Arase et al. 2009 ²²	Ca ⁺⁺ channels	apical surface of endometrial epithelial cells	controls cervical mucous secretions	activation stimulates [Ca ²⁺]-dependent, chloride secretion and osmotic water efflux	increased transepithelial fluid secretion
Cretoiu et al. 2012 ⁴ Aleksandrovych et al. 2019 ¹²	P2RY14	endometrial epithelial cells (+epithelial cells of cervix, fallopian tubes, placenta)	mucosal function, mediate induction of endo/trial epithelial IL-8	constant UDP-glucose expression through menstrual cycle	more abundant in endometria with PID
Bernstein et al. 2014 ²³	anoctamin ANO1 ANO2	myometrial SMCs	transmembrane protein functions as Ca ⁺⁺ activated Cl ⁻ channel	determine protein expression in myometrial tissue	uterine smooth muscle contractility
Wray et al. 2003 ²⁴	Ca ⁺⁺ channels	myometrium	role in excitability and contractility	basic mechanism of uterine contractions; uncertainty which channels are present in myometrium and how action potential is initiated	unclear which channels are present in myometrium and the nature of the pacemaker mechanism
Khan et al. 2001 ²⁵	K ⁺ channels	myometrial and endometrial cells	membrane-spanning regions (M1 and M2) uterus	plays a major role in cell homeostasis and cell signaling	M1/M2 dysregulation within the intrauterine environment during adverse pregnancy outcomes
Richter et al. 2004 ²⁶	OXTR	uterine endometrial and myometrial cells	control of cycle length, minor significance for contractility in the nonpregnant uterus	involved in parturition and lactation, increases production of prostaglandins	OXTR expression is modulated by stimulation with E ₂ and OT
Cretoiu et al. 2012 ⁴ Aleksandrovych et al. 2019 ¹² Varga et al. 2018 ²⁷	TCs	interstitial cells found in all sublayers of myometrium	extracellular vesicles along the telopodes	active intercellular signaling, express ER and PR, estrogens influence the development of uterine innervation	telocytes regulate uterine SMC expression; regulating uterine innervation and contractility

Table 1. Summary of key function cells, hormones and receptors involved in uterine neural network and contractility – cont.

References	Structure	Location	Function	Physiological response	Comments
Popescu et al. 2007 ²⁸	pacemaker cells (Cajal)	triangular-shaped cells located throughout the myometrium on the borders of smooth muscle bundles	myogenic regulation in uterus and fallopian tubes	CLC might have other physiological roles, depending on tissue type (e.g., intercellular signaling, immune surveillance, steroid sensors)	interstitial Cajal-like cells with dense cytoplasm, and numerous mitochondria
Zefferino et al. 2019 ²⁹	GJ	myometrium cell–cell contacts formed by Cx	large number of GJs rapidly formed prior to and during parturition	rate of gap junction formation also affected by estrogen/progesterone	major mechanism in parturition

ER – estrogen receptor; PR – progesterone receptors; GJ – gap junction; Cx – connexin; TCs – telocytes; ATP – adenosine triphosphate; OT – oxytocin; OXTR – oxytocin receptor; IL-8 – interleukin 8; SMC – smooth muscle cell; UDP – uridine diphosphate glucose; PR – progesterone receptor; GJ – gap junction; ANO – anoctamin; PID – pelvic inflammatory disease; SMC – smooth muscle cell; NF – neurofilament; PGP – protein gene product; PGE2 – prostaglandin E2; PGF2a – prostaglandin F2a; P2RY – purinergic receptor; CLC – Cajal-like cells.

Sensory nerve fibers and neural transmitters in the endometrium and myometrium

Table 2 summarizes identifiable sensory nerve fibers in the endometrial functional layer. Following immunohistochemical analysis, several neurotransmitters and signaling proteins, including VIP, SP, neurofilament (NF), PGP9.5, neuropeptide Y (NPY), and calcitonin gene-related protein (CGRP), were examined.³⁶ Nerve fibers reactive to neurotensin (NT), NPY, VIP, and SP are found in normal

human endometrium,³⁷ although little is known about their function in the uterus. In the healthy human endometrium, immunoreactive nerve fibers are restricted to the basal layer and the functional layer of the endometrium is devoid of innervation.

Neuromodulation of the uterus

Neurotrimin (NTM) is a glycosphatidylinositol. This neuronal cell adhesion molecule belongs to the immunoglob-

Table 2. Reported nerve fibers and neurotransmitters found in the uterus

References	Structure	Location	Function	Physiological response	Associated pathologies	Comments
Nerve fibers						
Zhang et al. 2010 ³⁰	PGP9.5 immunoreactive nerve fibers	basal layer of endometrium, myometrium	PGP9.5 neuronal marker for autonomic and sensory nerve fibers	found in myometrium, occasionally present in endometrium	in the endometrium of women with pain	their presence is related to the absence of pain
Zhang et al. 2010 ³⁰	NF immunoreactive nerve fibers	basal layer of endometrium, myometrium	NF – neurospecific cellular component	present only in myometrium	infiltration of endometrium cause pain	nerve fibers are related to pain
Taneike et al. 1999 ³¹	cholinergic nerve fibers	abundant in cervix uteri, uncommon in uterine body	inner circular muscle layer more controlled by cholinergic innervation	associated with the uterine arteries and myometrial smooth muscles	used to control blood flow to the uterine region with medication	–
Stjernholm et al. 1998 ³²	small unmyelinated nerve fibers	functional layer of the endometrium	controlled by adrenergic and postganglionic fibres of the sympathetic nerves	involved in pain, thermoregulation, mechanoreceptors	involved in endometriosis	in chronic deep pain, temperature receptors, pressure or mechanoreceptors
Tokushige et al. 2006 ³³	cytokines	stroma of endometrial cells	IL-8	endometrial glandular cells	present in endometriosis, absent in women without endometriosis	present in functional endometrium
Neurotransmitters						
Egarter et al. 1992 ³⁴ , Mueller et al. 2006 ³⁵	PGE ₂ , PGF _{2a}	endometrium, myometrium	PGE ₂ and PGF _{2a} contract the myometrium by acting as a calcium ionophores	direct stimulation of myometrial contractions	inflammatory cytokine	promotes neutrophil chemotaxis
Arase et al. 2009 ²²	PGE ₁	myometrial SMCs	–	increase in uterine contractility	estrogen increases the production of PGF _{2a} by the decidua	–

IL-8 – interleukin 8; NF – neurofilament; PGP9.5 – protein gene product 9.5; PGE – prostaglandin E; PGF_{2a} – prostaglandin F_{2a}; SMC – smooth muscle cell.

ulin-like cell adhesion molecule protein family. It is found in the uterus and is regulated by estrogen. Neurotrimin regulates the development and outgrowth of neuronal projections (neurites). Its expression is increased in patients with leiomyoma and in in vitro models after estrogen and progesterone treatment. In human, the *NTM* gene is situated on chromosome 11q25 and encodes a 39-kDa protein.³⁸ The BDNF belongs to the neurotrophin family and exerts its physiological functions through the neurotrophic tyrosine receptor kinase type 2 (Ntrk2) receptor, which is expressed in the luminal and glandular epithelium, as well as in the myometrium and vascular smooth muscle. The BDNF and Ntrk2 have an autonomous expression in the uterus.³⁹ The ligand and receptor are both colocalized and co-expressed in the uterus. The BDNF–Ntrk2 binding activates the adhesion formation, apoptosis, angiogenesis, and proliferation pathways, which are prominently involved in the physiology of reproduction.⁴⁰ Some transient receptor potential vanilloid type-1 (TRPV1)-immunoreactive fibers are found in nerve fascicles in the body of the nongravid uterus, but not of the gravid uterus. These fibers are sparsely distributed around the blood vessels and throughout the stroma of the cervix, but occur more frequently in the subepithelium.⁴⁰

Purinergic receptors are classified as either P1 or P2. The P2 purinergic receptors – P2X17, P2Y1, 2, 4, 6, 11, 12, 13, and 14, have been identified using molecular cloning.^{41–43} Burnstock demonstrated high affinity for extracellular adenosine in P1 receptors, while P2 receptors had high affinity for adenosine triphosphate (ATP).⁴² The P2U/P2Y2 purinergic receptor has demonstrated an equal or greater response to uridine-5'-triphosphate (UTP) compared to ATP. The P2U/P2Y2 receptor mRNA is expressed in human endometrial stromal cells (hESCs). Adenosine triphosphate activates the extracellular signal-regulated kinases 1/2 (ERK1/2), inducing the phosphorylated ERKs nuclear translocation, while simultaneously increasing matrix metalloproteinase (MMP)-2, -3, -10, and -24 expression in hESCs.²¹ The P2X7 receptors are also expressed in human endometrial epithelial cells. Throughout the endometrial cycle, endometrial differentiation and apoptosis are mediated by changes in the P2X receptor subtypes expression in uterine epithelial cells.¹⁸ The P2X receptors are known to exist on sensory nerves,⁴⁴ and have been identified on uterine and cervical sensory nerves. The G-protein-coupled estrogen receptor 1 (GPER-1) mRNA, which might play a role in endometrial biology, was found in all endometrial and decidual tissue samples.^{5,45,46}

Interactions between hormones and neurotransmitters involved in uterine innervation

The afferent innervation of the myometrium is immunoreactive for multiple co-transmitters, including SP, CGRP, VIP, nitric oxide synthase (NOS), neurokinin A, galanin,

and secretoneurin.⁴⁷ Estrogen incites a surge in protein production, which negatively affects sympathetic nerves. Semaphorin 3F, BDNF, *NTM*, as well as substrate-bound signals and pro-NGF all contribute to remodeling of the uterine innervation, which is induced by estrogen. Pro-neuritogenic factors such as NGF and NT3 remain undiminished, while estrogen elicits alterations in favor of p75NTR and TrkA neurotrophin receptors of sympathetic neurons.⁴⁸ Estrogen in the dorsal root ganglion (DRG) sensory neurons of the uterus supply causes changes in TrkA levels,⁴⁹ which in turn affect neuronal receptivity to the pro-neuritogenic effects of NGF and NT3, while promoting BDNF inhibition.⁵⁰ The TrkA signaling in sympathetic neurons, which is stimulated by NGF, is antagonized by Sema3F.⁵¹ The p75NTR is bound to neurotrophins in uterine-projecting sympathetic neurons required for growth by the inhibition of sympathetic neuron responses to Sema3F.⁵² The p75NTR expression is increased by estrogen. Cajal-like interstitial cells have been described outside the gastrointestinal tract, including in the uterus,⁵³ which further contributes to spontaneous uterine contractions. The complexities of myometrial innervation remain unclear, and the impact of neuromodulation on uterine contractility is still under investigation.

Discussion

The uterovaginal plexus gives rise to the uterine sympathetic nerve fibers. The biggest component of the uterovaginal plexus is the inferior hypogastric plexus and more specifically, its anterior and intermediate components. Furthermore, the pelvic splanchnic nerve roots S2–S4 give rise to the parasympathetic fibers of the uterus. Premature labor⁵⁴ is a complication of poor uterine adaptation during fetal growth, and pathologies such as adenomyosis,⁵⁵ endometriosis,^{10,55} dysmenorrhea,¹⁰ as well as infertility⁵⁶ are complications that arise after irregular myometrial or peristaltic contractions. However, the functional mechanisms of these muscles are still unclear.

Embryological development of myometrium

The organogenesis and maturation of the human uterus take longer than in other vital organs. The myometrial smooth muscle differentiation initiates after 18 weeks of gestation and the outer myometrial layer matures after 31 weeks of gestation. This stage is also characterized by increased activity of granular endoplasmic reticulum and Golgi apparatus, which suggests early protein production. The mesh muscle identified among the longitudinal and circular muscle layers anatomically blends the 2 layers together and coordinates the uterine contractions. Kuijsters et al. based this hypothesis on the embryological merging of the 2 Müllerian ducts and the development

of mesh-like structures.⁷ Endometrial cancer is considered to be in an advanced stage when malignant cells are found beyond the 50% of the myometrium, i.e., over the borders of the mesh muscle. At this point, distant metastasis and poor prognosis are expected.

Vascularization

Neural pathways follow the arterial supply. The anthropoid uterus is supplied with blood vessels from the ovarian, uterine and vaginal arteries.⁵⁷ The circumferential arcuate arteries are formed from the uterine arteries which penetrate the myometrium bilaterally.⁵⁸ This allows for a uniform capillary distribution and creation of a gradient of decreasing vascular smooth muscle richness from the exterior to the innermost layer of the myometrium.⁵⁸ Considering that the vascular layer of the myometrium is controlled by the autonomic nervous system, a correlation can be made. According to histological studies, a heavy plexus of nerve fibers with vasomotor function was identified medial to the main uterine artery, but no such structure was identified on the secondary uterine or the ovarian-uterine arteries.⁵⁹

Localization of nerve fibers

Neurofilament and PGP9.5 are pan-neuronal cytoplasmic proteins that are used as markers for unmyelinated and myelinated autonomic and sensory nerves.³⁰ Nerve fibers immunoreactive with NF and PGP9.5 are mostly restricted to the myometrium, with minimal presence in the endometrial basal layer. The endometrium is largely devoid of innervation. The inner circular layer of the myometrium is mostly cholinergic, while the outer longitudinal layer is mostly adrenergic.³¹ Cholinergic nerve fibers are abundant in the cervix uteri, but uncommon in the body of the uterus.³² Additionally, in patients with endometriosis, NF-immunoreactive myelinated fibers were found in the deeper portion of the basal endometrium. In contrast, patients who did not have endometriosis had myelinated nerve fibers – except for 1 patient who did not have endometriosis, but her symptomatology was consistent with that of endometriosis (i.e., uterine fibroids, menorrhagia, pelvic pain, and chronic cervical inflammation).

Interestingly, in the functional endometrial layer, there were no NF-immunoreactive myelinated nerve fibers. This was true both for patients with and without endometriosis. Occasionally, small unmyelinated nerve fibers were noted in the deeper basal layer in women without endometriosis. Tokushige et al. identified 31 women without endometriosis who had no nerve fibers in the basal endometrial layer.³³ Furthermore, there were 4 women without endometriosis who presented with deeper basal endometrial nerve fibers, but were also diagnosed with uterine fibroids. Multiple small unmyelinated nerve fibers marked for PGP9.5 are present in the functional endometrial layer of all patients

with endometriosis. However, in patients without endometriosis, no nerve fibers were detected in the endometrial functional layer.⁶ The PGP 9.5 is used in the primary identification of both unmyelinated and myelinated uterine nerve fibers. Patients with PGP 9.5-immunoactive nerve fibers in the endometrial functional layer experience pain. However, patients who do not have PGP 9.5-immunoactive nerve fibers do not suffer from pain. Consequently, PGP 9.5-immunoreactive nerves can be part of a pain mechanism in gynecological conditions such as adenomyosis. Most $\alpha 1$ -adrenergic receptors in the uterus are found in spherical bundles of the isthmo-cervical area. In contrast, $\beta 2$ -adrenergic receptors are mostly found in the uterine body. Tyrosine hydroxylase immunoreactivity was used to demonstrate the adrenergic contribution to the uterine innervation in myometrial tissue. The α -adrenergic receptors play a role in contraction, whereas $\beta 2$ -adrenergic receptors are involved in tocolysis. However, the clear roles of $\beta 1$ -, $\beta 3$ - and $\alpha 2$ -receptors in the myometrial contractility remain incompletely understood.

Different neuronal factors can be used to create a picture of normal uterine sensory and motor function. For example, sensory function in the nonpregnant uterus can be estimated through the investigation of NTM, a fixed neuronal cell adhesion molecule that regulates the development of neuronal projections in the uterus, and is in turn regulated by estrogen.⁵ The *NTM* expression is increased in painful uterine diseases such as leiomyoma, suggesting its role in transmitting sensory information in normal uterine neurophysiology.³⁸

Chemical factors affecting myometrial contractility

A prominent inward (depolarizing) current is activated by Ca^{2+} entry into cells, and this process plays a functionally important role in myometrial contractility by contributing to membrane potential and firing frequency in myometrial cells. Other chemicals that influence contractility are hormones affecting both estrogen receptor proteins and progesterone receptor proteins. Estrogen and progesterone play a role as neuromodulators and have a hormonal effect on neurotransmission.

Hormonal control

Estrogen also contributes to an increased uterine contractility in indirect ways. Egarter and Husslein showed that estrogen leads to an increased production of prostaglandins (e.g., PGE_1 , PGE_2 , PGF_2) from endometrial decidua.³⁴ Prostaglandins also increase the contractility of the uterus.³⁵ Prostaglandins act as neurotransmitters (Table 2). The female genital ducts, in contrast to the male ducts, which are controlled by testicular androgens,⁶⁰ differentiate autonomously without the need for any external regulatory factors.⁶¹ Estrogen and progesterone surge in the plasma

of both the mother and fetus during gestation. The decrease in size of the uterus following oophorectomy may negatively affect female genitalia development.⁶² Hence, during pregnancy, the fetal uterus is likely influenced by both estrogen and progesterone, particularly its mesenchymal components, i.e., smooth muscle and endometrial stroma. Further research is needed to verify the relationship between sex steroids and fetal uterus development.

Limitations

The limitations of our review were largely due to the limited number of studies that met the criteria for inclusion. The scarcity of suitable studies can be attributed to the limitations of the research design that would be necessary in order to collect this data. It is logistically and ethically difficult to carry out the necessary research aimed at identifying the neural network of the living, nongravid, human uterus at the ideal level of detail and quality.

Conclusions

The organogenesis and maturation of the human uterus takes longer to occur than in other vital organs. Signs of smooth muscle differentiation are observed as early as 18 weeks of gestation. However, maturation and increase in organelles in the outer layer of myometrium, which suggests early protein production, is not observed prior to 31 weeks of gestation. The newborn uterus continues to develop during childhood and teenage until reaching adulthood, changing its dimensions in favor of the corpus, while the cervical length decreases. Given the later development of the uterus, it can be speculated that there is an increased risk of myometrium microstructure malformations and malfunctions due to the influence of epigenetic factors (e.g., malnutrition, stress, hormonal levels, pollutants, and hypoxia). Hence, each uterus reaches maturity after exposure in utero, during labor and delivery, and later in life. The organ adapts to the conditions of every stage and forms a unique complex of neural network elements and microstructure, especially in the area of the mesh muscle. These findings reflect the development of an autonomous neural network of the uterus, and the subsequent contractility and propagation patterns that affect uterine health and potential to reproduction, pregnancy and delivery. Further knowledge on uterine neural networks and mesh muscle ultrastructure may lead to new ideas and solutions regarding intrauterine pressure and distending fluid intravasation during hysteroscopy, as well as to the improvement of the operative techniques of myomectomy, adenoma cytoreductive surgery and metroplasty. Prenatal and antenatal care are of paramount importance to minimize the risks associated with malnutrition and exposure to pollutants. Studies examining the neural network, function and contractility

of the nongravid uterus represent a new benchmark in gynecology research, providing significant information for better understanding and early diagnosis and treatment of uterine pathologies.

ORCID iDs

Vasilios Tanos  <https://orcid.org/0000-0002-4695-4630>

Panayiotis Tanos  <https://orcid.org/0000-0001-5742-0995>

References

- Konishi I, Fujii S, Okamura H, Mori T. Development of smooth muscle in the human fetal uterus: An ultrastructural study. *J Anat.* 1984;139(Pt 2): 239–252. PMID:6490516.
- Noe M. The cyclic pattern of the immunocytochemical expression of oestrogen and progesterone receptors in human myometrial and endometrial layers: Characterization of the endometrial-subendometrial unit. *Hum Reprod.* 1999;14(1):190–197. doi:10.1093/humrep/14.1.190
- Kagami K, Ono M, Iizuka T, et al. A novel third mesh-like myometrial layer connects the longitudinal and circular muscle fibers: A potential stratum to coordinate uterine contractions. *Sci Rep.* 2020;10(1):8274. doi:10.1038/s41598-020-65299-0
- Cretoiu D, Cretoiu SM, Simionescu AA, Popescu LM. Telocytes, a distinct type of cell among the stromal cells present in the lamina propria of jejunum. *Histol Histopathol.* 2012;27(1):1067–1078. doi:10.14670/HH-27.1067
- Takala H, Al-Hendy A, Yang Q. Neurotrimin: A novel neural cell adhesion molecule correlating with uterine fibroid phenotype. *Fertil Steril.* 2020;113(1):83–84. doi:10.1016/j.fertnstert.2019.09.026
- Tokushige N, Markham R, Russell P, Fraser IS. High density of small nerve fibres in the functional layer of the endometrium in women with endometriosis. *Hum Reprod.* 2006;21(3):782–787. doi:10.1093/humrep/dei368
- Kuijsters NPM, Methorst WG, Kortenhorst MSQ, Rabotti C, Mischi M, Schoot BC. Uterine peristalsis and fertility: Current knowledge and future perspectives. A review and meta-analysis. *Reprod BioMed Online.* 2017;35(1):50–71. doi:10.1016/j.rbmo.2017.03.019
- Cao M, Chan RWS, Cheng FHC, et al. Myometrial cells stimulate self-renewal of endometrial mesenchymal stem-like cells through WNT5A/ β -catenin signaling. *Stem Cells.* 2019;37(11):1455–1466. doi:10.1002/stem.3070
- Arulkumaran S, Ledger W, Denny L, Doumouchtsis S, eds. *Oxford Textbook of Obstetrics and Gynaecology.* Oxford, UK: Oxford University Press; 2020. doi:10.1093/med/9780198766360.001.0001
- Bulletti C, De Ziegler D, Setti PL, Cicinelli E, Polli V, Flamigni C. The patterns of uterine contractility in normal menstruating women: From physiology to pathology. *Ann N Y Acad Sci.* 2004;1034(1):64–83. doi:10.1196/annals.1335.007
- Fanchin R, Harmas A, Benaoudia F, Lundkvist U, Olivennes F, Frydman R. Microbial flora of the cervix assessed at the time of embryo transfer adversely affects in vitro fertilization outcome. *Fertil Steril.* 1998;70(5):866–870. doi:10.1016/S0015-0282(98)00277-5
- Aleksandrovych V, Pasternak A, Gil K. Telocytes in the architecture of uterine fibroids. *Folia Med Cracov.* 2019;59(4):34–44. doi:10.24425/FMC.2019.131378
- Latini C, Frontini A, Morroni M, Marzioni D, Castellucci M, Smith PG. Remodeling of uterine innervation. *Cell Tissue Res.* 2008;334(1):1–6. doi:10.1007/s00441-008-0657-x
- Zoubina EV, Fan Q, Smith PG. Variations in uterine innervation during the estrous cycle in rat. *J Comp Neurol.* 1998;397(4):561–571. PMID:9699916.
- Krizsan-Agbas D, Pedchenko T, Smith PG. Neurotrimin is an estrogen-regulated determinant of peripheral sympathetic innervation. *J Neurosci Res.* 2008;86(14):3086–3095. doi:10.1002/jnr.21768
- Gibson DA, Saunders PT. Estrogen dependent signaling in reproductive tissues: A role for estrogen receptors and estrogen related receptors. *Mol Cell Endocrinol.* 2012;348(2):361–372. doi:10.1016/j.mce.2011.09.026
- Bengtsson LP. Hormonal effects on human myometrial activity. *Vitam Horm.* 1973;31:257–303. doi:10.1016/s0083-6729(08)61000-6

18. Burnstock G. Purinergic signalling in the reproductive system in health and disease. *Purinergic Signal*. 2014;10(1):157–187. doi:10.1007/s11302-013-9399-7
19. Bottari SP, Vokaer A, Kaivez E, Lescairier JP, Vauquelin G. Regulation of alpha- and beta-adrenergic receptor subclasses by gonadal steroids in human myometrium. *Acta Physiol Hung*. 1985;65(3):335–346. PMID:2990161.
20. Hayashida DN, Leung R, Goldfien A, Roberts JM. Human myometrial adrenergic receptors: Identification of the beta-adrenergic receptor by [3H] dihydroalprenolol binding. *Am J Obstet Gynecol*. 1982;142(4):389–393. doi:10.1016/S0002-9378(16)32378-X
21. Chang SJ, Wang TY, Lee YH, Tai CJ. Extracellular ATP activates nuclear translocation of ERK1/2 leading to the induction of matrix metalloproteinases expression in human endometrial stromal cells. *J Endocrinol*. 2007;193(3):393–404. doi:10.1677/JOE-06-0168
22. Arase T, Uchida H, Kajitani T, et al. The UDP-glucose receptor P2RY14 triggers innate mucosal immunity in the female reproductive tract by inducing IL-8. *J Immunol*. 2009;182(11):7074–7084. doi:10.4049/jimmunol.0900001
23. Bernstein J, Vink JY, Wen Fu X, et al. Calcium-activated chloride channels anoctamin 1 and 2 promote murine uterine smooth muscle contractility. *Am J Obstet Gynecol*. 2014;211(6):688.e1–688. doi:10.1016/j.ajog.2014.06.018
24. Wray S, Jones K, Kupittayanant S, et al. Calcium signaling and uterine contractility. *J Soc Gynecol Investig*. 2003;10(5):252–264. doi:10.1016/s1071-5576(03)00089-3
25. Khan RN, Matharoo-Ball B, Arulkumaran S, Ashford MLJ; Uterine Contractility Symposium. Potassium channels in the human myometrium. *Exp Physiol*. 2001;86(2):255–264. <https://physoc.onlinelibrary.wiley.com/doi/pdf/10.1113/eph8602181>
26. Richter ON, Kübler K, Schmollung J, et al. Oxytocin receptor gene expression of estrogen-stimulated human myometrium in extracorporeally perfused non-pregnant uteri. *Mol Hum Reprod*. 2004;10(5):339–346. doi:10.1093/molehr/gah039
27. Varga I, Kyselovič J, Danišovič L, et al. Recently discovered interstitial cells termed telocytes: Distinguishing cell-biological and histological facts from fictions. *Biologia*. 2019;74:195–203. doi:10.2478/s11756-018-0162-y
28. Popescu LM, Ciontea SM, Cretoiu D. Interstitial Cajal-like cells in human uterus and fallopian tube. *Ann N Y Acad Sci*. 2007;1101:139–165. doi:10.1196/annals.1389.022
29. Zefferino R, Piccoli C, Gioia SD, Capitano N, Conese M. Gap junction intercellular communication in the carcinogenesis hallmarks: Is this a phenomenon or epiphenomenon? *Cells*. 2019;8(8):896. doi:10.3390/cells8080896
30. Zhang G, Dmitrieva N, Liu Y, McGinty KA, Berkley KJ. Endometriosis as a neurovascular condition: Estrous variations in innervation, vascularization, and growth factor content of ectopic endometrial cysts in the rat. *Am J Physiol Regul Integr Comp Physiol*. 2008;294(1):R162–R171. doi:10.1152/ajpregu.00649.2007
31. Taneike T, Kitazawa T, Funakura H, et al. Smooth muscle layer-specific variations in the autonomic innervation of bovine myometrium. *Gen Pharmacol*. 1999;32(1):91–100. doi:10.1016/S0306-3623(98)00089-5
32. Stjernholm YM, Sahlin L, Eriksson HA, Byström BE, Stenlund PM, Ekman GE. Cervical ripening after treatment with prostaglandin E2 or antiprogesterin (RU486): Possible mechanisms in relation to gonadal steroids. *Eur J Obstet Gynecol Reprod Biol*. 1999;84(1):83–88. doi:10.1016/S0301-2115(98)00329-7
33. Tokushige N, Markham R, Russell P, Fraser IS. High density of small nerve fibres in the functional layer of the endometrium in women with endometriosis. *Hum Reprod*. 2006;21(3):782–787. doi:10.1093/humrep/dei368
34. Egarter CH, Husslein P. Biochemistry of myometrial contractility. *Baillieres Clin Obstet Gynaecol*. 1992;6(4):755–769. doi:10.1016/S0950-3552(05)80187-7
35. Mueller A, Maltaris T, Siemer J, et al. Uterine contractility in response to different prostaglandins: Results from extracorporeally perfused non-pregnant swine uteri. *Hum Reprod*. 2006;21(8):2000–2005. doi:10.1093/humrep/del118
36. Bokor A, Kyama CM, Vercruyse L, et al. Density of small diameter sensory nerve fibres in endometrium: A semi-invasive diagnostic test for minimal to mild endometriosis. *Hum Reprod*. 2009;24(12):3025–3032. doi:10.1093/humrep/dep283
37. Heinrich D, Reinecke M, Forssmann WG. Peptidergic innervation of the human and guinea pig uterus. *Arch Gynecol*. 1986;237(4):213–219. doi:10.1007/BF02133783
38. Parikh TP, Malik M, Britten J, Aly JM, Pilgrim J, Catherino WH. Steroid hormones and hormone antagonists regulate the neural marker neurotrophin in uterine leiomyoma. *Fertil Steril*. 2020;113(1):176–186. doi:10.1016/j.fertnstert.2019.08.090
39. Tingåker BK, Ekman-Ordeberg G, Facer P, Irestedt L, Anand P. Influence of pregnancy and labor on the occurrence of nerve fibers expressing the capsaicin receptor TRPV1 in human corpus and cervix uteri. *Reprod Biol Endocrinol*. 2008;6(1):8. doi:10.1186/1477-7827-6-8
40. Wessels JM, Wu L, Leyland NA, Wang H, Foster WG. The brain–uterus connection: Brain derived neurotrophic factor (BDNF) and its receptor (Ntrk2) are conserved in the mammalian uterus. *PLoS ONE*. 2014;9(4):e94036. doi:10.1371/journal.pone.0094036
41. Burnstock G, Knight GE. Cellular distribution and functions of P2 receptor subtypes in different systems. *Int Rev Cytol*. 2004;240:31–304. doi:10.1016/S0074-7696(04)40002-3
42. Burnstock G. Pathophysiology and therapeutic potential of purinergic signaling. *Pharmacol Rev*. 2006;58(1):58–86. doi:10.1124/pr.58.1.5
43. Gordon JL. Extracellular ATP: Effects, sources and fate. *Biochem J*. 1986;233(2):309–319. doi:10.1042/bj2330309
44. Cook SP, Vulchanova L, Hargreaves KM, Elde R, McCleskey EW. Distinct ATP receptors on pain-sensing and stretch-sensing neurons. *Nature*. 1997;387(6632):505–508. doi:10.1038/387505a0
45. Kolkova Z, Noskova V, Ehinger A, Hansson S, Casslen B. G protein-coupled estrogen receptor 1 (GPER, GPR 30) in normal human endometrium and early pregnancy decidua. *Mol Hum Reprod*. 2010;16(10):743–751. doi:10.1093/molehr/gaq043
46. Richeri A, Bianchimano P, Marmol NM, Viettro L, Cowen T, Brauer MM. Plasticity in rat uterine sympathetic nerves: The role of TrkA and p75 nerve growth factor receptors. *J Anat*. 2005;207(2):125–134. doi:10.1111/j.1469-7580.2005.00435.x
47. Brauer MM, Smith PG. Estrogen and female reproductive tract innervation: Cellular and molecular mechanisms of autonomic neuroplasticity. *Autonom Neurosci*. 2015;187:1–17. doi:10.1016/j.autneu.2014.11.009
48. Hasan W, Smith HJ, Ting AY, Smith PG. Estrogen alters trkA and p75 neurotrophin receptor expression within sympathetic neurons. *J Neurobiol*. 2005;65(2):192–204. doi:10.1002/neu.20183
49. Chalar C, Richeri A, Viettro L, et al. Plasticity in developing rat uterine sensory nerves: The role of NGF and TrkA. *Cell Tissue Res*. 2003;314(2):191–205. doi:10.1007/s00441-003-0799-9
50. Krizsan-Agbas D, Pedchenko T, Hasan W, Smith PG. Oestrogen regulates sympathetic neurite outgrowth by modulating brain derived neurotrophic factor synthesis and release by the rodent uterus. *Eur J Neurosci*. 2003;18(10):2760–2768. doi:10.1111/j.1460-9568.2003.03029.x
51. Atwal JK, Singh KK, Tessier-Lavigne M, Miller FD, Kaplan DR. Semaphorin 3F antagonizes neurotrophin-induced phosphatidylinositol 3-kinase and mitogen-activated protein kinase signaling: A mechanism for growth cone collapse. *J Neurosci*. 2003;23(20):7602–7609. doi:10.1523/JNEUROSCI.23-20-07602.2003
52. Naska S, Lin DC, Miller FD, Kaplan DR. p75NTR is an obligate signaling receptor required for cues that cause sympathetic neuron growth cone collapse. *Mol Cell Neurosci*. 2010;45(2):108–120. doi:10.1016/j.mcn.2010.05.015
53. Ciontea SM, Radu E, Regalia T, et al. C-kit immunopositive interstitial cells (Cajal-type) in human myometrium. *J Cell Mol Med*. 2005;9(2):407–420. doi:10.1111/j.1582-4934.2005.tb00366.x
54. Ravanos K, Dagklis T, Petousis S, Margioulas-Siakou C, Prapas Y, Prapas N. Factors implicated in the initiation of human parturition in term and preterm labor: A review. *Gynecol Endocrinol*. 2015;31(9):679–683. doi:10.3109/09513590.2015.1076783
55. Tamura H, Kishi H, Kitade M, et al. Clinical outcomes of infertility treatment for women with adenomyosis in Japan. *Reprod Med Biol*. 2017;16(3):276–282. doi:10.1002/rmb2.12036
56. Eytan O, Halevi I, Har-Toov J, Wolman I, Elad D, Jaffa AJ. Characteristics of uterine peristalsis in spontaneous and induced cycles. *Fertil Steril*. 2001;76(2):337–341. doi:10.1016/S0015-0282(01)01926-4
57. Chard T, Grudzinskas JG, eds. *The Uterus*. New York, USA: Cambridge University Press; 1994. ISBN: 978-0-521-41403-6 978-0-521-42453-0.

58. Farrer-Brown G, Beilby JOW, Tarbit MH. The blood supply of the uterus. 1. Arterial vasculature. *BJOG*. 1970;77(8):673–681. doi:10.1111/j.1471-0528.1970.tb03592.x
59. Bell C. Evidence for dual innervation of the human extrinsic uterine arteries. *BJOG*. 1969;76(12):1123–1128. doi:10.1111/j.1471-0528.1969.tb05796.x
60. Jost A. The role of fetal hormones in prenatal development. *Harvey Lect*. 1961;55:201–226. PMID:13790784.
61. Pelliniemi LJ, Dym M, Karnovsky MJ. Peroxidase histochemistry using diaminobenzidine tetrahydrochloride stored as a frozen solution. *J Histochem Cytochem*. 1980;28(2):191–192. doi:10.1177/28.2.6986432
62. Tulchinsky D, Hobel CJ. Plasma human chorionic gonadotropin, estrone, estradiol, estriol, progesterone, and 17 α -hydroxyprogesterone in human pregnancy. *Am J Obstet Gynecol*. 1973;117(7):884–893. doi:10.1016/0002-9378(73)90057-4

Phenotyping in heart failure with preserved ejection fraction: A key to find effective treatment

Magdalena Maria Zawadzka^{A–D}, Marcin Grabowski^{E,F}, Agnieszka Kapłon-Cieślicka^{A–F}

1st Chair and Department of Cardiology, Medical University of Warsaw, Poland

A – research concept and design; B – collection and/or assembly of data; C – data analysis and interpretation; D – writing the article; E – critical revision of the article; F – final approval of the article

Advances in Clinical and Experimental Medicine, ISSN 1899–5276 (print), ISSN 2451–2680 (online)

Adv Clin Exp Med. 2022;31(10):1163–1172

Address for correspondence

Agnieszka Kapłon-Cieślicka
E-mail: agnieszka.kaplon@gmail.com

Funding sources

None declared

Conflict of interest

Dr. Zawadzka has nothing to disclose. Dr. Kapłon-Cieślicka reports personal fees from Boehringer Ingelheim, outside the submitted work. Prof. Grabowski reports personal fees from AstraZeneca and Boehringer Ingelheim, outside the submitted work.

Received on February 10, 2022

Reviewed on March 4, 2022

Accepted on May 4, 2022

Published online on May 18, 2022

Abstract

Heart failure with preserved ejection fraction (HFpEF) is an increasingly widespread medical condition, with excessive morbidity and mortality. Recently, for the first time in HFpEF, a reduction in the primary composite outcome of cardiovascular death or HF hospitalization was shown with empagliflozin. The failure of previous clinical trials in HFpEF might have resulted from suboptimal patient selection and inclusion of patients without “true” or clinically significant HFpEF. Another important factor might be the heterogeneity of HFpEF, and thus there is a growing interest in HFpEF phenotyping. This phenotyping can be based on clinical presentation (e.g., subtypes with predominant atrial fibrillation, obesity, pulmonary hypertension and right ventricular failure, coronary artery disease (CAD), or noncardiac comorbidities), but also on HFpEF etiology. Specific therapies, such as tafamidis in transthyretin-related amyloidosis (ATTR) or mavacamten in hypertrophic cardiomyopathy, have demonstrated their efficacy. However, pathomechanisms leading to the development of different phenotypes of HFpEF seem more complex and subtle. Machine learning and neural network models might help identify specific subgroups within the HFpEF population that either cluster patients with similar genetic, biochemical, echocardiographic or clinical characteristics, or respond similarly to a given treatment. Herein, we review different approaches to HFpEF phenotyping and present some distinct HFpEF subtypes.

Key words: diastolic dysfunction, phenotype, artificial intelligence, heart failure with preserved ejection fraction

Cite as

Zawadzka MM, Grabowski M, Kapłon-Cieślicka A. Phenotyping in heart failure with preserved ejection fraction: A key to find effective treatment. *Adv Clin Exp Med.* 2022;31(10):1163–1172. doi:10.17219/acem/149728

DOI

10.17219/acem/149728

Copyright

Copyright by Author(s)

This is an article distributed under the terms of the Creative Commons Attribution 3.0 Unported (CC BY 3.0) (<https://creativecommons.org/licenses/by/3.0/>)

Introduction

Heart failure with preserved ejection fraction (HFpEF) constitutes as much as half of all heart failure (HF) cases.¹ However, the diagnosis of HFpEF is challenging, and no simple, unified definition of HFpEF exists (Table 1).^{1–4} Furthermore, until recently, no treatment was available to improve outcomes in HFpEF – in contrast to HF with reduced EF (HFrEF). Even the latest 2021 guidelines of the European Society of Cardiology (ESC) provide only 2 recommendations regarding HFpEF therapy, i.e., diuretics for decongestion and symptomatic relief, and adequate treatment of comorbidities.⁵ These ESC guidelines were released during the 2021 ESC Congress. At the same congress, the results of the EMPEROR-Preserved trial were announced, showing, for the first time in HFpEF, a reduction in the primary composite outcome of cardiovascular death or HF hospitalization with empagliflozin compared to placebo.¹ Thus, empagliflozin becomes the first drug with proven benefits in HFpEF. The DELIVER trial, with results expected in 2022, will show whether another sodium-glucose co-transporter-2 (SGLT2) inhibitor, dapagliflozin, is also beneficial in HFpEF.⁶ The most recent 2022 American guidelines recommend SGLT2 inhibitors in the treatment of HFpEF.⁴ However, the fact that after years of extensive research there is potentially only 1 effective drug class for HFpEF (compared to the broad armamentarium of drugs for HFrEF) is somewhat disappointing. The failure

of previous clinical trials in HFpEF might be, at least in part, attributable to the heterogeneity of HFpEF and thus, there is a growing interest in HFpEF phenotyping.

Pathogenesis and phenotypes

Pathogenesis of HFpEF is complex and multifactorial, and involves not only left ventricle (LV) diastolic dysfunction (impaired relaxation and increased stiffness) due to LV hypertrophy in course of arterial hypertension, but also subtle impairment of LV systolic function, coronary and peripheral microvascular dysfunction, oxidative stress, myocardial fibrosis, metabolic disturbances, skeletal muscle pathology, and systemic low-grade inflammation mediated through tumor necrosis factor alpha (TNF- α), transforming growth factor beta (TGF- β) and interleukin 6 (IL-6).^{7,8} Microvascular dysfunction and inflammation precede symptomatic myocardial diastolic dysfunction.^{9–11} Those mechanisms seem to be mediated by micro ribonucleic acids (miRNA).^{5,12–14} The HFpEF hearts also have significantly higher calcium ion levels (Ca²⁺) than those with HFrEF.¹⁵ Furthermore, extracardiac comorbidities are extremely frequent in HFpEF, and may add to the development of the disease.

The multiplicity of pathomechanisms leading to HFpEF results in its heterogeneous manifestations, and might also provide an explanation for failure of most hitherto

Table 1. Diagnosis of HFpEF and recommended HFpEF treatment in European and American guidelines and consensus documents

Guidelines/consensus documents	HFpEF diagnostic criteria	HFpEF treatment
AHA/ACC/HFSA 2022 guidelines ⁴	LVEF \geq 50% + symptoms \pm signs + evidence of spontaneous or provokable increased LV filling pressures (e.g., elevated NPs, noninvasive and invasive hemodynamic measurement)	# diuretics for symptom control (strong recommendation) [§] SGLT2i & ARNI, MRA, ARB
ESC 2021 guidelines ¹	LVEF \geq 50% + symptoms \pm signs + objective evidence of cardiac structural and/or functional abnormalities consistent with the presence of LV diastolic dysfunction/raised LV filling pressures, including elevated NPs*, concentric LVH, left atrial enlargement*, increased E/e' ratio and/or elevated estimated systolic pulmonary artery pressure	# diuretics for symptom control (class I recommendation) # treatment of etiologies and CV and non-CV comorbidities (class I recommendation)
HFA-PEFF score 2019 ²	HFpEF diagnosis in a symptomatic patient with preserved LVEF: 5–6 points in the HFA-PEFF score 0–2 points in each of the 3 domains: 1) functional (reduced e' velocity, increased E/e' ratio, elevated estimated systolic pulmonary artery pressure, reduced GLS); 2) morphological (left atrial enlargement*, concentric LVH); 3) biochemical (elevated NPs*).	N/A
ASE/EACVI diagnostic algorithm 2016 ³	Echocardiographic diagnosis of diastolic dysfunction (not overt HFpEF) in a patient with LVEF \geq 50% – over half of the following criteria positive: 1) reduced e' velocity; 2) increased E/e' ratio; 3) left atrial enlargement; 4) elevated estimated systolic pulmonary artery pressure.	N/A

* cutoffs based on presence or absence of atrial fibrillation; # – therapies with strong or class I recommendation; § – moderate recommendation;

& – weak recommendation. ACC – American College of Cardiology; AHA – American Heart Association; ARB – angiotensin receptor blocker;

ARNI – angiotensin receptor-nephtrilysin inhibitor; ASE – American Society of Echocardiography; CV – cardiovascular; EACVI – European Association of Cardiovascular Imaging; ESC – European Society of Cardiology; GLS – global longitudinal strain; HFA – Heart Failure Association; HFpEF – heart failure with preserved ejection fraction; HFSA – Heart Failure Society of America; LVH – left ventricular hypertrophy; LVEF – left ventricular ejection fraction; MRA – mineralocorticoid receptor antagonist; NPs – natriuretic peptides; N/A – not applicable; SGLT2i – sodium-glucose co-transporter-2 inhibitor.

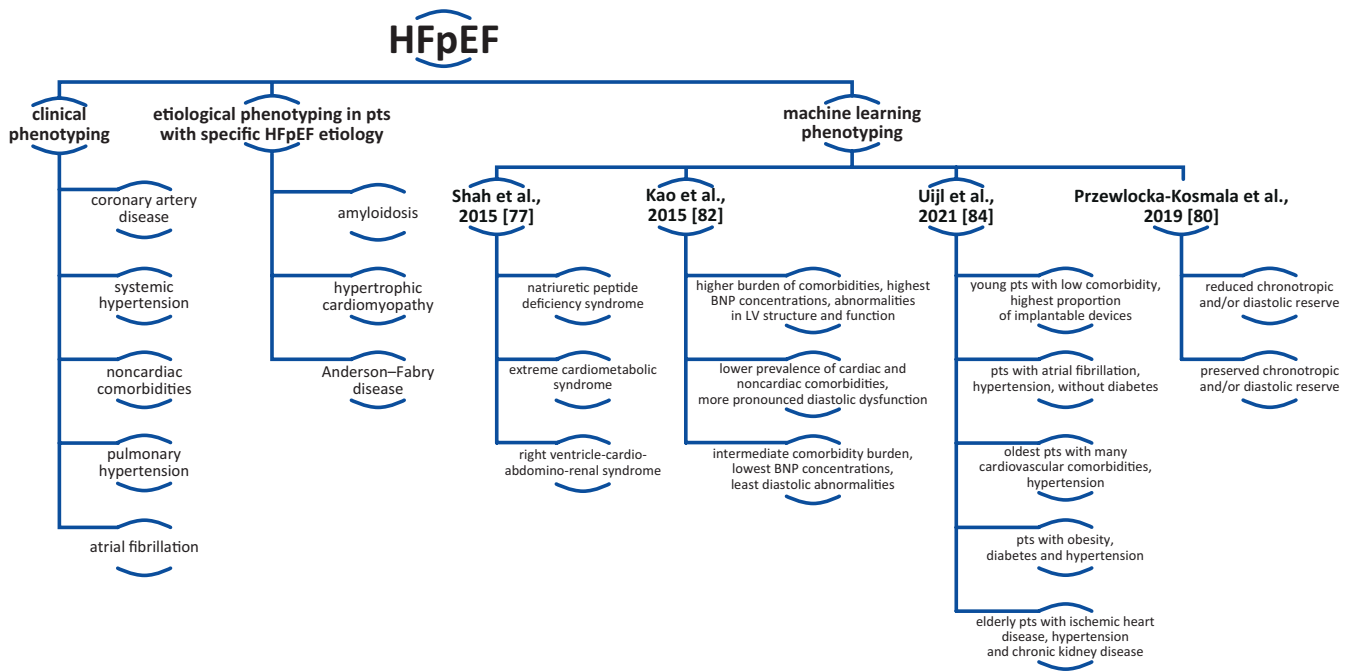


Fig. 1. Phenotyping of heart failure with preserved ejection fraction (HFpEF)
BNP – B-type natriuretic peptide; LV – left ventricle; pts – patients.

HFpEF trials. Appropriate phenotyping of HFpEF might help to guide its treatment.¹⁶ Such phenotyping might be based on clinical presentation, etiology, but also phenotyping with the help of machine learning and artificial intelligence (Fig. 1).

Clinical phenotyping

The HFpEF is characterized by polymorbidity, and in a single HFpEF patient, different cardiac and noncardiac diseases usually coexist. Still, distinct clinical phenotypes can be identified based on the domination of a given pathology and clinical presentation (Table 2).^{15,17–22}

Systemic hypertension

Arterial hypertension, especially long-standing and untreated or poorly controlled, leads to arterial stiffness, LV hypertrophy due to increased afterload, and multiorgan inflammatory response. As such, hypertension plays a crucial role in HFpEF pathogenesis and should be controlled from the early onset, as normalization of blood pressure prevents structural changes in myocardium and blood vessels, and improves outcomes.^{23–25} The landmark Antihypertensive Lipid-Lowering Treatment to Prevent Heart Attack Trial (ALL-HAT) showed that well-controlled hypertension reduces hospitalizations and the incidence of new-onset HFpEF.²⁶ In patients with symptomatic HFpEF and uncontrolled hypertension, adequate hypotensive treatment, including a diuretic, results in relief of dyspnea and decongestion.²⁷

Pulmonary hypertension

Pulmonary hypertension (PH) can occur in the majority of HFpEF patients at rest, and even more so with exercise.^{28–30} Pulmonary artery endothelial dysfunction was reported in an animal model of HFpEF with coexisting normal aortic endothelial function and intracardiac pressures.³¹ This suggests that pulmonary vascular endothelial dysfunction might precede the onset of systemic endothelial dysfunction, explaining the observed high prevalence of PH in HFpEF. Normally, pulmonary arteries are not subjected to high pressures, in contrast to systemic arteries. Therefore, pulmonary circulation is more prone to oxidative stress and inflammatory reaction in response to increased pressures. In obese hypertensive rats with HFpEF, in which vascular endothelial growth factor (VEGF) receptors were blocked, oral nitrites prevented the development of new-onset PH. However, they did not reverse the already preexisting PH.^{32–34} Patients with HFpEF and PH may develop right ventricular dilation and dysfunction, tricuspid regurgitation, and, ultimately, symptoms of right ventricular HF, which may dominate the clinical presentation of those patients.

Atrial fibrillation

Atrial fibrillation (AF) can cause HF symptoms such as dyspnea and impaired exercise capacity, but also lead to the development of tachycardia-induced cardiomyopathy and HFpEF.¹ On the other hand, AF often develops in patients with HF, as a consequence of elevated left

Table 2. Key concepts and therapies in different clinical phenotypes of HFpEF

Clinical phenotype	Key concepts	Therapy
Ischemic heart disease	In HFpEF pts, angina is often caused by CMD. The CMD affects arterioles and capillaries (<200 µm in diameter). ³⁹ Impaired coronary flow reserve in the absence of obstructive CAD is present in up to 3/4 of HFpEF pts. In pts with the metabolic syndrome, systemic inflammation and oxidative stress cause endothelial dysfunction with decreased nitric oxide availability, leading to both CMD with subendocardial ischemia, and impaired lusitropy – hallmarks of CMD-HFpEF phenotype.	So far, studies targeting the cGMP pathway (e.g., the RELAX trial with sildenafil ¹⁹) did not meet their primary endpoints in HFpEF. New studies targeting the nitric oxide-cGMP pathway are warranted.
	Obstructive CAD (atherosclerosis of epicardial coronary arteries).	Statins, antiplatelets, ACE inhibitors, β-blockers and other antianginal drugs; coronary revascularization if needed.
Systemic hypertension	Systemic hypertension plays a central role in HFpEF pathogenesis through the development of concentric hypertrophy and diastolic dysfunction. The ALLHAT showed that well-controlled hypertension reduces HF hospitalizations and new HFpEF cases.	Antihypertensive treatment decreases dyspnea and congestion.
Noncardiac comorbidities	Both a study by Kapłon-Cieślicka et al. and an analysis by Chioncel et al. recorded that: 1) almost 1/2 pts with HFpEF have T2DM and >1/2 are obese; 2) approx. 1/4 suffer from CKD; 3) 1/5 of pts are recorded to have COPD; 4) circa 5% of all pts suffer from sleep apnea as well. ^{21,22}	Treatment of concomitant noncardiac diseases (in particular T2DM, obesity, pulmonary diseases) remains the mainstay of HFpEF therapy.
Pulmonary hypertension	Pulmonary vascular endothelial dysfunction precedes systemic endothelial dysfunction, explaining high prevalence of PH in HFpEF. In obese hypertensive rats with HFpEF with blocked VEGF receptors, oral nitrates prevented PH.	So far, treatment with sildenafil was ineffective in HFpEF-PH. ²⁰
Atrial fibrillation	The prevalence of AF in HFpEF is estimated at 45–60% and is higher than in HFpEF.	Oral anticoagulation in all HFpEF pts with AF. Rate compared to rhythm control (in HFpEF, there is a paucity of data regarding advantage of any strategy (rate compared to rhythm control), or any drug class (e.g., β-blockers) for rate control). ¹

ACE – angiotensin-converting enzyme; AF – atrial fibrillation; ALLHAT – Antihypertensive Lipid-Lowering Treatment to Prevent Heart Attack Trial; cGMP – cyclic guanosine monophosphate; CMD – coronary microvascular disease; cGMP – cyclic guanosine monophosphate; COPD – chronic kidney pulmonary disease; CAD – coronary artery disease; CKD – chronic kidney disease; VEGF – vascular endothelial growth factor; T2DM – type 2 diabetes mellitus; HFpEF – heart failure with preserved ejection fraction; HFrEF – heart failure with reduced ejection fraction; PH – pulmonary hypertension; pts – patients.

atrial pressure. The prevalence of AF in HFpEF is estimated at 40–65%,³⁵ and is higher than in HFrEF,³⁶ which might be attributable to the fact that HFpEF not only leads to an increase in left atrial pressure, but also shares common risk factors with AF (hypertension, obesity, metabolic syndrome).³⁷ In a patient with HF symptoms, AF and preserved EF, it might be difficult to both diagnose HFpEF (given left atrial dilation and elevation of natriuretic peptides in AF even in the absence of HF) and determine whether the symptoms are attributable to AF or HFpEF. Whether patients with HFpEF and concomitant AF would benefit from rhythm control strategy remains to be determined. Even in patients with preserved EF, AF may lead to the development of functional mitral regurgitation, related to atrial and annular dilation (so-called functional atrial mitral regurgitation). On the other hand, severe primary mitral regurgitation often results in AF. Recently, the Atherosclerosis Risk in Communities (ARIC) study showed that in the setting of HFpEF with concomitant significant mitral regurgitation, AF is associated with increased mortality.³⁸

Coronary artery disease

Although coronary artery disease (CAD), especially in patients after myocardial infarction (MI), is commonly

related to HFrEF, it may also lead to HFpEF. In a substantial proportion of HFpEF patients, angina is caused by the dysfunction of coronary microcirculation rather than by the disease of the epicardial coronary arteries.^{39,40} This is often referred to as ischemia with no obstructive coronary artery disease (INOCA).⁴¹ Coronary microvascular dysfunction (CMD) can account for up to 2/3 of all ischemic clinical conditions with chest pain symptoms but without atherosclerosis in coronary arteries.⁴¹ The CMD cannot be diagnosed with classic computed tomography coronary angiography (CTCA) or invasive coronary angiography, as it mainly affects arterioles and capillaries (<200 µm in diameter).⁴² Nondirect invasive methods for CMD diagnosis include the assessment of 1) delayed flow of contrast, 2) coronary flow reserve and 3) index of microvascular resistance, all measured during invasive coronary angiography.

Noncardiac comorbidities

Almost half of patients with HFpEF have type 2 diabetes mellitus (T2DM) and over half of them are obese.⁴³ These proportions have grown in the last decade. Recently, a new group of DM drugs, SGLT2 inhibitors, has been investigated in HF, including HFpEF, showing an improvement

in prognosis even in non-DM patients.^{43–48} Apart from obesity, metabolic syndrome and DM, other common noncardiac comorbidities in HFpEF include chronic kidney disease (CKD), chronic obstructive pulmonary disease (COPD), obstructive sleep apnea, and anemia. The treatment of concomitant diseases remains the mainstay of HFpEF therapy.^{8,10}

Etiological phenotyping

While in most patients with HFpEF, its development is multifactorial and related to older age, hypertension, obesity, metabolic syndrome, T2DM, and other noncardiac comorbidities, in some, HFpEF occurs due to a specific condition which, in some cases, may be a subject to a targeted treatment (Table 3). This has been recently referred to as “secondary” HFpEF. Important causes of such “secondary” HFpEF include restrictive and infiltrative cardiomyopathies (with amyloidosis being the most common), as well as hypertrophic cardiomyopathy, but also other conditions with HF symptoms and preserved EF but with no permanent damage to the left ventricular myocardium (such as mitral stenosis, pericardial diseases, acute tachyarrhythmias, or high-output HF in patients with severe anemia, fever/sepsis, thyrotoxicosis, or large arteriovenous fistulas).⁴⁹ Below, we decided to focus on those “secondary” HFpEF causes that are related to permanent diastolic dysfunction of the LV.

Amyloidosis

Amyloidosis in myocardium is in most cases caused by immunoglobulin light chain amyloid (AL) or transthyretin amyloid (TTR). The latter causes transthyretin-related

amyloidosis (ATTR), which may be of particular interest since specific treatment of cardiac ATTR has been recently introduced. Amyloidosis is an increasing cause of HFpEF, might constitute up to 15% of HFpEF cases, and should be excluded during differential diagnosis of HF, especially in elderly patients without typical risk factors for HFpEF (hypertension, obesity, T2DM) and in those with amyloidosis “red flags”.^{50,51} The ATTR may be either hereditary – caused by autosomal dominant mutations in the TTR gene, or acquired – due to the aggregation of wild-type transthyretin. Amyloid is deposited in the myocardium and/or peripheral nervous system. The most common cardiac symptoms are dyspnea, angina, edema, and syncope.^{50–53} Noncardiac manifestations, often referred to as “red flags”, include peripheral neuropathy, neuropathic pain, numbness, and loss of muscle strength in the lower extremities. Gastrointestinal symptoms such as diarrhea and weight loss can be a consequence of autonomic neuropathy. Other autonomic manifestations include erectile dysfunction, orthostatic hypotension and neurogenic bladder.^{50,53–55} Biopsy used to be required for the diagnosis of amyloidosis as a gold standard. Congo red or Direct Fast Scarlet 4BS staining binds to amyloid fibrils and creates characteristic apple-green birefringence under polarized light microscopy. However, genetic testing and innovative imaging techniques are becoming vital in the diagnostic process.^{53,56–59} Echocardiography is used as the first diagnostic step, and some indicators, such as 1) thickened LV wall with granular sparkling appearance, with concomitant thickening of the atrial septum; 2) free right ventricle (RV) wall and valves; 3) atrial enlargement; 4) restrictive LV filling pattern; 5) pericardial effusion, and; 6) reduced LV strain with relative apical sparing pattern might hint towards amyloidosis.^{56,58,59} Compared to a similar degree of LV wall thickening due to hypertrophy, the QRS amplitude is smaller, and natriuretic

Table 3. Key concepts and recommended therapies for proposed etiological phenotypes of HFpEF

Etiological phenotype	Key concepts	Recommended therapy
Amyloidosis	Amyloidosis might constitute up to 15% of HFpEF cases.	Tafamidis is recommended in pts with ATTR (hereditary or wild-type) with cardiac involvement and NYHA class I or II symptoms to improve prognosis (class I recommendation) ¹ ; maintenance of euvoolemia; diuretics if needed (with caution due to orthostatic hypotension).
Hypertrophic cardiomyopathy	LVH leads to diastolic dysfunction. LVOTO in HOCM additionally impairs hemodynamics. LVOTO occurs due to asymmetric LVH, SAM of the mitral leaflet and dyssynchrony. Apart from those anatomic macroscopic abnormalities, functional changes at the level of the sarcomere (an increased number of actin-myosin crossbridges) are also responsible for LVOTO.	In symptomatic HOCM: – β -blockers/verapamil/diltiazem \pm disopyramide; – septal reduction therapy; – sequential pacing; – as per ESC guidelines. ⁶³ Mavacamten is a new drug that decreases the number of actin-myosin crossbridges leading to an improvement in LVOTO and symptoms. ^{68–70}
Anderson–Fabry disease	Thickening of LV wall in AFD leads to restrictive cardiomyopathy, and vascular dysfunction – to CAD.	Enzyme replacement therapy; chaperone therapy (for pts with <i>GLA1</i> gene mutation).

AFD – Anderson–Fabry disease; ATTR – transthyretin-related amyloidosis; CAD – coronary artery disease; ESC – European Society of Cardiology; HFpEF – heart failure with preserved ejection fraction; HOCM – hypertrophic obstructive cardiomyopathy; LV – left ventricle; LVH – left ventricular hypertrophy; LVOTO – left ventricular outflow tract obstruction; NYHA – New York Heart Association; pts – patients; SAM – systolic anterior motion.

peptides concentrations are higher in amyloidosis. Cardiac magnetic resonance is indicated in patients suspected of cardiac amyloidosis. For the diagnosis of AL amyloidosis, laboratory tests for the detection of monoclonal light chains in serum and/or urine are performed. In ATTR, nuclear imaging techniques using technetium-99m (^{99m}Tc) provide relatively high sensitivity (>90%) and specificity (86%), yet are noninvasive in comparison to classic biopsy and histopathological assessment. High uptake of ^{99m}Tc in the cardiac muscle area in comparison to bones and other peripheral structures suggests ATTR cardiomyopathy and might substitute as a diagnostic method in the future.^{50,56,58,59} Genetic testing can prove hereditary ATTR. Recently, an oral medication, tafamidis, previously used for the treatment of ATTR neuropathy, has proven effective in the treatment of ATTR cardiomyopathy. Tafamidis binds to transthyretin, preventing tetramer dissociation and amyloid genesis. Studies such as ATTR-ACT show that tafamidis is a safe oral medication that reduces mortality and morbidity, and improves New York Heart Association (NYHA) class in patients with HF caused by both hereditary and wild-type ATTR.^{60–62} Thus, the new 2021 ESC guidelines on HF, recommend treatment with tafamidis in patients with ATTR (hereditary or wild-type) with cardiac involvement and NYHA class I or II symptoms to improve prognosis (class I recommendation).¹⁰

Hypertrophic cardiomyopathy

Hypertrophic cardiomyopathy (HCM) is the most common genetic heart disease. It affects people of all ages and with different comorbidities.⁶³ Its phenotypic expression ranges from mild symptoms and almost standard life-length expectancy up to sudden cardiac death (SCD) in seemingly healthy young people.^{64–66} Hypertrophic cardiomyopathy is characterized by LV muscle hypertrophy which is not secondary to increased afterload (i.e., with no identifiable cause). Histopathological findings are myocytes hypertrophy, disarray and fibrosis. Common symptoms are dyspnea at rest, ventricular tachycardia and syncope. The first symptom may be SCD in young adults and adolescents.^{64,67,68} In patients with symptomatic hypertrophic obstructive cardiomyopathy (HOCM), hitherto pharmacotherapy, based on β -blockers or non-dihydropyridine calcium channel blockers with or without disopyramide, is often inadequate, poorly tolerated and not disease-specific.^{67,68} Mavacamten is a cardiac myosin inhibitor. In HOCM, diastolic dysfunction and hypercontractility with left ventricular outflow tract obstruction (LVOTO) result not only from anatomic, macroscopic abnormalities (asymmetric left ventricular hypertrophy), but also from functional changes at the level of sarcomeres: an increased number of actin-myosin cross-bridges. Mavacamten is a cutting-edge allosteric inhibitor of cardiac-specific myosin adenosine triphosphatase,

reducing the number of actin-myosin crossbridges. Its use in HOCM results in normalized contractility, improved relaxation and improved myocardial energetics.^{69–73} In the EXPLORER-HCM trial, in HOCM, mavacamten, compared to placebo, alleviated the symptoms and exercise capacity, reduced LVOTO and natriuretic peptides, and consequently received a “breakthrough therapy designation” from the American Food and Drug Administration (FDA).^{69,70} The VALOR-HCM trial, whose results were recently announced during the American College of Cardiology’s 71st Scientific Sessions, showed that mavacamten alleviated the symptoms and significantly reduced the need for septal reduction therapy among symptomatic patients with HOCM who were on maximally tolerated medical therapy.

Anderson–Fabry disease

Anderson–Fabry disease (AFD) is a genetic storage disorder. It is caused by X-linked mutations in the *GLA* gene, resulting in deficiency of the enzyme alpha-galactosidase A, which should metabolize neutral glycosphingolipids.^{74,75} The increased amount of those molecules leads to their accumulation in various tissues including vascular endothelium, kidneys, heart, eyes, skin, and nervous system.⁷⁶ The AFD causes thickening of LV wall, which leads to restrictive cardiomyopathy and vascular dysfunction, in consequence leading to CAD. Common symptoms and complications include HF symptoms, angina, arrhythmias, chronotropic incompetence, and SCD. Early AFD diagnosis enables timely introduction of enzyme replacement therapy. In recent years, a new form of treatment was introduced – chaperone therapy. However, it is reserved only for patients with *GLA1* gene mutation.⁷⁴

Machine learning phenotyping

Artificial intelligence, machine learning and the use of complex algorithms are more and more frequently applied in medicine. Recently, new phenotypes have emerged in HFpEF using machine learning to identify specific subgroups, and helping to stratify risks and predict outcomes (Table 4).

The study using phenomapping led by Shah et al. has collected data from 420 prospectively enrolled, symptomatic HFpEF patients, including: 1) demographic and clinical characteristics; 2) blood laboratory measurements; 3) electrocardiographic (ECG) features; and 4) echocardiographic measurements.⁷⁷ Data were systematically inserted into a specially designed computer algorithm called support vector machines (SVM), which identifies a separation boundary between classes of interest in a much higher dimensional feature space. The SVM is a robust nonlinear algorithm that can be used for classification or regression.⁷⁸

Table 4. Key concepts in machine-learning phenotyping of HFpEF

Study name	Phenotype	Key concepts
Shah et al. 2015 ⁷⁷	natriuretic peptide deficiency syndrome	This phenogroup had the least visible electric and myocardial remodeling, although 65% of pts had at least grade 2 diastolic dysfunction. In long-term follow-up, pts had the lowest risk of cardiovascular hospitalization or death.
	extreme cardiometabolic syndrome	This phenogroup pts with comorbidities (i.e., obesity, T2DM and obstructive sleep apnea) had the highest fasting glucose levels. Patients had the most impaired LV relaxation (lowest e' velocity) on echocardiography and the highest pulmonary capillary wedge pressure and pulmonary vascular resistance on invasive hemodynamic testing.
	right ventricle-cardio-abdomino-renal syndrome	This phenogroup consisted of the oldest pts who were most likely to have CKD (highest serum creatinine concentration and the lowest GFR). They had the most severe electric and myocardial remodeling with the longest QRS duration, highest LV mass index, worst RV function, and highest BNP concentrations. This phenogroup also had the highest mortality risk measured using MAGGIC risk score. In long-term follow-up, phenogroup 3 had the highest risk of cardiovascular hospitalization or death.
Segar et al. 2019 ⁸²	higher burden of comorbidities, highest BNP concentrations, abnormalities in LV structure and function	Phenogroups from the TOPCAT-subanalysis did not differ with respect to age. Phenogroup 1 had higher risk for all adverse clinical events, including all-cause death and HF hospitalization.
	lower prevalence of cardiac and noncardiac comorbidities, more pronounced diastolic dysfunction	Phenogroup 2 had higher risk of HF hospitalization but lower risk of atherosclerotic event (MI, stroke or cardiovascular death), and comparable risk of death. Patients had lower LV mass and intermediate burden of diastolic function abnormalities compared with other groups.
	intermediate comorbidity burden, lowest BNP concentrations, least diastolic abnormalities	Patients in phenogroup 3 had the lowest E/e' ratio on echocardiography.
Uijl et al. 2021 ⁸⁴	young pts with low comorbidity, highest proportion of implantable devices	This cluster had the best prognosis. Patients had the lowest BNP levels and the lowest number of zpts had NYHA class III–IV.
	pts with AF, hypertension, without T2DM	Patients in this cluster most often had implantable devices, AF prevalence and were most likely to use RAS inhibitors, β -blockers and diuretics.
	oldest pts with many cardiovascular comorbidities, hypertension	Together with cluster 2, pts in cluster 3 were most likely to use RAS inhibitors, β -blockers and diuretics. The majority of measured parameters oscillated on medium levels.
	pts with obesity, T2DM and hypertension	Patients had higher systolic blood pressure levels and the highest prevalence of DM.
	elderly pts with ischemic heart disease, hypertension and CKD	This cluster had the worst prognosis. Patients were often prescribed diuretics. Patients had the highest BNP levels and most pts had NYHA class III–IV.
Przewłocka-Kosmala et al. 2019 ⁸⁰	reduced chronotropic and/or diastolic reserve	Hierarchical clustering was used on continuous variables obtained from resting and post-exercise echocardiography. Patients in this subgroup had a higher risk of 1) HF hospitalization and 2) cardiovascular hospitalization or death during a 2-year follow-up.
	preserved chronotropic and/or diastolic reserve	Patients in this subgroup had a lower risk of 1) HF hospitalization and 2) cardiovascular hospitalization or death during a 2-year follow-up.

AF – atrial fibrillation; BNP – B-type natriuretic peptide; CKD – chronic kidney disease; T2DM – type 2 diabetes mellitus; GFR – glomerular filtration rate; LV – left ventricle; RV – right ventricle; HF – heart failure; MI – myocardial infarction; HFpEF – heart failure with preserved ejection fraction; NYHA – New York Heart Association; pts – patients; RAS – renin-angiotensin system; TOPCAT – Treatment of Preserved Cardiac Function Heart Failure With an Aldosterone Antagonist.

A total of 67 phenotypical variables were found, which then scientists blinded to the agenda of this trial merged into bigger subgroups using hierarchical clustering methods. That led to the extraction of 3 main phenogroups using Gaussian distribution for values calculated with the program. The final cohort included 397 HFpEF patients (mean age 65 years, 62% female) with complete data. Of those, 216 patients had additional data from invasive hemodynamic testing. Phenogroup 1 included younger HFpEF patients with the lowest B-type natriuretic peptide (BNP) levels. This HFpEF phenogroup had the least visible electric and myocardial remodeling, although 65% had at least grade 2 diastolic dysfunction. Phenogroup 2 included HFpEF patients with the highest burden of HF-associated comorbidities, such as obesity, T2DM and obstructive sleep

apnea, and the highest fasting glucose levels. This HFpEF phenogroup was characterized by the most impaired LV relaxation on echocardiography (lowest e' velocity) and the highest pulmonary capillary wedge pressure and pulmonary vascular resistance on invasive hemodynamic testing. Phenogroup 3 included the oldest HFpEF patients who were most likely to have CKD (with the highest serum creatinine concentration and the lowest estimated glomerular filtration rate (eGFR) compared to the other 2 phenogroups). Phenogroup 3 had the most severe electric and myocardial remodeling, with the longest QRS duration, highest LV mass index, highest E/e' ratio, worst RV function, and highest BNP concentrations. This phenogroup also had the highest mortality risk using the Meta-Analysis Global Group in Chronic Heart Failure (MAGGIC) risk

score.⁷⁹ In long-term follow-up, HFpEF phenogroup 1 had the lowest, and phenogroup 3 – the highest risk of cardiovascular hospitalization or death.⁷⁸ These results were then replicated in a prospective validation cohort consisting of 107 HFpEF patients.⁷⁸

In a study by Przewlocka-Kosmala et al., hierarchical clustering was used on continuous variables obtained from resting and post-exercise echocardiography in 177 patients with HFpEF.⁸⁰ This led to the identification of a subgroup of HFpEF patients with impaired chronotropic and/or diastolic reserve who had a higher risk of 1) HF hospitalization and 2) cardiovascular hospitalization or death during a 2-year follow-up.

A different approach was used by Kao et al., who applied latent class analysis allowing to include not only continuous, but also categorical variables.⁸¹ In 4113 HFpEF patients enrolled in the Irbesartan in Heart Failure with Preserved Ejection Fraction Study (I-PRESERVE), 6 subgroups were identified with significant differences in an event-free survival. Observations were then validated in 3203 patients from the Candesartan in Heart Failure: Assessment of Reduction in Mortality and Morbidity (CHARM)-Preserved study. A different type of phenomapping analysis based on a dataset from another randomized controlled trial, Treatment of Preserved Cardiac Function Heart Failure with an Aldosterone Antagonist (TOPCAT), was performed by Segar et al.⁸² Using unsupervised cluster analysis on 61 phenotypic variables in 654 HFpEF patients (TOPCAT participants enrolled in the Americas, who had available echocardiographic data), 3 mutually exclusive phenogroups were identified: phenogroup 1 had higher burden of comorbidities, the highest BNP concentrations, and abnormalities in LV structure and function; phenogroup 2 had lower prevalence of cardiac and noncardiac comorbidities but more pronounced diastolic dysfunction; and phenogroup 3 had intermediate comorbidity burden, the lowest BNP concentrations, and the least diastolic abnormalities (including the lowest E/e' ratio) on echocardiography.⁸³ Interestingly, in contrast to the previous study by Shah et al., the 3 phenogroups from the TOPCAT subanalysis did not differ with respect to age.⁷⁸ In comparison to phenogroup 3, phenogroup 1 had higher risk for all adverse clinical events including all-cause death and HF hospitalization, and phenogroup 2 had higher risk of HF hospitalization but a lower risk of atherosclerotic event (MI, stroke or cardiovascular death), and a comparable risk of death.⁸²

Other distinct HFpEF phenogroups were identified in different HFpEF cohorts depending on the type of analysis used.^{84,85} In 6909 HFpEF patients from the Swedish Heart Failure Registry (SwedeHF), latent class analysis identified 5 phenogroups: cluster 1 (10% of patients) – young patients with a low comorbidity burden and the highest proportion of implantable devices; cluster 2 (30%) – patients with AF and hypertension, without T2DM; cluster 3 (25%) – the oldest patients with many

cardiovascular comorbidities and hypertension; cluster 4 (15%) – patients with obesity, T2DM and hypertension; and cluster 5 (20%) – elderly patients with ischemic heart disease, hypertension and CKD, who were most often prescribed diuretics. Those clusters were externally validated in a cohort of 2153 patients from the Chronic Heart Failure ESC-guideline based Cardiology practice Quality project (CHECK-HF) registry. Patients in cluster 1 had the most favorable prognosis, and those in clusters 3 and 5 – the worst prognosis.⁸⁴

Conclusions

Recent studies have demonstrated the importance of identifying subgroups among HFpEF patients. Phenotyping based on HFpEF etiology (such as amyloidosis or hypertrophic cardiomyopathy) may guide the choice of specific treatment. Clinical HFpEF phenotyping (with division into patient subgroups with prevailing, e.g., hypertension, noncardiac comorbidities, CAD, or AF) can also point towards preferred therapies. In contrast to that “traditional”, clinical phenotyping, phenomapping based on machine learning enables clustering of common clinical and/or laboratory characteristics, leading to the identification of less obvious or “predictable” HFpEF subgroups. These subgroups were shown to have different prognosis. In future, machine learning phenotyping might change our approach to HFpEF treatment.

ORCID iDs

Magdalena Maria Zawadzka  <https://orcid.org/0000-0001-7581-2781>
 Marcin Grabowski  <https://orcid.org/0000-0003-3306-0301>
 Agnieszka Kapłon-Cieślicka  <https://orcid.org/0000-0003-2020-3027>

References

- McDonagh TA, Metra M, Adamo M, et al. 2021 ESC Guidelines for the diagnosis and treatment of acute and chronic heart failure. *Eur Heart J*. 2021;42(36):3599–3726. doi:10.1093/eurheartj/ehab368
- Pieske B, Tschöpe C, de Boer RA, et al. How to diagnose heart failure with preserved ejection fraction: The HFA-PEFF diagnostic algorithm. A consensus recommendation from the Heart Failure Association (HFA) of the European Society of Cardiology (ESC). *Eur Heart J*. 2019;40(40):3297–3317. doi:10.1093/eurheartj/ehz641
- Nagueh SF, Smiseth OA, Appleton CP, et al. Recommendations for the evaluation of left ventricular diastolic function by echocardiography: An update from the American Society of Echocardiography and the European Association of Cardiovascular Imaging. *J Am Soc Echocardiogr*. 2016;29(4):277–314. doi:10.1016/j.echo.2016.01.011
- Heidenreich PA, Bozkurt B, Aguilar D, et al. 2022 AHA/ACC/HFSA Guideline for the Management of Heart Failure: Executive summary. A report of the American College of Cardiology/American Heart Association Joint Committee on Clinical Practice Guidelines. *Circulation*. 2022;145(18):e876–e894. doi:10.1161/CIR.0000000000001062
- Nair N, Gupta S, Collier IX, Gongora E, Vijayaraghavan K. Can micro-RNAs emerge as biomarkers in distinguishing HFpEF versus HFrEF? *Int J Cardiol*. 2014;175(3):395–399. doi:10.1016/j.ijcard.2014.06.027
- Solomon SD, Boer RA, DeMets D, et al. Dapagliflozin in heart failure with preserved and mildly reduced ejection fraction: Rationale and design of the DELIVER trial. *Eur J Heart Fail*. 2021;23(7):1217–1225. doi:10.1002/ejhf.2249
- Mayet J. Cardiac and vascular pathophysiology in hypertension. *Heart*. 2003;89(9):1104–1109. doi:10.1136/heart.89.9.1104

8. Duca F, Zotter-Tufaro C, Kammerlander AA, et al. Gender-related differences in heart failure with preserved ejection fraction. *Sci Rep*. 2018;8(1):1080. doi:10.1038/s41598-018-19507-7
9. Paulus WJ, Tschöpe C. A novel paradigm for heart failure with preserved ejection fraction: Comorbidities drive myocardial dysfunction and remodeling through coronary microvascular endothelial inflammation. *J Am Coll Cardiol*. 2013;62(4):263–271. doi:10.1016/j.jacc.2013.02.092
10. Westermann D, Lindner D, Kasner M, et al. Cardiac inflammation contributes to changes in the extracellular matrix in patients with heart failure and normal ejection fraction. *Circ Heart Fail*. 2011;4(1):44–52. doi:10.1161/CIRCHEARTFAILURE.109.931451
11. van Heerebeek L, Hamdani N, Falcão-Pires I, et al. Low myocardial protein kinase G activity in heart failure with preserved ejection fraction. *Circulation*. 2012;126(7):830–839. doi:10.1161/CIRCULATIONAHA.111.076075
12. Rech M, Barandiarán Aizpurua A, van Empel V, van Bilsen M, Schroen B. Pathophysiological understanding of HFpEF: MicroRNAs as part of the puzzle. *Cardiovasc Res*. 2018;114(6):782–793. doi:10.1093/cvr/cvy049
13. van Empel V, Brunner-La Rocca HP. Inflammation in HFpEF: Key or circumstantial? *Int J Cardiol*. 2015;189:259–263. doi:10.1016/j.ijcard.2015.04.110
14. Su MYM, Lin LY, Tseng YHE, et al. CMR-verified diffuse myocardial fibrosis is associated with diastolic dysfunction in HFpEF. *JACC Cardiovasc Imaging*. 2014;7(10):991–997. doi:10.1016/j.jcmg.2014.04.022
15. Lewis GA, Schelbert EB, Williams SG, et al. Biological phenotypes of heart failure with preserved ejection fraction. *J Am Coll Cardiol*. 2017;70(17):2186–2200. doi:10.1016/j.jacc.2017.09.006
16. Donal E, L'officiel G, Kosmala W. Heart failure with preserved ejection fraction: Defining phenotypes. *J Cardiac Fail*. 2020;26(11):929–931. doi:10.1016/j.cardfail.2020.09.013
17. Samson R, Jaiswal A, Ennezat PV, Cassidy M, Le Jemtel TH. Clinical phenotypes in heart failure with preserved ejection fraction. *J Am Heart Assoc*. 2016;5(1):e002477. doi:10.1161/JAHA.115.002477
18. Shah SJ, Kitzman DW, Borlaug BA, et al. Phenotype-specific treatment of heart failure with preserved ejection fraction: A multiorgan roadmap. *Circulation*. 2016;134(1):73–90. doi:10.1161/CIRCULATIONAHA.116.021884
19. Redfield MM, Chen HH, Borlaug BA, et al. Effect of phosphodiesterase-5 inhibition on exercise capacity and clinical status in heart failure with preserved ejection fraction: A randomized clinical trial. *JAMA*. 2013;309(12):1268. doi:10.1001/jama.2013.2024
20. Hoendermis ES, Liu LCY, Hummel YM, et al. Effects of sildenafil on invasive haemodynamics and exercise capacity in heart failure patients with preserved ejection fraction and pulmonary hypertension: A randomized controlled trial. *Eur Heart J*. 2015;36(38):2565–2573. doi:10.1093/eurheartj/ehv336
21. Kapłon-Cieślicka A, Benson L, Chioncel O, et al. A comprehensive characterization of acute heart failure with preserved versus mildly reduced versus reduced ejection fraction: Insights from the ESC-HFA EORP Heart Failure Long-Term Registry. *Eur J Heart Fail*. 2022;24(2):335–350. doi:10.1002/ehjhf.2408
22. Chioncel O, Lainscak M, Seferovic PM, et al. Epidemiology and one-year outcomes in patients with chronic heart failure and preserved, mid-range and reduced ejection fraction: An analysis of the ESC Heart Failure Long-Term Registry. *Eur J Heart Fail*. 2017;19(12):1574–1585. doi:10.1002/ehjhf.813
23. Gu J, Fan YQ, Bian L, et al. Long-term prescription of beta-blocker delays the progression of heart failure with preserved ejection fraction in patients with hypertension: A retrospective observational cohort study. *Eur J Prev Cardiol*. 2016;23(13):1421–1428. doi:10.1177/2047487316636260
24. Kjeldsen SE, von Lueder TG, Smiseth OA, et al. Medical therapies for heart failure with preserved ejection fraction. *Hypertension*. 2020;75(1):23–32. doi:10.1161/HYPERTENSIONAHA.119.14057
25. Hummel SL, Seymour EM, Brook RD, et al. Low-sodium DASH diet improves diastolic function and ventricular-arterial coupling in hypertensive heart failure with preserved ejection fraction. *Circ Heart Fail*. 2013;6(6):1165–1171. doi:10.1161/CIRCHEARTFAILURE.113.000481
26. Davis BR, Kostis JB, Simpson LM, et al. Heart failure with preserved and reduced left ventricular ejection fraction in the antihypertensive and lipid-lowering treatment to prevent heart attack trial. *Circulation*. 2008;118(22):2259–2267. doi:10.1161/CIRCULATIONAHA.107.762229
27. Kosmala W, Przewlocka-Kosmala M, Marwick TH. Association of active and passive components of LV diastolic filling with exercise intolerance in heart failure with preserved ejection fraction: Mechanistic insights from spironolactone response. *JACC Cardiovasc Imaging*. 2019;12(5):784–794. doi:10.1016/j.jcmg.2017.10.007
28. Andersen MJ, Hwang SJ, Kane GC, et al. Enhanced pulmonary vasodilator reserve and abnormal right ventricular: Pulmonary artery coupling in heart failure with preserved ejection fraction. *Circ Heart Fail*. 2015;8(3):542–550. doi:10.1161/CIRCHEARTFAILURE.114.002114
29. Borlaug BA, Nishimura RA, Sorajja P, Lam CSP, Redfield MM. Exercise hemodynamics enhance diagnosis of early heart failure with preserved ejection fraction. *Circ Heart Fail*. 2010;3(5):588–595. doi:10.1161/CIRCHEARTFAILURE.109.930701
30. Mohammed SF, Hussain I, AbouEzzeddine OF, et al. Right ventricular function in heart failure with preserved ejection fraction: A community-based study. *Circulation*. 2014;130(25):2310–2320. doi:10.1161/CIRCULATIONAHA.113.008461
31. Nair N. Epidemiology and pathogenesis of heart failure with preserved ejection fraction. *Rev Cardiovasc Med*. 2020;21(4):531. doi:10.31083/j.rcm.2020.04.154
32. Driss AB, Devaux C, Henrion D, et al. Hemodynamic stresses induce endothelial dysfunction and remodeling of pulmonary artery in experimental compensated heart failure. *Circulation*. 2000;101(23):2764–2770. doi:10.1161/01.CIR.101.23.2764
33. Lai YC, Tabima DM, Dube JJ, et al. SIRT3-AMP-activated protein kinase activation by nitrite and metformin improves hyperglycemia and normalizes pulmonary hypertension associated with heart failure with preserved ejection fraction. *Circulation*. 2016;133(8):717–731. doi:10.1161/CIRCULATIONAHA.115.018935
34. Lam CSP, Brutsaert DL. Endothelial dysfunction: A pathophysiologic factor in heart failure with preserved ejection fraction. *J Am Coll Cardiol*. 2012;60(18):1787–1789. doi:10.1016/j.jacc.2012.08.004
35. Sartipy U, Dahlström U, Fu M, Lund LH. Atrial fibrillation in heart failure with preserved, mid-range, and reduced ejection fraction. *JACC Heart Fail*. 2017;5(8):565–574. doi:10.1016/j.jchf.2017.05.001
36. Oziarański K, Kapłon-Cieślicka A, Peller M, et al. Clinical characteristics and predictors of one-year outcome of heart failure patients with atrial fibrillation compared to heart failure patients in sinus rhythm. *Kardiol Pol*. 2016;74(3):251–261. doi:10.5603/KP.a2015.0180
37. Kapłon-Cieślicka A, Lund LH. Atrial fibrillation in heart failure with preserved ejection fraction: A risk marker, risk factor or confounder? *Heart*. 2020;106(24):1949–1949. doi:10.1136/heartjnl-2020-317978
38. Silvestre OM, Nadruz W, Querejeta Roca G, et al. Declining lung function and cardiovascular risk: The ARIC study. *J Am Coll Cardiol*. 2018;72(10):1109–1122. doi:10.1016/j.jacc.2018.06.049
39. Planer D, Mehran R, Ohman EM, et al. Prognosis of patients with non-ST-segment-elevation myocardial infarction and nonobstructive coronary artery disease: Propensity-matched analysis from the Acute Catheterization and Urgent Intervention Triage Strategy trial. *Circ Cardiovasc Interv*. 2014;7(3):285–293. doi:10.1161/CIRCINTERVENTIONS.113.000606
40. Bugiardini R, Manfrini O, De Ferrari GM. Unanswered questions for management of acute coronary syndrome: Risk stratification of patients with minimal disease or normal findings on coronary angiography. *Arch Intern Med*. 2006;166(13):1391. doi:10.1001/archinte.166.13.1391
41. Vancheri F, Longo G, Vancheri S, Henein M. Coronary microvascular dysfunction. *J Clin Med*. 2020;9(9):2880. doi:10.3390/jcm9092880
42. Sinha A, Rahman H, Webb A, Shah AM, Perera D. Untangling the pathophysiologic link between coronary microvascular dysfunction and heart failure with preserved ejection fraction. *Eur Heart J*. 2021;42(43):4431–4441. doi:10.1093/eurheartj/ehab653
43. Pieske B, Wachter R. Impact of diabetes and hypertension on the heart. *Curr Opin Cardiol*. 2008;23(4):340–349. doi:10.1097/HCO.0b013e3283031ab3
44. Packer M, Anker SD, Butler J, et al. Effect of empagliflozin on the clinical stability of patients with heart failure and a reduced ejection fraction: The EMPEROR-Reduced trial. *Circulation*. 2021;143(4):326–336. doi:10.1161/CIRCULATIONAHA.120.051783
45. Anker SD, Butler J, Filippatos G, et al. Effect of empagliflozin on cardiovascular and renal outcomes in patients with heart failure by baseline diabetes status: Results from the EMPEROR-Reduced trial. *Circulation*. 2021;143(4):337–349. doi:10.1161/CIRCULATIONAHA.120.051824

46. Volpe M, Gallo G. Cardiometabolic phenotype of heart failure with preserved ejection fraction as a target of sodium-glucose co-transporter 2 inhibitors and glucagon-like peptide receptor agonists. *Cardiovasc Res.* 2021;117(9):1992–1994. doi:10.1093/cvr/cvaa334
47. Hou YC, Zheng CM, Yen TH, Lu KC. Molecular mechanisms of SGLT2 inhibitor on cardiorenal protection. *Int J Mol Sci.* 2020;21(21):7833. doi:10.3390/ijms21217833
48. Williams DM, Nawaz A, Evans M. Renal outcomes in type 2 diabetes: A review of cardiovascular and renal outcome trials. *Diabetes Ther.* 2020;11(2):369–386. doi:10.1007/s13300-019-00747-3
49. Del Buono MG, Buckley L, Abbate A. Primary and secondary diastolic dysfunction in heart failure with preserved ejection fraction. *Am J Cardiol.* 2018;122(9):1578–1587. doi:10.1016/j.amjcard.2018.07.012
50. Kapoor M, Rossor AM, Laura M, Reilly MM. Clinical presentation, diagnosis and treatment of TTR amyloidosis. *J Neuromuscul Dis.* 2019;6(2):189–199. doi:10.3233/JND-180371
51. Manolis AS, Manolis AA, Manolis TA, Melita H. Cardiac amyloidosis: An underdiagnosed/underappreciated disease. *Eur J Intern Med.* 2019;67:1–13. doi:10.1016/j.ejim.2019.07.022
52. Alkhwam H, Patel D, Nguyen J, et al. Cardiac amyloidosis: Pathogenesis, clinical context, diagnosis and management options. *Acta Cardiol.* 2017;72(4):380–389. doi:10.1080/00015385.2017.1335034
53. Ando Y, Coelho T, Berk JL, et al. Guideline of transthyretin-related hereditary amyloidosis for clinicians. *Orphanet J Rare Dis.* 2013;8(1):31. doi:10.1186/1750-1172-8-31
54. Rapezzi C, Merlini G, Quarta CC, et al. Systemic cardiac amyloidoses: Disease profiles and clinical courses of the 3 main types. *Circulation.* 2009;120(13):1203–1212. doi:10.1161/CIRCULATIONAHA.108.843334
55. Shin SC, Robinson-Papp J. Amyloid neuropathies. *Mt Sinai J Med.* 2012;79(6):733–748. doi:10.1002/msj.21352
56. Gillmore JD, Maurer MS, Falk RH, et al. Nonbiopsy diagnosis of cardiac transthyretin amyloidosis. *Circulation.* 2016;133(24):2404–2412. doi:10.1161/CIRCULATIONAHA.116.021612
57. Gopal DM, Ruberg FL, Siddiqi OK. Impact of genetic testing in transthyretin (ATTR) cardiac amyloidosis. *Curr Heart Fail Rep.* 2019;16(5):180–188. doi:10.1007/s11897-019-00436-z
58. Perugini E, Guidalotti PL, Salvi F, et al. Noninvasive etiologic diagnosis of cardiac amyloidosis using ^{99m}Tc-3,3-diphosphono-1,2-propanodixcarboxylic acid scintigraphy. *J Am Coll Cardiol.* 2005;46(6):1076–1084. doi:10.1016/j.jacc.2005.05.073
59. Treglia G, Glaudemans AWJM, Bertagna F, et al. Diagnostic accuracy of bone scintigraphy in the assessment of cardiac transthyretin-related amyloidosis: A bivariate meta-analysis. *Eur J Nucl Med Mol Imaging.* 2018;45(11):1945–1955. doi:10.1007/s00259-018-4013-4
60. Damy T, Garcia-Pavia P, Hanna M, et al. Efficacy and safety of tafamidis doses in the Tafamidis in Transthyretin Cardiomyopathy Clinical Trial (ATTR-ACT) and long-term extension study. *Eur J Heart Fail.* 2021;23(2):277–285. doi:10.1002/ejhf.2027
61. Park J, Egom U, Parker S, Andrews E, Ombengi D, Ling H. Tafamidis: A first-in-class transthyretin stabilizer for transthyretin amyloid cardiomyopathy. *Ann Pharmacother.* 2020;54(5):470–477. doi:10.1177/1060028019888489
62. Rapezzi C, Elliott P, Damy T, et al. Efficacy of tafamidis in patients with hereditary and wild-type transthyretin amyloid cardiomyopathy: Further analyses from ATTR-ACT. *JACC Heart Fail.* 2021;9(2):115–123. doi:10.1016/j.jchf.2020.09.011
63. Elliott PM, Anastasakis A, Borger MA, et al. 2014 ESC Guidelines on diagnosis and management of hypertrophic cardiomyopathy: The Task Force for the Diagnosis and Management of Hypertrophic Cardiomyopathy of the European Society of Cardiology (ESC). *Eur Heart J.* 2014;35(39):2733–2779. doi:10.1093/eurheartj/ehu284
64. Kogut J, Popjes ED. Hypertrophic cardiomyopathy 2020. *Curr Cardiol Rep.* 2020;22(11):154. doi:10.1007/s11886-020-01381-3
65. Marian AJ, Braunwald E. Hypertrophic cardiomyopathy: Genetics, pathogenesis, clinical manifestations, diagnosis, and therapy. *Circ Res.* 2017;121(7):749–770. doi:10.1161/CIRCRESAHA.117.311059
66. Ryu AJ, Kumar V, Borlaug BA, et al. Systolic-to-diastolic myocardial volume ratio as a novel imaging marker of cardiomyopathy. *Int J Cardiol.* 2021;322:272–277. doi:10.1016/j.ijcard.2020.08.004
67. Teekakirikul P, Zhu W, Huang HC, Fung E. Hypertrophic cardiomyopathy: An overview of genetics and management. *Biomolecules.* 2019;9(12):878. doi:10.3390/biom9120878
68. Tuohy CV, Kaul S, Song HK, Nazer B, Heitner SB. Hypertrophic cardiomyopathy: The future of treatment. *Eur J Heart Fail.* 2020;22(2):228–240. doi:10.1002/ejhf.1715
69. Olivetto I, Oreziak A, Barriales-Villa R, et al. Mavacamten for treatment of symptomatic obstructive hypertrophic cardiomyopathy (EXPLORER-HCM): A randomised, double-blind, placebo-controlled, phase 3 trial. *Lancet.* 2020;396(10253):759–769. doi:10.1016/S0140-6736(20)31792-X
70. Rapezzi C. Mavacamten for the treatment of symptomatic obstructive hypertrophic cardiomyopathy. *G Ital Cardiol (Rome).* 2021;22(1):30–32. doi:10.1714/3502.34878
71. Spertus JA, Fine JT, Elliott P, et al. Mavacamten for treatment of symptomatic obstructive hypertrophic cardiomyopathy (EXPLORER-HCM): Health status analysis of a randomised, double-blind, placebo-controlled, phase 3 trial. *Lancet.* 2021;397(10293):2467–2475. doi:10.1016/S0140-6736(21)00763-7
72. Papadakis M, Basu J, Sharma S. Mavacamten: Treatment aspirations in hypertrophic cardiomyopathy. *Lancet.* 2020;396(10253):736–737. doi:10.1016/S0140-6736(20)31793-1
73. Ho CY, Mealiffe ME, Bach RG, et al. Evaluation of mavacamten in symptomatic patients with nonobstructive hypertrophic cardiomyopathy. *J Am Coll Cardiol.* 2020;75(21):2649–2660. doi:10.1016/j.jacc.2020.03.064
74. Miller JJ, Kanack AJ, Dahms NM. Progress in the understanding and treatment of Fabry disease. *Biochim Biophys Acta Gen Subj.* 2020;1864(1):129437. doi:10.1016/j.bbagen.2019.129437
75. Akhtar MM, Elliott PM. Anderson-Fabry disease in heart failure. *Biophys Rev.* 2018;10(4):1107–1119. doi:10.1007/s12551-018-0432-5
76. Hagège A, Réant P, Habib G, et al. Fabry disease in cardiology practice: Literature review and expert point of view. *Arch Cardiovasc Dis.* 2019;112(4):278–287. doi:10.1016/j.acvd.2019.01.002
77. Shah SJ, Katz DH, Selvaraj S, et al. Phenomapping for novel classification of heart failure with preserved ejection fraction. *Circulation.* 2015;131(3):269–279. doi:10.1161/CIRCULATIONAHA.114.010637
78. Nouretdinov I, Costafreda SG, Gammerman A, et al. Machine learning classification with confidence: Application of transductive conformal predictors to MRI-based diagnostic and prognostic markers in depression. *NeuroImage.* 2011;56(2):809–813. doi:10.1016/j.neuroimage.2010.05.023
79. Pocock SJ, Ariti CA, McMurray JJV, et al. Predicting survival in heart failure: A risk score based on 39 372 patients from 30 studies. *Eur Heart J.* 2013;34(19):1404–1413. doi:10.1093/eurheartj/ehs337
80. Przewlocka-Kosmala M, Marwick TH, Dabrowski A, Kosmala W. Contribution of cardiovascular reserve to prognostic categories of heart failure with preserved ejection fraction: A classification based on machine learning. *J Am Soc Echocardiogr.* 2019;32(5):604–615.e6. doi:10.1016/j.echo.2018.12.002
81. Kao DP, Lewsey JD, Anand IS, et al. Characterization of subgroups of heart failure patients with preserved ejection fraction with possible implications for prognosis and treatment response. *Eur J Heart Fail.* 2015;17(9):925–935. doi:10.1002/ejhf.327
82. Segar MW, Patel KV, Ayers C, et al. Phenomapping of patients with heart failure with preserved ejection fraction using machine learning-based unsupervised cluster analysis. *Eur J Heart Fail.* 2020;22(1):148–158. doi:10.1002/ejhf.1621
83. Kosmala W, Przewlocka-Kosmala M, Rojek A, Mysiak A, Dabrowski A, Marwick TH. Association of abnormal left ventricular functional reserve with outcome in heart failure with preserved ejection fraction. *JACC Cardiovasc Imaging.* 2018;11(12):1737–1746. doi:10.1016/j.jcmg.2017.07.028
84. Uijl A, Savarese G, Vaartjes I, et al. Identification of distinct phenotypic clusters in heart failure with preserved ejection fraction. *Eur J Heart Fail.* 2021;23(6):973–982. doi:10.1002/ejhf.2169
85. Hedman ÅK, Hage C, Sharma A, et al. Identification of novel phenotypes in heart failure with preserved ejection fraction using machine learning. *Heart.* 2020;106(5):342–349. doi:10.1136/heartjnl-2019-315481